"Modeling of
Friant Water Management and Groundwater "

by

Nels C. Ruud, Thomas Harter
Department of Land, Air, and Water Resources

Guilherme F. Marques, Marion W. Jenkins, Jay R. Lund
Department of Civil and Environmental Engineering

University of California, Davis

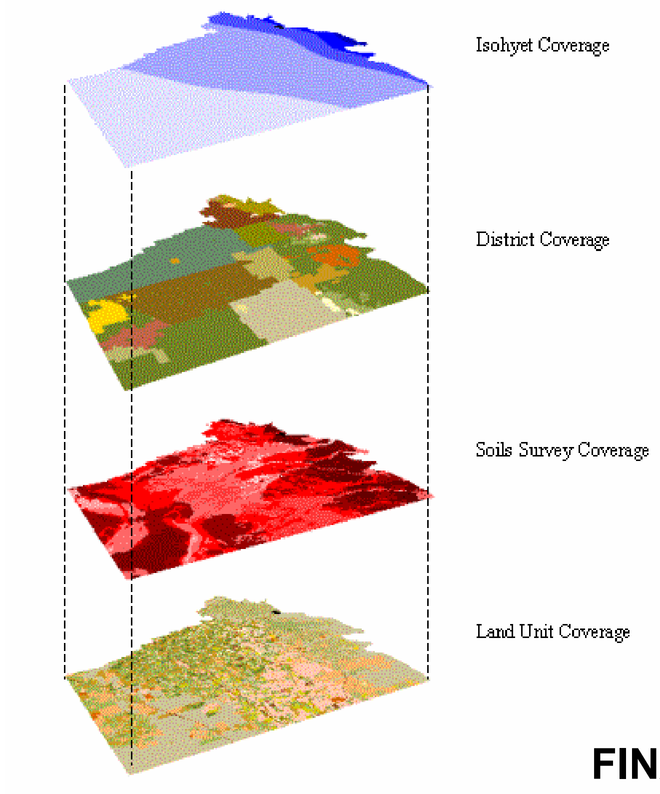

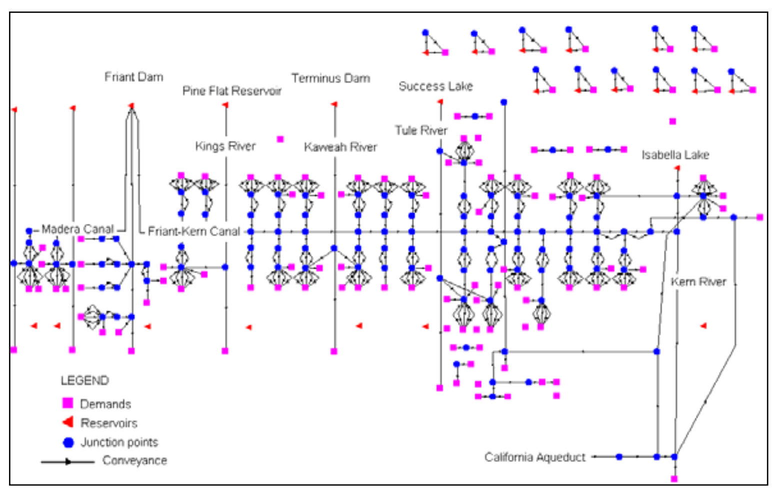

FINAL REPORT
30 September 2003

Submitted to U.S. Bureau of Reclamation
- Cooperative Agreement 22FC200213 -
David Haisten, Planning Division
U.S. Bureau of Reclamation, Mid-Pacific Region
Sacramento, California

Executive Summary

Introduction

The Friant Division is a dynamic, highly developed system. Intense agricultural development has relied in the use of both surface and groundwater supplies, which are commonly stored, sold, and transferred among users for mutual benefit and profit. The often uncoordinated use of groundwater and surface water supplies has led to aquifer overdraft and related problems in most of the region. This project develops simulation tools to aid in examining water issues within the Tulare Basin and Friant Division and in examining the effects of external water management issues on Tulare Basin activities. The project combines detailed groundwater simulation with economically-driven simulation techniques to provide an integrated modeling approach able to represent the dynamics behind users' decisions and their impact in the system.

The model development includes four tasks presented in three reports. Report 1 – "**A Conjunctive Use Model for the Tule Groundwater Sub-Basin Area in the Southern-Eastern San Joaquin Valley, California**" describes the conceptual basis and development of a hydrology model applicable for the hydrologic conditions in the Friant Division of the Tulare Basin. It includes a surface-water supply model, an unsaturated zone water budget model and a groundwater model. The report also describes the implementation of this hydrology model for the Tule River sub-basin including model calibration and validation; and provides all relevant data. Report 2 – "**Development of a GIS database for a Conjunctive Use Model for the combined Tule and Kaweah Groundwater Sub-Basins Area in the Southern-Eastern San Joaquin Valley, California**" includes all necessary data (excluding surface water supply data, which are currently being developed by the Kaweah Delta Water Conservation District) necessary for an extension of the hydrology model to the Kaweah Basin just north of the Tule Basin (Task 2), and report 3 – "**Modeling of Friant Water Management and Groundwater**" includes the description of improvements on a water management model and links the water management model with the hydrology model (Tasks 3 and 4).

Approach

A two-pronged approach was used:

1. Hydrologic modeling provided the basis for the development of a regionally calibrated physical groundwater - surface water model for the Tule-Kaweah basin, which includes almost two dozen Friant Kern contractors.

2. A water management and economic model for the Friant-Kern Unit allowed for a quantitative assessment of changes in deliveries and system reliabilities in response to changes in water operations, environmental restrictions, water prices, and other regulations.

Hydrology Model: We developed a GIS-based sub-basin scale conjunctive use model for a semi-arid agricultural area in the eastern part of the southern San Joaquin Valley, California. The base period are the fiscal water years of 1970-99. The study area is 541,580 acres in size, and consists of 9,114 land units and 26 water service districts. The conjunctive use model consists of three sub-models: 1) a surface water supply (SWS) model, 2) an unsaturated zone water budget (UZWB) model, and 3) a groundwater flow model.

The SWS model calculates the surface water balance for the source and diversion channels in the conveyance network supplying surface water to individual districts. Its primary outputs are monthly surface water deliveries to each district and the monthly seepage and evaporative losses from the modeled channels. The surface water deliveries become input for the UZWB model and the channel seepage are input into the groundwater flow model as a localized source of aquifer recharge.

The subsurface of each land unit is conceptualized as consisting of a soil root zone and a deep vadose zone overlying the aquifer system. For each land unit, the UZWB model calculates the monthly applied water demand; its allotment of delivered surface water; the groundwater pumping required to meet the balance of its applied water demand; and any aquifer recharge resulting from deep percolation of surface applied water and precipitation. Its primary outputs are the diffuse recharge to the aquifer system from surface applied water and precipitation, and the groundwater pumping demand from the aquifer system.

The diffuse aquifer recharge and groundwater pumping become input into the groundwater flow model. Its purpose is to calculate the hydraulic head and groundwater storage changes in the aquifer system subject to transient groundwater recharge and pumping stresses. The main model output is the simulated hydraulic head distribution in the modeled area for each stress period. A post-processing routine calculates the cumulative annual groundwater storage changes over each district and the entire study area. An automated calibration of the transient groundwater flow model was performed from 1970-85. The model was then validated from 1986-99. Using the calibrated model, we computed the annual inter-district groundwater fluxes between adjacent districts.

Water Management Model: The water management model – FREDSIM – simulates water operations in the Friant Division as a system driven by economic performance at the irrigation district level. The model uses a computer based decision support system based on a capacitated network flow approach for simulation and optimization of water resources systems (MODSIM).

Land use and water demand data provided by the hydrology model is used to develop water penalty functions at the irrigation district level with the SWAP (Statewide Agricultural Production) model. Penalty functions are integrated into the water management model to represent economic decisions on water use by irrigation districts.

Groundwater data from the hydrology model is used to delineate groundwater reservoirs and identify their connection with the irrigation districts that pump groundwater. The groundwater model is used to develop response parameters (hydraulic conductance) so that groundwater flows can be calculated and groundwater reservoirs head tracked based on storage variation. Groundwater pumping costs are updated every time step based on head changes.

Results

Hydrology Model

The Tule Sub-basin study area is 541,580 acres in size and contains the entire Tule groundwater sub-basin and parts of the Kaweah and Tulare Lake groundwater sub-basins. The incorporated land in the study area is divided into 26 water service districts: 21 irrigation, water, or public utility districts; 2 major cities; 2 private contractors; and 1 water company. These districts are either completely or partially located within the study area. The study area is further delineated into 9,114 individual land units from a 1985 land use survey of Tulare County. Agriculture is the largest land use, comprising 72% of the study area. Native and urban land use comprise 22% and 4% of the study area, respectively. Semi-agricultural and special conditions (i.e. fallow) land use each comprise 1%. Twelve crops account for 95% of the area under agricultural production. Cotton, grain & grass hay, citrus, vineyards, and alfalfa individually represent 20.3, 18.6, 13.6, 13, and 10.3% of the total productive acreage, respectively.

The total imported surface water for 1970-99 from the CVP and the Success Reservoir are 13,329,262 and 4,653,501 acre-feet (af), respectively. The SWP and the Kings River imported the lesser amounts of 88,625 and 7,332 af, respectively. Annual CVP diversions varied from 125,970 af in 1977 to 679,298 af in 1993 with a 30-year annual average of 444,309 af. The Tule River and Pioneer Ditch both receive regulated releases from Success Reservoir. Tule River annual imports varied from 11,034 af in 1977 to 607,154 af in 1983 while the Pioneer Ditch varied from 3,445 af in 1973 to 5,874 af in 1990. The total natural runoff from the Deer Creek and White River from 1970-99 were 703,444 and 219,098 af, respectively. Deer Creek runoff varied from 4,082 af in 1992 to 103,716 af in 1983 while the White River runoff varied from 422 af in 1977 to 37,985 af in 1998.

From 1970-99, a total of 15 million af of surface water was applied by the service districts in the study area. The applied surface water varied from a low of 135,482 af in 1977 to a high of 708,293 af in 1996. The Lower Tule River Irrigation District and the Delano-Earlimart Irrigation District together account for 59% of the total applied surface water while occupying approximately 40% of the incorporated area in the study area. Over the 30-year base period, an estimated total of 3.5 million af of seepage conveyance loss occurred in all surface water channels. Seepage in the Tule River, Deer Creek, and White River accounted for 85% of the total seepage. Total annual seepage varied from a low of 8,128 af in 1977 to 467,084 af in 1983.

The total annual agricultural and urban consumptive use ranged from 872,100 af in 1970 to 1,250,700 af in 1999. The estimated total pumping ranged from 143,100 af in 1978 to 560,600 af in 1990. As expected, pumping was heaviest during the droughts of 1975-77 and 1987-92, and lightest during the wet years of 1973, 1978, 1982-83, 1995, and 1998. Precipitation totals varied from 176,500 af in 1990 to 967,400 af in 1998. Diffuse recharge from surface applied water ranged from 110,000 af in 1992 to 270,100 af in 1983.

The trends in cumulative annual groundwater storage changes computed from the water balance and the water table fluctuation (WTF) method from 1970-99 were quite similar. The minimum and maximum differences between them were 28,479 af (1996) and 1,027,693 af (1991), respectively. From 1970, the maximum amount of groundwater accumulation occurred in the spring of 1987 with the WTF method and the water balance estimating positive storage changes of 1,146,286 and 907,155 af, respectively. The maximum groundwater overdraft occurred in 1993 with the WTF method estimating a negative storage change of 1,610,210 af while the water balance method maximum overdraft was 992,906 af in 1995. The 1987 and 1993 fiscal water years marked the beginning and ending of a major 6-year drought in California, respectively.

Three different conceptual models of the aquifer system horizontal hydraulic conductivity, K_h, structure were evaluated in the calibration process: 1) K_h as an exponential function of the specific yield, S_y, distribution, 2) K_h as a linear function of the saturated hydraulic conductivity of the soil survey mapping units, and 3) division of the model domain into square zones of uniform size. The models were calibrated against both spatially distributed hydraulic head targets and cumulative groundwater storage change targets for seven of the largest districts. The discretization of the model domain into uniform square zones provided the most robust K_h structure and produced the most reasonable estimates of hydraulic head and district groundwater storage changes from the three conceptual models over the 1971-85 calibration period. The calibrated model was then used to compute the annual net inter-district groundwater fluxes between adjacent districts. In general, groundwater flux directions were consistent with the large-scale hydraulic gradients. Annual inter-district net fluxes between adjacent districts ranged from negligibly small (< 100 af) to as much as 50,000 af (e.g. net flux from Lower Tule River ID to Pixley ID). Net interdistrict fluxes were generally a function of the local transmissivity, the length of the shared border between adjacent districts, and the differences in their surface water supplies.

Water Management Model

The water management model was run for three initial alternatives. A FPlow run (original groundwater pumping costs), a FPhigh run (updated groundwater pumping costs based on new head data, and a VP run (variable groundwater pumping cost). Multiple runs were made under the VP alternative with varying surface water and energy prices. The higher groundwater pumping costs on runs FPhigh and VP resulted in reduction in groundwater pumping, reduction in overdraft and increase in scarcity and scarcity costs (Table ES-1).

Table ES-1. Overall average results – all FRIANT contractors

	Variable pmp cost **FPlow run**		Fixed pmp cost **VP run**	
Totals (taf/yr avg)		% Total		% Total
Demand	2,984	100.0%	2,984	100.0%
Total Supply	2,891	96.9%	2,865	96.0%
Scarcity	93	3.1%	119	4.0%
Total Supply	2,891	100.0%	2,865	100.0%
Surface contract supply	867	30.0%	1,004	35.0%
Surface other supply[1]	613	21.2%	613	21.4%
GW supply	1,411	48.8%	1,248	43.6%

[1]Excluding artificial recharge

The lower groundwater pumping cost run (FPlow) results in 21 maf of total overdraft over 73 years and a $19 million/yr average penalty in scarcity costs. Avoiding this overdraft would require reducing groundwater pumping by either cutting back in production or acquiring supplemental non-local surface supplies averaging 288 kaf/yr. The groundwater pumping curtailment seen in VP run could reduce the overdraft to 9.2 maf at a cost of $24 million/yr in scarcity costs, if no supplemental surface supply is available. To eliminate the 9.2 maf overdraft 126 kaf/yr average of supplemental surface supplies would be needed.

Reduction of this overdraft requires reduction of groundwater pumping. In terms of surface water this is equivalent to 33% of contract surface supplies that would be required as non-local transfers. Without additional surface supplies, a 49% reduction in overdraft (9.8 maf) would cost an additional $5 million/yr average in scarcity costs, a 26% increase.

Uses

Results from the models developed provide better understanding of the groundwater system under Friant Division, particularly the important role of irrigation and pumping in driving the dynamics of the groundwater system. The model points towards significant groundwater exchanges among districts. The non-uniqueness of the groundwater model calibration provides the basis for defining future data needs. The integration of this information into the management model enables it to simulate operational changes consequence of management policies modifying surface water and energy prices.

Conclusions

Users change supply sources and quantities, and transfer water reacting to variations in water and energy price, economic value and water availability. Groundwater is a critical component of the system and the differences in the approaches used to model it demonstrate that efforts dedicated to evaluate it accurately are important in modeling the Friant system.

Significant increases in surface water prices are seen to compromise current conjunctive use operations. The historical overdraft pattern is still occurring despite the increase in groundwater prices and it is a consequence of the irrigation districts economic decisions. Reduction of this overdraft requires reduction of groundwater pumping. In terms of surface water this is equivalent to 33% of contract surface supplies that would be required as non-local transfers. Without additional surface supplies, a 49% reduction in overdraft (9.8 maf) would cost an additional $5 million/yr average in scarcity costs, a 26% increase

High spatial and temporal variability in groundwater pumping was found by processing data from the groundwater model for use in FREDSIM. This variability is included as a constraint in the simulation model to enable a better characterization of present conditions when the model optimizes the water allocation for a given time step.

Recommendations

Recommendations to address some of the model limitations include:

1. Extend groundwater model to include remaining irrigation districts and the Kaweah Basin
2. Collect field data on groundwater hydraulic conductivity and incorporate into the groundwater model
3. Include carry-over value functions for surface and groundwater storage
4. Improve information regarding applied water demands and evapotranspiration.
5. Implement sensitivity study on the coupled hydrology-water management model to determine interdependency between input data to the hydrologic model and the output from the water management model

The model should also be applied in further investigation of conjunctive use operations and water-market scenarios in the region. Currently only non-contract water is allowed to be exchanged among irrigation districts.

Attachments

- Attachment 1: Report “A Conjunctive Use Model for the Tule Groundwater Sub-Basin Area in the Southern-Eastern San Joaquin Valley, California”
- Attachment 2: Report “Development of a GIS database for a Conjunctive Use Model for the combined Tule and Kaweah Groundwater Sub-Basins Area in the Southern-Eastern San Joaquin Valley, California”
- Attachment 3: Report “Modeling of Friant Water Management and Groundwater”

INSERT SLIP SHEET (P1) INSTEAD OF THIS PAGE

ATTACHMENT 1

A Conjunctive Use Model for the Tule Groundwater Sub-Basin Area in the Southern-Eastern San Joaquin Valley, California

Nels Ruud, Thomas Harter, and Alec Naugle
Department of Land, Air, and Water Resources, University of California, Davis

Prepared for:
United States Bureau of Reclamation
Submitted: September 30, 2003

List of Tables

List of Figures

List of Plates

1 Executive Summary

The Tule groundwater sub-basin is an agriculturally-intensive area located in the eastern-central part of the southern San Joaquin Valley, California. Urban and agricultural stakeholders in the Tule sub-basin depend on a combination of imported surface water and pumped groundwater to meet their water demands. The water service districts there receive surface water deliveries from the Friant Unit of the Central Valley Project (CVP) (United States Bureau of Reclamation), the State Water Project (SWP) (California Department of Water Resources), the Kings River (United States Army Corps of Engineers), or the Success Reservoir (United States Army Corps of Engineers). All of these surface water sources develop their supplies from run-off and snow melt in the foothills and watersheds of the Sierra Nevada mountain range. The state of California is prone to recurring droughts, some lasting several years. During drought periods, irrigated agriculture depends more heavily on groundwater pumping as surface water supplies are generally less available. To buffer the effects of drought, districts in the Tule sub-basin have cooperatively managed their surface water and groundwater resources conjunctively. During a normal to wet year, excess available surface water supplies (e.g. releases for flood control) are used by some districts to recharge their groundwater reservoirs. However, a prolonged multi-year drought invariably leads to an increased dependence on groundwater pumping and overdraft of the groundwater sub-basin storage. In addition to climate variability, changes in future surface water supplies may also occur due to the passage of the Central Valley Project Improvement Act of 1992 which mandates that 400,000 acre-feet per year of CVP water be released from the Friant Unit into the San Joaquin River for restoration purposes.

To better understand the impacts of irrigated agriculture, fluctuating surface water supplies, and groundwater pumping practices on water levels and groundwater storage in the Tule sub-basin area, we developed a GIS-based conjunctive use model to study them. The study area is 541,580 acres in size and contains the entire Tule groundwater sub-basin and parts of the Kaweah and Tulare Lake groundwater sub-basins. The incorporated land in the study area is divided into 26 water service districts: 21 irrigation, water, or public utility districts; 2 major cities; 2 private contractors; and 1 water company. These districts are either completely or partially located within the study area. The study area is further delineated into 9,114 individual land units from a 1985 land use survey of Tulare County. Agriculture is the largest land use, comprising 72% of the study area. Native and urban land use comprise 22% and 4% of the study area, respectively. Semi-agricultural and special conditions (i.e. fallow) land use each comprise 1%. Twelve crops account for 95% of the area under agricultural production. Cotton, grain & grass hay, citrus, vineyards, and alfalfa individually represent 20.3, 18.6, 13.6, 13, and 10.3% of the total productive acreage, respectively.

Surface water supplies are distributed to the districts and ultimately to the individual land units by a surface water supply system. The surface water supply system in the model is divided into two parts: 1) an inter-district surface water channel network, and 2) an intra-district surface water distribution system. The inter-district channel network consists of the explicitly modeled source and diversion channels which import surface water into the study area and deliver it to individual districts. The intra-district distribution system consists of the implicitly modeled district channels (e.g. laterals, ditches, canals, farm turnouts) which deliver surface water to individual land units within each district.

The conjunctive use model consists of three loosely-coupled sub-models: 1) a surface water supply (SWS) model, 2) an unsaturated zone water budget (UZWB) model, and 3) a groundwater flow model. The base period of the study covers the fiscal water years of 1970-99. The purpose of the SWS model is to calculate the surface water balance for the source and diversion channels in the inter-district channel network. For each modeled surface water channel, the SWS model computes surface water deliveries from it to each district and conveyance losses from it due to evaporation and channel seepage. The primary model outputs are monthly surface water deliveries to each district and monthly seepage rates from modeled channels. The surface water deliveries became input for the UZWB model. The channel seepage became input for the groundwater flow model as localized aquifer recharge. The allocation of surface water within each district, via the implicitly modeled intra-district surface water distribution system, is estimated by the UZWB model.

The total imported surface water for 1970-99 from the CVP and the Success Reservoir are 13,329,262 and 4,653,501 acre-feet (af), respectively. The SWP and the Kings River imported the lesser amounts of 88,625 and 7,332 af, respectively. Annual CVP diversions varied from 125,970 af in 1977 to 679,298 af in 1993 with a 30-year annual average of 444,309 af. The Tule River and Pioneer Ditch both receive regulated releases from Success Reservoir. Tule River annual imports varied from 11,034 af in 1977 to 607,154 af in 1983 while the Pioneer Ditch varied from 3,445 af in 1973 to 5,874 af in 1990. The total natural runoff from the Deer Creek and White River from 1970-99 were 703,444 and 219,098 af, respectively. Deer Creek runoff varied from 4,082 af in 1992 to 103,716 af in 1983 while the White River runoff varied from 422 af in 1977 to 37,985 af in 1998.

From 1970-99, a total of 15 million af of surface water was applied by the service districts in the study area. The applied surface water varied from a low of 135,482 af in 1977 to a high of 708,293 af in 1996. The Lower Tule River Irrigation District and the Delano-Earlimart Irrigation District together account for 59% of the total applied surface water while occupying approximately 40% of the incorporated area in the study area. Over the 30-year base period, an estimated total of 3.5 million af of seepage conveyance loss occurred in all surface water channels. Seepage in the Tule River, Deer Creek, and White River accounted for 85% of the total seepage. Total annual seepage varied from a low of 8,128 af in 1977 to 467,084 af in 1983.

The UZWB model then calculates the monthly water storage changes in the soil root zone and deep vadose zone of each land unit, where the land unit is the UZWB model scale of resolution. It also models the intra-district surface water distribution system by estimating the monthly allocation of surface water to individual land units within each district. The main model outputs were the recharge to the unconfined aquifer from surface applied water and precipitation, and the groundwater pumping demand from the unconfined and confined aquifers. The recharge and groundwater pumping rates became input for the groundwater flow model.

The total annual agricultural and urban consumptive use ranged from 872,100 af in 1970 to 1,250,700 af in 1999. The estimated total pumping ranged from 143,100 af in 1978 to 560,600 af in 1990. As expected, pumping was heaviest during the droughts of 1975-77 and 1987-92, and lightest during the wet years of 1973, 1978, 1982-83, 1995, and 1998. Precipitation totals varied from 176,500 af in 1990 to 967,400 af in 1998. Diffuse recharge from surface applied water ranged from 110,000 af in 1992 to 270,100 af in 1983.

The net aquifer recharge for the entire study area was computed by aggregating the aquifer recharge and groundwater pumping of each land unit to this scale and adding the contribution to aquifer recharge from channel seepage. The monthly net recharge was then summed to produce a cumulative annual net recharge from 1970 to each fiscal water year from 1971-99. The water balance computed for the entire study area neglects horizontal groundwater inflows and outflows through its vertical boundaries. Groundwater fluxes undoubtedly exist along these boundaries. However, net fluxes are likely small in comparison to the total changes in storage due to vertical stresses applied to the entire study area (e.g. groundwater pumping, evapotranspiration, applied surface water, channel seepage). Horizontal groundwater flow on the inter-land unit and inter-district scales is expected to be more significant. For computing a total water balance, however, we made the simplifying assumption that the study area behaves as a relatively closed system where the net horizontal groundwater inflows through its vertical boundaries are small. Invoking this assumption, we then use the cumulative net recharge as an estimate of the cumulative groundwater storage change in the aquifer system. Ideally, verification of these estimates is performed by comparing them with an objective measure of the study area aquifer storage changes. However, changes in groundwater storage are not directly observable and must always be estimated using non-direct measures. As such, an objective measure for verification does not exist. As an alternative, we compare the water balance model results with those produced by the water-table fluctuation (WTF) method.

The trends in cumulative annual groundwater storage changes computed from the water balance and the WTF method from 1970-99 were quite similar. The minimum and maximum differences between them were 28,479 af (1996) and 1,027,693 af (1991), respectively. From 1970, the maximum amount of groundwater accumulation occurred in the spring of 1987 with the WTF method and the water balance estimating positive storage changes of 1,146,286 and 907,155 af, respectively. The maximum groundwater overdraft occurred in 1993 with the WTF method estimating a negative storage change of 1,610,210 af while the water balance method maximum overdraft was 992,906 af in 1995. The 1987 and 1993 fiscal water years marked the beginning and ending of a major 6-year drought in California, respectively.

Finally, the groundwater flow model calculates the changes in water levels in the aquifer system subject to transient groundwater recharge and pumping stresses. A post-processing routine calculates the cumulative groundwater storage changes over each district and the entire study area for each stress period. An automated calibration of the groundwater flow model was performed to refine the conceptual model of the hydrogeology and to estimate the spatial distributions of the aquifer system horizontal hydraulic conductivity. The calibration period of the groundwater flow model is 1970-85 and the validation period is 1986-99.

Three different conceptual models of the aquifer system horizontal hydraulic conductivity, K_h, structure were evaluated in the calibration process: 1) K_h as an exponential function of the specific yield, S_y, distribution, 2) K_h as a linear function of the saturated hydraulic conductivity of the soil survey mapping units, and 3) division of the model domain into square zones of uniform size. The models were calibrated against both spatially distributed hydraulic head targets and cumulative groundwater storage change targets for seven of the largest districts. The discretization of the model domain into uniform square zones provided the most robust K_h structure and produced the most reasonable estimates of hydraulic head and district groundwater storage changes from the three conceptual models over the 1971-85 calibration period. The calibrated model was then used to compute the annual net inter-district groundwater fluxes between adjacent districts. In general, groundwater flux directions were consistent with the large-scale hydraulic gradients. Annual inter-district net fluxes between adjacent districts ranged from negligibly small (< 100 af) to as much as 50,000 af (e.g. net flux from Lower Tule River ID to Pixley ID). Net interdistrict fluxes were generally a function of the local transmissivity, the length of the shared border between adjacent districts, and the differences in their surface water supplies.

2 Abstract

We developed a GIS-based sub-basin scale conjunctive use model for a semi-arid agricultural area in the eastern part of the southern San Joaquin Valley, California. The base period are the fiscal water years of 1970-99. The study area is 541,580 acres in size, and consists of 9,114 land units and 26 water service districts. The conjunctive use model consists of three sub-models: 1) a surface water supply (SWS) model, 2) an unsaturated zone water budget (UZWB) model, and 3) a groundwater flow model. The SWS model calculates the surface water balance for the source and diversion channels in the conveyance network supplying surface water to individual districts. Its primary outputs are monthly surface water deliveries to each district and the monthly seepage and evaporative losses from the modeled channels. The surface water deliveries become input for the UZWB model and the channel seepage are input into the groundwater flow model as a localized source of aquifer recharge. The subsurface of each land unit is conceptualized as consisting of a soil root zone and a deep vadose zone overlying the aquifer system. For each land unit, the UZWB model calculates the monthly applied water demand; its allotment of delivered surface water; the groundwater pumping required to meet the balance of its applied water demand; and any aquifer recharge resulting from deep percolation of surface applied water and precipitation. Its primary outputs are the diffuse recharge to the aquifer system from surface applied water and precipitation, and the groundwater pumping demand from the aquifer system. The diffuse aquifer recharge and groundwater pumping become input into the groundwater flow model. Its purpose is to calculate the hydraulic head and groundwater storage changes in the aquifer system subject to transient groundwater recharge and pumping stresses. The main model output is the simulated hydraulic head distribution in the modeled area for each stress period. A post-processing routine calculates the cumulative annual groundwater storage changes over each district and the entire study area. An automated calibration of the transient groundwater flow model was performed from 1970-85. The model was then validated from 1986-99. Using the calibrated model, we computed the annual inter-district groundwater fluxes between adjacent districts. We describe the development of the conjunctive use model and present a discussion of its results and the invoked modeling assumptions.

3 Introduction

The Tule groundwater sub-basin is an agriculturally-intensive area located in the eastern-central part of the southern San Joaquin Valley, California (Plate 1). Urban and agricultural stakeholders in the Tule sub-basin depend on a combination of imported surface water and pumped groundwater to meet their water demands. The water service districts which distribute surface water to the individual stakeholders receive these supplies from four potential sources: 1) the Friant Unit of the Central Valley Project (CVP), 2) the State Water Project (SWP), 3) regulated flows in the Tule River and the Pioneer Ditch released from the Success Reservoir, and 4) diversions from the Kings River from Pine Flat Reservoir. The CVP and the SWP are operated by the United States Bureau of Reclamation (USRB) and the California Department of Water Resources (CDWR), respectively, while the Success Reservoir and the Pine Flat Reservoir are operated by the United States Army Corps of Engineers (USACE), respectively.

The primary sources of surface water are the CVP and the Tule River. The SWP is not a major supplier of surface water in the Tule sub-basin and the other unregulated rivers and creeks have significant flows only during severe storm events. Nevertheless, all surface water sources develop their supplies from run-off and snow melt in the foothills and watersheds of the Sierra Nevada mountain range. Surface water availability varies considerably during the fiscal water year due to the timing, duration, and severity of storm events, to the amount of accumulated snow pack in the Sierra Nevada mountains during the fall and winter months, and the rate of snow melt. Surface water availability also varies annually as the state of California in general is prone to recurring drought.

Not all districts in the Tule sub-basin possess contracts with the CVP or entitlements to the Tule River. In addition, the contract amounts and entitlements of all districts are not equal; nor are they proportional to the acreage or number of stakeholders served by them. Districts with large contracts or entitlements are able to meet most or all of the crop water demands of their farmers with surface water during years of normal precipitation. Farmers in unincorporated areas (i.e. areas not residing in a district) or in districts with relatively small contracts or entitlements are often required to satisfy a substantial portion of their crop water demands with pumped groundwater, even during normal to wet years.

To buffer the effects of drought and variable surface water supplies, districts in the Tule sub-basin have cooperatively managed their surface water and groundwater resources conjunctively. During a normal to wet year, excess available surface water supplies (e.g. releases for flood control) are used by some districts to recharge their groundwater reservoirs. However, a prolonged multi-year drought invariably leads to an increased dependence on groundwater pumping and the consequent overdraft of the sub-basin groundwater storage. For example, in Bulletin 118-80 the CDWR report an estimated average annual groundwater overdraft in the Tule sub-basin of 163,000 acre-feet as of 1975

(CDWR, 1980).

Variability in future surface water supplies from the CVP may also occur due to federal legislation intended in part to restore the ecological health of the San Joaquin River. In 1992, the United States Congress enacted the Central Valley Project Improvement Act (CVPIA). The act calls for major changes in the management of the CVP and covers five primary areas: 1) limitations on new and renewed CVP contracts, 2) water conservation actions, 3) water transfers, 4) fish and wildlife restoration actions, and 5) establishment of an environmental restoration fund (USBR, 1997). In particular, the CVPIA mandates that 400,000 acre-feet per year of CVP water be released from Friant Unit into the San Joaquin River for protection of fish habitat in the Sacramento-San Joaquin River Delta ecosystem. This action may result in severe cut-backs in future surface water supplies for Friant Unit contractors and lead to greater dependence on groundwater pumping by many farmers to meet crop water demands. An understanding of the impact of changes in surface water supplies and dependencies on groundwater pumping is necessary to evaluate the ability of the Tule sub-basin area to manage its water resources conjunctively.

3.1 Purpose and Objectives

The purpose of this report is to present the development of a GIS-based conjunctive use model for the Tule groundwater sub-basin area. The objective of the model is to simulate the historical impacts of urban and agricultural water demands, fluctuating surface water supplies, and groundwater pumping practices on the spatial and temporal distribution of groundwater storage in the sub-basin area.

3.2 Conjunctive Use Modeling

Groundwater storage changes at the sub-basin scale in the San Joaquin Valley can be estimated by solving a water balance of inputs and outputs in the subsurface. The base period of the water balance model should include several distinct hydrologic conditions (i.e. wet and dry periods) to adequately characterize the storage changes with respect to climate variability. The hydrologic sub-basin inputs are typically precipitation, applied irrigation, seepage from flows in natural or constructed surface water channels, and groundwater inflows through subsurface boundaries. The hydrologic outputs from the sub-basin are crop evapotranspiration, evaporation from surface water bodies and bare soil, urban consumptive use, and groundwater outflows through subsurface boundaries.

The conjunctive use model consists of three sub-models: 1) a surface water supply (SWS) model, 2) an unsaturated zone water budget (UZWB) model, and 3) a groundwater flow model. The relationships between the three sub-models is illustrated in Figure 1. The SWS model computes surface water deliveries from the major natural and constructed channels to each water service district and the channel conveyance losses due to evaporation and channel seepage. The surface water deliveries become input into the UZWB model and the channel seepage become input into the groundwater flow model as recharge to the unconfined aquifer. The UZWB model then solves the soil root zone and deep vadose zone water balances for each land unit in the study area. For each land unit, it computes the applied water demand; the allotment of delivered surface water from its service district; the groundwater pumpage required to meet the balance of the applied water demand; and any aquifer recharge resulting from the deep percolation of the surface applied water. The recharge from surface applied water becomes input into the groundwater flow model which then computes changes in water levels and groundwater storage in response to the pumping and recharge stresses. The modeling base period are the fiscal water years from 1970-99 and the minimum modeling time step is monthly.

3.3 Report Organization

This report is organized as follows. In Section 4, we describe the study area setting, including its geographic location, climate, soils, land uses, and water service districts. In Section 5, we describe the study area geology and in Section 7 we define the aquifer system and the sources of groundwater recharge and discharge. In Section 6, we describe the surface hydrology, including a description of the major natural and constructed surface water channels. In Section 8, we present the conceptual model of the surface water supply system and the development of the SWS model. In Section 9, we present the conceptual model of the soil root and deep vadose zones and the development of the UZWB model. In Section 10, we describe the development and calibration of the transient groundwater flow model. Finally, in Section 11 we assess the development of the conjunctive use model including a discussion of the simplifying assumptions invoked in the development of each sub-model.

4 Setting

The study area is located in the southwest corner of Tulare County in the eastern-central part of the southern San Joaquin Valley, California. It is 541,580 acres in size and consists of the entire Tule groundwater sub-basin and small portions of the Kaweah and Tulare Lake groundwater sub-basins (Plate 2). Each of these sub-basins are within the greater San Joaquin Valley groundwater basin (CDWR, 1980).

4.1 Climate

The local climate is semi-arid (Steppe) with most precipitation falling between November and March. From 1970-99, annual precipitation varied between 5-22 inches with a mean of approximately 9 inches (Figure 2). Precipitation is greatest along the eastern boundary of the study area and decreases westwardly (Plate 3). The annual evaporation ranged from 55-70 inches with a mean of 64 inches (Figure 3). Average monthly daytime temperatures vary from 56 F^{o} in

December to 98 F^{o} in July. Average monthly nighttime temperatures vary from 36 F^{o} in December to 63 F^{o} in July. The region experiences alternating periods of drought (1975-77, 1987-92) and wet conditions (1973, 1978, 1982-83, 1995, 1998) (Figure 2).

4.2 Soils

The major soil types in the study area were identified in a 1935 soils survey of western Tulare County (Storie, 1942) and later digitized into a GIS by Zhang (1993) (Plate 4). The soil types range from low-permeable clay and clay loam to highly-permeable sand and loamy fine sand. The associated field capacities range from 8% for fine sandy loam and sand to 41% for adobe clay (Plate 5), and the saturated hydraulic conductivity ranges from 0.06 ft/day in adobe clay to 16.5 ft/day in sandy soils (Plate 6).

4.3 Land Units and Land Use

The study area is delineated into 9,114 land units from a 1985 land use survey and digitized into a GIS by Zhang (1993) (Plate 7). The land units are generally classified as agricultural, semi-agricultural, urban, native, or special conditions land use (Tables 1-4). Land use is further delineated into classes and sub-classes. There are 61 land use sub-classes in the land use survey. Agriculture is the largest land use, comprising 72% of the study area (Figure 4). Native and urban land use comprise 22% and 4% of the study area, respectively. Semi-agricultural and special conditions (i.e. fallow) land use each comprise 1%. Twelve crops account for 95% of the area under agricultural production (Figure 5). Cotton, grain & grass hay, citrus, vineyards, and alfalfa individually represent 20.3, 18.6, 13.6, 13, and 10.3% of the total productive acreage, respectively.

4.4 Water Service Districts

The study area is also delineated into 26 water service districts: 21 irrigation, water, or public utility districts; 2 major cities; 2 private contractors; and 1 water company (Plate 8). The remaining area is unincorporated agricultural and non-agricultural lands. Not all districts completely reside within the study area. The fraction of area and acreage of each district within the study area are given in Table 5. The service areas may also be located in different groundwater sub-basins. Lindmore Irrigation District (LID), Lindsay-Strathmore Irrigation District (LSID), Lewis Creek Water District (LCWD), and the city of Lindsay are located within the Kaweah groundwater sub-basin. Small fractions of Angiola Water District (AWD) and Alpaugh Irrigation District (AID) are located within the Tulare Lake groundwater sub-basin. All other districts are partially or entirely located in the Tule sub-basin.

5 Geology

5.1 Regional Geology

The San Joaquin Valley covers approximately the southern two-thirds of the Central Valley, extending from the Sacramento-San Joaquin River Delta in the north to the Tehachapi Mountains in the south. The Central Valley is a structural trough whose major axis trends northwest to southeast. The valley is bordered on the east by the granitic complex of the Sierra Nevada mountain range and on the west by the folded and faulted sedimentary, volcanic, and metamorphic rocks of the Coast Ranges.

From the late Cretaceous Period through the late Tertiary Period, the San Joaquin Valley underwent marine deposition. From the late Tertiary Period to present, thousands of feet of continental deposits were deposited above these marine sediments. The marine and continental deposits together form a wedge that thickens from east to west and from north to south. Deposit thickness ranges from 15,000 feet thick to a maximum of 28,000 feet at the extreme southern end of the valley (Lofgren and Klausing, 1969).

5.2 Study Area Geology

The study area is bordered on the east by the foothills of the Sierra Nevada mountains and on the west by the Tulare Lake Bed. The major geomorphic units in this region include: (1) the Sierra Nevada mountain granitic basement complex, (2) the dissected uplands at the base of the Sierra Nevada mountains, (3) low lying alluvial plains and fans, (4) river flood plains and channels, and (5) overflow lands and lake bottom deposits (Figure 6) (Lofgren and Klausing, 1969). The undulating foothills are formed from the dissected uplands and separate the crystalline rocks of the Sierra Nevada mountains from the alluvial plain. The uplands consist primarily of uplifted marine and continental sedimentary rocks. The Tulare Lake Bed is composed of the overflow lands and lake bottom deposits. Except in the foothill region, the study area ground surface gently slopes from an elevation of 500-600 feet in the east to 200-250 feet along the western boundary in the Tulare Lake Bed (Plate 9) (Lofgren and Klausing, 1969). Foothill elevations reach a maximum of approximately 1300 feet.

5.2.1 Sierra Nevada Mountain Granitic Basement Complex

The basement complex includes the metamorphic and igneous rocks of the westward-tilted Sierra Nevada fault block. The metamorphic rocks include quartzite, schist, gneiss, and crystalline limestone; and the igneous rocks range in composition from granite to gabbro. The basement complex dips steeply westward as it plunges below the aquifer system in the study area to depths greater than 15,000 feet. In the study area, the basement complex is insignificant as a water supply source except along the eastern boundary where fractures may yield sufficient water for domestic and stock use (Hilton et al., 1963).

5.2.2 Tertiary and Quaternary Deposits

The Tertiary and Quaternary Period sediments were deposited in alternating marine and continental environments above the basement complex and are described extensively by Hilton et al. (1963), Croft (1969), and Lofgren and Klausing (1969). The consolidated marine and non-marine rocks of Tertiary age underlie unconsolidated continental deposits of late Tertiary and Quaternary age.
The vertical sequence of deposits in the east-west direction are illustrated in Figures 7-9 (Lofgren and Klausing, 1969).

Marine Rocks Two marine-deposited stratigraphic units of Tertiary age are significant sources of groundwater in the southeastern portion of the study area: the Santa Margarita Formation and the Olcese Sand (Hilton et al., 1963). The Santa Margarita Formation consists of well-sorted, fine- to coarse-grained sand. It underlies the ground surface at depths of 3,000-4,000 feet east of Highway 99 and of 1,000-1,500 feet near Highway 65 (Figures 7-9) (Hilton et al., 1963; Lofgren and Klausing, 1969). The areal extent of the formation north of Terra Bella is unknown. From east to west, the Santa Margarita Formation thickness diminishes from approximately 600 feet to less than 150 feet. An interface between fresh and saline groundwater exists at the midpoint between Highways 65 and 99, with freshwater occurring east of this point. In the southeastern corner of the study area near Richgrove, the Santa Margarita Formation is 150-250 feet thick, highly permeable, and is a significant source of groundwater (Hilton et al., 1963).

The Olcese Sand consists mainly of unconsolidated, medium- to coarse-grained sand. The top of the unit underlies the base of the Santa Margarita Formation by 200-300 feet and is separated from the Santa Margarita Formation by the low permeable Round Mountain Silt. The areal extent of the Olcese Sand is similar to that of the Santa Margarita Formation. Near Richgrove, the Olcese Sand thickness varies from 100-450 feet and is a confined aquifer. Like the Santa Margarita Formation, the Olcese Sand is highly permeable and is a significant source of groundwater (Hilton et al., 1963).

Continental Deposits The continental deposits are fluvial and lacustrine of late Tertiary and Quaternary age. The unconsolidated deposits are divided into seven units. From oldest to youngest, they are: (1) undifferentiated continental deposits, (2) the Tulare Formation, (3) old alluvium, (4) terrace deposits, (5) young alluvium, (6) flood-basin deposits, and (7) dune sands. The lithologic character of these units is determined by the competence and capacity of the depositing channel, the depositional environment, and the source rock (Hilton et al., 1963; Lofgren and Klausing, 1969).

Undifferentiated Continental Deposits The undifferentiated continental deposits include the Kern River Formation and the older continental deposits above or inter-bedded with marine rocks of Tertiary age. The contact between the marine rocks and the overlying continental deposits dips westward from near the eastern boundary and reaches a maximum depth of 2,600 feet near the western boundary. These continental deposits consist of poorly-sorted, lenticular sediments of clay, silt, sand, and gravel derived from the Sierra Nevada mountains, and range in thickness from 500-2,000 feet. They are moderately to highly permeable, and together with the overlying Tulare Formation and older alluvium, are the most significant source of groundwater in the study area (Hilton et al., 1963).

Tulare Formation The Tulare Formation consists of poorly-sorted, lenticular deposits of gypsiferous clay, silt, sand, and gravel derived predominantly from the Coast Ranges. These deposits often exhibit a yellowish or bluish coloring. The Tulare Formation was formed by an alternating sequence of lake bottom, swamp, and meandering stream depositional environments. Along the western boundary, the Tulare Formation is up to 2,200 feet thick. The thickness of the Tulare Formation diminishes from west to east and eventually becomes indistinguishable from the undifferentiated continental deposits in the eastern half of the study area (Hilton et al., 1963).

The Corcoran Clay Member of the Tulare Formation is a laterally extensive stratum consisting of a well-sorted diatomaceous silty clay. The Corcoran Clay Member acts as a confining layer to groundwater flow and separates the upper unconfined aquifer from the lower confined aquifer west of Highway 99. The sediments in the Tulare Formation above the Corcoran Clay Member are moderately permeable. In the western half of the study area, the unconfined aquifer above the Corcoran Clay Member and the confined aquifer below it are significant sources of groundwater (Hilton et al, 1963; Lofgren and Klausing, 1969).

The lateral extent, and top and bottom elevations of the Corcoran Clay Member are illustrated in Plates 10 and 11. Its average thickness is between 50-100 feet in the study area with a maximum of +200 feet below the former Tulare Lake Bed. The top and bottom elevation ranges are -50 to -500 feet and -100 to -600 feet, respectively.

Old Alluvium The old alluvium consists of poorly-sorted, lenticular deposits of clay, silt, sand, and gravel that are loosely consolidated to cemented. These sediments were likely deposited from ancestral rivers. They are often reddish-brown in the hardpan and cemented zones. The older alluvium is diff-cult to distinguish from the underlying Tulare Formation. Although its thickness is not well characterized, it is considered less than 200 feet thick. The older alluvium is moderately to highly permeable and together with the underlying Tulare Formation and undifferentiated continental deposits is a moderate to high source of groundwater (Hilton et al., 1963).

Terrace Deposits The terrace deposits border the lower and middle reaches of the larger streams in the study area. They consist of poorly-sorted, poorly-bedded sand and gravel with some clay, and may be cemented in areas. Terrace deposits are typically less than 50 feet thick, moderately-permeable, and occur mostly above the saturated zone (Hilton et al., 1963).

Young Alluvium Young alluvium includes stream channel deposits and deposits underlying active alluvial fans. It consists of inter-stratified and discontinuous beds of poorly- to well-sorted sand, silt, gravel, and clay, yet lacks the hardpan or cemented zones common in the old alluvium. The young alluvium is less than 100 feet thick and is inter-bedded with flood-basin deposits associated with the ancestral Tulare Lake Bed in the western part of the study area. The young alluvium often occurs above the saturated zone, is moderately to highly permeable, and is suitable as a percolation site to recharge deeper aquifers in the older underlying geologic units (Hilton et al., 1963).

Flood-Basin Deposits The flood-basin deposits include the fine-grained materials of the ancestral Tulare Lake and the overflow lands bordering it that occur in the western and southwestern portion of the study area. These deposits consist of low-permeable silts and clays inter-bedded with poor- to moderately-permeable sands. Their thickness is approximately 50 feet. Due to their low permeability and the poor quality of shallow groundwater in the area, these deposits are not used as a significant source of groundwater (Hilton et al., 1963).

Dune Sands Dune sands are the ancient beach deposits along the shores of the ancestral Tulare Lake. They are limited in extent and occur as ridges parallel to the lake shoreline. The dune sands are typically composed of loose, well-sorted, gray quartz sand that has been reworked by winds and wave action. These deposits are often less than four feet thick and occur above the unsaturated zone (Hilton et al., 1963).

6 Surface Hydrology

Surface water flows in the natural and constructed channels characterize the study area surface hydrology. The natural channels are the streams, rivers, and creeks that carry runoff from catchments in the Sierra Nevada mountains and foothill regions along the eastern border of the study area. The constructed channels are a system of hydraulically inter-connected canals and ditches that import surface water into the study area, divert it for delivery to contracting service districts, and distribute it to individual land units within each district. Some natural channels receive diversions of imported surface water and divert it to other diversion channels or deliver it to contracting districts. In this section, we describe the major natural and constructed channels in the study area. This includes a description of the following: 1) the classification of each as a source, diversion, or distribution channel, 2) the types of channel flow data used for developing the surface water supply model, 3) the inter-connectedness of these channels, and 4) the districts served by them.

6.1 Source, Diversion, and Distribution Channels

We distinguish three types of natural and constructed surface water channels: 1) source channels, 2) diversion channels, and 3) distribution channels. Source channels import developed surface water or natural runoff into the study area and deliver it directly to the contracting districts, release it to diversion channels for later delivery, or allow it to infiltrate through its channel bed into the subsurface as recharge. Diversion channels convey the surface water releases from the source channels to the borders or interiors of contracting districts or redirect it to other diversion channels for later delivery. The distribution channels within each district receive the surface water from these source or diversion channels and allocate it to its members. Source and diversion channels transport surface water between districts and thus constitute the inter-district surface water conveyance network. The distribution channels deliver surface water to individual land units within each district. Therefore, each district has an associated intra-district surface water distribution system. The inter-district conveyance network and the intra-district distribution system together constitute the study area surface water supply system.

6.2 Channel Flow Data

Flow data for the individual channels constituting each intra-district surface water distribution systems are not available. However, limited flow data are available for the most significant source and diversion channels in the interdistrict surface water conveyance network. There are five types of flow data for source and diversion channels: 1) channel inflow, 2) channel outflow, 3) point discharges, 4) metered diversions, and 5) district deliveries. Channel inflow is the gauged flow at the point at which the channel crosses the study area perimeter or at the point within the study area at which channel flow begins. Channel outflow is the gauged flow at the point at which the channel exits the study area. If the channel flow terminates within the study area interior, then the channel outflow at the terminal point is assumed zero. Point discharges are measured flows at known locations along the channel reach. Diversions into or out of the channel are metered at the point of diversion. Finally, deliveries are often unmetered although the point of delivery from the channel to the district is known.

Limited availability of flow data prohibits the explicit modeling of every source and diversion channel in the study area. Consequently, a channel is explicitly modeled if: 1) it is a major source or diversion channel, 2) it is unlined (i.e. experiences seepage losses), 3) there exists monthly metered diversion, point discharge, or channel inflow and outflow data at known locations along its reach, and 4) its reach is digitized in an available GIS.

The known sources of surface water for the districts are listed in Table 6. Many districts report the diversion amount released from the source channel rather than the delivered amount received by the intra-district distribution system. A diversion is the amount of water a district contracts for from the source agency. The diversion is released from a source channel into a diversion channel or from a source channel directly into a district distribution system. Between the point of release from the source channel and the point of receipt by the distribution system, a fraction of the diversion is lost through conveyance seepage and evaporation. This loss is called the carry water. If the diversion is released from a source channel directly into a distribution system then the carry water is negligible. However, carry water may be considerable in diversion channels. The diversion minus the carry water is the district delivery, which is the actual amount of surface water received by the distribution system. Each district is assumed to receive these deliveries at their borders. Within each district, additional conveyance losses occur from surface water in transit to individual land units. The difference between the delivery and the intra-district conveyance losses is the applied surface water. In the surface water supply model section, a methodology is presented for estimating district deliveries from diversion data and applied surface water from the estimated deliveries.

6.3 Surface Water Channels

The major natural and constructed surface water channels are presented in Plate 12. Each channel is represented by a line segment. In some cases, a channel is divided into multiple line segments. The locations and identification numbers of the channel metering stations are also presented in Plate 13 and the corresponding station names in Table 8. Additional information describing channel inflows, outflows, diversions, and deliveries are provided for reference in Table 9. Here we briefly describe the major channels, including their interconnectedness
and the districts they serve.

6.3.1 Constructed Channels

Friant-Kern Canal The Friant-Kern Canal (FKC) is the most significant source channel in the basin. It is owned and operated by the USBR and is part of the CVP Friant Unit. This concrete-lined canal begins at the Friant Dam where it receives controlled releases from Millerton Lake and terminates approximately 152 miles to the south at the Kern River. It has an initial flow capacity of 5,000 cubic feet per second which decreases to 2,000 cubic feet per second at its terminus. The canal conveys surface water for urban and agricultural needs to water service districts in Fresno, Tulare, and Kern counties.

The FKC enters the study area through the LSID and exits at the Tulare-Kern county line through the Delano-Earlimart ID. As it traverses the study area, the FKC makes direct deliveries of surface water to LSID, LID, Porterville Irrigation District (PID), Saucelito Irrigation District (SID), Terra Bella Irrigation District (TBID), and Delano-Earlimart ID (DEID). The FKC also makes metered releases into diversion channels for possible delivery to the Lower Tule River ID (LTRID), PID, Pixley Irrigation District, AID, and Atwell Island Water District (AIWD).

A list of the CVP contractors in the study area and their contract amounts are given in Table 10 (USBR, 1991). Two classes of surface water (Class 1 and Class 2) are delivered to contracting districts by the Friant Unit. Class 1 water is called the "firm" supply. This supply is available for most years except during drought conditions. The Class 2 water supply is available during wet years and only after the Class 1 supply is met. The majority of Class 2 water is used for irrigation in lieu of pumping or as direct recharge into percolation basins or channels. In a dry year when little or no Class 2 water is available, the Class 2 water used in previous years as recharge is pumped back out of storage and used for irrigation. The conjunctive management of surface water and groundwater resources throughout the Friant Unit service area is predicated on this two-class water system.

Pioneer Ditch The Pioneer Ditch is an unlined source channel which begins at the Success Dam, where it receives controlled releases from the Success Reservoir, and terminates 6 miles to the west. The Pioneer Ditch serves the Pioneer Water Company (PWC).

Constructed Diversion Channels The major constructed diversion channels are the Rankin, Casa Blanca, Poplar, Campbell-Moreland, Hubbs-Miner, Porter-Slough, Woods-Central, Tipton, and Vandalia ditches, the North Canal, and the Porter Slough (Plate 12). These channels receive diversions from the Tule River or Friant-Kern Canal and make deliveries to a number of districts as described in Table 9.

6.3.2 Natural Channels

The Tule River, Deer Creek, White River, Frazier Creek, and Lewis Creek are the major natural channels in the study area (Plate 12).

Tule River The Tule River is the only natural channel used explicitly as a source of irrigation water. It begins at the Success Dam and terminates approximately 52.6 miles to the west. The Tule River Association (TRA) contracts for the Success Reservoir releases to the Tule River. The TRA consists of the PWC, PID, Vandalia Irrigation District (VID), LTRID, and the Downstream Kaweah & Lower Tule River Association. Surface water in the Tule River is diverted into secondary diversion channels (Campbell-Moreland Ditch, Porter Slough, Vandalia Ditch, Poplar Ditch, Hubbs-Miner Ditch, Woods-Central Ditch) and delivered from them to TRA contractors. The Tule River also receives diversions from the FKC for delivery to the LTRID. Monthly diversions from Success Dam into the Tule River and the Pioneer Ditch for each fiscal water year from 1970-99 are documented in TRA annual reports (TRA, 1970-99). Included in these reports are the monthly releases from the Tule River into the secondary diversion channels.

The Tule River is also the only non-intermittent natural channel, with active flows in at least a portion of its reach year-round. During periods of heavy precipitation, it may exit the western boundary of the sub-basin discharging into the Tulare Lake Basin. In this study, the Tule River is divided into 3 segments: 1) the Upper Tule River, 2) the Middle Tule River, and 3) the Lower Tule River.

Deer Creek The Deer Creek is an unregulated, intermittent natural channel with natural flows occurring only in the winter and spring. None of its natural flows are explicitly used as a source of applied water. Some natural flows are diverted into side channels or spreading ponds to facilitate recharge; however, most recharge occurs within the creek. The Deer Creek receives diversions from the FKC for Pixley ID, AID, and Atwell Island WD. In this study, the Deer Creek is divided into 3 segments: 1) the Upper Deer Creek, 2) the Middle Deer Creek, and 3) the Lower Deer Creek.

White River The White River is also an unregulated, intermittent natural channel with natural flows occurring only in the winter and spring. Natural flows in the White River are not used directly by any district as a source of applied water. The White River is used as a primary diversion channel for FKC diversions to DEID. Flows are sometimes diverted into side channels or spreading ponds to facilitate recharge; however, most recharge occurs within the river. In this study, the White River is divided into 2 segments: 1) the Upper White River, and 2) the Lower White River.

Frazier and Lewis Creek Frazier Creek and Lewis Creek are both unregulated, intermittent natural channels. Neither is used as a source or diversion channel.

6.4 Other Surface Water Sources

AWD is reported to receive surface water supplies from the Kings River and the SWP. These supplies are not received directly from the Kings River or the SWP but instead are delivered from them to AWD via unmodeled diversion channels.

7 Hydrogeology

The most significant source of extractable groundwater in the study area resides in the thicker, permeable volumes of the unconsolidated continental deposits (Croft, 1969; Lofgren and Klausing, 1969; Croft and Gordon, 1968; and Hilton et al., 1963). Other significant sources reside in the old alluvium, the permeable unconfined aquifer in the Tulare Formation, and the undifferentiated continental deposits. In the southeastern corner of the study area, the consolidated marine rocks of the Santa Margarita Formation and the Olcese Sand are also an important source of groundwater but to a much lesser extent (Hilton et al., 1963).

The unconsolidated continental deposits form three differentiated aquifers: (1) a semi-confined aquifer located throughout the study area and above the Corcoran Clay Member, (2) a confined aquifer below the Corcoran Clay Member, and (3) a confined aquifer in the marine rocks of the Santa Margarita Formation and Olcese Sand in the southeastern corner near Richgrove. The confined aquifer in the Santa Margarita Formation and Olcese Sand is limited in lateral extent and its groundwater is too saline to be used as a source of water. Consequently, it will be excluded from the conceptual model of the aquifer system described later (Figure 10).

7.1 Semi-confined Aquifer

Above the Corcoran Clay Member, the semi-confined aquifer consists primarily of old alluvium, permeable sediments of the Tulare Formation, and young alluvium. There its thickness ranges from 150 feet near Highway 99 to 800 feet along the western boundary of the study area.

The thickness of the Corcoran Clay Member diminishes just east of Highway 99. From this point east, the semi-confined aquifer extends to the contact between the unconsolidated continental deposits and the consolidated marine rocks. In this region, the aquifer consists of undifferentiated continental deposits, permeable sediments of the Tulare Formation, old alluvium, and young alluvium. East of the Corcoran Clay Member, the semi-confined system is sometimes referred to as the forebay aquifer. The thickness of the forebay aquifer ranges from approximately 1700 feet thick near Highway 99 to less than 100 feet thick along the eastern boundary of the study area (Lofgren and Klausing, 1969).

The semi-confined aquifer is divided into two zones: a shallow zone and a principal-pumped zone (Hilton et al., 1963; Lofgren and Klausing, 1969). The shallow zone is approximately 300 feet deep, except where the Corcoran Clay Member is less than 300 feet deep and in the eastern uplands where the Sierra Nevada basement complex encroaches the surface. The principal-pumped zone extends from the shallow zone base to the top of the consolidated marine rocks east of Highway 99 and to the top of the Corcoran Clay Member west of Highway 99. In the eastern half of the study area, the principal-pumped zone is approximately 1500 feet thick near Highway 99 and is non-existent in the eastern uplands where the basement complex encroaches the surface.

The delineation of the shallow and principal-pumped zones is based on historical groundwater development. Initially, groundwater was pumped from shallow wells less than 300 feet deep. As water levels declined over time, shallow wells were replaced with deeper wells. Currently, most groundwater in the semiconfined aquifer is pumped from wells screened between 300-1600 feet below ground surface (Hilton et al., 1963).

In the eastern half, the shallow and principal-pumped zones are separated by discontinuous lenses of poorly-permeable materials which are 100-300 feet thick. These lenses give the aquifer its semi-confined character. Due to excessive pumping in the deeper principal-pumped zone, the drawdown in these wells is a 100 feet or greater than shallower wells (Lofgren and Klausing, 1969).

7.2 Confined Aquifer

The confined aquifer below the Corcoran Clay Member consists of unconsolidated continental deposits. From the eastern margin of the Corcoran Clay

Member to the western boundary of the study area, the confined aquifer is 1700-2600 feet thick (Lofgren and Klausing, 1969). Where the Corcoran Clay Member is less than 60 feet thick, the confined aquifer deposits have a greater sand content and are more permeable than in other areas (Hilton et al., 1963).

7.3 Groundwater Recharge and Discharge

There are four major sources of recharge to the semi-confined aquifer: 1) natural and constructed channel seepage, 2) intentional recharge of surface applied water, 3) deep percolation of surface applied water, and 4) deep percolation of precipitation (Erlewine, 1989). Recharge to the confined aquifer occurs as subsurface inflow from the principal-pumped zone east of the zone of confinement and from leakage through the Corcoran Clay Member (Hilton et al., 1963).

7.3.1 Natural and Constructed Channel Seepage

Natural channel seepage occurs primarily in the eastern half of the study area through channel beds underlain by permeable deposits. The upper reaches of the Tule River, Deer Creek, and White River are underlain by moderately to highly permeable deposits of Sierra Nevada mountain granitic-derived sands and, to a lesser extent, less permeable silts and clays from sedimentary rocks. Considerable seepage may occur along these reaches. Seepage also occurs in unlined constructed channels such as canals and ditches. Seepage rates from natural and constructed channels are estimated later by the SWS model.

7.3.2 Intentional Recharge

Some districts use intentional recharge as a method of augmenting groundwater supplies. Prior to the opening of the FKC in 1950, intentional recharge was performed mainly by districts located near the three primary natural channels (i.e. Tule River, Deer Creek, White River). Before the regulation of the Tule River in 1960, surface water supplies were often available only during winter and spring months when irrigation requirements are small. Natural channel flows were diverted to nearby spreading basins and percolation ponds or allowed to seep directly through the channel beds.

For normal to wet seasons, the FKC and the Tule River provide additional surface water imports throughout the year. Districts such as the LTRID, Pixley ID, TBID, and DEID cooperatively bank this excess water through artificial recharge programs.

Several districts implement conjunctive use management practices to facilitate water level recovery in the shallow and principal-pumped zones (Erlewine, 1989). Intentional recharge of surface water supplies occurs along the upper and middle reaches of the three major streams. For districts with excess surface water supplies, intentional recharge is performed in constructed sloughs, canals, percolation ponds, and spreading basins.

7.3.3 Percolation of Surface Applied Water

Due to irrigation inefficiencies, excess surface applied water increases the moisture content of the deep vadose zone and may recharge the underlying semiconfined aquifer. This can be a significant source of aquifer recharge.

7.3.4 Percolation of Precipitation

Deep percolation of precipitation may occur in extremely wet years during the winter and early spring when the crop water needs are small. In dry to normal years, precipitation may not completely saturate the soil root zone to field capacity. By early spring, excess soil root zone moisture is likely consumed by crops or native vegetation. During the late spring, summer, and early fall, precipitation is small and mostly evaporated or consumed by crops and native vegetation.

7.3.5 Groundwater Discharge

The regional groundwater flow direction in the semi-confined and confined aquifers is from east to west. Prior to intensive agricultural production, groundwater also discharged upward from the confined and semi-confined systems to surface drainages or to transpiring vegetation. Prior to 1920, artesian wells existed west of where Highway 99 is today (Lofgren and Klausing, 1969). Currently, pumping exceeds recharge in some years and is the principal form of groundwater discharge.

7.4 Historical Water Levels

Annual water level measurements in production wells are collected from early January to late March each year by the CDWR (Plate 14). The CDWR uses these measurements to generate contour maps of equal hydraulic head elevation for the semi-confined aquifer each year. The CDWR regards the semi-confined aquifer as unconfined and the measured hydraulic heads as representative of spring season unconfined water levels. The lines of equal elevation of unconfined water levels for 1970, 1975, 1980, 1985, 1990, and 1995 are displayed in Plates 15-20, respectively. Water levels increase from west to east with lows of 110 feet occurring in the southwest corner of Pixley ID and highs of 600 feet along the foothills in the east. Local water level depressions consistently occur in the southwest corner of Pixley ID, in an area north of LTRID, and just south of LID. Consistent water level mounds occur in DEID near the Tulare-Kings county line and along the Tule River west of Porterville.

Water level hydrographs from 1970-99 for 10 selected production wells (Plate 21) are shown in Figures 11-20. These hydrographs illustrate trends in water level changes throughout the study area over the 30-year base period. Water levels in wells 1-4 (i.e. eastern part of the study area) mostly fluctuate between 350-400 feet from 1970-99. Water levels in wells 5-7 (i.e. middle area) fluctuate between 100-250 feet and wells 8-10 (i.e. western area) between 0-200 feet. Water level fluctuations increase from east to west reflecting greater dependence on groundwater pumping in the western half of the study area. The water levels in most of the 10 wells appear to have recovered from 1970-99 despite significant intermittent fluctuations resulting from dry period overdraft (e.g. 1977) and wet year accretion (e.g. 1983). These hydrographs also reveal the varying quality of hydraulic head observations due to the presence of apparent measurement error (e.g. well 1). They also reveal the inability of the contour maps to characterize the actual range of water levels throughout the study area, particularly near the western boundary.

8 Surface Water Supply Model

As mentioned previously, the surface water supply system in the study area is divided into two parts: 1) an inter-district surface water channel network, and 2) an intra-district surface water distribution system. The inter-district channel network consists of the explicitly modeled source and diversion channels which import surface water into the study area and deliver it to individual districts (Figure 12). The intra-district distribution system consists of the implicitly modeled district channels (e.g. laterals, ditches, canals, farm turnouts) which deliver surface water to individual land units within each district.

The surface water supply (SWS) model is the first sub-model in the conjunctive use model. Its purpose is to calculate the surface water balance for the source and diversion channels in the inter-district channel network. The primary model outputs are monthly surface water deliveries to each district and monthly seepage rates from modeled channels. The surface water deliveries and seepage become input for the unsaturated zone water budget (UZWB) model and the groundwater flow model, respectively. The allocation of surface water within each district, via the implicitly modeled intra-district surface water distribution system, is estimated by the UZWB model and described in a later section. The SWS model is solved numerically in a spreadsheet.

8.1 Conceptual Model of the Surface Water Supply System

A conceptual model of the surface water supply system is presented in Figure 21. The SWS model solves for three major components: 1) the surface water deliveries to each district, 2) the seepage and evaporative conveyance losses from the channels comprising the inter-district conveyance network, and 3) the intradistrict distribution system evaporative losses. The surface water deliveries and intra-district distribution system evaporative losses are solved at the district scale; and the inter-district channel seepage and evaporation losses are solved at the lineal scale of the GIS objects representing the individual channels.

Due to the significant depth of the water table, the major channels behave ephemerally (Sophocleous, 2002). This implies that the saturated channel beds are always separated from the water table by a zone of partial saturation. In the model, we assume that channel seepage is unidirectionally downward with negligible return or base flows from the water table and unsaturated zone. However, we invoke the further simplifying assumption that the inter-district channel seepage directly recharges the unconfined aquifer. Consequently, channel seepage is not a water budget component in the unsaturated zones of individual land units in the UZWB model.

Intra-district distribution system seepage losses are not explicitly estimated by the SWS and UZWB models. Instead, we assume that all the surface water delivered to a district is actually applied to the land units in its interior. Since intra-district seepage and surface applied water both recharge the underlying aquifer system, these seepage losses are implicitly accounted for by uniformly applying them to the land units as surface applied water.

Modeled channels are divided into segments, where each segment is defined as the stretch of channel between successive flow measurement locations. The channel segment is therefore the scale of resolution in the SWS model. Each segment has associated inflows and outflows, and is subject to other potential reductions in surface water storage due to evaporation, seepage, and off-stream intentional recharge. The inflows consist of inflow from the upstream segment, diversions from source channels, or diversions from other diversion channels. Outflows consist of outflow into the downstream segment, diversions into other diversion channels, or deliveries to districts.

Inflow and outflow data may not be available at all of the measurement locations defining the segments. Most diversion channels only possess measured inflow data from the source channels supplying them. We assume that these channels terminate either at the district border or within its interior. Since measured outflow data is not available for them, a surface water balance cannot be computed and conveyance losses are estimated as a fixed percentage of the known inflows. Only the Tule River, Deer Creek, and White River are divided into more than one segment.

8.2 Inter-District Channel Network Surface Water Balance

For each segment, we solve the surface water balance using

$$L_{s(i)} = Q_{in(i)} + \sum_{k=1}^{p} \sum_{l-1}^{m(k)} D_{vi(i,l,k)} - Q_{out(i)} - \sum_{l=1}^{n} D_{vo(i.l)} - \sum_{k=1}^{p} \sum_{l=1}^{m(k)} D_{d(i,l,l)} \qquad (1)$$

where L_s is the total segment conveyance loss due to evaporation, seepage, and off-stream intentional recharge during the i-th month (L^3), Q_{in} is the segment upstream inflow (L^3), D_{vi} is a diversion into the segment (L^3), D_{vo} is a diversion out of the segment (L^3), Q_{out} is the segment downstream outflow (L^3), D_d is a delivery out of the segment (L^3), p is the number of districts in the basin, $m(k)$ is the number of diversions into the segment for the k-th district, and n is the total number of diversions out of the segment.

As mentioned previously, the diversions, D_{vi} and D_{vo}, rather than the actual deliveries, D_d, are usually reported by the districts. By assuming that a fixed percentage of D_{vi} is removed due to conveyance losses and intentional recharge between the point of diversion and the point of delivery, we estimate D_d using

$$D_{d(i,l,k)} = D_{vi(i,l,k)} - (\alpha_{(k)} + \beta_{(k)} + \gamma_{(k)}) \cdot D_{vi(i,l,k)}, \quad \alpha_{(k)} + \beta_{(k)} + \gamma_{(k)} \leq 1 \qquad (2)$$

where α is the fractional reduction of D_v due to evaporation, β is the fractional reduction due to seepage, and γ is the fractional reduction due to intentional recharge. The delivery is computed in (2) for the last segment in each channel from which the delivery is taken by the receiving district. For each modeled channel segment, we assume that 95% of the total conveyance loss is due to seepage and 5% to evaporation. Initial values of α, β, and γ for each district are given in Table 11. Substituting (2) into (1) we obtain

$$L_{s(i)} = Q_{in(i)} + \sum_{k=1}^{p} \sum_{l=1}^{m(k)} D_{vi(i,l,k)} - Q_{out(i)} - \sum_{l=1}^{n} D_{vo(i)}$$
$$- \sum_{k=1}^{p} \sum_{l=1}^{m(k)} \left[D_{vi(i,l,k)} - (\alpha_{(k)} + \beta_{(k)} + \gamma_{(k)}) \cdot D_{vi(i,l,k)} \right] \quad (3)$$

In (1), we assumed that groundwater flow into each channel is negligible. Consequently, to achieve a surface water balance over the segment $L_{s(i)}$ must Satisfy

$$L_{s(i)} \geq 0 \quad (4)$$

If $L_{s(i)} < 0$, then the total delivery in (3) is overestimated and must be reduced by increasing α or β or γ in (2) until (4) is satisfied. The monthly seepage loss, $Q_{c(i,l)}$, (L^3) is computed using

$$Q_{c(i)} = \sum_{k=1}^{p} \sum_{l=1}^{m(k)} (\beta_{(k)} + \gamma_{(k)}) \cdot D_{vi(i,l,k)} \quad (5)$$

and becomes input into the groundwater flow model as direct recharge from the channel segment to the unconfined aquifer.

8.3 Intra-District Distribution System Evaporative Loss

Surface water deliveries estimated by (2) are received by district distribution channels at their borders or within their interior. Additional conveyance losses occur within each district as the delivered surface water traverses the intradistrict distribution channels in transit to the individual land units. The difference between the district delivery and this conveyance loss is the applied surface water. Within each district, we don't regard channel seepage as a conveyance loss since it recharges the aquifer underlying the district and is theoretically available as a future source of irrigation water. However, evaporation is a loss and is accounted for by assuming that a fixed percentage of the delivery is evaporated using

$$S_{d(i,k)} = \sum_{l=1}^{m} (1 - \alpha_{d(k)}) \cdot D_{d(i,l,k)} \quad (6)$$

where S_d is the applied surface water to the *k*-th district during the *i*-th month (L^3) and α_d is the fractional reduction of D_d due to evaporation (Table 11). The monthly applied surface water to each district, $S_{d(i,k)}$, becomes input into the UZWB model which calculates its allocation to individual land units.

8.4 Model Results

8.4.1 Imported Surface Water and Unregulated Natural Runoff

The total imported surface water from the FKC from 1970-99 is 13,329,262 af (USBR, 1970-99). Annual FKC diversions varied from 125,970 af in 1977 to 679,298 af in 1993 (Figure 22) with a 30-year annual average of 444,309 af. The Tule River and Pioneer Ditch both receive regulated releases from Success Reservoir. The total imported surface water from the Tule River and Pioneer Ditch from 1970-99 are 4,502,153 and 151,348 af, respectively (TRA, 1970-99). Tule River annual imports varied from 11,034 af in 1977 to 607,154 af in 1983 (Figure 23). Pioneer Ditch annual imports varied from 3445 af in 1973 to 5874 af in 1990 (Figure 24). The SWP and the Kings River imported the smaller amounts of 88,625 and 7332 af, respectively, over the base period.

Unregulated natural runoff occurs in the Deer Creek, White River, Frazier Creek, and Lewis Creek. The total natural runoff from the Deer Creek and White River from 1970-99 are 703,444 and 219,098 af, respectively (USGS, 1970-99). Deer Creek runoff varied from 4082 af in 1992 to 103,716 af in 1983 (Figure 25). White River runoff varied from 422 af in 1977 to 37,985 af in 1998 (Figure 26). Unfortunately, monthly runoff in Frazier Creek and Lewis Creek are not gauged. Only a single flow measurement was available for each creek per annum. This measurement represented the maximum flow rate (in cubic feet per second) of the entire year and the date in which it occurred. It was impossible to estimate a monthly time series of channel flows for each year based on a single yearly maximum flow measurement. Consequently, we were forced to ignore the flows in the Lewis and Frazier Creeks and assume they were zero.

8.4.2 Exported Surface Water and Unregulated Natural Runoff

During months of heavy runoff, withdrawals from the Tule River into the Friant-Kern Canal are performed on behalf of the Downstream Kaweah & Tule Rivers Association to avoid discharge into and flooding of the normally empty Tulare Lake bed. Total annual diversions of 84851, 36447, and 95424 af of Tule River runoff were diverted during 1983, 1997, and 1998, respectively, for this purpose.

8.4.2 Applied Water from District Surface Water Deliveries

The annual total applied water from district surface water deliveries for the fiscal water years of 1970-99 are presented in Figure 27. From 1970 to 1999, a total of 15 million acre-feet of surface water was applied by the service districts in the study area. The applied surface water varied from a low of 135,482 acre-feet in 1977 to a high of 708,293 acre-feet in 1996. The percentage of the total applied surface water apportioned to each district from 1970-99 is given in Figure 28. The LTRID and DEID together account for 59% of the total applied surface water while occupying approximately 40% of the incorporated area in the study area.

8.4.3 Inter-District Network Conveyance Losses

The annual inter-district surface water conveyance network seepage and evaporation losses for the fiscal water years of 1970-99 are presented in Figures 29 and 30, respectively. Whether estimated by mass balance or as a fixed-percentage of flows, the total conveyance losses for all channels are apportioned as 95% for seepage and 5% for evaporation. Over the 30-year base period, an estimated total of 3.5 million acre-feet of seepage occurred for all surface water channels. Seepage in the Tule River, Deer Creek, and White River accounted for 85% of the total seepage. Total annual seepage varied from a low of 8,128 acre-feet in 1977 to 467,084 acre-feet in 1983. The estimated seepage in 1983 is substantial. It may be possible that flood control flows exited the western boundary of the study area that year, especially from the Tule River. However, no data is available to estimate these outflows from the study area. Therefore, we maintain the assumption that flows terminate within the study area and the associated seepage losses occur within its boundaries. Additional seepage no doubt occurs within Lewis Creek and Frazier Creek. However, insufficient flow data prevented the estimation of monthly channel seepage and evaporation losses from these creeks.

9 Unsaturated Zone Water Budget Model

The unsaturated zone water budget (UZWB) model is the second of the three sub-models in the conjunctive use model. Its purpose is to calculate monthly water storage changes in the soil root zone and deep vadose zone of each land unit (Figure 31), where the land unit is the UZWB model scale of resolution. It also models the intra-district surface water distribution system by estimating the monthly allocation of surface water to individual land units within each district. The main model outputs are the recharge to the unconfined aquifer from surface applied water and precipitation, and the groundwater pumping demand from the unconfined and confined aquifers. The recharge and groundwater pumping rates become input for the groundwater flow model. The UZWB model is solved numerically by a FORTRAN code.

9.1 Soil Root Zone Water Budget

The soil root zone of each land unit is bounded above by the atmosphere and below by the deep vadose zone (Figure 31). For vegetative land uses, the soil root zone storage change in the *j*-th land unit during the *i*-th month is computed by

$$\Delta D_{s(i,j)} = P_{(i,j)} + S_{w(i,j)} + G_{w(i,j)} - ET_{a(i,j)} - q_{v(i,j)} \tag{7}$$

where D_s is the depth of soil root zone water (L), P is atmospheric precipitation (L), S_w is surface applied surface water (L), G_w is the surface applied pumped groundwater (L), ET_a is evapotranspiration (L), and q_v is the depth of water percolating from the soil root zone into the deep vadose zone (L). The inputs into the soil root zone are precipitation, surface applied surface water, and surface applied pumped groundwater; and the outputs are evapotranspiration into the atmosphere and percolation into the deep vadose zone (Figure 31). In the UZWB model, we assume that no lateral flow occurs between the soil root zones of adjacent land units.

For urban land uses, the monthly soil root zone storage change of each land unit is

$$\Delta D_{s(i,j)} = P_{(i,j)} + S_{w(i,j)} + G_{w(i,j)} - M_{(i,j)} - q_{v(i,j)} \quad (8)$$

where M is the urban water demand (L). The inputs and outputs for (8) are the same as in (7) except that the water demands of the urban land units, M, are calculated differently than ET_a.

Soil root zone storage changes are computed by estimating the components on the right-hand sides of (7) and (8). The methodologies used for this are described below for the different land uses.

9.1.1 Crop Water Needs

In this study, unless specified otherwise, we refer to any vegetative land use as a 'crop'. Two concepts are used for calculating the water needs of a cropped land unit: 1) crop evapotranspiration, and 2) the theoretical applied water demand. Crop evapotranspiration is defined as the cumulative amount of water transpired by the crop, retained in its plant tissue, and evaporated from adjacent soil surfaces during its growing season. The evapotranspiration is given by

$$ET_{a(i,j)} = k^{*}_{c(i,j)} \cdot ET_{o(i)} \quad (9)$$

where ET_o is the evapotranspiration of a reference crop (L) (Figure 33) and k_c^* is the modified crop coefficient given by

$$k^{*}_{c(i,j)} = k_{c(i,j)} \cdot d_l \quad (10)$$

where k_c is the crop coefficient and d_l is an adjustment factor for the l-th year. The adjustment factor accounts for annual changes in land-use acreage in the study area and is described later.

The theoretical applied water demand, w^*, (L) accounts for the soil root zone moisture content available for crop uptake and for inefficiencies in the irrigation application methodology

$$w^{*}_{(i,j)} = \left[\frac{ET_{a(i,j)} - D_{s(i,j)}}{WE_j} \right] \quad (11)$$

where WE is the water use efficiency (Tables 1-4).

In the model, not all crops receive surface applications sufficient to meet their theoretical applied water demand. The amount of (11) satisfied by surface water or pumped groundwater is a function of land use

$$w_{(i,j)} = w^*_{(i,j)} \cdot \lambda_j, \qquad \lambda_j = \begin{cases} 1, & u_j = 1-45 \\ 0.25, & u_j = 46-50 \\ 0, & u_j = 56, 60 \end{cases} \qquad (12)$$

where $w_{(i,j)}$ is the adjusted applied water demand (L) and u_j is the land use designation of the j-th land unit (Tables 1-3). In equation (12), crops used primarily for food and fiber (u_j = 1-45) receive 100% of their theoretical applied water demand. We assume that other agriculturally-related land uses (u_j = 46-50), such as dairies and pastures, satisfy only 25% of their demands with applied water. Native vegetation (u_j = 56) and non-irrigated cemeteries (u_j = 60) do not receive any irrigation water. Their evapotranspiration rates are equal to those of pasture, but cannot exceed available soil moisture contents. Their sole source of root zone soil moisture is precipitation.

9.1.2 Urban Water Needs

The applied water demands of urban municipal and industrial land units (u_j = 51, 52, 53, 59) are estimated using water influent and effluent data for the city of Porterville (Baker, 1999). The urban land-use categories are: 1) produce packing houses, 2) wastewater treatment plants, 3) developed urban areas, and 4) miscellaneous industrial land use (Table 3). In urban areas, surface water or groundwater is pumped into a distribution system as influent for municipal and industrial use, and water effluent is sent to the wastewater treatment facilities for treatment, recycling, or recharging. Although not all industrial land units are associated with an urban center, most of them are.

From 1995-99, the average net water use, m_P, (L^3) for the i-th calendar month in Porterville (Table 13) is

$$m_{P(i)} = m_{I(i)} - m_{E(i)}, \qquad i = 1,\ldots,12 \qquad (13)$$

where m_I is the monthly average total water influent (L^3) and m_E is the monthly average total water effluent used for recharge (L^3). The monthly average net water use per acre, M, (L) is computed by

$$M_{P(i)} = \frac{m_{P(i)}}{a_P}, \qquad i = 1,\ldots,12 \qquad (14)$$

where a_P is the acreage of Porterville (L^2) in 1995.

The applied water demand, w, is equated to the average net water use per acre

$$w_{(i,j)} = M_{P(i)} \qquad (15)$$

for u_j = 51, 52, 53, and 59 (Table 13).

For all municipal and industrial land units, we assume that none of the applied water demand in (15) is satisfied by soil moisture. Except for land units residing within the city of Lindsay, (15) is satisfied exclusively by pumped groundwater. We also assume a 100% water use efficiency for these land units, with no aquifer recharge resulting from the use of pumped groundwater. In effect, we are ignoring water that is pumped by municipalities only to be returned to the treatment plant for recharge back into the groundwater. Lindsay has an existing CVP water contract. Consequently, the possibility of aquifer recharge exists there due to the availability and application of excess surface water supplies in the UZWB model. For all other urban land units, the only source of potential diffuse recharge is from modeled excess precipitation.

9.1.3 Miscellaneous Water Needs

Miscellaneous land units classified as ”fallow land”, ”idle land”, ”livestock feedlots”, and ”unspecified urban” (Tables 2-4) possess negligible vegetation and are assigned an adjusted applied water demand of zero. As a result, they do not receive any applications of surface water or groundwater. These land units do, however, experience bare-soil evaporation. If their evapotranspiration rate is in excess of the soil moisture content, then it is equated to that soil moisture content. Also, the sole source of soil moisture is supplied by precipitation.

9.1.4 Precipitation

In the model, we assume that overland runoff and evaporation of precipitation are negligible and that 100% of the precipitation infiltrates into soil root zone. Overland runoff is neglected due to the relatively flat topography of much of the study area and evaporation is ignored due to the cool temperatures which prevail during much of the rainfall season. Any evaporation of precipitation from the ground surface which might occur is assumed to implicitly contribute to the evaporative component of crop evapotranspiration. The precipitation in the *i*-th month for the *j*-th land unit is

$$P_{e(i,j)} = P_{(j)} \cdot \frac{p_{o(i)}}{P_o} \qquad (16)$$

where $P_{(j)}$ is the average annual precipitation for the *j*-th land unit (*L*), $p_{o(i)}$ is the *i*-th monthly precipitation at the reference location (*L*), and P_o is the average annual precipitation at the reference location (*L*). The spatial distribution of $P_{(j)}$ is defined by an isohyet map (Plate 3). Values of average annual precipitation are assigned to each land unit by overlaying the isohyet map on the land use map in GIS (Figure 32).

9.1.5 Surface Water Allocation and Groundwater Pumping

Solving (12) and (15) for each land unit, the total adjusted applied water demand of the *k*-th district, $W_{(i,k)}$, (L^3) is then computed using

$$W_{(i,k)} = 0.95 \cdot \sum_{j=1}^{n(k)} w_{(i,j)} \cdot a_{(j)} \cdot \gamma_{(j)}, \qquad \gamma_{(j)} = \begin{cases} 0, & u_j = 51-53, 59 \; and \; k \neq 4 \\ 1, & otherwise \end{cases} \qquad (17)$$

where *a* is the land unit acreage (L^2) and *n*(*k*) is the number of land units in the *k*-th district (Table 5). Equation (17) sums the applied water demands of those land units which are eligible to receive surface water allocations. Notice that the right-hand side of (17) is multiplied by 0.95. This factor imposes a 5% reduction in the estimated applied water demand for each land unit. This reduction accounts for the areas of the land unit which may be occupied by roads, vacant areas, or any other land use which does not have an applied water demand. Not included in (17) are urban land units which rely solely on groundwater pumping.

If the total available surface water to the *k*-th district during the *i*-th month, $S_{d(i,k)}$, is greater than or equal to the total applied water demand $W_{(i,k)}$ then each land unit receives an allotment of surface water equal to its applied water demand, $w_{(i,j)}$. The remaining surplus surface water, $S_{d(i,k)}-W_{(i,k)}$, is distributed uniformly over the land units in the *k*-th district for which u_j=1,…,45 or for urban land units in the city of Lindsay using

$$s'_{(i,j)} = \frac{(S_{d(i,k)} - W_{(i,k)})}{A^*_{(k)}} \tag{18}$$

where $s'_{(i,j)}$ is the applied surplus surface water (L) and

$$A^*_{(k)} = \sum_{j=1}^{n(k)} a_{(j)} \cdot \gamma_{(j)}, \qquad \gamma_{(j)} = \begin{cases} 1, & u_j = \{1-45\} \; or \; \{51, 52, 53, or\; 59 \; and \; k=4\} \\ 0, & otherwise \end{cases} \tag{19}$$

is the total acreage of land units in the *k*-th district (L^2) eligible to receive 100% of the available surface water to them. The total allotted surface water for the *j*-th land unit is

$$S_{w(i,j)} = \begin{cases} s'_{(i,j)} + w_{(i,j)}, & 1 \le u_j \le 45 \\ w_{(i,j)}, & 46 \le u_j \le 50 \end{cases} \tag{20}$$

If the total available surface water is less than the total applied water demand (i.e. $S_{(i,k)} - W_{(i,k)} < 0$) then the fractional amount of the total applied water demand which will have to be satisfied by groundwater pumping is

$$c_{(i,k)} = \frac{(W_{(i,k)} - S_{d(i,k)})}{W_{(i,k)}} \tag{21}$$

The groundwater pumping demand for the *j*-th land unit becomes

$$G_{w(i,j)} = c_{(i,k)} \cdot w_{(i,j)} \tag{22}$$

and its allotment of surface water is

$$S_{w(i,j)} = (1 - c_{(i,k)}) \cdot w_{(i,j)} \tag{23}$$

9.1.6 Soil Root Zone Percolation

The depth of water percolating from the soil root zone to the deep vadose zone, q_v, (L) is calculated using a simple "tipping bucket" model given by

$$q_{v(i,j)} = D_{s(i-1,j)} + P_{e(i,j)} + w_{(i,j)} + s'_{(i,j)} - ET_{a(i,j)} - D_{f(j)} \quad (24)$$

where D_f is the depth of soil root zone water at field capacity (L) (Plate 5) given by

$$D_{f(j)} = f_{c(j)} \cdot b_s \quad (25)$$

where f_c is the soil root zone field capacity (Plate 5) and b_s is the soil root zone thickness (L). We assume that b_s is a constant of 3 feet for every land unit. Field capacities are assigned to each land unit by overlaying the soils survey GIS coverage on the land use coverage (Figure 32). Solution of (24) requires an initial estimate of the depth of soil root zone water which is given by

$$D_{s(0,j)} = 0.25 \cdot f_{c(j)} \cdot b_s \quad (26)$$

Substitution of (9), (16), (22), (23), and (24) into (7) yields the soil root zone storage change during the i-th month in the j-th cropped land unit. Substitution of (14) into (8) yields the corresponding storage change for urban land units.

9.2 Deep Vadose Zone Water Budget

The deep vadose zone is directly underneath the soil root zone and directly above the water table in the unconfined aquifer. Input into the deep vadose zone is simply the percolation from the soil root zone and its output is recharge into the underlying unconfined aquifer. Similarly to the soil root zone, we assume that no lateral flow occurs between the deep vadose zones of adjacent land units. Recharge into the unconfined aquifer from the deep vadose zone, q_a, is calculated using a simplified form of the one-dimensional unsaturated flow equation

$$q_{a(i,j)} = K_s \cdot \left[\frac{D_{v(i-1,j)}}{\phi_e \cdot b_v} \right]^d \quad (27)$$

where K_s is the vadose zone saturated hydraulic conductivity (LT^{-1}), $D_{v(i,j)}$ is the vadose zone moisture content (L), ϕ_e is the vadose zone effective porosity, b_v is the vadose zone thickness (L), and d is a scaling factor. We assume a constant K_s = 5 ft/day and b_v = 100 feet for each land unit. Equation (27) assumes that flow during any given month is steady and is driven by gravity drainage. For the first time step, the solution of (27) requires an estimate of the initial vadose zone moisture content which is given by solving (27) for $D_{v(0,j)}$ as

$$D_{v(0,j)} = \phi_e \cdot b_v \cdot \left[\frac{q^*_{v(j)}}{K_s} \right]^{d^{-1}} \quad (28)$$

where $q^*_{v(j)}$ is the average percolation from the soil root zone over n months given by

$$q^*_{v(j)} = \frac{1}{n} \sum_{i=1}^{n} q_{v(i,j)} \quad (29)$$

We are able to solve (29) independently of (27) since we assume no upward flow of vadose zone moisture into the soil root zone. The deep vadose zone moisture content is then updated for the next time step using

$$D_{v(i,j)} = D_{v(i-1,j)} + q_{v(i,j)} - q_{a(i,j)} \quad (30)$$

Finally, the change in deep vadose zone moisture content ΔD_v is computed by

$$\Delta D_{v(i,j)} = D_{v(i,j)} - D_{v(i-1,j)} \quad (31)$$

9.3 Sub-basin Scale Net Aquifer Recharge

The net aquifer recharge for the entire study area is computed by aggregating the aquifer recharge and groundwater pumping of each land unit to the sub-basin scale and adding the contribution to aquifer recharge from channel seepage. The monthly total net recharge in the study area, Q^T, is given by

$$Q^T_{(i)} = q^T_{s(i)} + \sum_{j=1}^{n} [q_{a(i,j)} - G_{w(i,j)}] \quad (32)$$

where q^T_s is the total seepage from all channels and n is the total number of land units.

9.4 Crop Evapotranspiration and Changes in Land Use

As mentioned previously, 72% of the land is under agricultural production and 12 crop types account for nearly 95% of this area. The ET_a of these 12 crops largely determine the surface water and groundwater pumping needs in the study area. Different sets of reported crop coefficients for crops grown in the San Joaquin Valley will result in different estimates of monthly and annual crop ET_a in (9). It's important, therefore, to choose a set of crop coefficients which produce representative values of crop ET_a for the major crops grown. Seasonal and annual changes in land use also impact regional crop ET_a demands. In our model, a single land use survey was used to assign land use to each land unit. However, annual land use changes during 1970-99 for the 12 major crops in

Tulare County were significant. In the UZWB model, county land use records were obtained from Tulare County Agricultural Commissioners Reports and used to develop an annual crop coefficient adjustment factor to account for annual changes in land use acreage for the county. The monthly crop ET_a in (9) is adjusted by application of the adjustment factor in (10). The selection of the crop coefficients for the 12 major crops and the development of the adjustment factors for annual land use changes are described below.

9.4.1 Crop Coefficients

A number of resources were available from which to choose monthly crop coefficients for the 12 major crops. Experimentally-derived values or ranges of values of annual ET_a a for these crops in the region were obtained from publications and through personal communications with agricultural industry professionals (Table 14). Crop coefficients were chosen from these resources and in some cases adjusted such that the computed average annual ET_a for each crop from 1970-99 was similar to its derived value or within the range of the values given in Table 14. The chosen monthly crop coefficients for all crops are given in Tables 15-17. Monthly crop coefficients for citrus, cotton, field corn, alfalfa, and vineyards were adapted from Letey and Vaux (1984). Crop coefficients for olives, plums, almonds, walnuts, pistachios, and grain & grass hay were adapted from Goldhammer and Snyder (1989). Grain & corn refers to the double cropping of silage corn and winter grain. In the model, we assume that winter grain has a growing season from November through March. Silage corn is then planted in April and harvested at the end of August. The crop coefficients for silage corn are the same as field corn (Letey and Vaux, 1984). The crop coefficients for winter grain are from Goldhammer and Snyder (1989). All other crop coefficients were obtained from Naugle (2001). The estimated range of ET_a and average annual ET_a of the 12 major crops from 1970-99 are presented in Table 14.

9.4.2 Adjustment Factor for Annual Land Use Changes

The total acreage of each of the 12 major crops in Tulare County from 1970-99 are presented in Table 18. We assume that the land use changes in the study area are proportionally the same as those of Tulare County.

The monthly ET_a in (9) is modified for annual changes in land use for the 12 crops by multiplying the crop coefficients in (10) by an annual adjustment factor d_l. For each year from 1970-99, the total acreage of each crop in Table 18 is multiplied by the representative value of its average annual ET_a to produce a rough estimate of the total ET_a demands of the crop for the entire county. For each year, the estimated total ET_a demands of these crops are summed to produce a total annual ET_a demand for the county. Since the land use survey used in this study is for 1985, the total ET_a demands of each year are divided by the total ET_a demand of 1985. The resultant ratios are the values of d_l in (10) and are plotted in Figure 34.

9.5 Water-Table Fluctuation Method

The monthly net recharge computed in (32) can be summed to produce a cumulative annual net recharge from 1970 to each fiscal water year from 1971-99. The water balance computed for the entire study area neglects horizontal groundwater inflows and outflows through its vertical boundaries. Groundwater fluxes undoubtedly exist along these boundaries. However, these fluxes are assumed small in comparison to the total changes in storage due to vertical stresses applied to the entire study area (e.g. groundwater pumping, evapotranspiration, applied surface water, channel seepage). Horizontal groundwater flow on the inter-land unit and inter-district scales is expected to be more significant. For computing a total water balance, however, we make the simplifying assumption that the study area behaves as a relatively closed system where the net horizontal groundwater inflows through its vertical boundaries are small. Invoking this assumption, we then use the cumulative net recharge as an estimate of the cumulative groundwater storage change in the aquifer system. Ideally, verification of these estimates is performed by comparing them with an objective measure of the study area aquifer storage changes. However, changes in groundwater storage are not directly observable and must always be estimated using non-direct measures. As such, an objective measure for verification does not exist. As an alternative, we compare the water balance model results with those produced by the water-table fluctuation (WTF) method (Healy and Cook, 2002). The WTF method is used to compute the cumulative annual groundwater storage changes in the unconfined aquifer from 1970-99 using annually-measured hydraulic heads from production wells and point estimates of specific yield. To do this, a grid of uniformly-sized cells was superimposed on a GIS coverage of the study area. Each grid cell had a length of Δx in the x-direction (L) and Δy in the y-direction (L), where $\Delta x = \Delta y = 3280$ feet. Scattered point estimates of specific yield were then interpolated to the grid cells. A set of spatially distributed hydraulic head measurements from the production wells for each year were also interpolated to the grid. The cumulative groundwater storage change in ij-th cell from 1970 to the year l was estimated using

$$\Delta s_{ij}^{l} = (h_{ij}^{l} - h_{ij}^{1970}) \cdot S_{yij} \cdot \Delta x \cdot \Delta y, \qquad l = 1971,\ldots,1999 \tag{33}$$

where h^{1970}_{ij} is the spring-measured hydraulic head of 1970, h^{l}_{ij} is the hydraulic head of the year l, and S_{yij} is the unconfined aquifer specific yield (Plate 22). The cumulative storage change in the unconfined aquifer from 1970 to the year l is

$$\Delta S^{l} = \sum_{i=1}^{n_x} \sum_{j=1}^{n_y} \Delta s_{ij}^{l} \tag{34}$$

where n_x is the number of grid cells in the x-direction and n_y is the number of cells in the y-direction.

The hydraulic heads used in the WTF method are the spring measurements collected annually by CDWR in local production wells (Plate 14). Spring water levels are assumed to be negligibly influenced by localized drawdown due to pumping near or in the measured well. For specific yield, a relationship between texture and S_y was developed from a well log analysis in the study area by the USGS (Davis et al., 1959) (Table 19). The CDWR updated this well log

analysis by incorporating logs from wells drilled after the original USGS study and applied the texture-specific yield relationship to estimate a S_y for each quarter township-range over much of the San Joaquin Valley. For each quarter township-range, a relative percentage of each texture was determined from the well log analysis. The estimated S_y for each quarter township-range is the average of the specific yields of each texture, weighted by the relative percentages of each texture. The S_y estimates are assumed to characterize a depth of 300 feet below ground surface, a representative thickness of the well logs.
The WTF method neglects storage changes in the confined aquifer. This simplification is justifiable since the confined aquifer storage coefficient is several orders of magnitude smaller than the unconfined aquifer specific yield. Consequently, even if potentiometric water level changes in the confined aquifer significantly exceeded those in the unconfined aquifer, the effective confined water storage change would only be a small fraction of the unconfined storage change.

9.6 Model Results

9.6.1 Study Area Water Balance

A monthly water balance for the soil root zone and deep vadose zone was computed on a land unit scale by solving for the components in (7), (8), and (27). These components were then aggregated from the land unit scale to the subbasin scale to produce a water balance for the entire study area. The main components of the study area annual water balance from 1970-99 are displayed in Figure 35. The total annual agricultural and urban consumptive use ranged from 872,100 acre-feet (af) in 1970 to 1,250,700 af in 1999. The upward trend in consumptive use is due to a steady increase in acreage of land put into agricultural production during the base period; whereas annual fluctuations are due to yearly variations in seasonal climate (i.e. yearly variations in monthly ET_o). The estimated total pumping ranged from 143,100 af in 1978 to 560,600 af in 1990. As expected, pumping was heaviest during the droughts of 1975-77 and 1987-92, and lightest during the wet years of 1973, 1978, 1982-83, 1995, and 1998. Precipitation totals varied from 176,500 af in 1990 to 967,400 af in 1998.

Diffuse recharge from surface applied water and precipitation ranged from 110,000 af in 1992 to 270,100 af in 1983. The annual total diffuse recharge is also plotted against the annual total localized recharge from channel seepage in Figure 36. Over the base period, 5.75 million af (i.e. 62% of the total recharge) and 3.5 million af (i.e. 38% of the total recharge) of diffuse recharge and localized recharge, respectively, occurred in the entire study area. The average annual diffuse recharge and localized recharge were 191,616 af and 116,706 af, respectively. Only during years of heavy precipitation (1978, 1983, 1993, 1995, 1997, 1998) is localized recharge from channel seepage typically greater than the diffuse recharge.

The average water balance components for each calendar month over the base period for the study area are presented in Figure 37. This plot demonstrates the average temporal variation of each component. As expected, the precipitation is greatest during the winter and early spring months while surface water applications and groundwater pumping are greatest during the summer months when evapotranspiration demands are high. In Figure 37, the plotted recharge is actually the percolation from the soil root zone into the deep vadose zone rather than the recharge flux at the water table boundary. The diffuse recharge to the water table on a monthly time step is fairly uniform due to the buffering capacity of the deep vadose zone. By contrast, the percolation from the soil root zone to the deep vadose fluctuates more and its peak tends to lag behind that of the precipitation curve (Figure 37).

9.6.2 Study Area Groundwater Storage Changes

The cumulative annual groundwater storage changes from 1970-99 computed from the water balance and the WTF method are plotted in Figure 38. The trends in storage change produced by the two models are quite similar. The minimum and maximum differences between them are 28,479 acre-feet (1996) and 1,027,693 acre-feet (1991), respectively. From 1970, the maximum amount of groundwater accumulation occurred in the spring of 1987 with the WTF method and the water balance estimating positive storage changes of 1,146,286 and 907,155 acre-feet, respectively. The maximum groundwater overdraft occurred in 1993 with the WTF method estimating a negative storage change of 1,610,210 af while the water balance method maximum overdraft was 992,906 af in 1995. The 1987 and 1993 fiscal water years marked the beginning and ending of a major 6-year drought in California, respectively.

The WTF method calculates storage changes using water levels measured in the unconfined aquifer. In the UZWB model, pumping in the western half of study area is proportioned between the unconfined aquifer overlying the Corcoran Clay aquitard and the confined aquifer below (Figure 10). The proportions of pumping in each aquifer were determined by analysis of production well screen locations. From the UZWB model, pumping from the confined aquifer annually accounts for 7.1-12.5% of the total pumping in the study area from 1970-99. Since the long-term storage changes in the confined aquifer are negligibly small compared to those in the overlying unconfined aquifer, the confined aquifer, to balance its production, must receive recharge from the unconfined aquifer either as vertical leakage through the Corcoran Clay or as deep lateral transfer from the unconfined aquifer to the east.

9.6.3 Spatial Distribution of Groundwater Pumping

As mentioned previously, groundwater pumping at the land unit scale is estimated in the water balance as a closure term. Plots displaying the spatial distributions of total groundwater pumping at this scale for 1977 (dry year), 1980 (normal year), and 1983 (wet year) are displayed in Plates 23-25, respectively. These figures illustrate the land unit pumping demands as a function of both land use and service district for years of below-average, average, and above-average surface water supplies. Districts with substantial surface water supplies (e.g. LTRID, DEID) are required to augment their crop water demands with pumping mainly in drought years. However, districts with smaller surface water supplies (e.g. Pixley ID) annually rely on pumping to meet their irrigation demands. The average annual groundwater pumping over the base period is displayed in Plate 26. On average, districts with poor surface water supplies (e.g. Pixley ID, AID) pump between 1-3 feet of groundwater annually whereas districts with substantial supplies pump less than 1 foot. For districts with small surface water supplies and where crops with high water demands are grown (e.g. alfalfa), the annual pumping demand may be 4 feet or more in some land units.

9.6.4 Spatial Distribution of Diffuse Recharge

The spatial distributions of diffuse recharge are plotted for 1977, 1980, and 1983 in Plates 27-29, respectively. As with groundwater pumping, the distribution of diffuse recharge is illustrated here for years of below-average, average, and above-average surface water supplies. Generally, the diffuse recharge distribution is the negative image of the groundwater pumping distribution. During 1977, for example, most districts experienced less than 0.5 feet of diffuse recharge. In average-to-wet years, districts such as LSID, LTRID, DEID, PID, and SID experience at least 1-2 feet of diffuse recharge in contrast to other districts with smaller surface water supplies (e.g. Pixley ID) which still experience less than 0.5 feet. The higher recharge results from the additional availability of surface water, above the applied water demand. In groundwater dependent areas, pumping is (presumably) limited to meeting applied water demand (plus a leaching requirement) during the growing season. The average annual diffuse recharge rate over the base period is displayed in Plate 30 and also reflects differences in surface water supplies between districts. In addition to surface water supplies, the diffuse recharge distribution is also dependent on the spatial distribution of precipitation as defined by the isohyet map (Plate 3).

9.6.5 Service District Water Balances

The average water balance components for each calendar month over the base period for DEID, LID, LSID, LTRID, Pixley ID, PID, and SID are presented in Figures 42-48. The average monthly water balance for all the unincorporated areas is also displayed in Figure 49. These plots demonstrate the average temporal variability in the water balance components for these districts and the unincorporated areas. Generally, the groundwater pumping and deep percolation variability between districts is due to differences in surface water supplies, crop types and cropping patterns, and precipitation - estimated as a function of the isohyet map (Plate 3). The differences in deep percolation rates between districts with relatively large surface water supplies (DEID, LTRID), small supplies (Pixley ID), and no supplies (the unincorporated areas) is highlighted in Figure 50. This plot illustrates the relatively higher percolation in DEID and LTRID due to excess surface water supplies for average-to-wet years. For most years, the only source of percolation in the Pixley ID is from irrigation inefficiencies (i.e. excess irrigation applications) and precipitation. For the unincorporated areas, percolation is strictly due to irrigation inefficiencies and precipitation. Pre-irrigation of annual crops (e.g. cotton, grain) is not explicitly accounted for in the model. District farmers may use a combination of surface water and groundwater to pre-irrigate their fields. In the UZWB model, we apply all monthly surface water deliveries to the irrigated crops within each district either to satisfy the applied water demand or as surplus. In this way, we may implicitly account for pre-irrigations sourced solely from surface water for districts with substantial surface water supplies. For example, LTRID and DEID receive surface water deliveries in February and March which significantly exceed their applied water demands (Figures 42 and 45). Combined with excess precipitation, this results in high amounts of deep percolation from the saturated soil root zone during the early spring.

We do not, however, implicitly account for pre-irrigations sourced from groundwater since pumping is estimated only as a function of applied water demands and not for pre-irrigation purposes. For districts with small surface water supplies and which rely heavily on pumping (e.g. Pixley ID), the crop water demands in the late winter and early spring exceed the soil moisture content that is derived mainly from precipitation (Figure 46). Consequently, deep percolation resulting from pre-irrigations sourced predominantly from pumped groundwater is not expressed in the results of the UZWB model.

The monthly variation in water balances between a district with a relatively large surface water supply (i.e. LSID) and the unincorporated areas which have no surface water supplies is illustrated for a dry year (1990) and a wet year (1998) in Figures 51 and 52. Deep percolation is negligible in the dry year for the unincorporated areas but does occur in the wet year due to excess precipitation. However, LSID and other districts with substantial supplies experience deep percolation in both wet and dry years.

10 Groundwater Flow Model

The groundwater flow model is the third of the three sub-models in the conjunctive use model (Figure 1). Its purpose is to calculate the hydraulic head and groundwater storage changes in the aquifer system subject to transient groundwater recharge and pumping stresses. The main model output is the simulated hydraulic head distribution in the modeled area for each stress period. A post-processing routine calculates the cumulative annual groundwater storage changes over each district. In this section, we describe the development and calibration of the numerical groundwater flow model.

10.1 Numerical Model Development

The numerical groundwater flow model was developed in MODFLOW(Modular Finite-Difference Ground-Water Flow Model) (McDonald and Harbaugh, 1988). A MODFLOW plug-in-extension (PIE), developed as an application for Argus Open Numerical Environments (ONE)™ (Argus Interware, 1997), functions as a graphical-user-interface for MODFLOW to define the numerical groundwater flow model based on the conceptual model of the aquifer system hydrogeology (Winston, 2000). The PIE generates a list of empty input parameters for each user-defined model layer in the conceptual model which require data specification. The PIE imports input parameter data into Argus ONE™ in scattered point data, spreadsheet, and GIS formats; generates the MODFLOW input files; runs the MODFLOW model; and imports model results into Argus ONE™ for post-processing and visualization. Argus ONE™ also contains functionality for exporting model data and results in a shapefile format compatible with other commercial GIS software.

10.1.1 Conceptual Model of the Aquifer System Hydrogeology

A conceptual model of the aquifer system hydrogeology in the east-west direction is given in Figure 10. In the western part of the study area, the system consists of three hydrogeologic units: 1) an unconfined aquifer, 2) an underlying aquitard (i.e. the Corcoran Clay Member of the Tulare Formation), and 3) a confined aquifer. In this region, the aquifer system bottom boundary is the contact between the unconsolidated continental deposits constituting the confined aquifer and the underlying consolidated Quaternary Period marine deposits. In the eastern part of the study area, the system is conceptualized as an unconfined aquifer overlying a thick semi-confined aquifer. The aquifer system bottom boundary there is defined as the contact between the unconsolidated continental deposits and the underlying consolidated Tertiary Period marine deposits. Along the eastern border, the bottom boundary is the contact between the continental deposits and the Sierra Nevada mountain range basement complex.

10.1.2 Model Domain

The domain of the groundwater flow model is displayed in Plate 31. The model domain excludes several areas along the eastern boundary. These areas are associated with the undulating foothills formed from the dissected uplands. The finite-difference grid resolution used is too coarse to capture the dramatic changes in ground surface elevation there. In preliminary runs including these areas, problems were encountered with cells going dry in the numerical solution of the groundwater flow model. Since most of these areas are not in agricultural production and the aquifer storage capacity there is not considered significant, they were excluded from the model domain and are inactive in the groundwater flow model.

The groundwater flow model domain also includes a portion of the Kaweah groundwater sub-basin residing adjacent to and along the length of the LTRID northern boundary. As discussed later, the groundwater flow model domain was extended into this region to better approximate the northern study area boundary condition in the vicinity of LTRID.

10.1.3 Vertical and Horizontal Discretization

The aquifer system hydrogeologic units are modeled by three MODFLOW layers (Figure 53). The unconfined aquifers in the western and eastern parts of the study area are modeled as an unconfined MODFLOW layer (model layer 1). The Corcoran Clay aquitard and the adjacent semi-confined aquifer to its east are modeled as a convertible confined/unconfined MODFLOW layer (model layer 2). The confined aquifer underlying the Corcoran Clay and the adjacent semiconfined aquifer to its east are also modeled as a convertible confined/unconfined MODFLOW layer (model layer 3).

GIS coverages of the top and bottom elevations of the Corcoran Clay aquitard (Plates 10 and 11) are imported into Argus ONE™ and used to assign different hydrogeologic properties to the western and eastern regions of layer 2. The top elevation coverage is used to distinguish the boundary between the unconfined aquifer and the underlying Corcoran Clay. The bottom elevation coverage is used to distinguish the boundary between the confined aquifer and the overlying Corcoran Clay.

The Corcoran Clay terminates near the middle of the study area where its depth is approximately 250 feet below the ground surface and its top boundary elevation is -45 feet (Figure 10 and Plate 10). To avoid a horizontal discontinuity in the top and bottom elevations of adjacent cells in layer 2 at the vertical contact between the Corcoran Clay and the semi-confined aquifer to the east, the top elevation of layer 2 east of this contact is specified also as -45 feet. The thickness of the Corcoran Clay near the middle of the study area is approximately 45 feet. Consequently, the bottom elevation of layer 2 east of the Corcoran Clay is defined as 45 feet below the top elevation of layer 2 with an elevation of -90 feet. The bottom elevation of the aquifer system was adapted from a contour map of the aquifer bottom used in a previous study (Erlewine, 1989) (Plate32). The thickness of the aquifer system is known to decrease significantly near the eastern boundary. The bottom elevation of layer 3 was defined using the contour map except near the extreme eastern boundary. For cells where the bottom elevation of layer 2 crosses the aquifer system bottom elevation defined by this contour map, the bottom of the aquifer system was redefined as 45 feet below the bottom elevation of layer 2. Although the aquifer system thickness decreases significantly in the vicinity of the eastern boundary (Figures 8 and 9), allowing the thickness of the aquifer system to diminish to near zero there posed numerous numerical problems with model cells drying out.

The MODFLOW model finite-difference grid of the domain is presented in Plate 33. The grid consists of 52 rows and 59 columns, where the cell spacing in the x and y directions are $\Delta x = \Delta y$ = 3280 feet. The x-axis of the finite-difference grid is aligned approximately with the east-west direction and the y-axis aligns with the north-south direction. The finite difference grid is rotated by -1o about the east-west axis to align itself with the western boundary defined by the Kings-Tulare county line.

10.1.4 Temporal Horizon and Discretization

The simulation period is 29 years and consists of 116 stress periods (Table 21). The first stress period is the April-March stress period of 1970 and the last is the December-January-February-March stress period ending in 1999. The numerical model is defined by a daily time unit. For each stress period, the layer aquifer recharge and groundwater pumping from the UZWB model and the channel seepage from the SWS model were divided by the total number of days in that stress period to produce average daily recharge, pumping, and seepage rates. Twenty time steps were used for the April-May and October-November stress periods and 40 time steps were used for the June-July-August-September and December-January-February-March stress periods.

10.1.5 Boundary Conditions

No-flow boundary conditions in the horizontal direction are assigned around the model domain perimeter for each model layer. The no-flow condition along the eastern boundary occurs at the contact between the agriculturally-developed foothill regions and the Sierra Nevada mountain granitic complex and between the alluvial plain and the agriculturally-undeveloped foothills. No-flow conditions were assigned along the northern and southern study area boundaries along an approximate groundwater flow divide, as determined by inspection of unconfined aquifer hydraulic head contour maps from 1970-99 (Plates 15-20) (CDWR, 1970-99). A no-flow condition was also assigned to the western boundary of the model domain, where it is assumed that the net horizontal flow between the hydrostratigraphic units comprising the Tulare Lake Bed geomorphic unit and those of the alluvial plain region is insignificant; particularly in comparison to vertical fluctuations in the unconfined aquifer water levels due to recharge, pumping, and channel seepage stresses.

The northern boundary of the model domain was extended to include an area of unincorporated agricultural land above LTRID (Plate 31). Originally, the northern boundary of the model domain coincided with the northern boundary of LTRID. However, it was determined by re-examination of the contour maps of hydraulic head that net groundwater fluxes exist from LTRID into the unincorporated lands just north of it. To account for the effects of pumping stresses in this area on simulated heads in LTRID in the model calibration, the northern boundary was extended to include this unincorporated zone.

10.1.6 Initial Conditions

The initial conditions for hydraulic head in the unconfined aquifer were derived from a set of production well measurements taken from the unconfined aquifer during early-January to early-March of 1970. These point values were imported into Argus ONE™ where they were interpolated to the cells of the finite-difference grid. The resulting gridded values became the initial hydraulic heads for model layers 1 and 2. Originally, a set of confined aquifer hydraulic head measurements over the same period in 1970 was used to derive the initial conditions for the confined aquifer underlying the Corcoran Clay in model layer 3. However, the quality of these hydraulic heads were questionable and the spatial distribution sparse. Consequently, the initial conditions for the confined aquifer were assigned those of the unconfined aquifer. The initial conditions assigned to the cells east of the Corcoran Clay in layer 3 were also the overlying gridded values of unconfined aquifer hydraulic heads used for layers 1 and 2. In the eastern part of the study area, if the initial hydraulic head falls below the bottom elevation of layer 1 for a particular cell, the bottom elevation of the cell is redefined as 30 feet below the initial head prior to simulation. Cells in which the initial head generally falls below this mark are located in the foothills along the eastern border where the ground surface elevation increases dramatically.

The resulting distribution of heads in the model layers represents the initial conditions for the April-May stress period in 1970. The initial hydraulic heads in the unconfined aquifer vary from 90 feet in the south-west corner of the study area to over 600 feet along the eastern boundary.

10.1.7 Hydraulic Properties

The hydraulic parameters defining each model layer are the horizontal hydraulic conductivity K_h (L/T), the hydraulic conductivity anisotropy ratio a_r, and the storage coefficient S. The storage coefficient for the unconfined aquifer is the specific yield S_y, and the storage coefficient for the confined aquifer is the product of the specific storativity S_s (L^{-1}), and the confined aquifer thickness b_c which varies spatially. The anisotropy ratio is defined as the ratio of the horizontal hydraulic conductivity to the vertical hydraulic conductivity, K_h/K_z. The horizontal hydraulic conductivity and layer anisotropy ratios are calibration parameters. Their estimated spatial distributions will be described later in the model calibration section. The spatial distribution of S_y after interpolation to the finite-difference grid in Argus ONE™ is presented in Plate 22. The spatial distribution of S_y varies from 5% in the heavy-textured Tulare Lake Bed and foothill regions to 15% in the coarse-textured regions of the LTRID and Pixley ID within the Tule River alluvial fan. The S_s for the Corcoran Clay region of layer 2 is $2.7\text{x}10^{-6}$ (feet^{-1}) and the S_s for layer 2 east of the Corcoran Clay and for layer 3 is $2.7\text{x}10^{-4}$ (feet^{-1}).

10.1.8 Aquifer Recharge and Groundwater Pumping

Two sources of aquifer recharge are inputted into the groundwater flow model: 1) localized recharge from channel seepage, and 2) diffuse recharge from surface applied water. Seepage per channel segment is estimated by the SWS model and imported into Argus ONE™ as a GIS coverage of line objects. An Argus ONE™ export template overlays the channel coverage onto the finite-difference grid (Figure 54) and the seepage is assigned to the grid cells over which the channel line objects intersect. The localized recharge from seepage is then applied to model layer 1 as diffuse recharge using the MODFLOW recharge package. Aquifer recharge from surface applied water and groundwater pumping per land unit were computed by the UZWB model. The pumping is partitioned among the three model layers of each land unit using the proportions displayed in Plates 34-36. These proportions were determined by analysis of screen interval depth and location of selected production wells. No pumping occurs in model layer 2 where the Corcorcan Clay is present. The net recharge for layer 1 is computed by subtracting the pumping for layer 1 from the recharge for layer 1. An Argus ONE™ export template overlays the net recharge and pumping coverage onto the finite-difference grid (Figure 54). The net recharge is assigned to the grid cells in layer 1 over which the land unit polygon objects intersect. The pumping is assigned to layers 2 and 3 in the same manner. The net recharge and pumping are then applied to layers 1, 2, and 3 as wells using the MODFLOW well package.

10.2 Model Calibration and Validation Implementation

An automated calibration of the groundwater flow model was performed using the PEST (Parameter ESTimation) model-independent parameter estimation software (Doherty, 1998). PEST estimates the model parameters using a nonlinear estimation algorithm known as the Gauss-Marquardt-Levenberg method. Three conceptual models describing the structure of the spatial distribution of the aquifer system hydraulic parameters were evaluated by PEST. These structures were used to define zones of equal parameter value in the calibration procedure. Amongst the candidate conceptual models, the structure which led to the best fit between the calibration targets and the modeled results was chosen to represent the spatial distribution of the hydraulic parameters in the groundwater flow model. The calibrated model was then validated for a similar historical period. Here we describe the calibration and validation procedures and results.

10.2.1 Calibration Parameters

The calibration parameters are the spatial distributions of K_h in the unconfined aquifer, the Corcoran Clay aquitard, and the confined aquifer, and a single *a*r for each of the three model layers.

10.2.2 Conceptual Models of K_h Spatial Structure

We considered three different conceptual models of K_h spatial structure: 1) K_h as an exponential function of the *S*y distribution (Plate 22), 2) K_h as a linear function of the saturated hydraulic conductivity of the soil survey mapping units (Plate 6), and 3) division of the model domain into square zones of uniform size (Plate 37). For each conceptual model, we assume that the spatial distributions of K_h east of the Corcoran Clay in model layers 2 and 3 are equal to the calibrated distribution in layer 1 above them. In the first model, the K_h structure is an exponential function of the *S*y distribution given by

$$\log K_h = a + b \cdot S_y \qquad (35)$$

where *a* and *b* are calibration parameters. In the second model, the K_h structure is a linear function of the *K*s distribution given by

$$K_h = c + d \cdot K_s \qquad (36)$$

where *c* and *d* are calibration parameters. In the third model we simply divide the model domain into a uniform grid of square zones and calibrated a K_h for each zone (Plate 37). For the first and second models, we assume that the Corcoran Clay aquitard and the confined aquifer are homogeneous units, thereby estimating single K_h values for each. In the third model, the uniform zonation for model layer 1 is the same for model layers 2 and 3 where the Corcoran Clay and confined aquifer are present.

The first and second conceptual models represent an attempt to estimate the spatial distribution of K_h based on an actual geologic or textural structure derived from previous investigations. The third model represents a brute-force attempt to calibrate the groundwater flow model by allowing PEST to estimate a spatial distribution of K_h based on an arbitrary structure.

10.2.3 Calibration and Validation Periods

The calibration period was 15 years and consisted of 60 stress periods. It began in the April-May stress period of 1970 and ended after the December-January-February-March stress period in 1985. The calibration period encompassed several distinct hydrologic cycles: drought conditions during 1974-77 and 1979-81 and heavy precipitation in 1973, 1978, and 1983 (Figure 2). The validation period was 14 years and consisted of 56 stress periods. It began in the April-May stress period of 1985 and ended after the December-January-February-March stress period in 1999. Like the calibration period, it also encompassed several distinct hydrologic cycles: a sustained drought during 1987-92 and a wet period from 1995-98 (Figure 2).

10.2.4 Calibration Targets

For the calibration, two sets of weighted targets were used. The first set consisted of a distribution of hydraulic head values for the years 1978, 1981, and 1984, derived from spring-measured production well observations for the same years. These years were chosen to represent aquifer system storage changes under three different hydrologic conditions: 1) the spring-measured hydraulic heads in 1978 followed an extremely dry 1977, 2) 1981 followed the average year 1980, and 3) 1984 followed the above-average wet year 1983. The production well locations are displayed in Figure 38. Although these wells are spatially distributed throughout the study area, preliminary calibration runs indicated that dense clusters of observed heads in particular areas (e.g. LID) resulted in greater sensitivity to estimated K_h than in other areas. In addition, other clusters of observed heads (e.g. in the foothills along the eastern boundary) contributed significantly to the calibration objective function but were insensitive to changes in estimated K_h. We performed a pseudo de-clustering of the observed hydraulic heads by interpolating their values to the cells of the finite-difference grid in Argus ONE™. We also excluded from the distribution of calibration targets, measurements from production wells along the eastern foothills and in the region intersecting the Tulare Lake Bed geomorphic unit (Plate 38). The declustering operation and the exclusion of these areas had the effect of assigning an equal weight to the interpolated hydraulic head targets in the region of the study area where the quality of the measured heads were considered the highest and the changes in hydraulic head were the most sensitive to the estimated K_h distribution. The resulting distribution of hydraulic head targets are displayed in Plate 39.

The second set of calibration targets consisted of the individual cumulative annual groundwater storage changes in the unconfined aquifer from 1971-85 for DEID, LID, LSID, LTRID, Pixley ID, PID, and SID. These storage changes were estimated by applying the WTF method to each district individually. These districts were chosen because of their large sizes, substantial groundwater storage capacities, and the availability of quality hydraulic head measurements within their boundaries. The cumulative annual storage changes for each district are given in inches of water. The storage change targets for each district were weighted by the number of finite-difference cells (i.e. declustered hydraulic head targets) residing within the district (Plate 39). The choice of declustered hydraulic heads and annual storage changes as calibration targets was made to constrain the spatial distribution of calibrated hydraulic heads and to provide meaningful estimates of groundwater storage changes in the largest districts in the study area.

Model fit was assessed by spatial and temporal analysis of the hydraulic head residuals, *r*, (*L*) computed as

$$r = H - h \tag{37}$$

where *H* is the target head (*L*) and *h* is the modeled head (*L*). The observed regional difference in unconfined aquifer hydraulic head from the eastern to the western model domain boundary is approximately 350 feet. The modeled heads were considered acceptable if their residuals were within 20 feet (i.e. 6% of the regional hydraulic head difference) of the target heads and displayed no significant spatial correlations.

The calibrated cumulative annual storage changes of each district were computed by the MODFLOW utility ZONEBUDGET (Harbaugh, 1990). The modeled storage changes were considered acceptable if their temporal pattern approximated that of the target storage changes. No quantifiable criterion was used to assess the closeness of the modeled and target storage changes. The reasonableness of the fit was qualitatively assessed by visual inspection.

10.2.5 Parameter Composite Sensitivities

For each calibration optimization run, PEST computes a *m*x*n* Jacobian matrix **J** of the model-calculated ”observations” (i.e. derivative of the *i*-th observation with respect to the *j*-th parameter) where *m* is the number of observations and *n* is the number of adjustable parameters. The sensitivity of the *j*-th parameter, s_j, is

$$s_j = (\mathbf{J}^t \mathbf{Q} \mathbf{J})_{jj}^{1/2} \tag{38}$$

where **Q** is the cofactor matrix, a diagonal matrix whose elements are the squared weights of the observations. The computed sensitivities provide a composite measure of the relative sensitivity of each parameter to all of the weighted model-calculated ”observations” (i.e. hydraulic heads, district storage changes). The composite sensitivities were used during preliminary calibration runs to determine which zones to remain adjustable and which to exclude (i.e. fix the parameter value of) during later calibrations.

10.3 Model Calibration and Validation Results

Automated calibrations were performed for each of the three candidate conceptual models of K_h structure. Due to the complexity of the spatial and temporal aquifer recharge and pumping patterns over the 30-year base period, the discretization of the model domain into uniform square zones provided the most robust K_h structure and produced the most reasonable estimates of hydraulic head and district groundwater storage changes from the three conceptual models over the 1971-85 calibration period. This calibrated model was then validated from 1986-99.

10.3.1 Residual Analysis and Validation

District Aquifer Storage Changes The modeled versus target cumulative annual groundwater storage changes from 1970-99 for DEID, LID, LSID, LTRID, Pixley ID, PID, and SID are presented in Figures 55-61, respectively, for the three conceptual models. The general shapes of the storage change curves for each district are similar to that of the entire study area (Figure 38). By inspection, the uniform zonation clearly produces the best model fit for the majority of districts. The trends in storage change produced by the uniform zonation and the WTF model are particularly similar for DEID, LTRID, and SID for the entire 30-year base period. Close agreement also exists for LID and PID during the calibration period with divergences occurring over the validation period. In PID, the model reasonably estimates the cumulative storage changes from 1971-89. However, the model underestimates them from 1990-99. Districts in the eastern portion of the study area do not depend on multi-year intensive pumping programs since their aquifer systems lack sufficient storage capacities to sustain them. Consequently, it is possible that the UZWB model overestimated the groundwater pumping demands in PID from 1990-93, especially toward the end of the 1986-91 drought. The storage changes in LID are very similar to those of PID, with reasonable fits from 1971-91 and underestimates from 1992-99. Recall that we neglected localized recharge from Frazier and Lewis Creeks due to a lack of available flow data. The aquifer recharge that may have resulted from seepage in these two creeks could partially account for the differences in storage change for LID estimated by the groundwater flow model.

Greater differences occur for LSID and Pixley ID over the entire base period. However, the fluctuations in cumulative storage change in LSID are small relative to the other districts. The aquifer storage capacity there is not considered substantial as evidenced by its low estimated specific yield (5%) and the thin unconfined sediments overlying the Sierran bedrock. For Pixley ID, the model significantly underestimates the peak cumulative storage from 1983-90 and also for 1994-99. It's difficult to say whether the groundwater flow model or the WTF model produces a more accurate estimate of storage change in Pixley ID. The measured hydraulic heads there are probably representative of a mixture of unconfined, semi-confined, and perched water table conditions. The extreme heterogeneity of the hydrostratigraphy in this region coupled with questionable hydraulic head measurements hinders the estimation of an accurate storage change for this district.

Spatial Distribution of Residuals The spatial distribution of residuals for 1978, 1981, 1984, 1987, 1990, 1993, 1996, and 1999 are presented in Plates 40-47, respectively, for the uniform zonation conceptual model. The residuals should be 20 feet or less to satisfy the residual criterion and no significant spatial patterns should be apparent. These figures display spatial patterns occurring in some years. Although many of the residuals satisfy the criterion, the model fails to capture several local hydraulic head features. Notably, the model consistently overestimates the head targets in the KTWD and RGWD areas east of DEID and underestimates them in the unincorporated agricultural area just west of DEID. The distribution of residuals for 1978, 1981, and 1984 for the S_y-structure and soil K_s-structure conceptual models are also displayed in Plates 48-50 and Plates 51-53, respectively. By inspection, greater spatial correlation appears present in them in comparison to the uniform zonation conceptual model for these years.

The tendency of the groundwater flow model to underestimate or overestimate the regional distribution of target heads in a particular year is reflected in the difference in cumulative storage change estimates for the entire study area between the water balance and the WTF method for the same year (Figure 38). For example, the spatial distribution of residuals in 1987 indicates that the groundwater flow model underestimates the hydraulic heads in a several large areas throughout the domain (Plate 43). For 1987, the water balance also underestimates the cumulative storage changes estimated by the WTF method by 248,158 af. Conversely, in 1993 the calibrated model overestimates the target heads over a large area while the water balance also overestimates the cumulative storage change of the WTF method by 391,644 af. In 1981 however, many of the distributed residuals satisfy the residual criterion and the difference between the water balance and WTF method storage change is only 91,202 af (Figure 38). Close matches also result for 1984. These results are not totally surprising since the heads used to estimate the regional storage changes by the WTF method are the same as those used as calibration targets. Nevertheless, if the observed hydraulic heads in production wells are a realistic measure of the aquifer system water levels, then these calibration results highlight the importance of estimating accurate recharge and pumping distributions during the water balance modeling stage of the conjunctive use model development.

Modeled versus Target Hydraulic Heads The modeled versus target hydraulic heads for the spring of 1978, 1981, and 1984 are presented in Figures 62-64, respectively, for the uniform zonation conceptual model. Also presented in Figures 65-67 are the corresponding plots of the modeled hydraulic heads versus the residuals. Ideally, the plotted points in each figure should be tightly spread about the corresponding solid line. Moreover, deviations from the solid line should be distributed randomly with no patterns of randomness as a function of hydraulic head magnitude or time. The residual means for 1978, 1981, and 1984 are -11.6, 1.2, and 13 feet, respectively. Approximately 61.4, 66, and

55% of the residuals for 1978, 1981, and 1984, respectively, were within the 20 foot residual criterion. The bias towards more positive or negative residuals for any particular year is reflected again by the underestimation or overestimation of the cumulative storage change for the entire study area by the water balance model versus the WTF method.

The residual plots for the S_y-structure and soil K_s-structure conceptual models are presented in Figures 71-73 and Figures 77-79, respectively. These plots display a strong bias towards large negative residuals for large simulated hydraulic heads; indicating that both models severely overestimate the hydraulic head in the eastern part of the study area.

Hydraulic Head Residual Normal Probability Plots The hydraulic head residuals are expected to be independent and normally distributed (Hill, 1998). The normal probability plots for residuals in 1978, 1981, and 1984 are displayed for the uniform zonation model only in Figures 80-82, respectively. While most of the residuals fall near the straight line, significant deviations do occur along the tails of the distribution. These deviations are indicative of spatially correlated residuals along the eastern boundary where the calibrated model tends to severely overestimate the target hydraulic heads in some areas while severely underestimating them in others.

10.3.2 Estimated Parameters

For the uniform zonation conceptual model, preliminary calibration runs were conducted to compute the composite sensitivities for the K_h zones in the three model layers and for the model layer anisotropy ratios. These sensitivities were used to fix the parameter values associated with certain zones which were considered relatively insensitive and to allow the more sensitive parameters to remain adjustable in the calibration. The initial zonation consisted of 141 calibration parameters: 1) an anisotropy ratio for each model layer, 2) 28 K_h zones in the confined aquifer (model layer 3), 3) 28 K_h zones in the Corcoran Clay aquitard, and 4) 82 K_h zones in the unconfined aquifer (model layer 1). The final calibrated model consisted of 87 adjustable hydraulic parameters: 1) the anisotropy ratio for model layer 2, 2) 20 K_h zones in the confined aquifer, 3) 3 K_h zones in the Corcoran Clay aquitard, and 4) 63 K_h zones in the unconfined aquifer (model layer 1).

The spatial distributions of estimated K_h for the three model layers with the uniform zonation are presented in Plates 54-56. For layer 1, K_h ranges from 0.67-328 ft/day. The spatial distribution does not vary smoothly everywhere, with many large contrasts existing between adjacent zones. Although the estimated K_h for the uniform zones are within a range of reasonable values, its spatial structure does not really reflect the study area geomorphology as evidenced by the calibrated K_h from the soil K_s-structure model (Plate 57) or the K_h from the S_y-structure model (Plate 58).

Most of the computed sensitivities in the zones representing the Corcoran Clay aquitard were small relative to those for the confined and unconfined aquifers. The K_h values for 25 zones were assigned the estimates PEST had computed for them during a preliminary run and held constant during the remainder of the calibration process; while the 3 remaining zones remained adjustable. Despite the relatively low sensitivities, the estimated K_h in the Corcoran Clay reveal an apparent structure with values increasing from west to east. This could reflect an increasing aquitard hydraulic conductivity and a transition to a semi-confined condition as the thickness of the Corcorcan Clay diminishes towards the middle of the study area. The calibrated K_h in the aquitard ranged from $4x10^{-4}$-$7.1x10^{-2}$ ft/day.

The estimated K_h in the confined aquifer varied from 0.33-328 ft/day. This range corresponds to the user-specified lower and upper bounds of estimation in which K_h values are restricted by PEST. The largest K_h estimates occurred directly below Pixley ID and below the boundary between Pixley ID and LTRID where significant inter-district groundwater fluxes are expected. These results reflect both the complexity of the aquifer system heterogeneity in the western half of the study area and the uncertainty in observed hydraulic heads there used as calibration targets and for estimating district storage changes. The estimated anisotropy ratio for model layer 2 is 2.8. The fixed values of *a*r for layers 1 and 3 are 1.4 and 1.0, respectively. These small anisotropy ratios imply that the zones are nearly homogeneous units. A more realistic range for them would be 5-20.

Linear Confidence Intervals Linear confidence intervals were computed by PEST for each calibrated parameter. The ratio of the upper limit to the lower limit of the 95% confidence interval for K_h in model layer 1 is plotted in Plate 59 for the uniform zonation conceptual model. The confidence intervals are reasonably narrow (i.e. less than a factor 100) for the large districts east of the Corcoran Clay aquitard. Confidence intervals are the greatest for zones above the Corcoran Clay and along the eastern groundwater flow model domain. Although not shown, the confidence intervals for the zones in model layer 3 representing the confined aquifer were extremely large (i.e. > 10,000). Wide confidence intervals for estimated K_h in the vicinity of the Corcoran Clay aquitard reflect the simplistic model characterization of the complex aquifer stratigraphy there and the perhaps questionable quality of the local hydraulic heads used for generating head and district storage change calibration targets.

Parameter Composite Sensitivities Composite sensitivities for the K_h parameters in model layers 1, 2, and 3 are displayed in Plates 60-62, respectively, for the uniform zonation conceptual model. For model layer 1, parameter sensitivities are greatest in districts east of the Corcoran Clay and where calibration targets are present. The most sensitive zones correspond to areas at the interface between districts where significant inter-district groundwater fluxes occur (e.g. LTRID, Pixley ID). For model layer 3, large sensitivities are computed at the interface between the confined aquifer and the unconfined aquifer below LTRID, Pixley ID, and DEID, where significant groundwater fluxes occur and sharp K_h contrasts exist between the Corcoran Clay aquitard and the adjacent unconfined and confined aquifers.

Parameter Correlation Coefficients Correlation between calibrated parameters is considered significant if greater than 0.95 (Hill, 1998). Using this criterion, significant correlations were detected for K_h estimates from the uniform zonation conceptual model in layer 1 between zones 22 and 12, zones 48 and 59, and zones 68 and 90; in model layer 3 between zones 53 and 63; and between model layer 1 and 3 for zone 31 (layer 3) and zone 31 (layer 1), zone 42 (layer 3) and zone 40 (layer 1), and zone 75 (layer 3) and zone 77 (layer 1) (Plate 37). These zone pairs are either adjacent to one another or separated by a single zone. Four of the zone pairs were located near the eastern edge of the Corcoran Clay aquitard where significant hydraulic conductivity contrasts exist between the unconfined and confined aquifers and the Corcoran Clay. In this region, we expect significant vertical fluxes between model layers due to these contrasts and to pumping in the confined aquifer.

10.3.3 Estimated Inter-District Groundwater Fluxes

The hydraulic head distribution in the study area and the cumulative aquifer storage changes in select districts were reproduced during the calibration and validation process. The calibrated model was then used in conjunction with ZONEBUDGET to estimate the annual net groundwater fluxes between adjacent districts from 1970-99 (Figures 83-89). In general, groundwater flux directions are consistent with large-scale hydraulic gradients (Figure 15-20). Annual inter-district net fluxes between adjacent districts ranged from negligibly small (< 100 af) to as much as 50,000 af (e.g. net flux from LTRID to Pixley ID). Net fluxes are largely a function of the local transmissivity, and the length of the shared border between adjacent districts and their contrasting surface water supplies (i.e. different reliance on groundwater pumping). For example, the aquifer system underlying Pixley ID receives significant groundwater influxes from LTRID, SID, and DEID due to the large amount of pumping which is believed to occur in Pixley ID. Significant groundwater inflows from PID to LTRID and to LID likely occur due to channel seepage from the middle Tule River. LTRID and LID also contribute groundwater inflows to the northern area in the Kaweah sub-basin (i.e. extended model domain) which is also believed to rely predominantly on groundwater pumping to satisfy its applied water demands.

10.3.4 Calibration Summary

Three conceptual models of the K_h structure for model layer 1 were evaluated by PEST: 1) K_h as an exponential function of the S_y distribution (Plate 22), 2) K_h as a linear function of the saturated hydraulic conductivity of the soil survey mapping units (Plate 6), and 3) division of the model domain into square zones of uniform size (Plate 37). Each model was calibrated against the same set of hydraulic head targets and service district groundwater storage change targets. Overall, the uniform zonation conceptual model provides the best model fit among the three models. However, the uniform zonation model consisted of 87 adjustable parameters whereas the S_y - and soil K_s-structure models consisted of only 7 each. The improvement of model fit by the uniform zonation model over the other models comes at the expense of a loss of degrees of freedom. The estimated K_h for the uniform zonation, S_y-structure, and K_s-structure models are presented in Plates 54, 58, and 57, respectively. The uniform zonation and K_s-structure models provide better fits to LID storage changes over the calibration period than the S_y-structure model. Both the S_y- and K_s-structure models overestimated storage changes in PID whereas the uniform zonation model matched them reasonably at least over the calibration period. All three models provided a good fit to the LTRID storage changes over the calibration and validation periods (i.e. 1970-99); however, all three failed to reproduce the changes in Pixley ID beyond 1982.

Although the uniform zonation model provides the best overall fit, the resultant K_h distribution does not really resemble the spatial patterns of the study area geology as evidenced by the S_y or soil K_s maps. This is not completely surprising since as the final step in the conjunctive use model development, the estimated K_h distribution embodies the cumulative uncertainty in the all input parameter values used by the SWS and UZWB models, and the uncalibrated groundwater flow model.

With future data collection efforts aimed to improve the spatial and temporal resolution of the model input data, the calibration process may eventually produce a spatial distribution of hydraulic parameters which better reflects the true aquifer system hydrogeology. Potential sources of error in the parameter data used in this study and the simplifying assumptions invoked in the development of the sub-models are discussed in the next section.

11 Conjunctive Use Model Assessment

As re-stated from the introduction, the objective of the conjunctive use model is to simulate the historical impacts of urban and agricultural water demands, fluctuating surface water supplies, and groundwater pumping practices on the spatial and temporal distribution of groundwater storage in the Tule sub-basin area. The ability of the model to achieve these goals depends to a large extent on the validity of the simplifying assumptions invoked during the model development process, and the severity by which they are violated and lead to hydrologically indefensible results. Since the inter-relationships of the sub-models are serial rather than dynamic, the errors associated with the SWS and UZWB model outputs are cumulative and express themselves as uncertainty in the estimated hydraulic parameters during the groundwater flow model calibration process.

Discrepancies between the groundwater flow model simulations and the calibration targets are due to potential errors in: 1) the model inputs, 2) the conceptual model of the hydrogeology, and 3) the quality of hydraulic head observations used to generate the calibration targets. Potential errors in model inputs refer to incorrectly estimated diffuse recharge, localized recharge, and groundwater pumping rates by the UZWB and SWS models. Errors in the conceptual model of the hydrogeology are related to: 1) the number of model layers used to vertically delineate the aquifer hydrostratigraphy, 2) the specific yield and specific storativity distributions, 3) the specified boundary conditions, 4) specification of aquifer system upper and lower boundaries, and 5) the vertical allocation of pumping among model layers. Issues related to the quality of hydraulic head measurements include: 1) the aquifer depth which the head measurements represent, 2) the thickness of the aquifer formation over which the well is screened, 3) whether the measurements represent unconfined, semiconfined, confined, or perched water levels, and 4) field measurement error. In this section, we re-state the purpose of each sub-model and these issues with respect to the major simplifying assumptions invoked in their development.

11.1 Surface Water Supply Model

The SWS model calculates the surface water balance for the source and diversion channels in the inter-district channel network. Its primary outputs are the estimated monthly seepage and evaporative conveyance losses in the channel reaches and the monthly service district surface water deliveries. The major simplifying assumptions of the SWS model are listed below and discussed.

1. *We explicitly modeled the major unlined natural and constructed source and diversion channels in the inter-district conveyance network.*

Diversion channels were explicitly modeled if they are unlined and traverse other districts or unincorporated lands along their destination routes. The inter-district conveyance network included the known major diversion channels for all districts except for AWD. However, this district accounts for less than 1% of the total surface water supplies in the study area. Otherwise, most CVP contractors intersect with the Friant-Kern Canal and are assumed to receive deliveries from it directly into their respective distribution systems.

2. *For diversion channels possessing only measured inflow data, conveyance losses are estimated as a fixed-percentage of these inflows.*

Conveyance losses in these channels were estimated as a function of the destination district of the surface water diversion. Percent conveyance losses of diversions into the Deer Creek for delivery to AID, AIWD, and AWD were assumed to be 15%. For all other diversion channels, the percent conveyance losses were 3%. For all channels, we assume that 95% of the conveyance loss is due to seepage and 5% to evaporation. These percent conveyance losses likely underestimate the actual rates, of which seepage is the dominant component. Underestimated conveyance losses result in overestimates of surface water deliveries and underestimates of groundwater pumping. This is probably not a significant issue for constructed channels which do not span long distances or traverse multiple districts.

3. *We assume that the seepage along channel segments are uniformly distributed.*

Actual seepage rates are a function of the channel's geometry, bed transmissivity, slope, and stage. The assumption of uniform seepage may be an issue for some of the longer natural channels which possess significant flows and traverse multiple districts (e.g. Tule River, Deer Creek).

4. *We assume that all explicitly modeled channels are ephemeral and return flows are negligible.*

This assumption implies that each channel (e.g. ditch, river, canal) is permanently separated from the water table by an unsaturated zone. This assumption is probably valid given the intermittent nature of surface water deliveries and natural channel flows in the study area, and groundwater depths of 20-300 feet below the ground surface in many areas during the spring season when water levels are expected to be highest.

5. *We assume that all conveyance seepage losses directly recharge the unconfined aquifer water table (i.e. no seepage flow in the unsaturated zone).*

Although this assumption contradicts the previous assumption of channel ephemerality, we invoke it nevertheless since the unsaturated zone is not rigorously modeled in this study and long-term storage changes in the unsaturated zone are small in comparison to changes in unconfined aquifer storage. In addition, the unsaturated zone is most permeable in the vicinity of the natural channels due to the coarse sediments deposited there.

6. *For those districts which intersect the source channels that provide surface water supplies to them, we assume that these deliveries are received directly into their intra-district distribution systems and no conveyance seepage losses occur within the district interior.*

Delivered surface water to the district distribution system is conserved in the district water balance. Since we assume that channel seepage directly recharges the underlying unconfined aquifer and is theoretically available as a future source of applied water to the district via groundwater pumping, we do not factor out seepage losses within the district distribution system.

7. *We assume that flows within the natural channels (e.g. Tule River, Deer Creek) terminate within the study area boundaries (i.e. no channel out-flows from the study area).*

For most years this assumption is valid. Outflows from the Tule River into the Tulare Lake Bed west of the study area western boundary may have occurred in the winter months during years of heavy precipitation such as 1982, 1983, 1997, and 1998. However, outflow data were not available to quantify this possibility.

8. *Due to a lack of historical discharge data, we did not solve a water balance for Lewis and Frazier Creeks; thereby ignoring their contribution to aquifer recharge from seepage losses.*

Only a single flow measurement was available for each creek per annum. This measurement represented the maximum flow rate in cfs for the entire year and the date in which it occurred. These data were collected for Lewis Creek from 1974-98 and from 1974-94 for Frazier Creek. The peak discharges ranged from 33-1550 cfs for Lewis Creek and 2-216 cfs for Frazier Creek. The total discharges into the creeks during these events may be considerable depending on the duration of the storm. The underestimated storage changes for LID and LSID in the groundwater flow model calibration during the late 1990's could be partially explained by not accounting for the aquifer recharge contributions from channel seepage in these creeks. However, any estimate of a monthly time series of creek flows for each year based on a single yearly maximum flow measurement would be extremely uncertain.

11.2 Unsaturated Zone Water Budget Model

The UZWB model calculates the monthly water storage changes in the soil root zone and deep vadose zone of each land unit. It also models the intra-district surface water distribution system by estimating the monthly allocation of surface water to individual land units within each district. The soil root zone water storage changes were computed using a simple tipping-bucket model. The deep vadose zone water storage changes were computed using a one-dimensional unsaturated flow equation in which we assume that flow during any given month is steady and driven by gravity drainage. The primary model outputs are the recharge to the unconfined aquifer from surface applied water and precipitation, and the groundwater pumping demand from the unconfined and confined aquifers. The major simplifying assumptions of the UZWB model are listed below and discussed.

1. *We assumed that no lateral flow occurs between the unsaturated zones (soil root zone, deep vadose zone) of adjacent land units.*

This assumption is justified due to the large areal extent of the land units in comparison to the depth of the soil root and deep vadose zones.

2. *We used a single land use survey to define the spatial distribution of agricultural and urban land use over the 30-year base period.*

This is probably the most limiting assumption invoked in the UZWB model. As mentioned previously, land use changes in crop type over the 30-year base period in Tulare County were substantial. The use of a single land use survey to define the spatial distribution of land use and land unit acreage is potentially a large source of error. The adjustment of monthly consumptive use on the land unit scale for annual changes in major crop acreage on the county scale using (10) improved the estimate of total consumptive use for the study area and perhaps for large districts but obviously does not account for consumptive use changes on the land unit scale.

3. *We assumed that the irrigation efficiencies for each individual crop are temporally constant (i.e. do not vary by month or year).*

The efficiency of irrigation technologies and practices is widely acknowledged to have improved in the San Joaquin Valley over the 30-year base period, particularly during severe droughts. Irrigation efficiencies for some crops also vary throughout the growing season. However, irrigation overapplications due to inaccurate efficiencies in the model merely result in increased deep percolation to the deep vadose and increased recharge to the unconfined aquifer. Groundwater pumping may also be overestimated for some land units; however, overapplications of surface applied groundwater are conserved in the water balance.

4. *We assumed a uniform application of surface water supplies to the land units within each district which are eligible to receive surface water applications.*

Spatial and temporal variations of surface water distributions to member farmers and other end users no doubt exist in most service districts. Farmers may receive larger or smaller deliveries depending on their access to district distribution channels, their ability to pump groundwater more easily or cheaply, and other factors. Accurate characterization of the surface water distribution is likely a more important issue for large districts than for smaller ones since it impacts regional estimates of groundwater pumping and aquifer recharge.

5. *We used a single coarsely-contoured isohyet map to define the spatial distribution of precipitation.*

Although the spatial distribution of precipitation is accurately characterized as increasing from west to east, the contour lines representing this variation are broadly spaced for much of the study area and differ from each other by 1-2 inches. This results in differences in precipitation of 30-60 inches between adjacent areas over the 30-year base period. However, insufficient data prevented a more accurate estimation of its spatial distribution.

6. *We assumed that 100% of the estimated precipitation infiltrates into the soil root zone of each land unit (i.e. no surface runoff or evaporation of precipitation) and is available for plant uptake.*

This is one the most contentious issues in the UZWB model. Changes in the soil root zone moisture content are calculated using a simple tipping-bucket model. As a result, precipitation infiltration will be stored as soil moisture until it is either consumed by the crop or percolates into the deep vadose zone once the field capacity is exceeded. Since flows in the soil root zone are not explicitly modeled, high soil moisture contents due to high monthly precipitation inputs and low crop water demands can persist for months. This point is illustrated by examination of the monthly water balances for years of below-average, normal, and above-average annual precipitation (Figures 39-41). In 1977, the study area was subjected to a drought with an annual precipitation total of only 177,800 af. Precipitation for crop uptake was minimal and the region depended more heavily on groundwater pumping that year as surface water supplies were also less available (Figure 39). During 1980, annual precipitation was normal and mostly occurred from January through March. Precipitation and surface water supplies satisfied most of the crop water demands until the midsummer months when the soil moisture due to precipitation is exhausted and surface water supplies are normally augmented by groundwater pumping (Figure 40). In 1998, however, annual precipitation was above average, with 974,400 af of rain falling between November, 1997 and June, 1998. According to the estimated water balance, the soil root zone moisture content satisfied most of the crop consumptive use from late winter through June (Figure 41). However, in the semi-arid San Joaquin Valley soil moisture content would not be sufficient to meet crop water demands in the late spring without large surface applications of irrigation, even in a wet year. It is therefore possible that the UZWB model, for years of above-average precipitation, underestimates groundwater pumping in the late-spring and early-summer.

7. *We estimated the spatial and temporal distribution of groundwater pumping as a water balance closure term.*

Groundwater pumping records in the study area are not regularly maintained or made available to the public. As a result, the groundwater pumping distribution had to be estimated as a closure term in the water balance.

8. *We used the estimated net recharge at the study area scale as an estimate of the groundwater storage changes in the aquifer system.*

For this, we assume that the net horizontal groundwater fluxes through the vertical boundaries of the study area are negligible (i.e. the aquifer system is relatively closed with respect to significant groundwater fluxes through the perimeter). By invoking this assumption, we were able to compare the water balance estimates of groundwater storage change to those computed by the WTF method. This provided a means of verification of the water balance approach at least at the study area scale.

11.3 Groundwater Flow Model

The groundwater flow model calculated the hydraulic head and groundwater storage changes in the aquifer system subject to transient groundwater recharge and pumping stresses. Its primary output was the modeled hydraulic head distribution in the modeled area for each stress period. A post-processing routine calculated the cumulative annual groundwater storage changes over each district and the entire study area. The calibrated model was also used to compute the net annual inter-district groundwater fluxes between adjacent districts. The major simplifying assumptions of the groundwater flow model are listed below and discussed.

1. *We modeled the aquifer system hydrostratigraphy using three MODFLOW model layers.*

Since we lacked more detailed information delineating the vertical sequence of hydrostratigraphic units and the screened intervals of production wells in them, we limited the representation of the aquifer system to three MODFLOW model layers.

2. *We assumed no-flow boundary conditions around the perimeter of the study area.*

Reliable historical hydraulic head data were not available to estimate horizontal fluxes across the western and southern boundaries in the study area. Along the western boundary, a high proportion of the groundwater pumping is known to occur in the confined aquifer below the Corcoran Clay aquitard. The confined aquifer there is more likely to receive its recharge from the unconfined aquifer either as vertical leakage through the Corcoran Clay or as deep lateral transfer from the unconfined aquifer to the east. Consequently, we assumed that the horizontal fluxes in the confined aquifer across the western boundary are small.

Assignment of a no-flow condition in the aquifer system across the eastern boundary is justifiable given the prevalence of impermeable bedrock in the foothill areas. Characterization of the runoff occurring in these foothills is partially accounted for by the assignment of higher precipitation rates from the isohyet map. However, runoff flows in non-gauged ephemeral streams derived from precipitation at higher elevations beyond the eastern model boundary may be considerable during extreme storm events and underestimated by the assigned precipitation in the foothills.

The northern boundary location in the groundwater flow model was extended partially into the Kaweah sub-basin to better approximate the groundwater flow divide there inferred from the contour maps of unconfined water levels. This had a significant effect on the calibrated groundwater storage changes in LTRID by accounting for horizontal fluxes across LTRID into the Kaweah sub-basin.

3. *We used hydraulic head measurements obtained from production wells to calibrate the model.*

The quality of the hydraulic head measurements and the conditions under which they were obtained are not known. These data may represent ambient water levels in production wells not in use at the time or wellbore drawdown recovery in wells recently pumped. Moreover, the measurements are obtained annually from approximately early January to late March thus spanning a 3-4 month observation period. For these reasons, the observed hydraulic heads are considered an unreliable measure of the water levels

in the aquifer formation away from the production wells in which they were obtained for any given year. However, if the measurements in a well for consecutive years were obtained under similar pumping/recovery circumstances, then the head difference between years can be used to infer groundwater storage changes rather than a single year measurement representing actual formation groundwater levels. Consequently, we used cumulative annual groundwater storage changes on the district scale as a calibration target for the groundwater flow model and on the study area scale to verify the water balance results from the UZWB model.

12 References

Argus Interware, Inc. (1997) User's Guide Argus ONETM, Argus Open Numerical Environments - A GIS Modeling System, Version 4.0, Jerico, NY, Argus Holdings, Limited, 506 pp

Baker J (1999) Written communication

California Department of Water Resources (CDWR) (1970-99) Historical Unconfined Ground Water Trends In The San Joaquin Valley, preliminary update report and electronic files, 1970-99.

California Department of Water Resources (CDWR) (1980) Groundwater basins in California, bulletin 118-80. Sacramento, California

California Department of Water Resources (CDWR) (1981) Standard land use legend, Land and Water Use Section, Statewide Planning Branch, Division of Planning, 12 pp

California Department of Water Resources (CDWR) (1993) Standard land use legend, Land and Water Use Section, Statewide Planning Branch, Division of Planning, 15 pp

Croft MG, Gordon GV (1968) Geology, hydrology, and quality of water in the Hanford-Visalia area San Joaquin Valley, California, USGS Open-File Report, 63 pp

Croft MG (1969) Subsurface geology of the late Tertiary and Quaternary waterbearing deposits of the southern part of the San Joaquin Valley, California. USGS Open-File Report 1999-H, 29 pp

Davis GH, Green JH, Olmsted FH, Brown DW (1959) Ground-water conditions and storage capacity in the San Joaquin Valley, California. USGS Water-Supply Paper 1469, 287 pp

Doherty J (1994) PEST: Model-Independent Parameter Estimation.Watermark Computing

Erlewine T (1989) Development of a groundwater model for the Tule groundwater basin. MS Thesis, University of California, Davis, California, 102 pp

Goldhammer DA, Snyder RL (1989) Irrigation scheduling: a guide for efficient on-farm water management. University of California, Division of Agriculture and Natural Resources, Publication 21454. Oakland, California

Harbaugh AW (1990) A computer program for calculating subregional water budgets using results from the U.S. Geological Survey modular three dimensional ground-water flow model: U.S. Geological Survey Open-File Report 90-392, 46 pp

Healy RW, Cook PG (2002) Using groundwater levels to estimate recharge. Hydrogeol J 10:91-109

Hill MC (1998) Methods and guidelines for effective model calibration. USGS Water-Resources investigations Report 98-4005, 90 pp

Hilton GS, McClelland EJ, Klausing RL, Kunkel F (1963) Geology, hydrology, and quality of water in the Terra Bella-Lost Hills area, San Joaquin Valley, California. USGS Open-File Report 63-47, 158 pp

Letey J, Vaux HJ (1984) Water duties for California agriculture. Report prepared for the California State Water Resources Control Board. Sacramento, California. Agreement No. 2-043-300-0, 110 pp

Lofgren BE, Klausing RL (1969) Land subsidence due to ground-water withdrawal, Tulare-Wasco area, California. USGS Professional Paper 437-B, 103 pp

McDonald MG, Harbaugh AW(1988) A modular three-dimensional finite-difference ground-water flow model, in Techniques of Water-Resources Investigations of the United States Geological Survey, Book 6, chap. A1, U.S. Geol. Surv., Washington, D.C.

Naugle AW(2001) A hydrologic budget model for the Tule basin area, southeastern San Joaquin Valley, California. MS Thesis, University of California, Davis, California, 227 pp

Tule River Association Annual Report for Water Years 1970-99.

Sophocleous MA (2002) Interactions between groundwater and surface water: the state of the science. Hydrogeol J 10:52-67

Storie RE, Owen BC, Layton MH, Anderson AC, Leighty WJ, Kikiforoff CC (1942) Soil survey of the Pixley area, California. United States GPO, Washington D.C., 113 pp

Tule River Association (TRA) (1970-99) Annual Report For Water Years 1970-99

United States Department of the Interior Bureau of Reclamation (USBR) (1997) Central Valley Project Improvement Act: Supplement to the Draft Programmatic

Environmental Impact Statement, Sacramento, California, 163 pp

United States Department of the Interior Bureau of Reclamation (USBR) (1970-99) Reports of Operations of the Central Valley Project 1970-99

United States Department of the Interior Bureau of Reclamation (USBR) (1991) Fortieth Annual Water Supply Report for the Central Valley Project 1990, Fresno, California, 158 pp

United States Geological Survey (USGS) (1970-99) National Water Information System (NWIS) database - Daily Mean Discharge data for Rivers and Streams 1970-99

Winston RB (2000) Graphical User Interface for MODFLOW, Version 4: U.S. Geological Survey Open-File Report 00-315, 27 pp 72

Zhang M (1993) The impact of agriculture and groundwater dynamics and qualities, PhD Dissertation, University of California, Davis, California, 237 pp

Agricultural Class	Agricultural Sub-classes	Class Symbol & Sub-class Number	Model ID	Acreage	Water Use Efficiency
Subtropical Fruits	Grapefruit	C1	1	241	0.85
	Lemons	C2	2	1580	0.85
	Oranges	C3	3	49872	0.85
	Avocados	C5	4	323	0.85
	Olives	C6	5	11125	0.85
	Misc. subtropical fruit	C7	6	53	0.85
	Kiwis	C8	7	1259	0.85
	Eucalyptus	C10	8	68	0.85
Deciduous Fruits and Nuts	Apples	D1	9	561	0.80
	Apricots	D2	10	177	0.80
	Cherries	D3	11	4	0.80
	Peaches	D5	12	1129	0.80
	Pears	D6	13	10	0.80
	Plums	D7	14	6947	0.80
	Prunes	D8	15	759	0.80
	Figs	D9	16	0	0.80
	Misc. deciduous fruits	D10	17	2014	0.80
	Almonds	D12	18	10012	0.80
	Walnuts	D13	19	6464	0.80
	Pistachios	D14	20	3922	0.80
Field Crops	Cotton	F1	21	77419	0.70
	Safflower	F2	22	3442	0.70
	Flax	F3	23	28	0.70
	Sugar beets	F5	24	977	0.67
	Corn	F6	25	27383	0.70
	Sudan	F8	26	466	0.70
	Dry beans	F10	27	2410	0.70
	Misc. field crops	F11	28	10	0.70
	Sunflower	F12	29	25	0.70
Grain and Hay Crops	Grain & hay	G	30	70885	0.65
	Grain & corn	G/F6	31	9220	0.68
Pasture Land	Alfalfa	P1	32	39217	0.75
	Mixed pasture	P3	46	1709	0.67
	Native pasture	P4	47	572	0.67
Truck and Berry Crops	Green beans	T3	33	835	0.70
	Cole crops	T4	34	1020	0.70
	Lettuce	T8	35	149	0.70
	Melons	T9	36	1112	0.70
	Onions	T10	37	23	0.70
	Tomatoes	T15	38	1	0.72
	Flowers & nursery	T16	39	157	0.70
	Misc. truck crops	T18	40	265	0.70
	Peppers	T21	41	329	0.70
Vineyards	Vineyards	V	45	49573	0.80
Idle Land	Idle land	L1	55	2198	1.00

Table 1: Agricultural land use: classes, sub-classes, class symbol & sub-class number, model identification number (ID), acreage, and water use efficiency (CDWR, 1981; CDWR, 1993).

Semi-agricultural Classes	**Semi-agricultural Sub-classes**	**Class Symbol Sub-class Number**	**Model ID**	**Acreage**	**Water Use Efficiency**
Semi-Agricultural and Incidental to Agriculture	farmsteads	S1	48	1883	1.0
	livestock feedlots	S2	58	723	1.0
	dairies	S3	49	4300	1.0
	poultry farms	S4	50	335	1.0

Table 2: Semi-agricultural land use: classes, sub-classes, class symbol & subclass number, model identification number (ID), acreage, and water use efficiency (CDWR, 1981; CDWR, 1993).

Urban Classes	**Urban Sub-classes**	**Class Symbol Sub-class Number**	**Model ID**	**Acreage**	**Water Use Efficiency**
Urban	urban	U	59	18112	1.0
Urban Industrial	produce canneries	UI11	51	1119	1.0
	misc. high water use	UI12	52	26	1.0
	sewage treatment plants	UI13	53	33	1.0
Urban Landscape	lawn	UL	42	217	1.0
	golf courses	UL2	43	8	1.0
	cemeteries	UL4	44	81	1.0
	non-irrigated cemeteries	UL5	60	13	1.0
Urban Vacant	unspecified urban	UV	61	3019	1.0

Table 3: Urban land use: classes, sub-classes, class symbol & sub-class number, model identification number (ID), acreage, and water use efficiency (CDWR, 1981; CDWR, 1993).

Native Classes	**Native Sub-classes**	**Class Symbol**	**Model ID**	**Acreage**	**Water Use Efficiency**
Native Vegetation	native vegetation	NV	56	115369	1.0
Water Surface	water surface	NW	57	4404	1.0
Special Conditions	**Special Conditions Sub-classes**	**Special Condition Symbol**	**Model ID**	**Acreage**	**Water Use Efficiency**
Fallow Land	n/a	F	54	5995	1.0

Table 4: Native land use and special conditions: classes, sub-classes, class symbol, model identification number (ID), acreage, and water use efficiency (CDWR, 1981; CDWR, 1993).

Water Service District	Fraction of District in Study Area	Acreage in Study Area	Land Units in District
Alpaugh Irrigation District (AID)	0.9	10662	238
Angiola Water District (AWD)	0.32	10661	73
Atwell Island Water District (AIWD)	0.78	5661	84
City of Lindsay	1.0	1462	43
City of Porterville	1.0	7922	23
Delano-Earlimart Irrigation District (DEID)	0.85	47861	806
Ducor Irrigation District (DID)	1.0	10355	146
Earlimart Public Utilities District (EPUD)	1.0	789	23
Kern-Tulare Water District (KTWD)	0.32	15165	116
Lewis Creek Water District (LCWD)	1.0	1268	76
Lindmore Irrigation District (LID)	1.0	21114	958
Lindsay-Strathmore Irrigation District (LSID)	1.0	15615	595
Lower Tule River Irrigation District (LTRID)	1.0	102810	1713
Pioneer Water Company (PWC)	1.0	892	40
Pixley Irrigation District (Pixley ID)	1.0	68891	964
Porterville Irrigation District (PID)	1.0	17112	497
Rag Gulch Water District (RGWD)	0.44	2659	44
Saucelito Irrigation District (SID)	1.0	19779	380
Smallwood Vineyards	1.0	155	4
Strathmore Public Utilities District (SPUD)	1.0	362	20
Styro-Tek Inc.	1.0	11	2
Teapot Dome Water District (TDWD)	1.0	3482	145
Terra Bella Irrigation District (TBID)	1.0	13795	488
Tipton Public Utilities District (TPUD)	1.0	637	10
Vandalia Irrigation District (VID)	1.0	1378	48
Unincorporated Land	n/a	163294	1573

Table 5: Fractions and acreages of districts within the study area and number of land units delineated in each district.

Water Service District	Surface Water Sources
Alpaugh Irrigation District	CVP
Angiola Water District	CVP, SWP, Kings River, Tule River
Atwell Island Water District	CVP
City of Lindsay	CVP
City of Porterville	none
Delano-Earlimart Irrigation District	CVP
Ducor Irrigation District	CVP
Earlimart Public Utilities District	none
Kern-Tulare Water District	CVP
Lewis Creek Water District	CVP
Lindmore Irrigation District	CVP
Lindsay-Strathmore Irrigation District	CVP
Lower Tule River Irrigation District	CVP, Tule River
Pioneer Water Company	Tule River
Pixley Irrigation District	CVP
Porterville Irrigation District	CVP, Tule River
Rag Gulch Water District	CVP
Saucelito Irrigation District	CVP
Smallwood Vineyards	CVP
Strathmore Public Utilities District	CVP
Styro-Tek Inc.	CVP
Teapot Dome Water District	CVP
Terra Bella Irrigation District	CVP
Tipton Public Utilities District	none
Vandalia Irrigation District	Tule River

Table 6: Sources of imported surface water for the water service districts.

Data Type	Source
Natural and Constructed Channels Map	Teale Data Center
Imported Surface Water Supplies - Central Valley Project	USBR
Imported Surface Water Supplies - Tule River	Tule River Association
Imported Surface Water Supplies - Pioneer Ditch	Tule River Association
Imported Surface Water Supplies - Kings River	Provost & Pritchard
Imported Surface Water Supplies - State Water Project	Provost & Pritchard
Natural Channel Flows - Deer Creek, White River	USGS
Inter-District Channel Network Conveyance Loss Factors	Naugle (2001)

Table 7: Data type and source for the SWS model.

Station ID	Station Name
1	Tule River near Springville
2	Pioneer Ditch below Success Dam
3	Tule River below Success Dam
4	Campbell-Moreland Ditch above Porterville
5	Porter Slough at Porterville
6	Porter Slough Ditch at Porterville
7	Vandalia Ditch near Porterville
8	Poplar Ditch near Porterville
9	Hubbs-Miner Ditch at Porterville
10	Woods-Central Ditch near Porterville
11	Friant-Kern Canal to Porter Slough
12	Friant-Kern Canal to Tule River
13	Friant-Kern Canal to Woods-Central Ditch
14	Friant-Kern Canal to Poplar Ditch
15	Porter Slough at Road 192
16	Tule River below Porterville (Rd 208/Rockford Stn.)
17	Tule River at Oettle Bridge (Rd 192)
18	Tule River at Turnbull Weir
19	Deer Creek near Fountain Springs
20	Deer Creek near Terra Bella
21	Friant-Kern Canal to Deer Creek
22	White River near Ducor
23	Friant-Kern Canal to White River
24	Lewis Creek near Lindsay
25	Frazier Creek near Strathmore

Table 8: Identification number (ID) and name of flow stations for modeled surface water channels.

Channel Segment	Segment Inflows	Diversions Inflows	Diversions Outflows	District Deliveries	Segment Outflows
Campbell-Moreland Ditch	Upper Tule River	none	none	Vandalia ID	none
Casa Blanca Ditch	Friant-Kern Canal	none	none	Lower Tule River ID	none
Frazier Creek	none	none	none	none	none
Hubbs-Miner Ditch	Upper Tule River	none	none	Porterville ID	none
Lewis Creek	none	none	none	none	none
Lower Deer Creek	Middle Deer Creek	Friant-Kern Canal Cross Valley Canal	none	Pixley ID Alpaugh ID Atwell Island WD	none
Lower Tule River	Middle Tule River (at Oettle Bridget)	none	none	Lower Tule River ID	Tule River (at Turnbull Weir)
Lower White River	Upper White River	none	none	none	none
Middle Deer Creek	Upper Deer Creek	none	none	none	Lower Deer Creek
Middle Tule River	Upper Tule River (at Road 208)	none	none	none	Lower Tule River (at Oettle Bridget)
North Canal	Friant-Kern Canal	none	none	Lower Tule River ID	none
North Canal/Rankin Ditch	Friant-Kern Canal	none	none	Lower Tule River ID	none
Pioneer Ditch	Success Reservoir	none	none	Pioneer Water Company	none
Poplar Ditch	Upper Tule River	Friant-Kern Canal	none	Lower Tule River ID Porterville ID	none
Poplar/Tipton Ditch	Friant-Kern Canal	none	none	Lower Tule River ID	none
Porter Slough	Upper Tule River	Friant-Kern Canal	Porter Slough Ditch	Porterville ID	Lower Porter Slough (at Road 192)
Porter Slough Ditch	Upper Porter Slough	none	none	Porterville ID	none
Upper Deer Creek	none	none	none	none	Middle Deer Creek (near Terra Bella)
Upper Tule River	Success Reservoir	Friant-Kern Canal	Campbell-Moreland Ditch Porter Slough Ditch Vandalia Ditch Poplar Ditch Hubbs-Miner Ditch Woods-Central Ditch	none	Middle Tule River (at Road 208)
Upper White River	none	none	none	none	Lower White River (near Ducor)
Vandalia Ditch	Upper Tule River	none	none	Vandalia ID	none
Woods-Central Ditch	Upper Tule River	Friant-Kern Canal	none	Lower Tule River ID	none

Table 9: Modeled surface water channel segment inflows, diversions, deliveries, and outflows.

CVP Contractors	Class 1 Contract	Class 2 Contract
City of Lindsay	2500	0
Delano-Earlimart Irrigation District	108,800	74,500
Kern-Tulare Water District	40,000	0
Lewis Creek Water District	1450	0
Lindmore Irrigation District	33,000	22,000
Lindsay-Strathmore Irrigation District	27,500	0
Lower Tule River Irrigation District	61,200	238,000
Pixley Irrigation District	31,102	0
Porterville Irrigation District	16,000	30,000
Rag Gulch Water District	13,300	0
Saucelito Irrigation District	21,200	32,800
Teapot Dome Water District	7500	0
Terra Bella Irrigation District	29,000	0

Table 10: Central Valley Project (CVP) contractors in the study area.

	Fractional loss from inter-district source and diversion channels			Fractional loss from intra-district distribution channels
Water Service District	Evaporation, α	Seepage, β	Intentional Recharge, γ	Evaporation, α_d
Alpaugh ID	0.0075	0.1425	0	0.066
Angiola WD	0.0075	0.1425	0	0
Atwell Island ID	0.0075	0.1425	0	0.01
City of Lindsay	0	0	0	0
City of Porterville	0	0	0	0
Delano-Earlimart ID	0	0	0	0.01
Ducor ID	0	0	0	0
Earlimart PUD	0	0	0	0
Exeter ID	0	0	0	0
Kern-Tulare WD	0	0	0	0.01
Lewis Creek WD	0	0	0	0
Lindmore ID	0	0	0	0
Lindsay-Strathmore ID	0	0	0	0
Lower Tule River ID	0.0015	0.0285	0	0.01
Pioneer Water Co.	0.0015	0.0285	0	0.01
Pixley ID (Mar-Aug)	0.0015	0.0285	0.7	0.01
(Sep-Feb)	0.0015	0.0285	0.2	0.01
Porterville ID	0.0015	0.0285	0	0.01
Rag Gulch WD	0	0	0	0
Saucelito ID	0	0	0	0
Smallwood Vineyards	0	0	0	0
Strathmore PUD	0	0	0	0
Styro-Tek Inc.	0	0	0	0
Teapot Dome WD	0	0	0	0
Terra Bella ID	0	0	0	0
Tipton PUD	0	0	0	0
Vandalia ID	0.0015	0.0285	0	0.01

Table 11: Fractional losses due to evaporation, seepage, and intentional recharge from modeled inter-district source and diversion channels and unmodeled intradistrict distribution channels.

Data Type	Source
Reference Precipitation	USGS, 1970-73 Vestal Station (C09304) USGS, 1974-95 Tulare ID Station (C0905101) DWR, 1996-99 Visalia Station (VSL)
Reference Evapotranspiration	DWR
Reference Evaporation	DWR
Crop Coefficients	Goldhammer and Snyder (1989) Letey and Vaux (1984)
Irrigation Efficiencies	Erlewine (1989)
Urban Water Use	City of Porterville
Specific Yield	DWR
Production Well Hydraulic Head Observations	DWR
Tulare County Reported Crop Acreage	Tulare County Agricultural Commissioners Reports
Land Use Map	Zhang (1993)
Water Service District Map	DWR
Isohyet Map	Naugle (2001)
Soils Survey Map	Zhang (1993)

Table 12: Data type and source for the UZWB model.

Land Use Category	Jan	Feb	Mar	Apr	May	Jun	Jul	Aug	Sep	Oct	Nov	Dec
produce canneries	0.012	0.006	0.033	0.064	0.109	0.136	0.157	0.168	0.112	0.111	0.043	0.014
misc. high water use	0.012	0.006	0.033	0.064	0.109	0.136	0.157	0.168	0.112	0.111	0.043	0.014
sewage treatment plants	0.012	0.006	0.033	0.064	0.109	0.136	0.157	0.168	0.112	0.111	0.043	0.014
unspecified urban	0.012	0.006	0.033	0.064	0.109	0.136	0.157	0.168	0.112	0.111	0.043	0.014

Table 13: Monthly net water use (acre-feet per acre) for urban land uses (e.g. municipal, industrial) which have 100% of their theoretical applied water demands satisfied by surface water or groundwater.

Major Crop	**Reported Annual ET_a (inches)**	Estimated Range of **Annual ET_a, 1970-99 (inches)**	**Estimated Average Annual ET_a, 1970-99 (inches)**
Cotton	27.4-35.5	26.2-34.2	31
Grain & Grass Hay	15.0-17.0	11.1-17.4	15.1
Citrus	28.9-38.1	28.3-38.4	34.8
Vineyards	23.8-31.3	23.3-30.4	27.6
Alfalfa	40.9-53.5	39.6-53.4	48.8
Grain & Corn	36	28.6-38.3	34.8
Olives	39.2	32.3-43.7	39.7
Almonds	38.7	31.0-41.3	37.4
Corn	27.4	23.8-30.5	27.5
Plums	33.8-43.4	31.0-41.3	37.4
Walnuts	41.8	33.7-44.4	40.2
Pistachios	40.7	33.1-43.0	38.8

Table 14: For the 12 major crops: reported typical values of or ranges of annual ET_a (inches); and estimated ranges and averages of annual ET_a (inches) from 1970-99.

Land Use Sub-Classes	Jan	Feb	Mar	Apr	May	Jun	Jul	Aug	Sep	Oct	Nov	Dec
grapefruit	0.83	0.8	0.74	0.72	0.72	0.67	0.67	0.67	0.68	0.75	0.77	0.8
lemons	0.83	0.8	0.74	0.72	0.72	0.67	0.67	0.67	0.68	0.75	0.77	0.8
oranges	0.83	0.8	0.74	0.72	0.72	0.67	0.67	0.67	0.68	0.75	0.77	0.8
avocados	0.83	0.8	0.74	0.72	0.72	0.67	0.67	0.67	0.68	0.75	0.77	0.8
olives	0.8	0.8	0.8	0.8	0.8	0.8	0.8	0.8	0.8	0.8	0.8	0.8
misc. subtropical fruit	0.82	0.78	0.84	0.77	0.76	0.71	0.74	0.73	0.74	0.77	0.7	0.66
kiwis	0	0	0	0.23	0.8	1.05	1.05	1.05	1.05	1.05	0	0
eucalyptus	0.82	0.78	0.84	0.77	0.76	0.71	0.74	0.73	0.74	0.77	0.7	0.66
apples	0	0.29	0.67	0.8	0.93	1	1	1	0.92	0.72	0.19	0
apricots	0	0.26	0.61	0.72	0.84	0.9	0.9	0.9	0.83	0.65	0.18	0
cherries	0	0.29	0.67	0.8	0.93	1	1	1	0.92	0.72	0.19	0
peaches	0	0.26	0.61	0.72	0.84	0.9	0.9	0.9	0.83	0.65	0.18	0
pears	0	0.26	0.61	0.72	0.84	0.9	0.9	0.9	0.83	0.65	0.18	0
plums	0	0.26	0.61	0.72	0.84	0.9	0.9	0.9	0.83	0.65	0.18	0
prunes	0	0.26	0.61	0.72	0.84	0.9	0.9	0.9	0.83	0.65	0.18	0
figs	0	0.26	0.61	0.72	0.84	0.9	0.9	0.9	0.83	0.65	0.18	0
misc. deciduous fruit	0	0.26	0.61	0.72	0.84	0.9	0.9	0.9	0.83	0.65	0.18	0
almonds	0	0.26	0.61	0.72	0.84	0.9	0.9	0.9	0.83	0.65	0.18	0
walnuts	0	0	0.27	0.64	0.83	1.01	1.14	1.14	0.98	0.57	0.13	0
pistachios	0	0	0	0.13	0.76	1.14	1.19	1.19	1.04	0.64	0.17	0
cotton	0	0	0	0.14	0.3	0.81	1.28	1.25	0.81	0	0	0
safflower	0	0	0.2	0.55	0.93	1.1	0.65	0.2	0	0	0	0
flax	0.54	0.9	1.07	1.09	0.58	0.52	0.38	0.2	0	0	0.05	0.35
sugar beets	0	0.09	0.22	0.59	1.1	1.17	1.18	1.18	1.14	1.11	0.41	0.4
corn	0	0	0	0.22	0.58	1.18	1.17	0.75	0	0	0	0
sudan	0	0	0	0.7	1	1.1	1.1	1	0	0	0	0
dry bean	0	0	0	0.05	0.27	1.12	1.08	0.52	0.27	0	0	0
misc. field crops	0	0.01	0.04	0.18	0.5	0.89	1.09	0.93	0.43	0.13	0.03	0.03
sunflower	0	0	0	0	0.35	0.75	1.1	1	0.4	0	0	0
grain and grass hay	0.54	0.95	1.17	1.1	0.64	0	0	0	0	0	0	0.22
grain and corn	1	1.2	1.19	0.22	0.58	1.18	1.17	0.75	0	0	0.25	0.38
alfalfa hay	1.05	1.02	1	0.97	0.97	0.97	0.97	0.97	0.98	1.01	1.04	1.08
green beans	0	0.35	0.7	0.98	0.8	0	0	0	0	0	0	0
cole crops	0.35	0.35	0.5	0.75	0.75	1.05	0.45	0	0	0.1	0.2	0.3
lettuce	0	0	0.35	0.75	0.95	0.5	0	0	0	0	0	0
melons	0	0.05	0.13	0.3	0.91	1.1	0.58	0.05	0	0	0	0
onions	0.7	0.8	0.9	1.1	1.05	1.05	1.05	0.5	0.1	0.25	0.35	0.55
tomatoes	0	0	0.09	0.26	0.37	0.91	1.18	0.97	0.36	0	0	0
flowers and nursery	1	1	1	1	1	1	1	1	1	1	1	1
misc. truck crops	0.15	0.22	0.38	0.64	0.79	0.8	0.59	0.28	0.07	0.05	0.08	0.12
peppers	0	0	0	0.35	0.7	1.02	0.9	0.45	0	0	0	0
lawn areas	1.05	1.05	1.05	1.05	1.05	1.05	1.05	1.05	1.05	1.05	1.05	1.05
golf courses	1.05	1.05	1.05	1.05	1.05	1.05	1.05	1.05	1.05	1.05	1.05	1.05
cemeteries	1.05	1.05	1.05	1.05	1.05	1.05	1.05	1.05	1.05	1.05	1.05	1.05
vineyards	0	0	0.18	0.57	0.78	0.85	0.83	0.71	0.38	0	0	0

Table 15: Monthly crop coefficients for land uses which have 100% of their theoretical applied water demands satisfied by surface water or groundwater.

Land Use Sub-classes	Jan	Feb	Mar	Apr	May	Jun	Jul	Aug	Sep	Oct	Nov	Dec
mixed pasture	0.90	0.90	0.90	0.90	0.90	0.90	0.90	0.90	0.90	0.90	0.90	0.90
native pasture	1.00	1.00	1.00	1.00	1.00	1.00	1.00	1.00	1.00	1.00	1.00	1.00
farmsteads	0.27	0.27	0.27	0.27	0.27	0.27	0.27	0.27	0.27	0.27	0.27	0.27
dairies	1.08	1.08	1.08	0.54	0.11	0.11	0.11	0.11	0.11	0.11	0.54	1.08
poultry farms	1.08	1.08	1.08	0.54	0.11	0.11	0.11	0.11	0.11	0.11	0.54	1.08

Table 16: Monthly crop coefficients for land uses which have 25% of their theoretical applied water demands satisfied by surface water or groundwater.

Land Use Sub-classes	Jan	Feb	Mar	Apr	May	Jun	Jul	Aug	Sep	Oct	Nov	Dec
fallow land	0.45	0.44	0.51	0.25	0.00	0.00	0.00	0.00	0.00	0.00	0.21	0.37
Idle land	1.07	1.06	1.22	0.58	0.00	0.00	0.00	0.00	0.00	0.00	0.49	0.90
native vegetation	0.89	0.88	1.02	0.96	0.95	0.95	1.00	0.98	0.98	0.94	0.82	0.75
surface water	1.09	1.08	1.24	1.18	1.16	1.17	1.22	1.20	1.20	1.14	1.00	0.91
feed lots	1.07	1.06	1.22	0.58	0.00	0.00	0.00	0.00	0.00	0.00	0.49	0.90
unirrigated cemeteries	1.05	1.05	1.05	1.05	1.05	1.05	1.05	1.05	1.05	1.05	1.05	1.05
vacant urban	0.80	0.80	0.80	0.53	0.26	0.26	0.26	0.26	0.26	0.26	0.53	0.80
none	0.90	0.90	0.90	0.90	0.90	0.90	0.90	0.90	0.90	0.90	0.90	0.90

Table 17: Monthly crop coefficients for miscellaneous land uses which do not satisfy any of their theoretical applied water demands with surface water or groundwater.

Year	Cotton	Grain & Hay	Citrus	Vineyards	Alfalfa	Field Corn	Olives	Almonds	Silage Corn	Plums	Walnuts	Pistachios	Total Acreage
1970	118400	125735	87140	69341	100000	11500	14263	3578	26900	9430	23544	305	590136
1971	118000	103793	87658	68739	109000	12100	14318	4140	33200	9588	25081	489	586106
1972	126800	81152	87755	71797	118600	6100	14417	4131	13100	9531	23197	493	557073
1973	135400	123076	90245	76068	102000	25000	15106	5522	22100	11111	30162	685	636475
1974	171400	105520	90062	79633	95350	16500	14949	4430	40300	11067	28832	675	658718
1975	104000	189785	89803	79983	88700	8000	14956	8128	58500	1629	29948	760	674192
1976	143000	148564	90978	75367	84000	15000	15000	8240	51540	12171	28502	845	673207
1977	209830	51632	90463	74636	52000	3272	14996	8256	44000	12447	28874	935	591341
1978	214145	101845	90112	74988	75000	3120	16384	8337	40400	12951	29104	935	667321
1979	218845	94375	90067	75322	75000	3000	15128	25404	56000	13126	29135	933	696335
1980	176680	148950	84517	77414	80000	16800	13864	9774	47300	14257	26201	1497	697254
1981	167540	130820	84835	82002	85000	18000	13823	10989	46070	14435	26688	2060	682262
1982	152470	119750	84803	84032	81400	11700	13780	11247	60670	14718	26704	2246	663520
1983	115315	87760	85361	84810	85000	10000	13910	11314	59900	14697	26696	2285	597048
1984	181280	80100	84505	85873	90000	14000	13735	11227	72400	14918	26349	2291	676678
1985	156160	74900	84966	84152	93500	14000	13876	10898	71000	15762	26228	2696	648138
1986	124720	73400	85658	79324	100000	11000	14164	10490	69000	15987	25911	2746	612400
1987	148300	69400	88588	73769	100000	8200	14297	10150	66100	16895	25639	3382	624720
1988	170800	54600	89123	70575	90000	7000	14536	10183	67200	17154	25565	3619	620355
1989	137000	90500	89280	68146	90000	10600	14315	9296	48300	17764	24832	3806	603839
1990	136000	112700	94258	71044	105000	8000	15409	10747	60200	18625	26082	5030	663094
1991	146000	93100	99236	73942	103000	5000	16502	12198	61500	19486	27331	6254	663549
1992	145000	107500	107171	77797	87800	10200	17485	11877	61500	21508	27822	6065	681725
1993	144600	115210	108350	76431	76900	10200	17916	11119	56100	21382	26800	6201	671209
1994	139800	123860	109839	75912	83900	12200	19120	12861	60700	20832	27322	6764	693110
1995	139400	134000	112320	76535	82800	8000	18518	13317	71200	19608	28569	7782	712049
1996	110900	146430	112256	79949	76900	10800	18410	14100	97500	19692	28765	7594	723296
1997	88300	126910	115851	81574	84800	25400	18547	14602	98000	18245	30613	8704	711546
1998	62100	138104	116187	82528	104000	35000	17496	15576	104000	18591	30384	9316	733282
1999	67200	144579	120164	87015	103000	17000	18641	16466	103000	20292	33334	10578	741269

Table 18: Acreage of major crops in Tulare County, California from 1970-99.

Major Texture Category	**Specific Yield (%)**
Gravel	25
Medium- to coarse-grained sand	25
Fine-grained sand	10
Silt	5
Clay	3
Crystalline bedrock	0

Table 19: Percent specific yield values for major texture categories.

Data Type	**Source**
Specific Yield	DWR
Specific Storativity	Lofgren and Klausing (1969)
Production Well Hydraulic Head Observations	DWR
Ground Surface Boundary Elevation	USGS
Corcoran Clay Member Boundary Elevations	Erlewine (1989)
Aquifer System Bottom Boundary Elevation	Erlewine (1989)

Table 20: Data type and source for the groundwater flow model.

Calendar months in stress period	**Approximate season of stress period**	**Number of days in stress period**
April, May	Spring	61
June, July, August, September	Summer	122
October, November	Fall	61
December, January, February, March	Winter	121

Table 21: Quasi-seasonal stress periods.

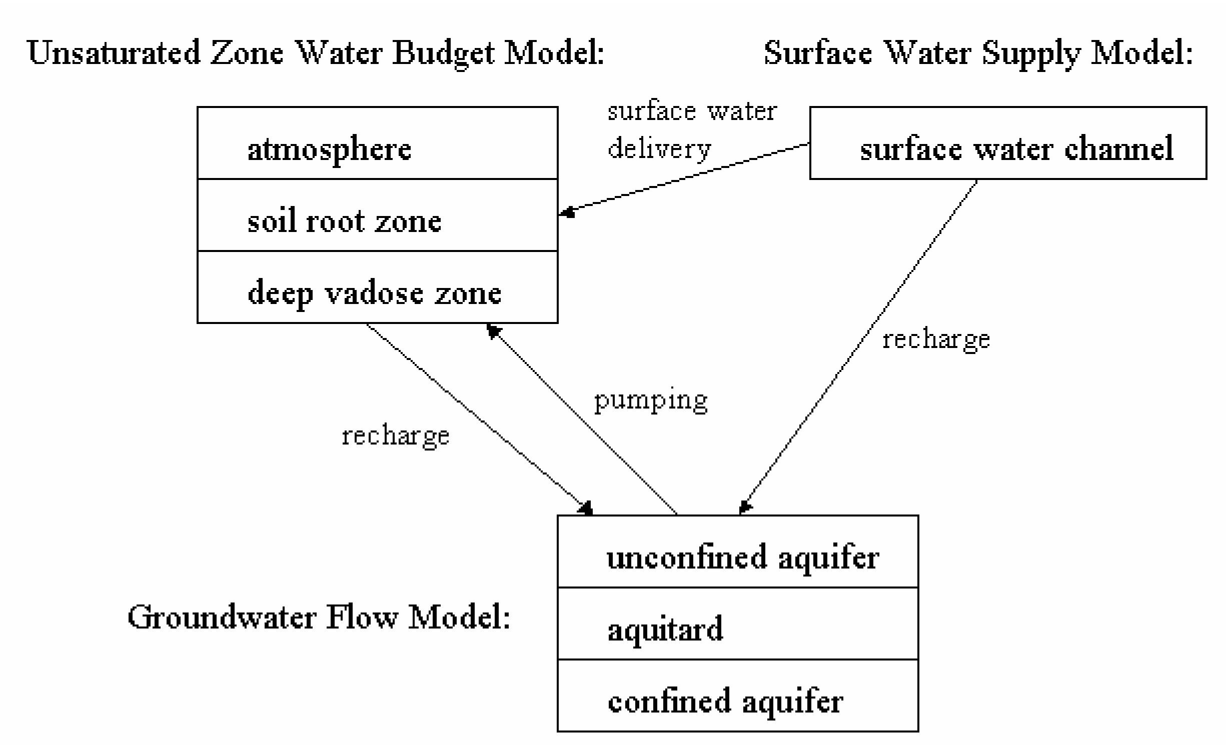

Figure 1: Relationships between the conjunctive use sub-models.

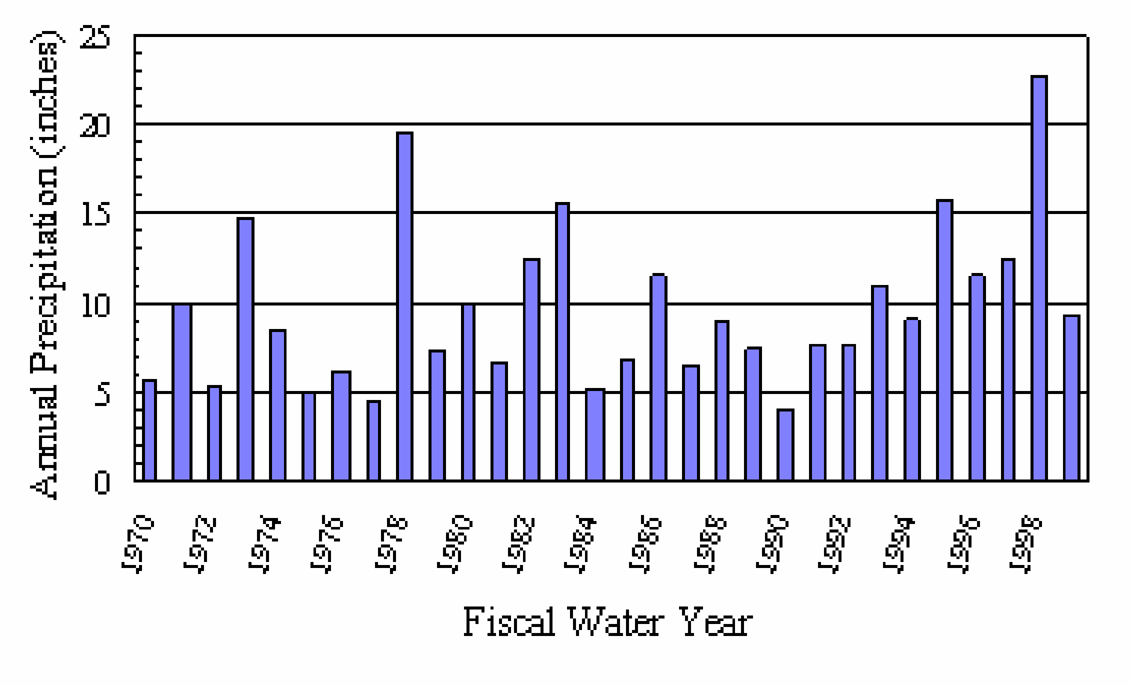

Figure 2: Annual precipitation (inches) for the fiscal water years of 1970-99 measured at the Tulare Irrigation District and Vistal gauging stations (1970-95) and at the Visalia gauging station (1996-99).

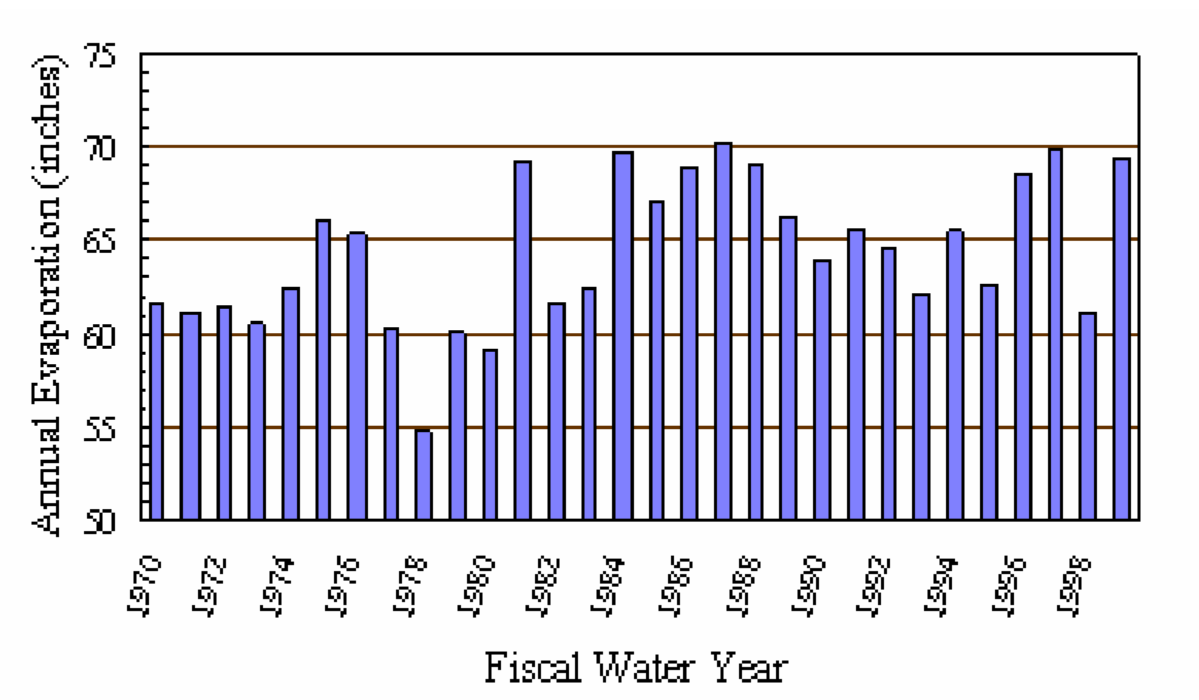

Figure 3: Annual pan evaporation (inches) representative of the southern San Joaquin Valley for the fiscal water years of 1970-99.

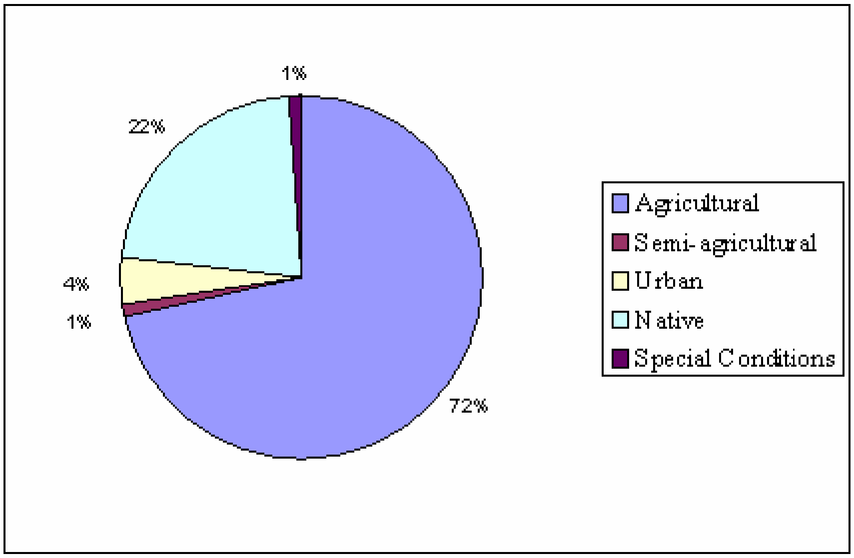

Figure 4: Percentages of major land-use categories from 1985 land-use survey.

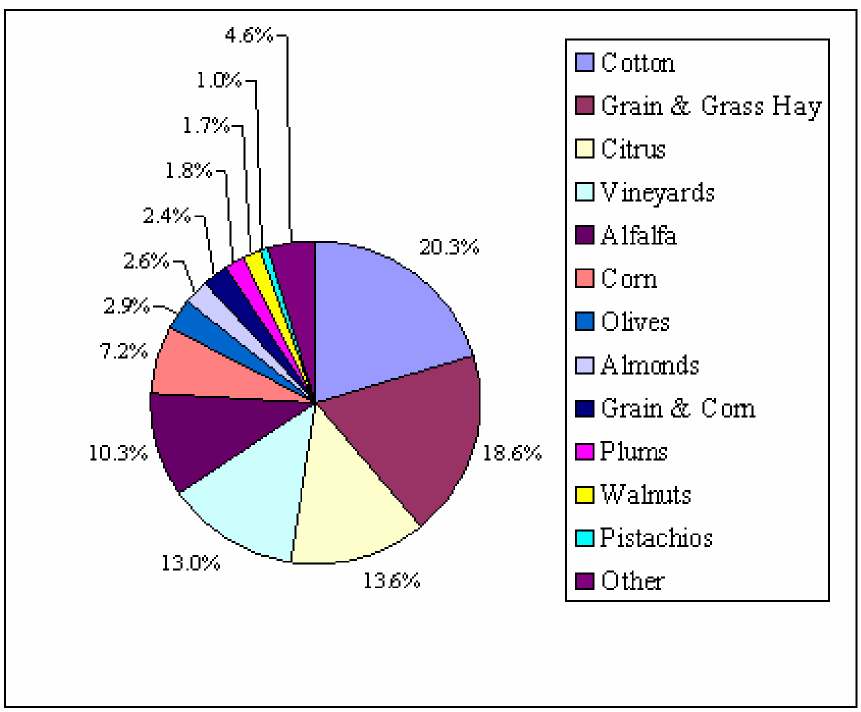

Figure 5: Percentages of major crops grown from 1985 land-use survey.

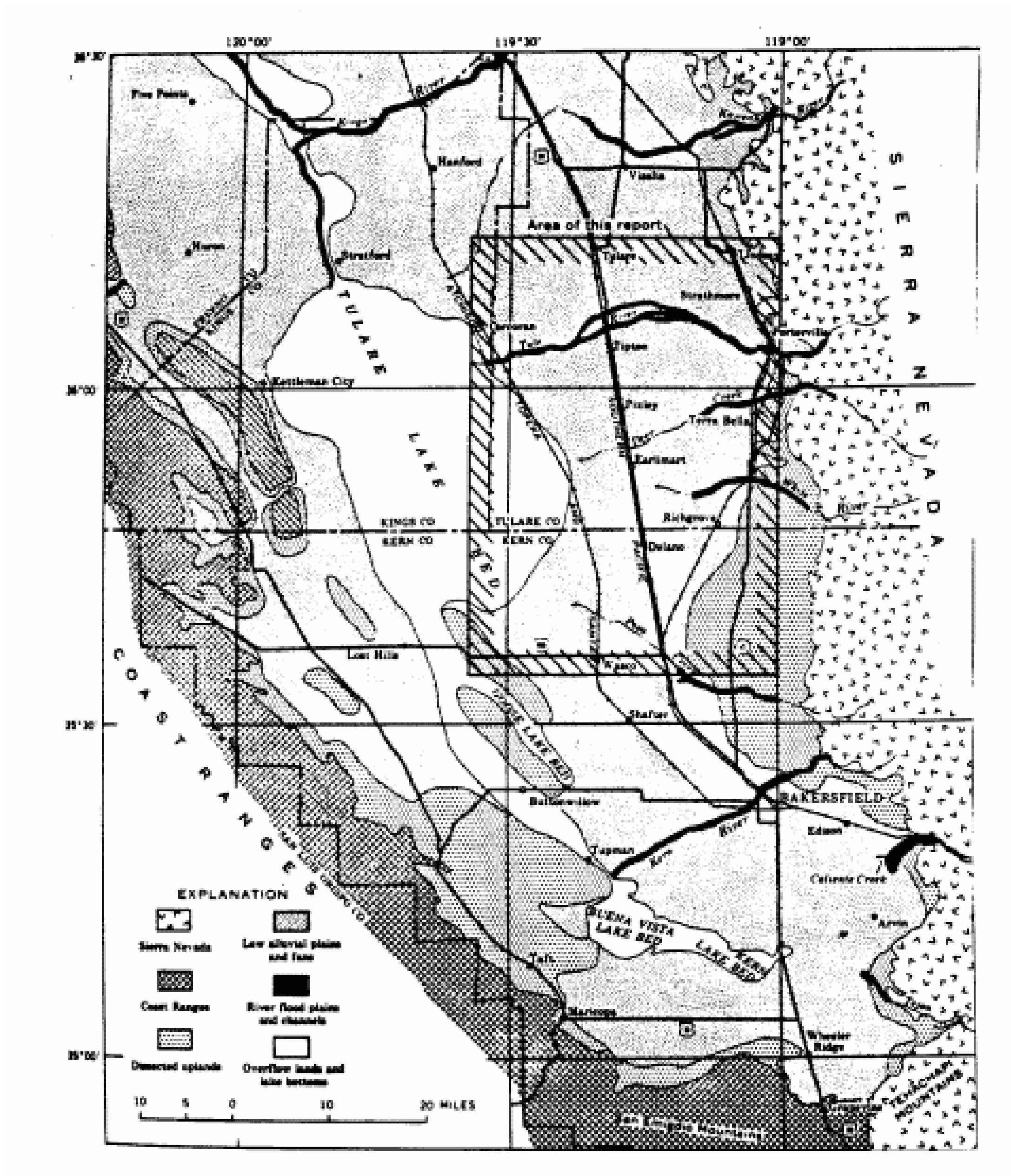

Figure 6: Geomorphic units in the study area.

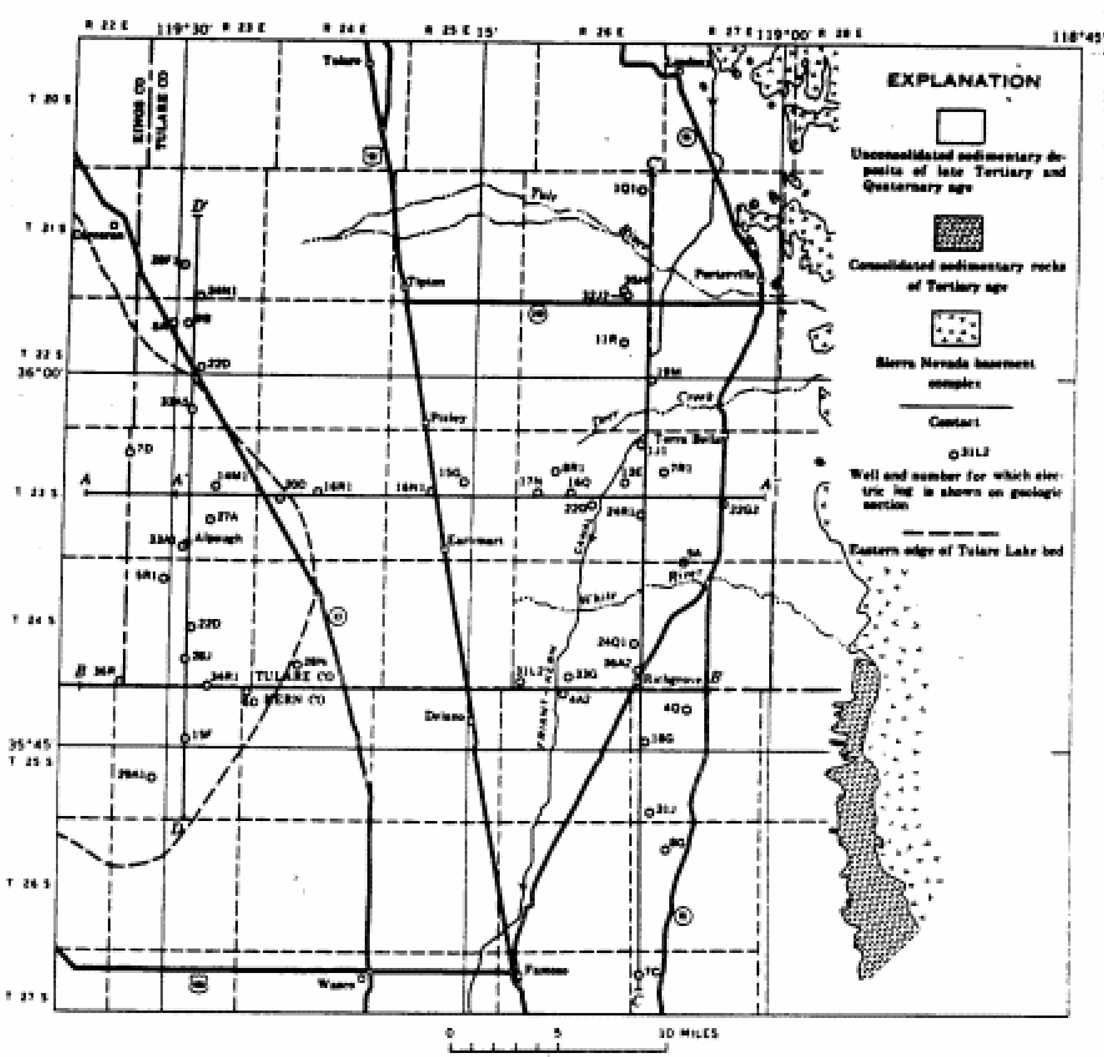

Figure 7: Locations of geologic cross-sections in the Tulare-Wasco area.

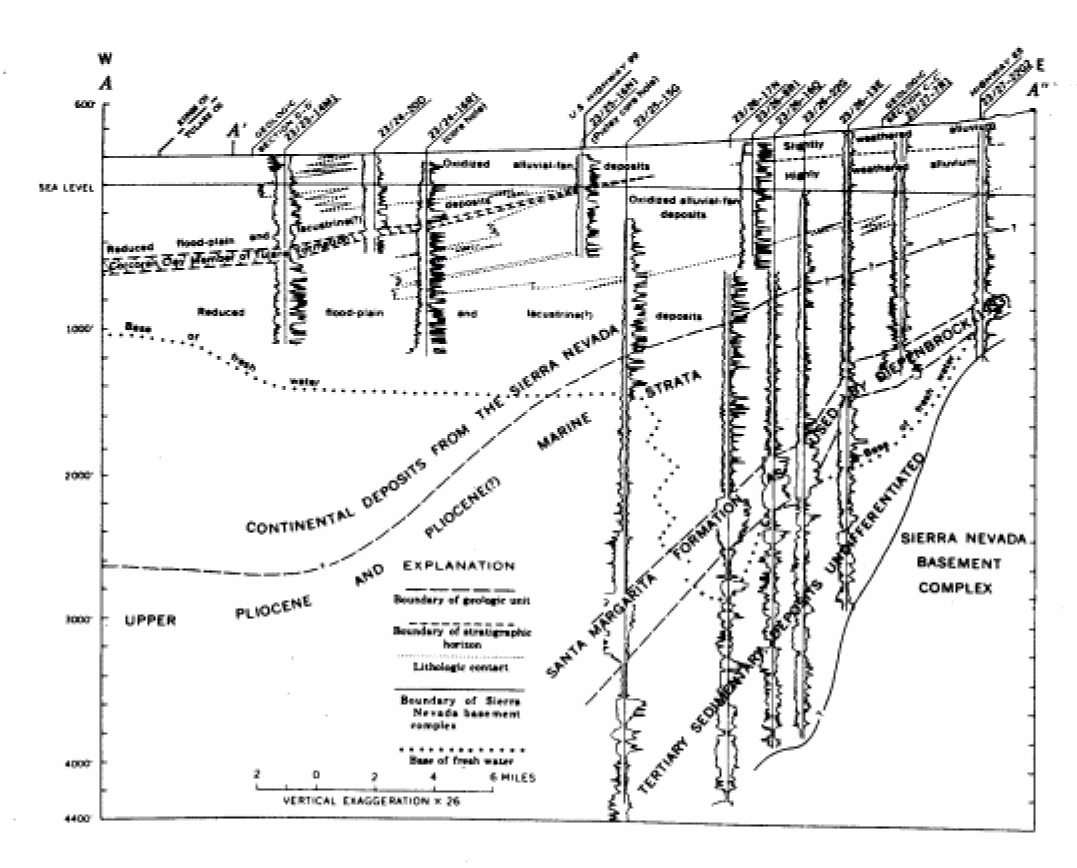

Figure 8: Geologic cross-section *A – A'*.

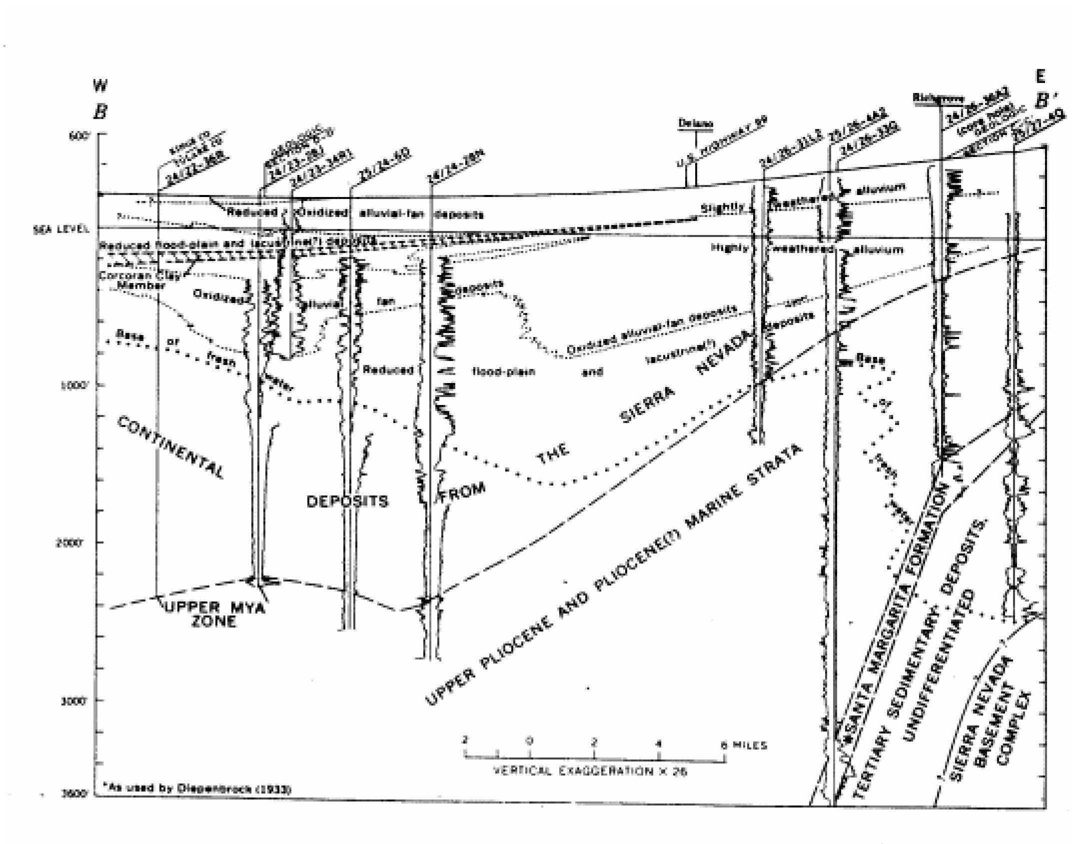

Figure 9: Geologic cross-section *B* – *B*'.

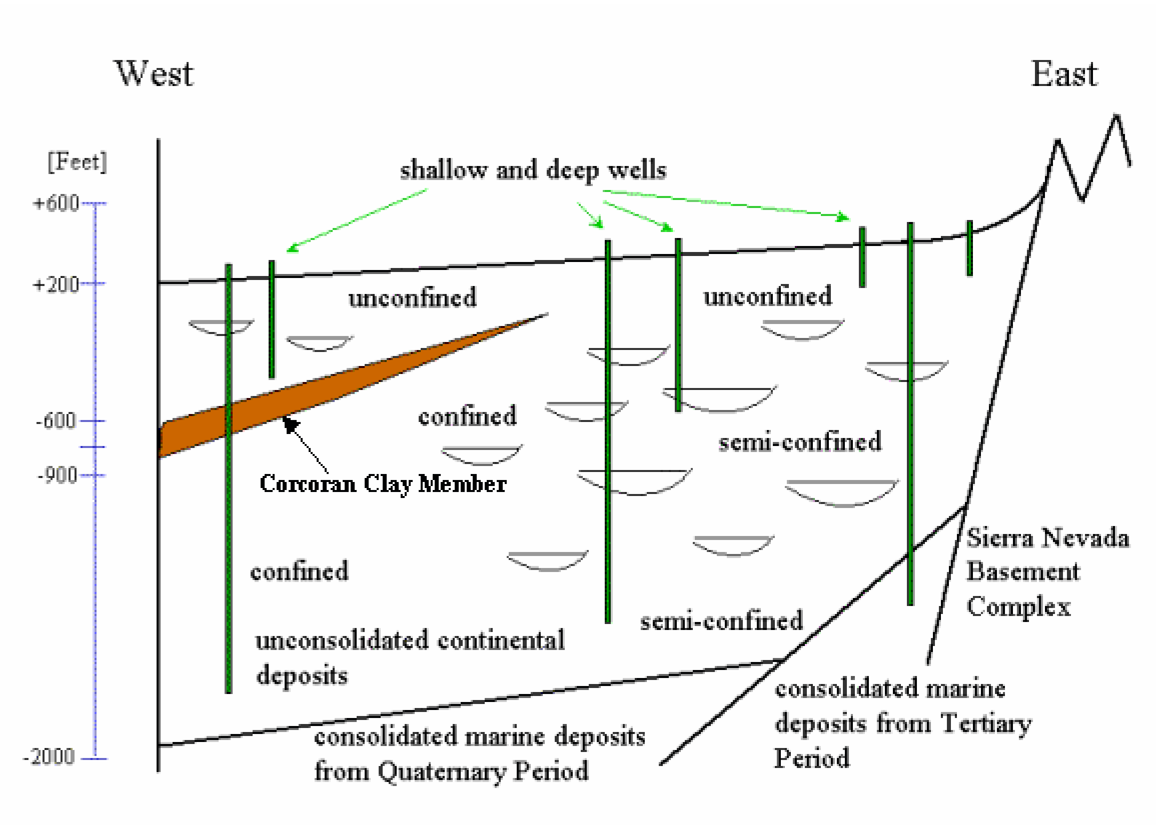

Figure 10: Conceptual model of the aquifer system hydrogeology in the east-west direction.

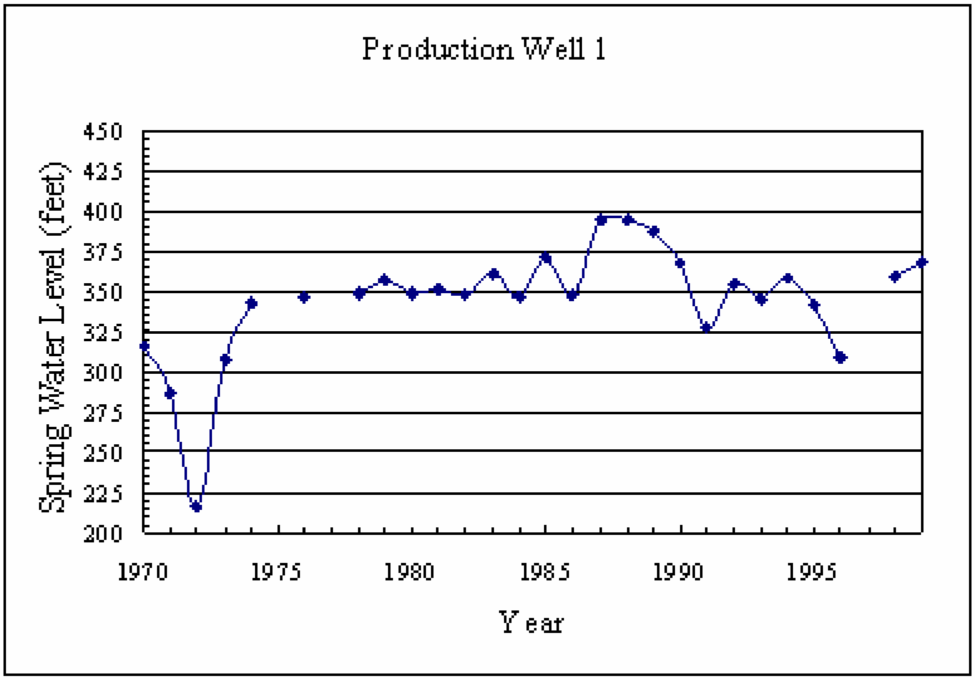

Figure 11: Hydraulic head hydrograph (feet) for production well 1 (Plate 21) from 1970-99.

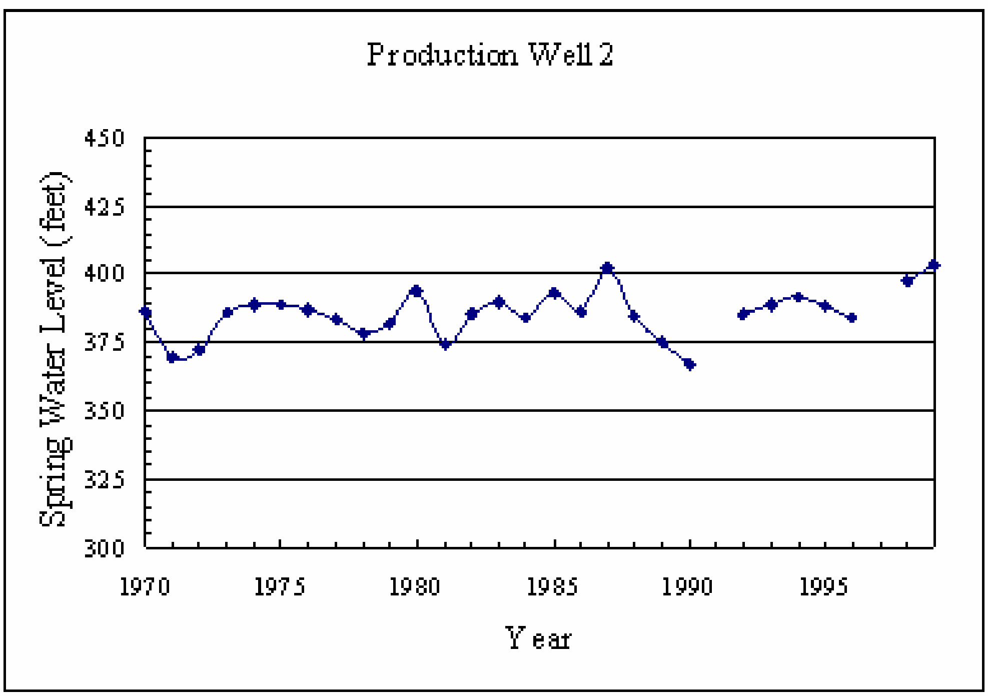

Figure 12: Hydraulic head hydrograph (feet) for production well 2 (Plate 21) from 1970-99.

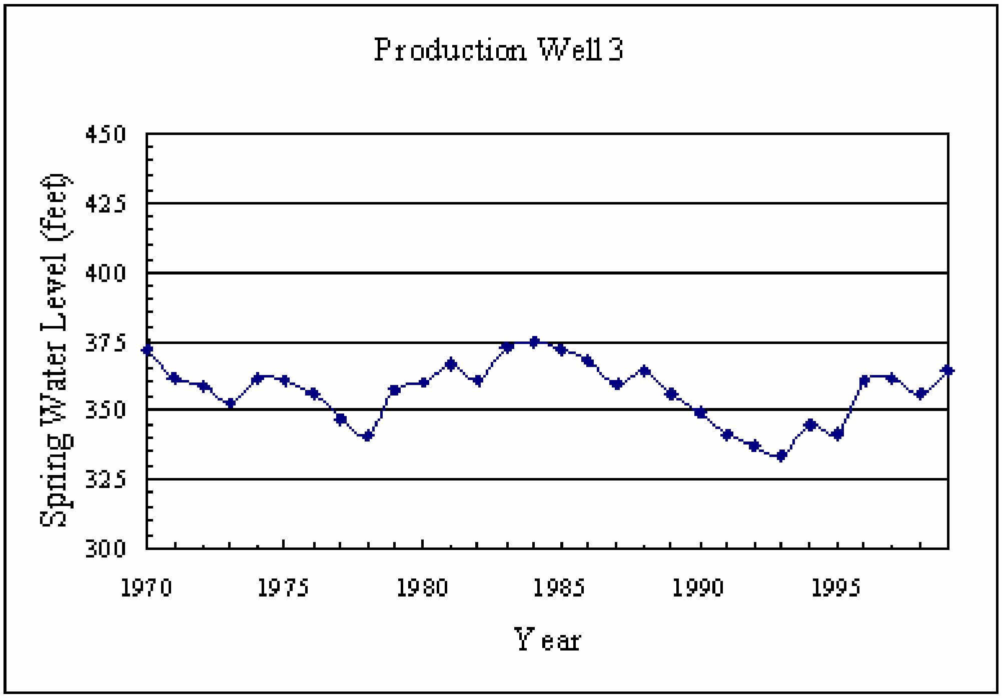

Figure 13: Hydraulic head hydrograph (feet) for production well 3 (Plate 21) from 1970-99.

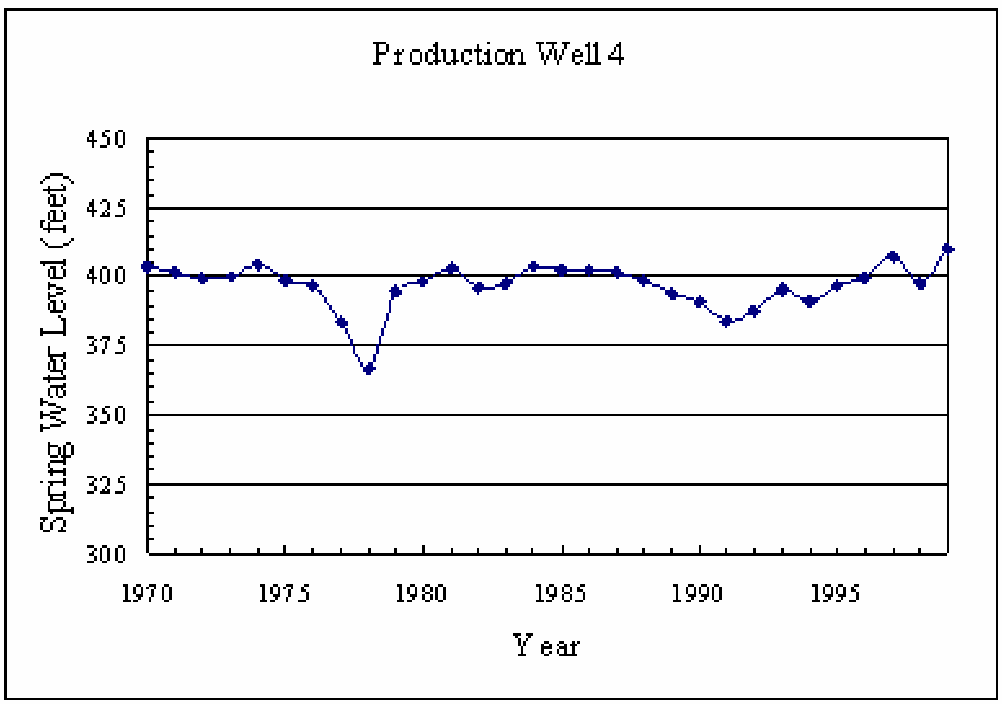

Figure 14: Hydraulic head hydrograph (feet) for production well 4 (Plate 21) from 1970-99.

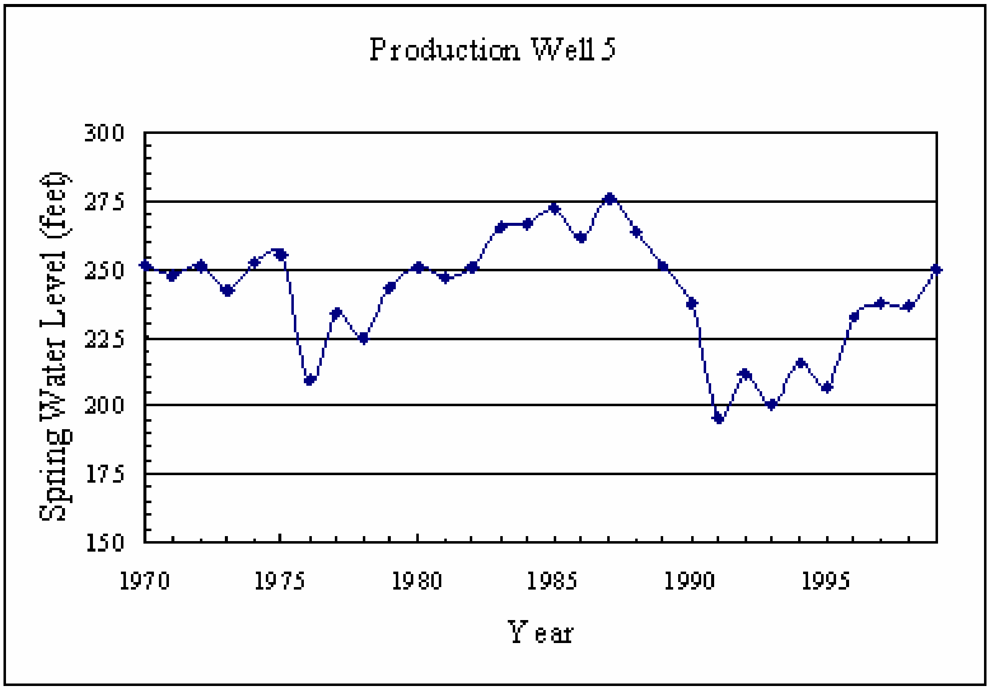

Figure 15: Hydraulic head hydrograph (feet) for production well 5 (Plate 21) from 1970-99.

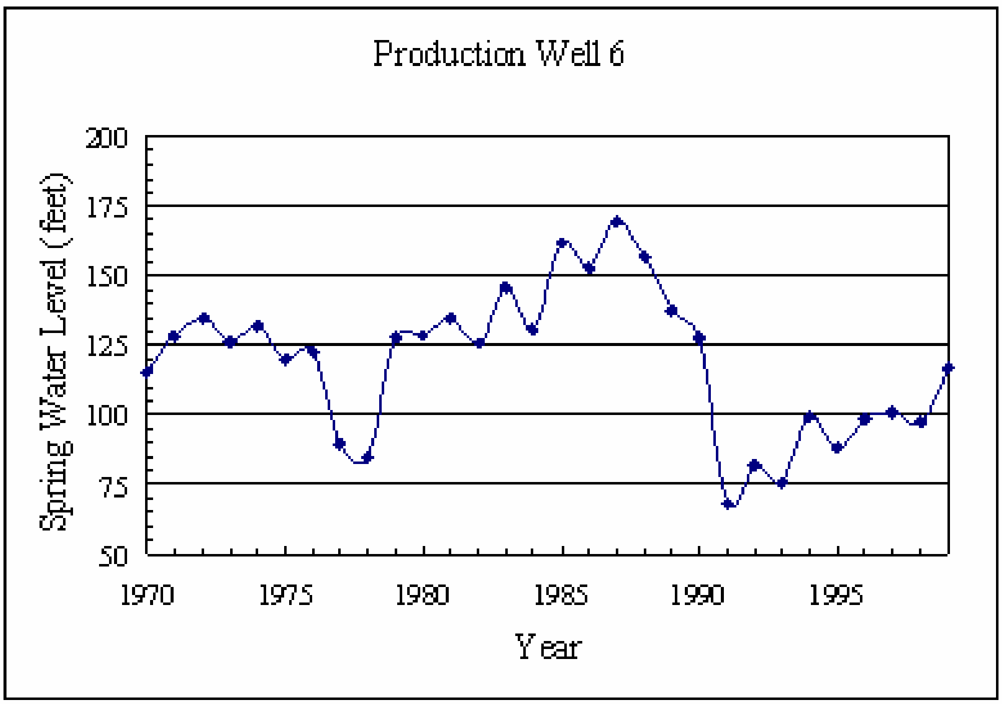

Figure 16: Hydraulic head hydrograph (feet) for production well 6 (Plate 21) from 1970-99.

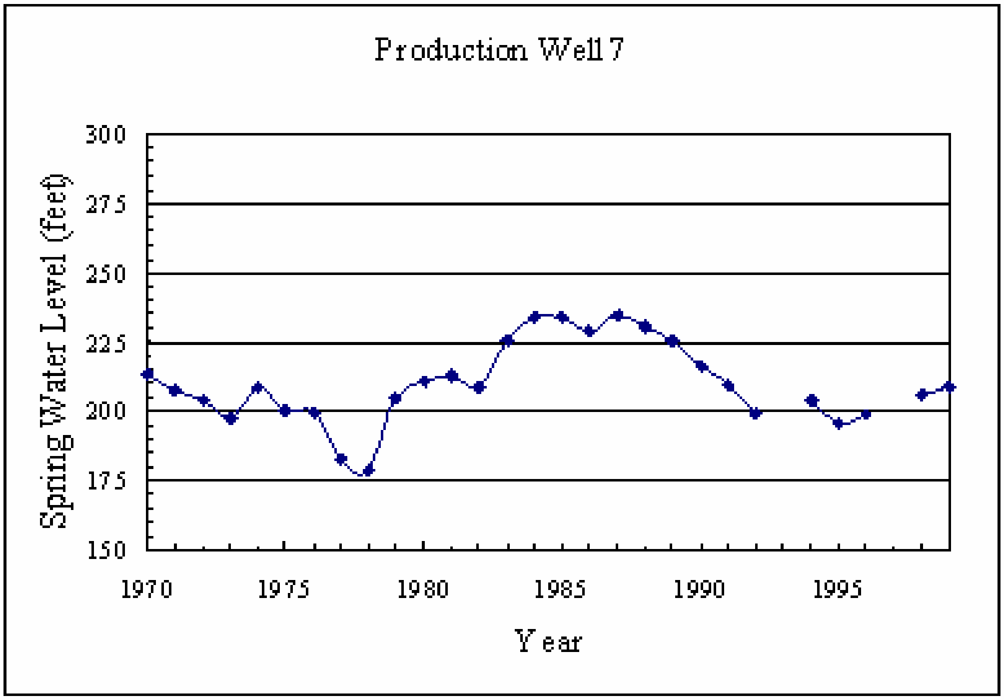

Figure 17: Hydraulic head hydrograph (feet) for production well 7 (Plate 21) from 1970-99.

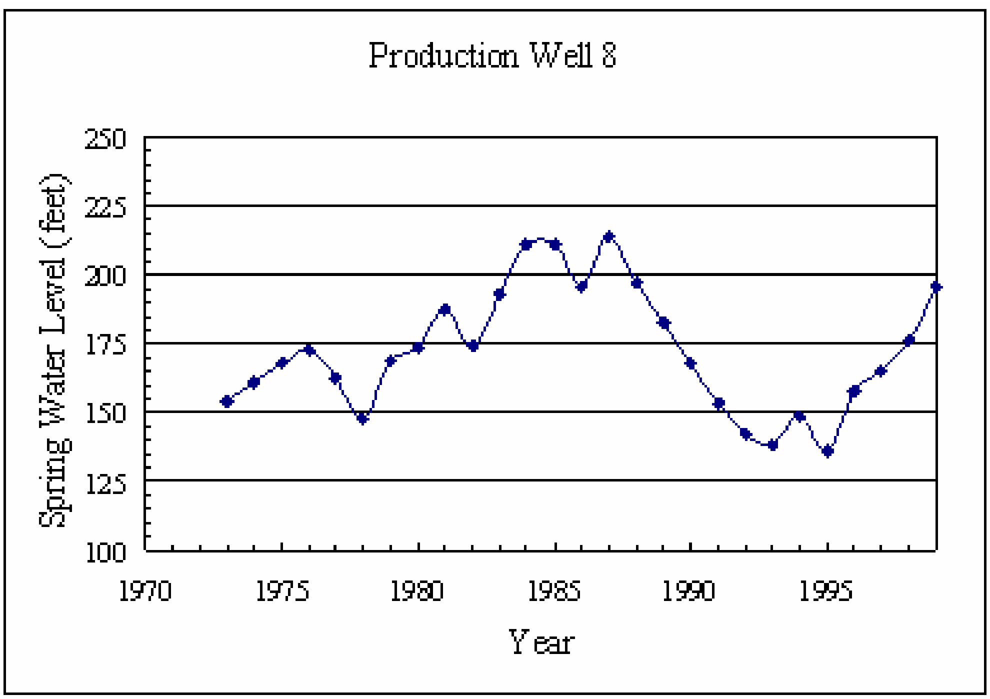

Figure 18: Hydraulic head hydrograph (feet) for production well 8 (Plate 21) from 1970-99.

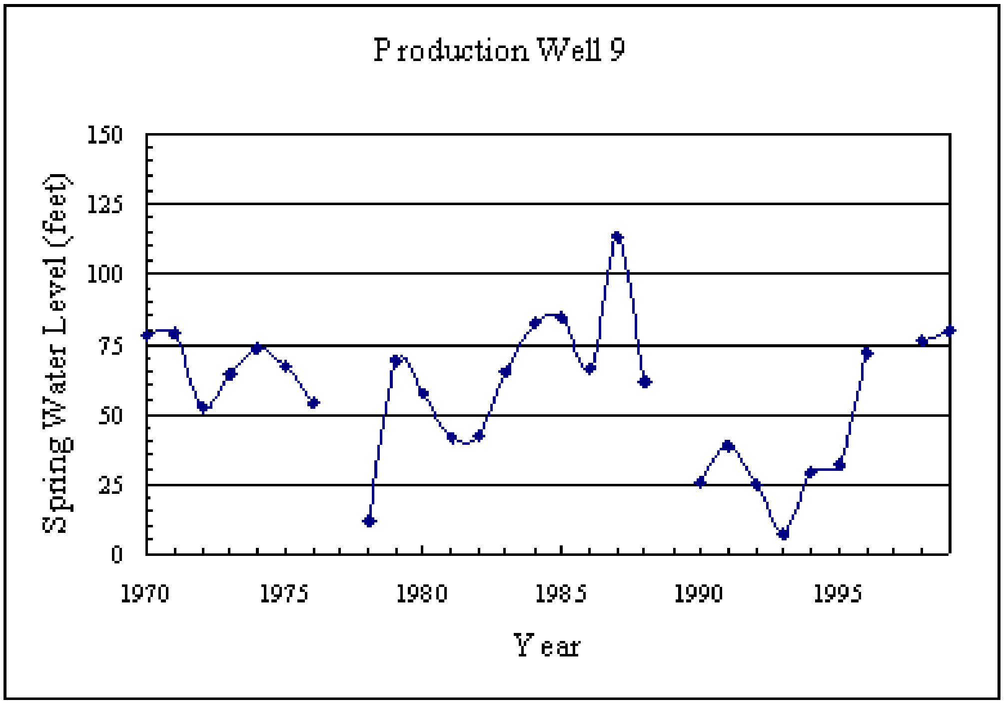

Figure 19: Hydraulic head hydrograph (feet) for production well 9 (Plate 21) from 1970-99.

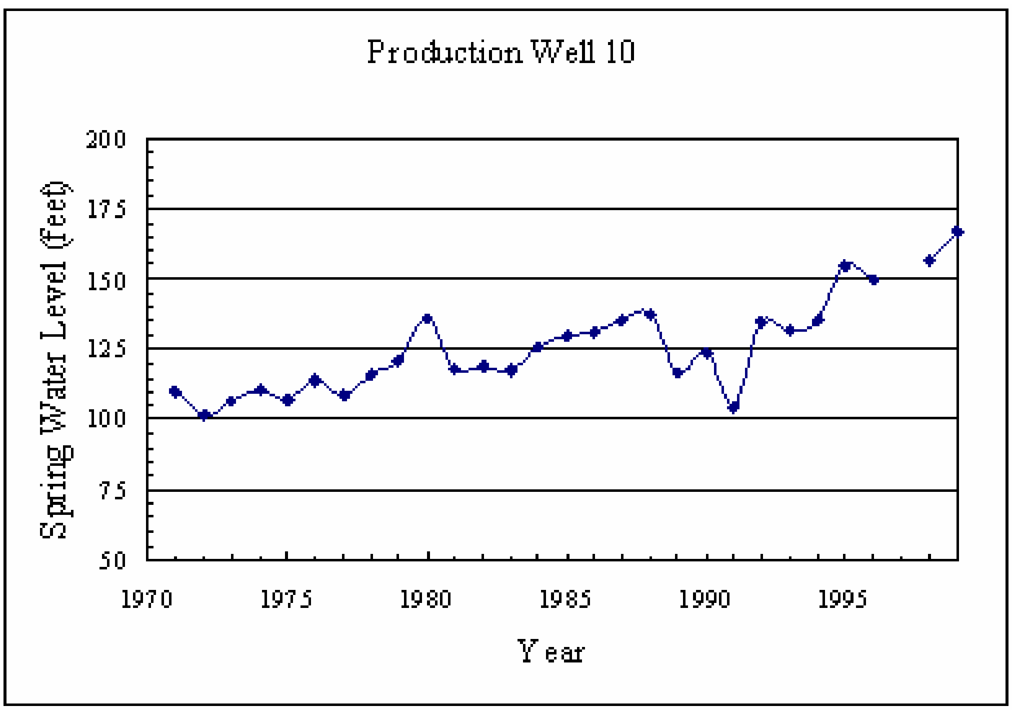

Figure 20: Hydraulic head hydrograph (feet) for production well 10 (Plate 21) from 1970-99.

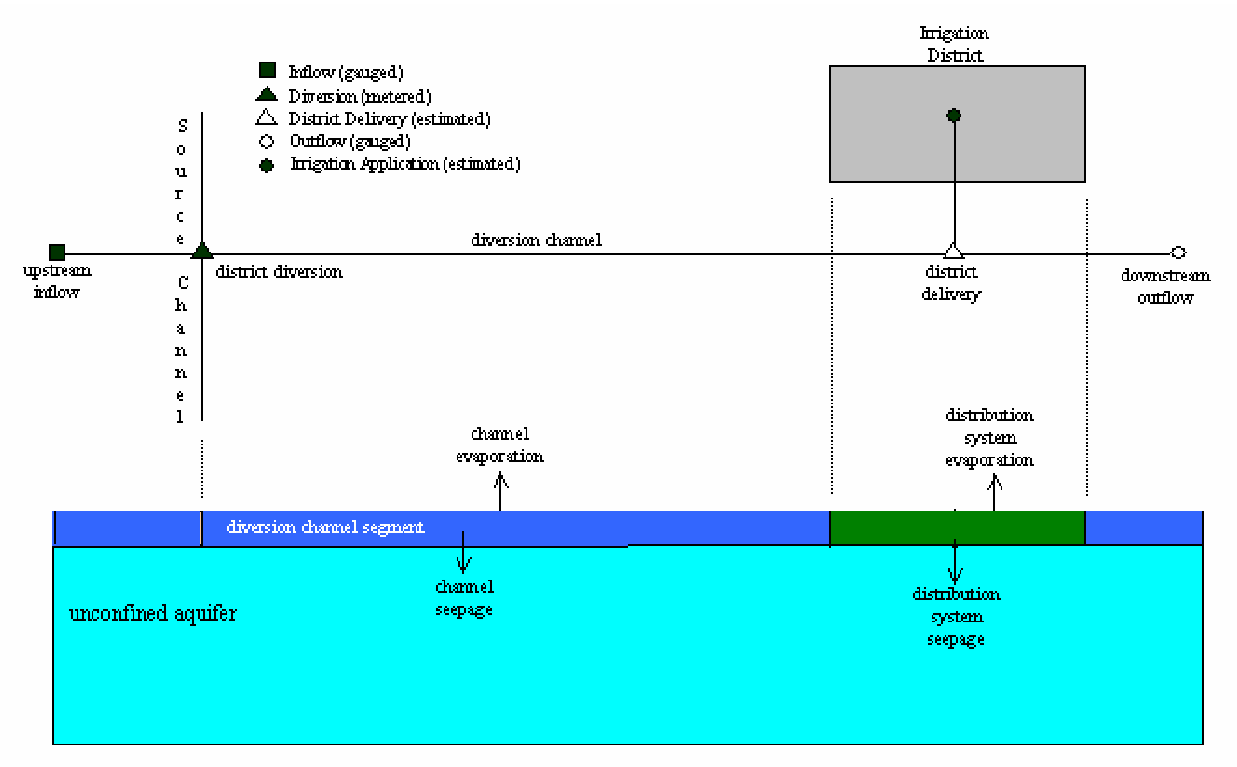

Figure 21: Conceptual model of the surface water supply system.

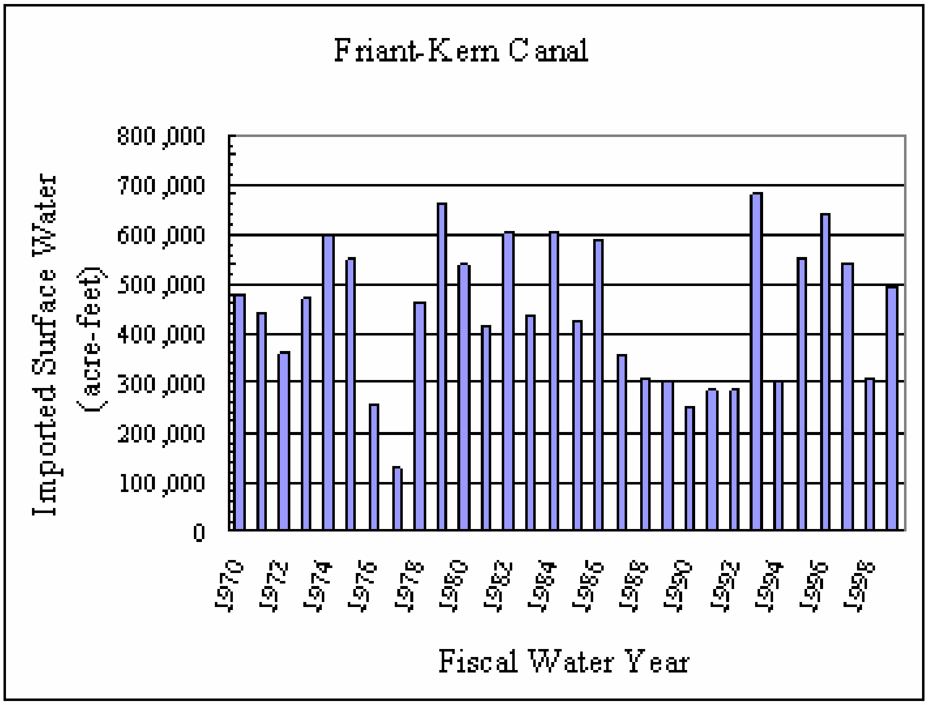

Figure 22: Annual imported surface water (acre-feet) from the Friant-Kern Canal for fiscal water years 1970-99.

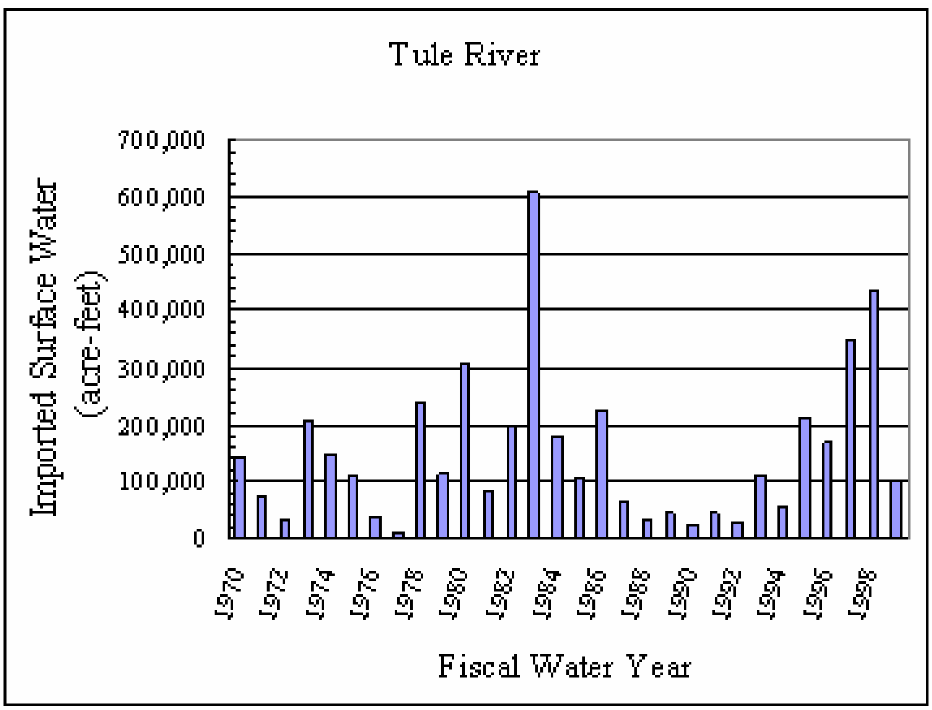

Figure 23: Annual imported surface water (acre-feet) from the Tule River for fiscal water years 1970-99.

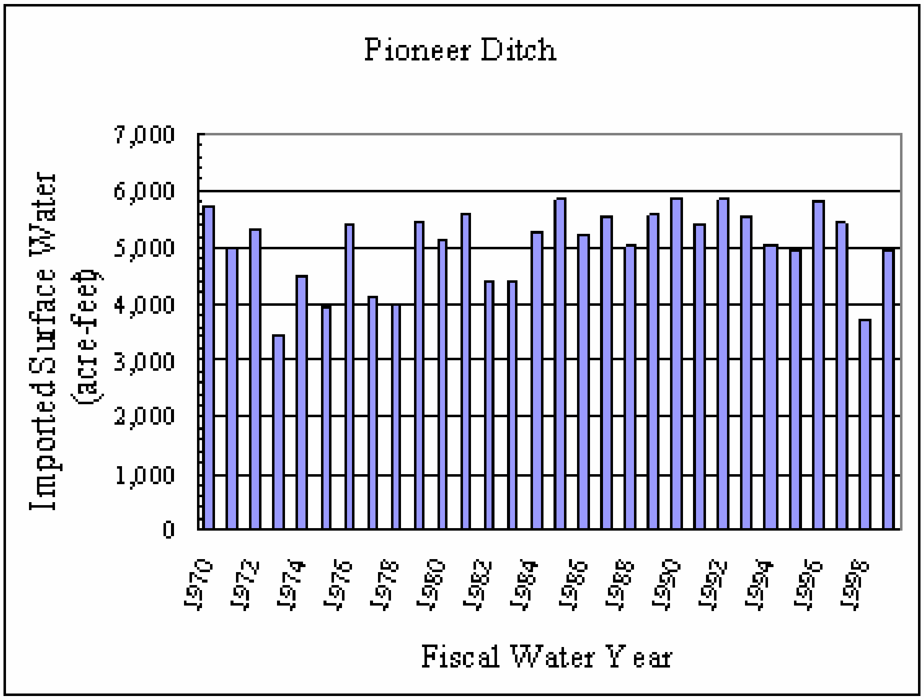

Figure 24: Annual imported surface water (acre-feet) from the Pioneer Ditch for fiscal water years 1970-99.

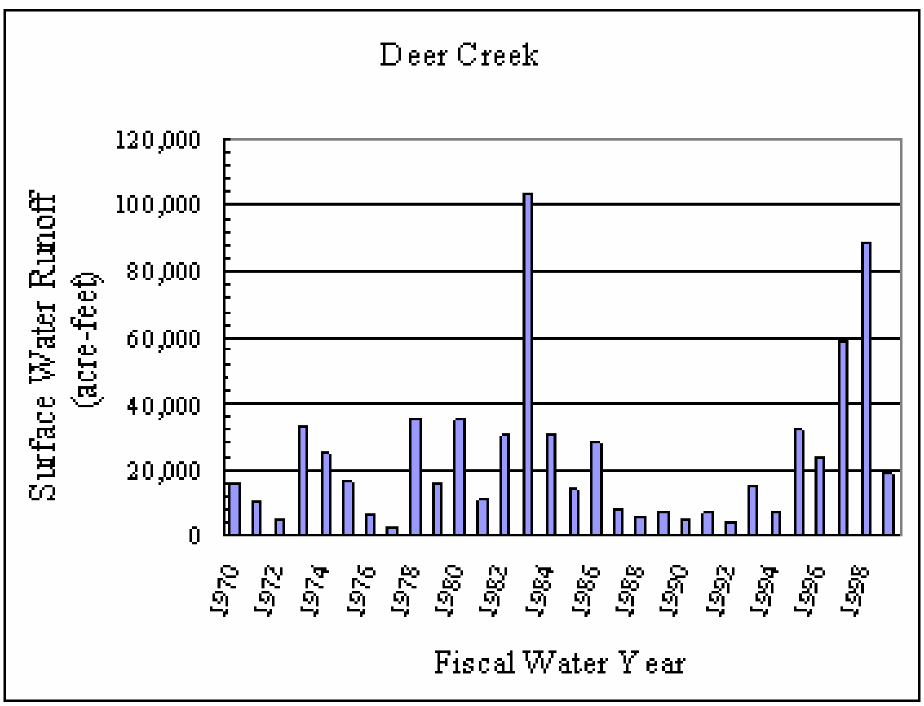

Figure 25: Annual unregulated natural runoff (acre-feet) in the Deer Creek for fiscal water years 1970-99.

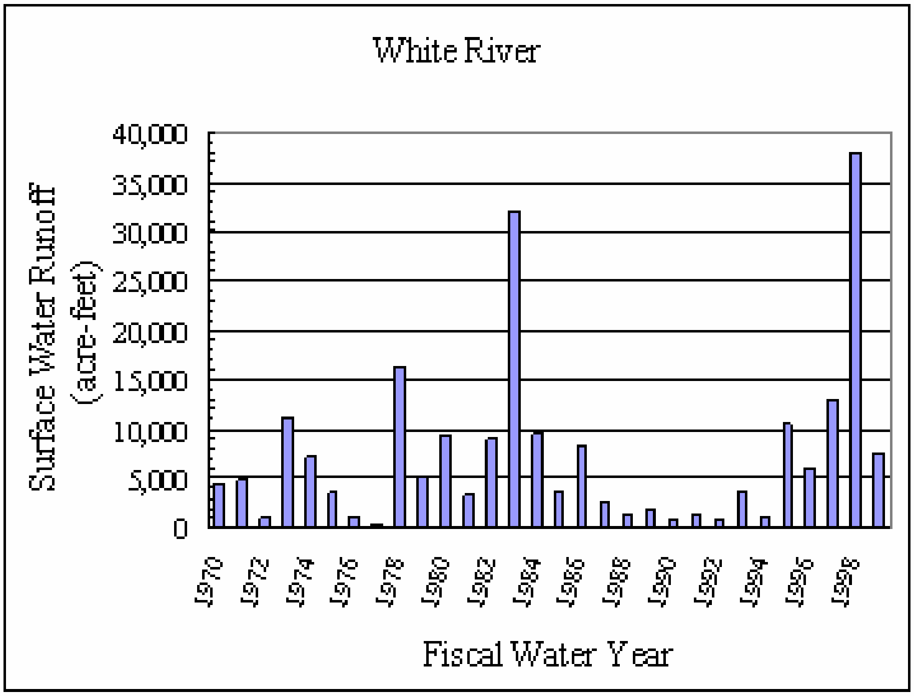

Figure 26: Annual unregulated natural runoff (acre-feet) in the White River for fiscal water years 1970-99.

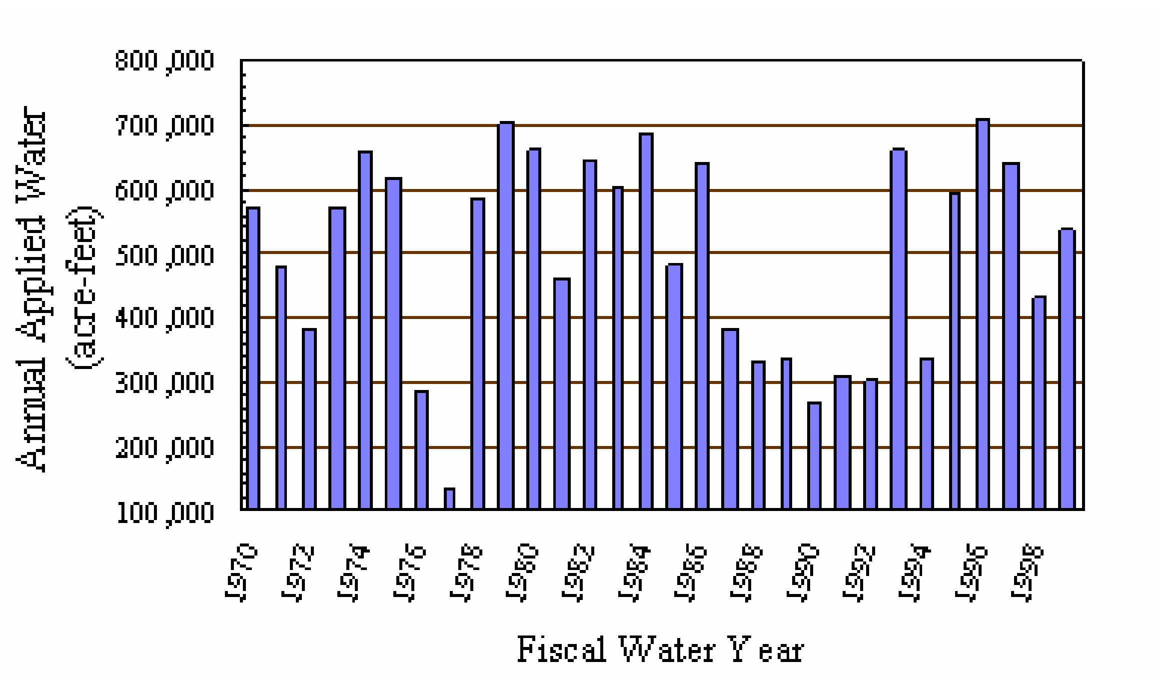

Figure 27: Annual applied water (acre-feet) from surface water deliveries for the fiscal water years of 1970-99.

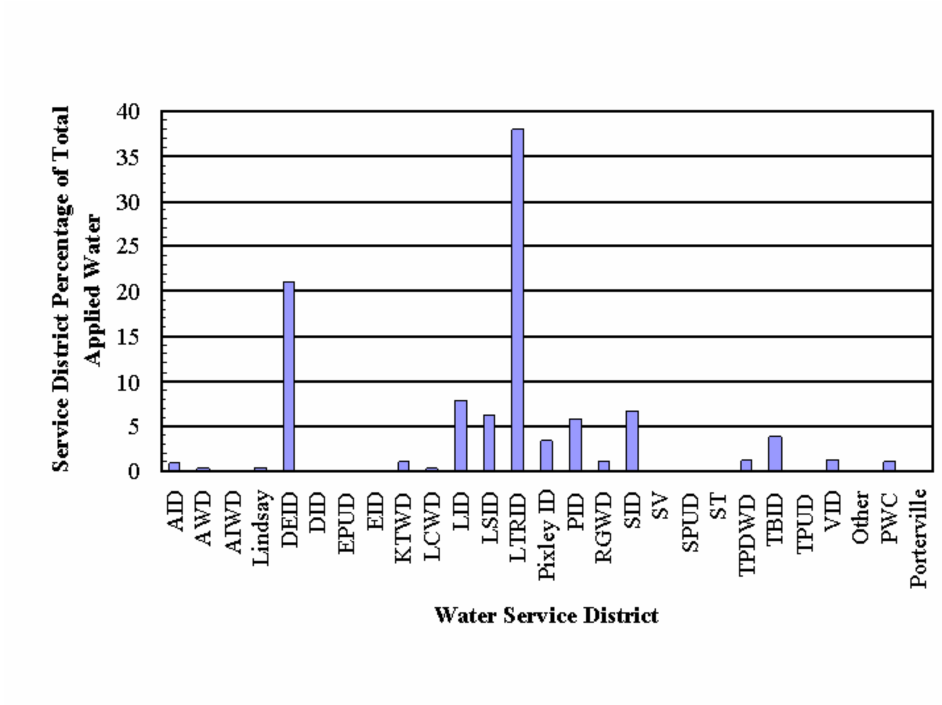

Figure 28: Percentage of applied water from 1970-99 allocated to each water service district.

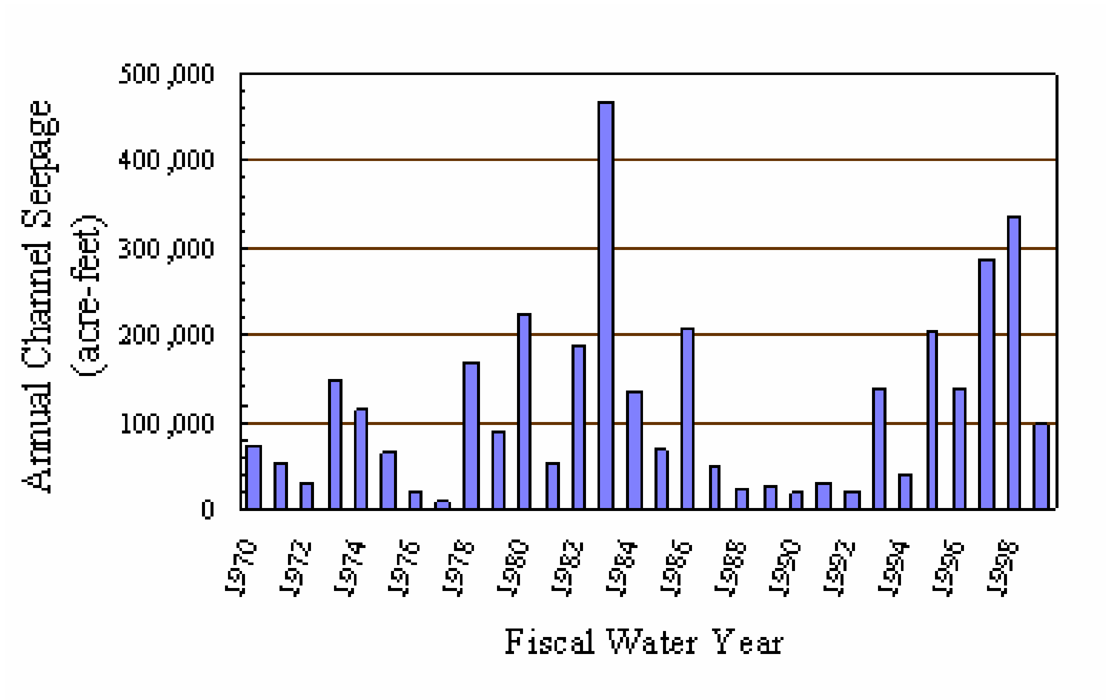

Figure 29: Annual inter-district surface water conveyance network seepage loss (acre-feet) for the fiscal water years of 1970-99.

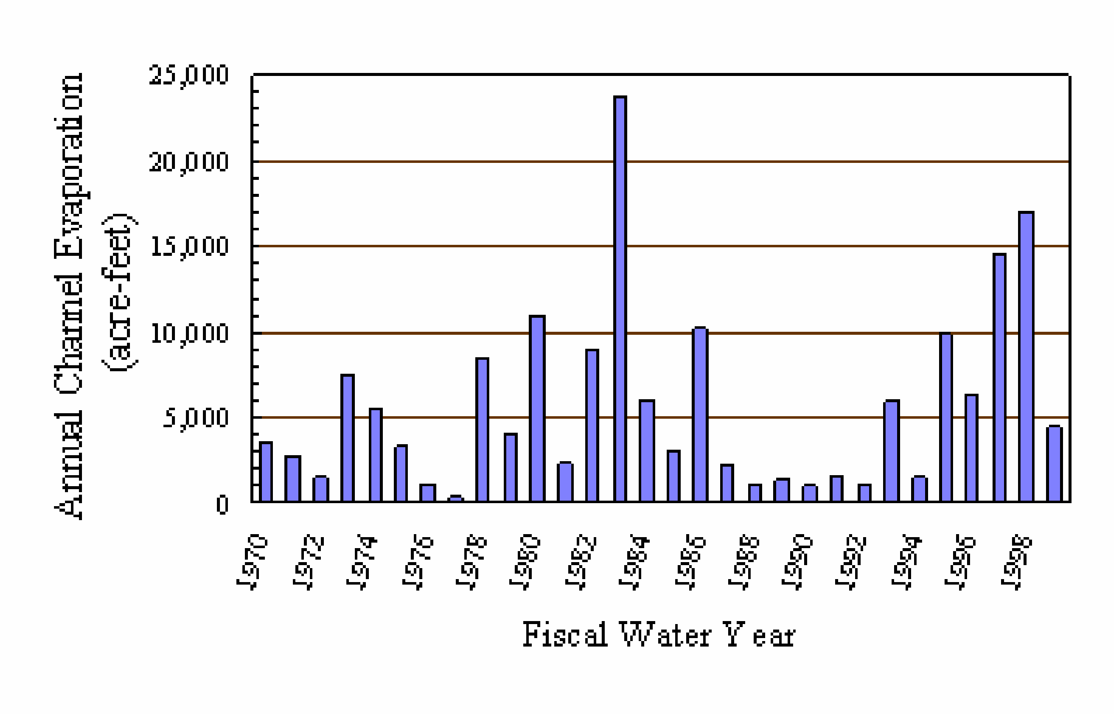

Figure 30: Annual inter-district surface water conveyance network evaporation loss (acre-feet) for the fiscal water years of 1970-99.

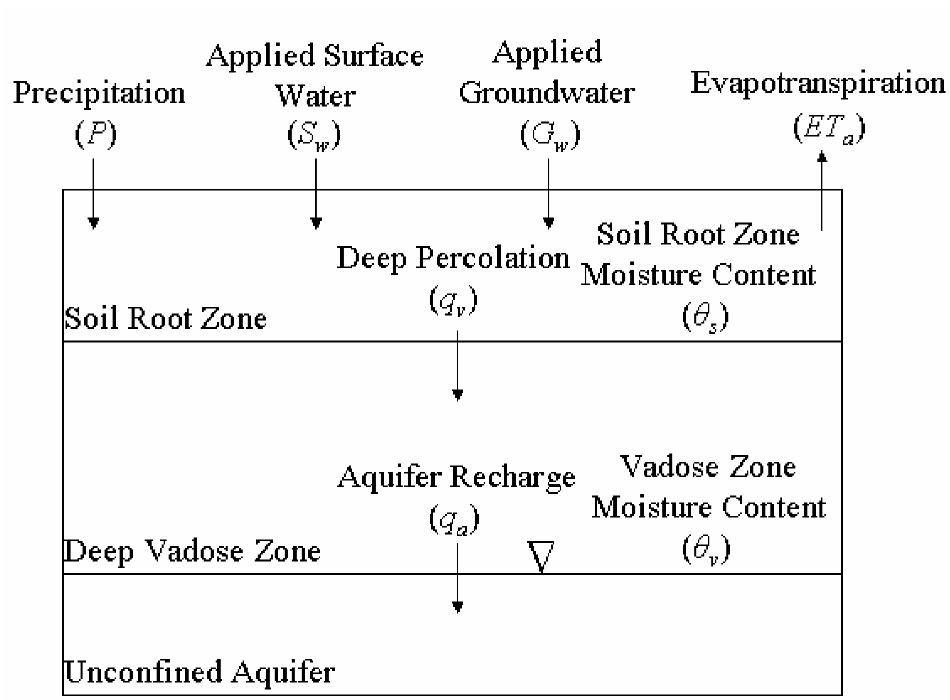

Figure 31: Conceptual model of the unsaturated zone water budget.

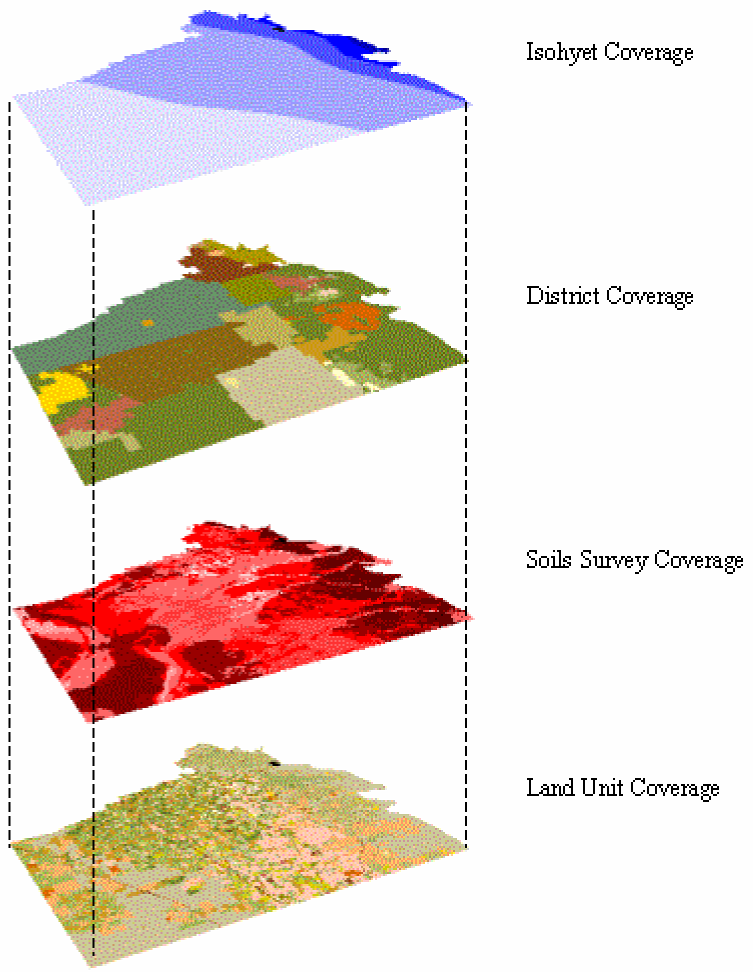

Figure 32: Illustration of GIS overlaying of isohyet, water service district, and soils survey coverage onto the land use coverage.

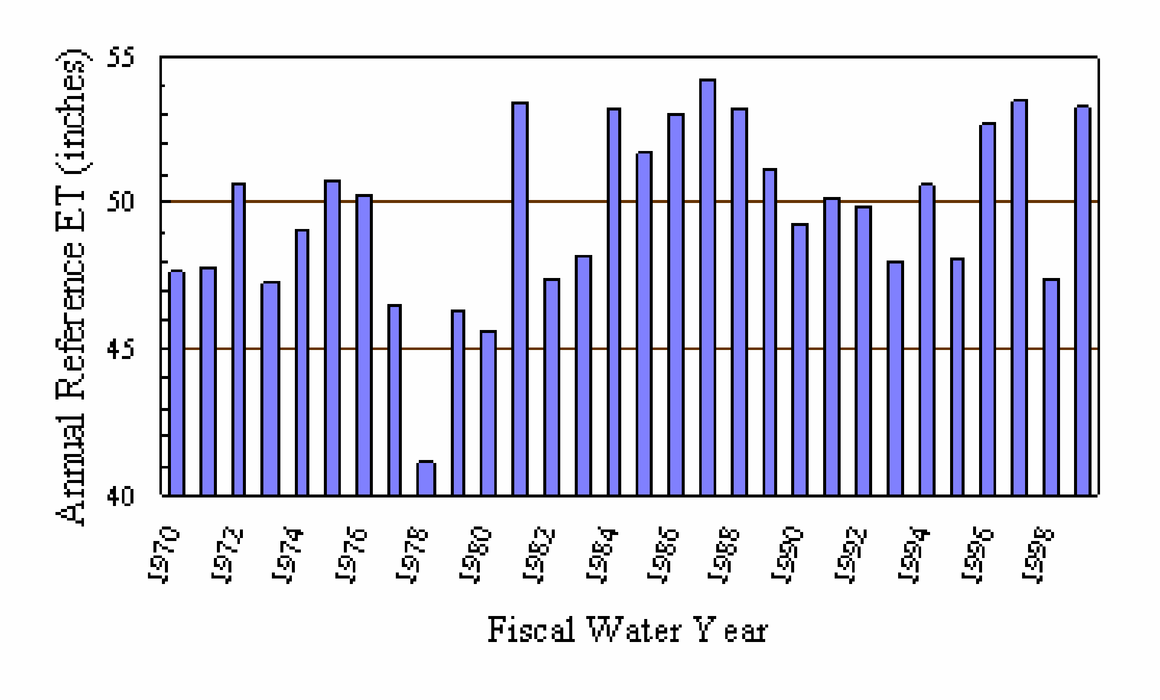

Figure 33: Annual reference (grass) evapotranspiration (*ET*o) (inches) for the fiscal water years of 1970-99 measured at the Wasco gauging station.

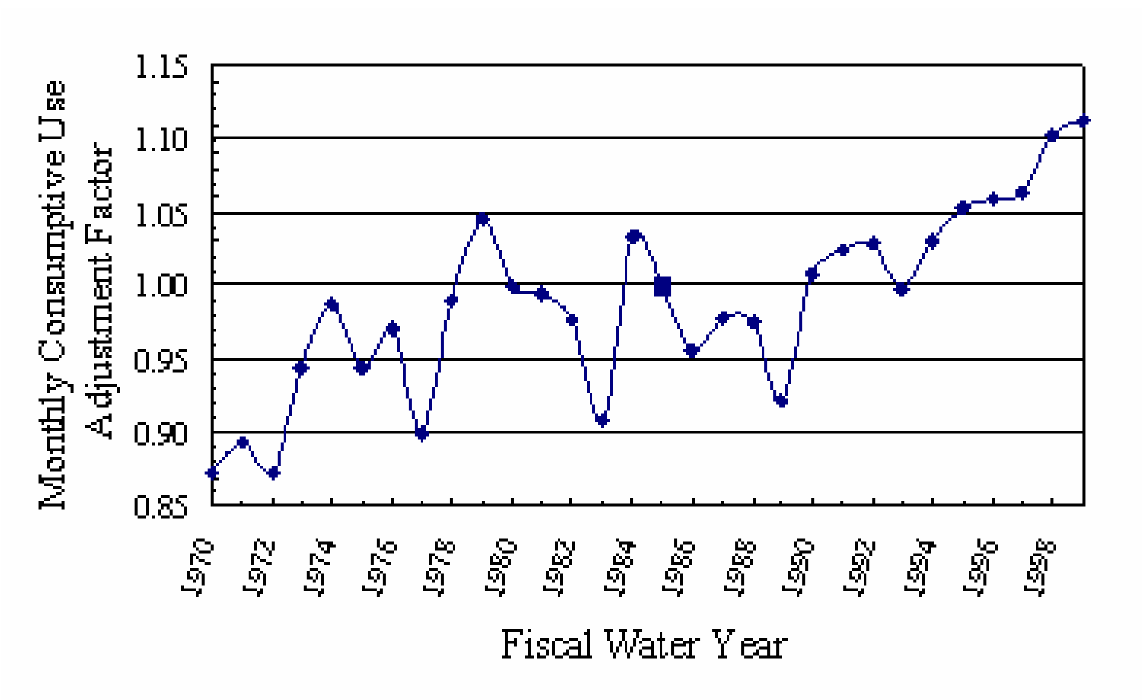

Figure 34: Monthly consumptive use adjustment factors for annual changes in acreage for the 12 major crops in Tulare County, California from 1970-99.

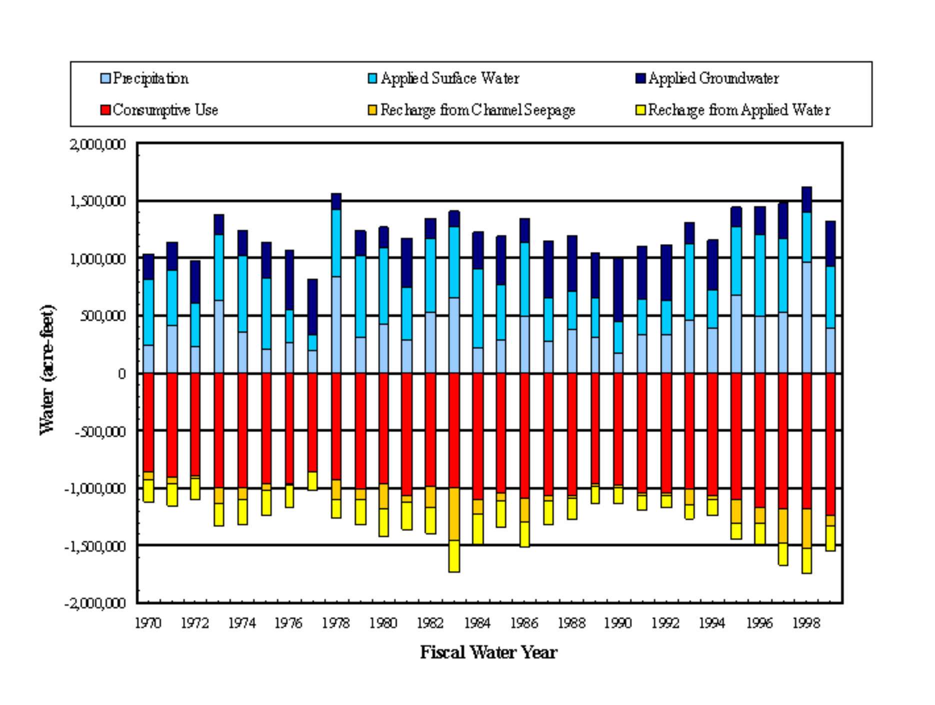

Figure 35: Annual water balance components (acre-feet) for the fiscal water years of 1970-99: precipitation, applied surface water, applied groundwater, consumptive use, diffuse recharge from applied water, and localized recharge from channel seepage.

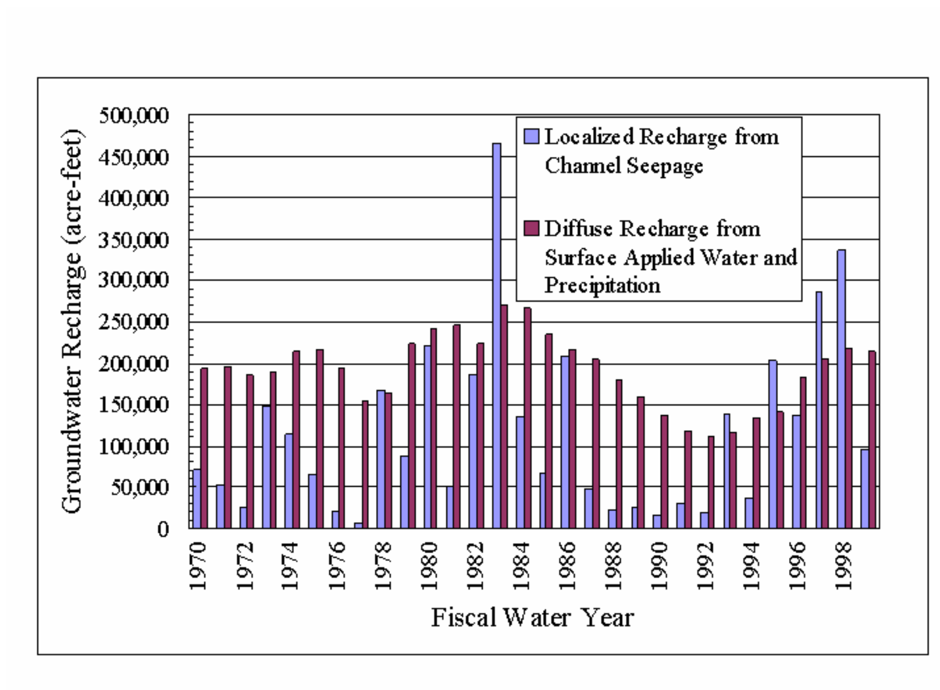

Figure 36: Annual localized recharge from channel seepage and diffuse recharge from surface applied water and precipitation (acre-feet) from 1970-99.

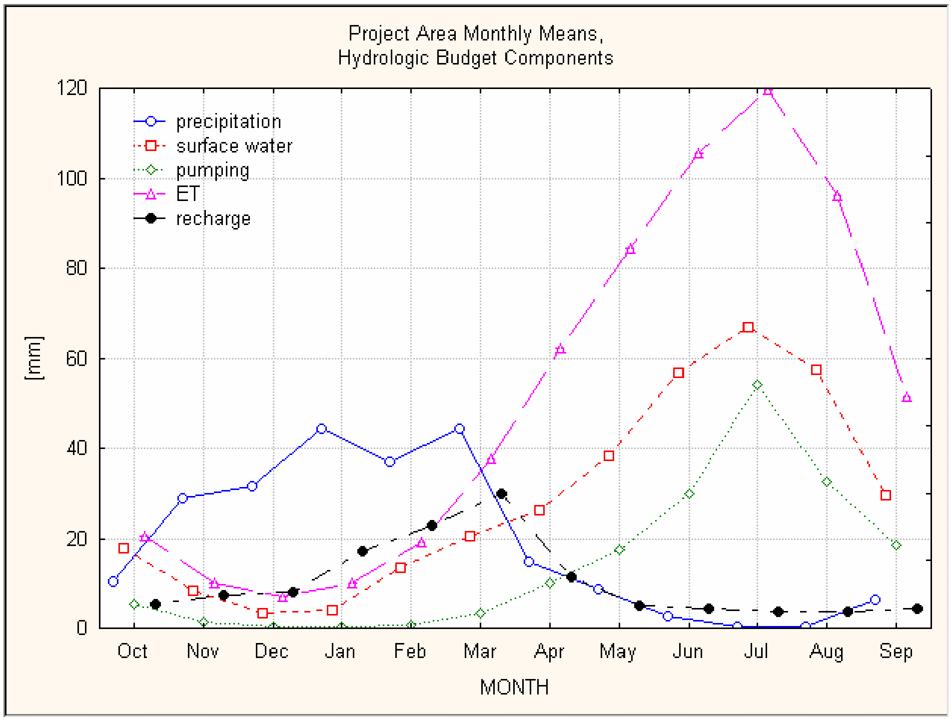

Figure 37: Average monthly water balance components (mm) for the fiscal water years of 1970-99: precipitation, applied surface water, applied groundwater, evapotranspiration, and diffuse recharge from applied water and precipitation.

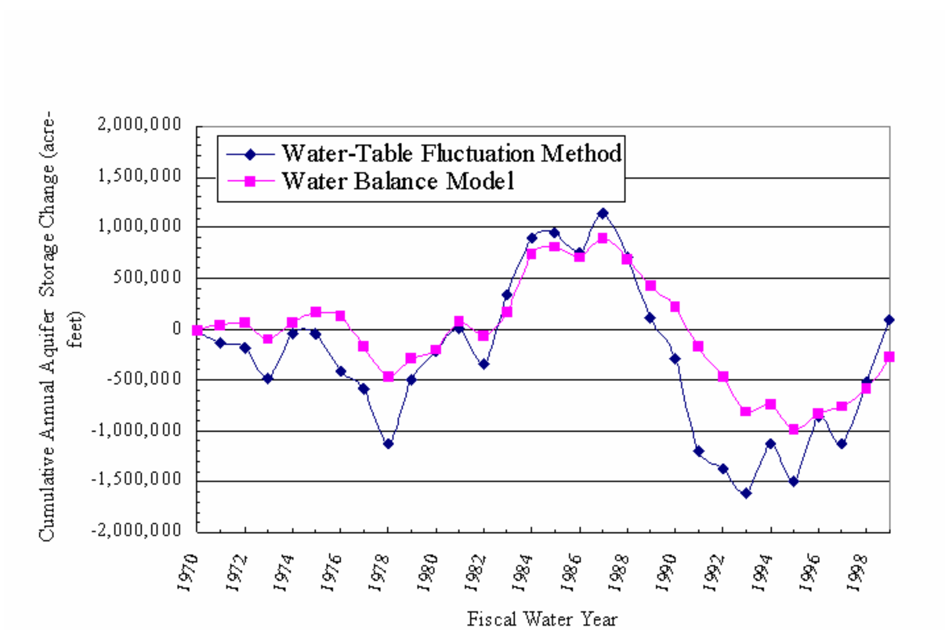

Figure 38: Water-table fluctuation method versus the modeled water balance: cumulative annual groundwater storage changes (acre-feet) for the study area for the fiscal water years of 1970-99.

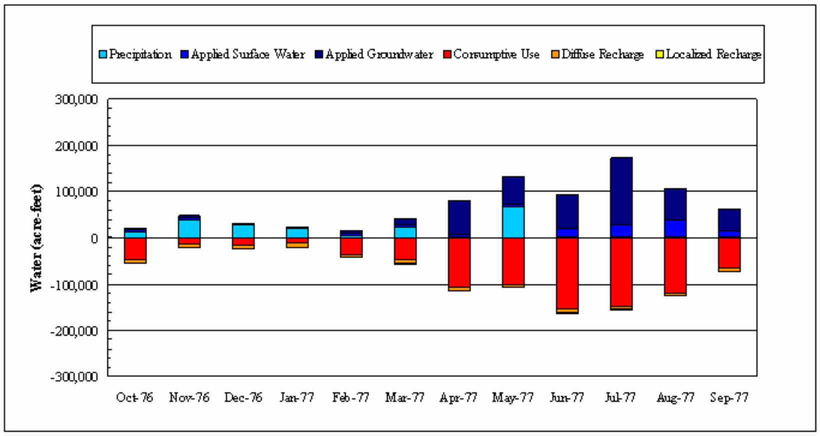

Figure 39: Water balance components for the study area for 1977, a year of below-average annual precipitation.

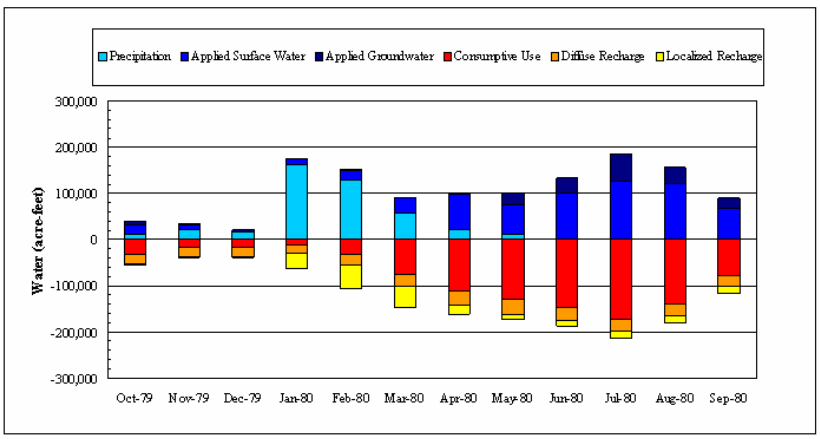

Figure 40: Water balance components for the study area for 1980, a year of normal annual precipitation.

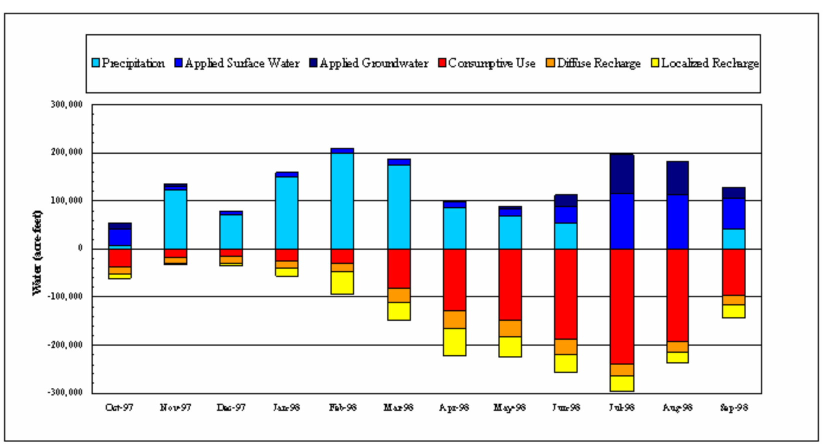

Figure 41: Water balance components for the study area for 1998, a year of above-average annual precipitation.

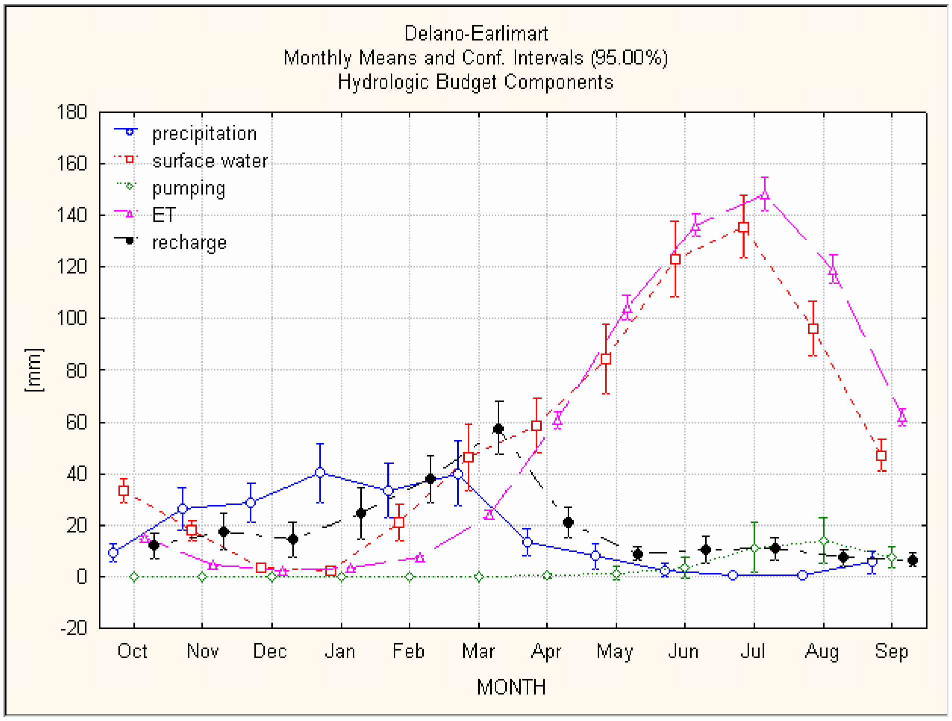

Figure 42: Average monthly water balance components (mm) for Delano-Earlimart Irrigation District from 1970-99.

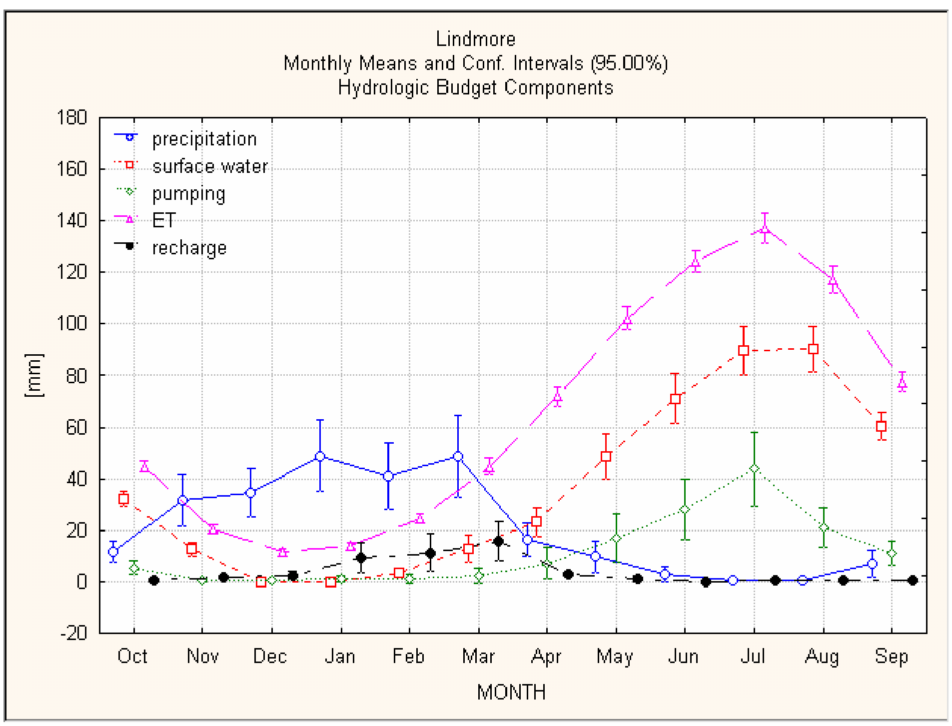

Figure 43: Average monthly water balance components (mm) for Lindmore Irrigation District from 1970-99.

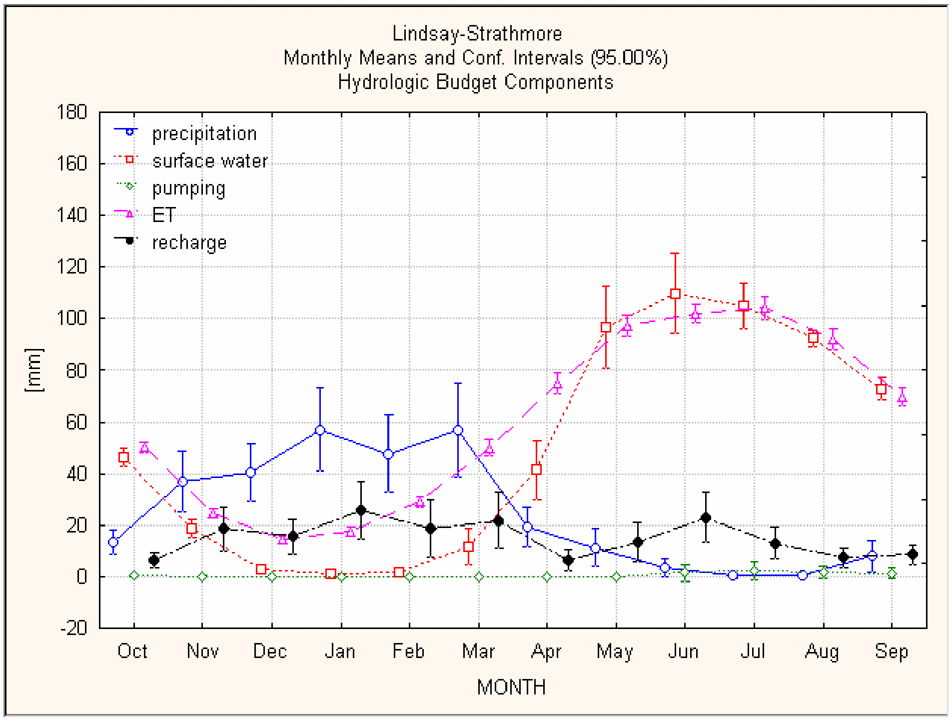

Figure 44: Average monthly water balance components (mm) for Lindsay-Strathmore Irrigation District from 1970-99.

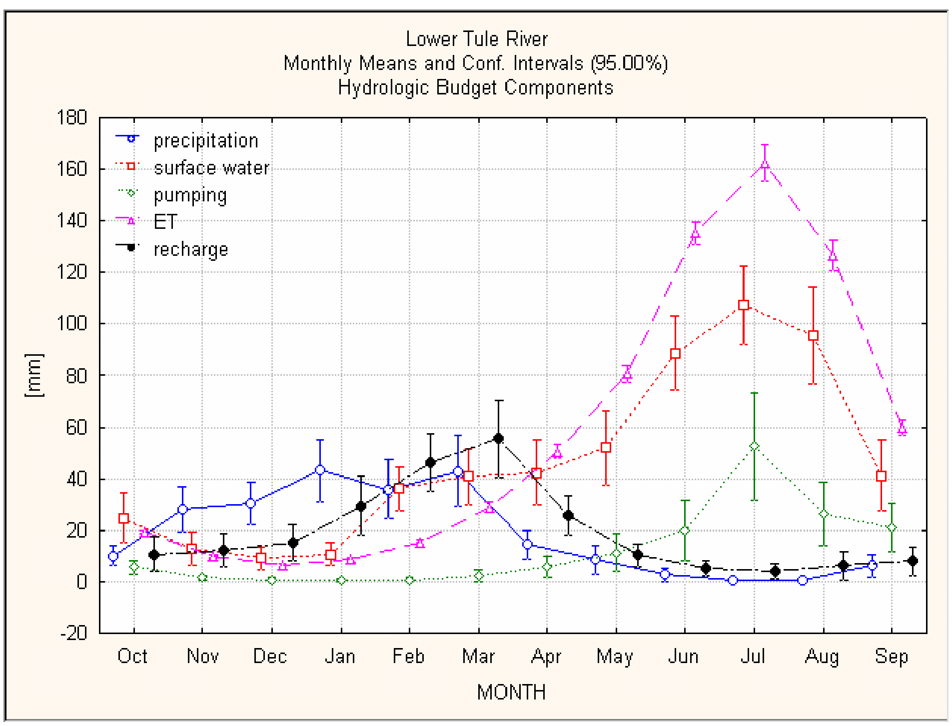

Figure 45: Average monthly water balance components (mm) for Lower Tule River Irrigation District from 1970-99.

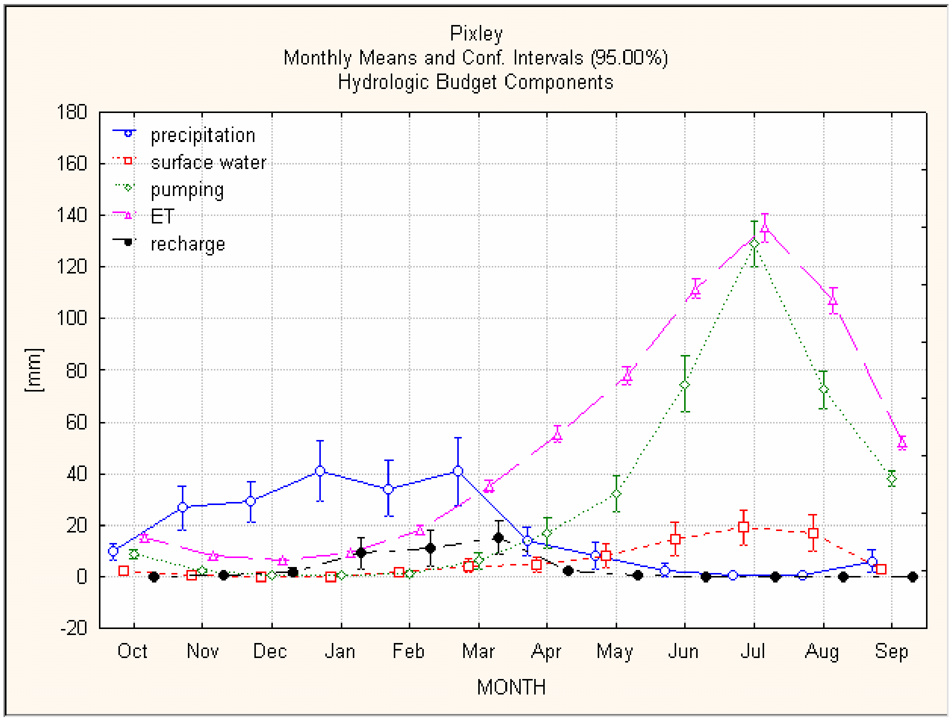

Figure 46: Average monthly water balance components (mm) for Pixley Irrigation District from 1970-99.

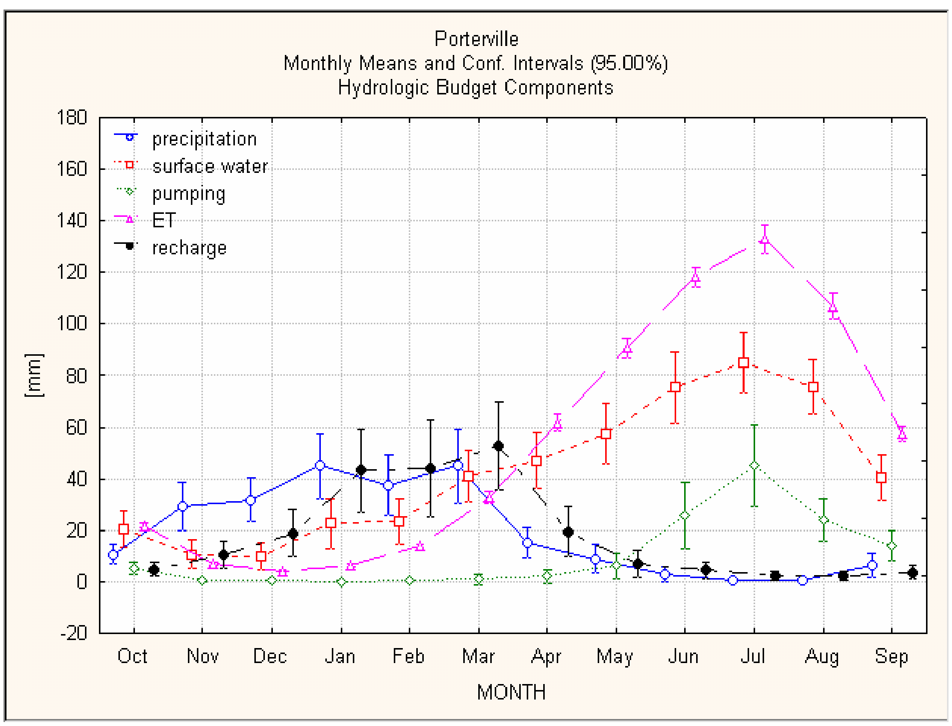

Figure 47: Average monthly water balance components (mm) for Porterville Irrigation District from 1970-99.

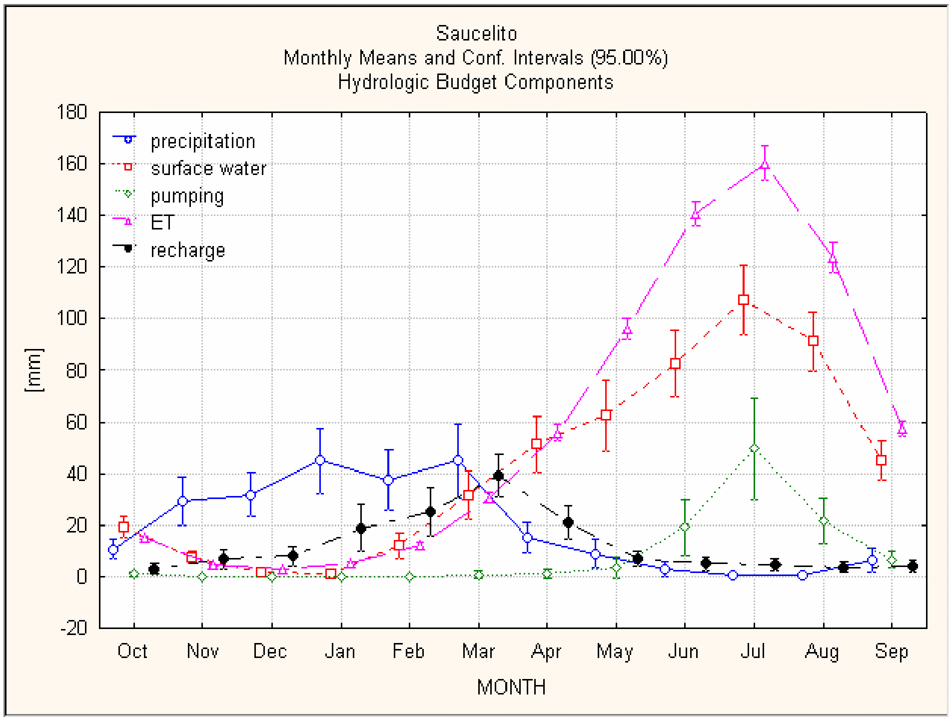

Figure 48: Average monthly water balance components (mm) for Saucelito Irrigation District from 1970-99.

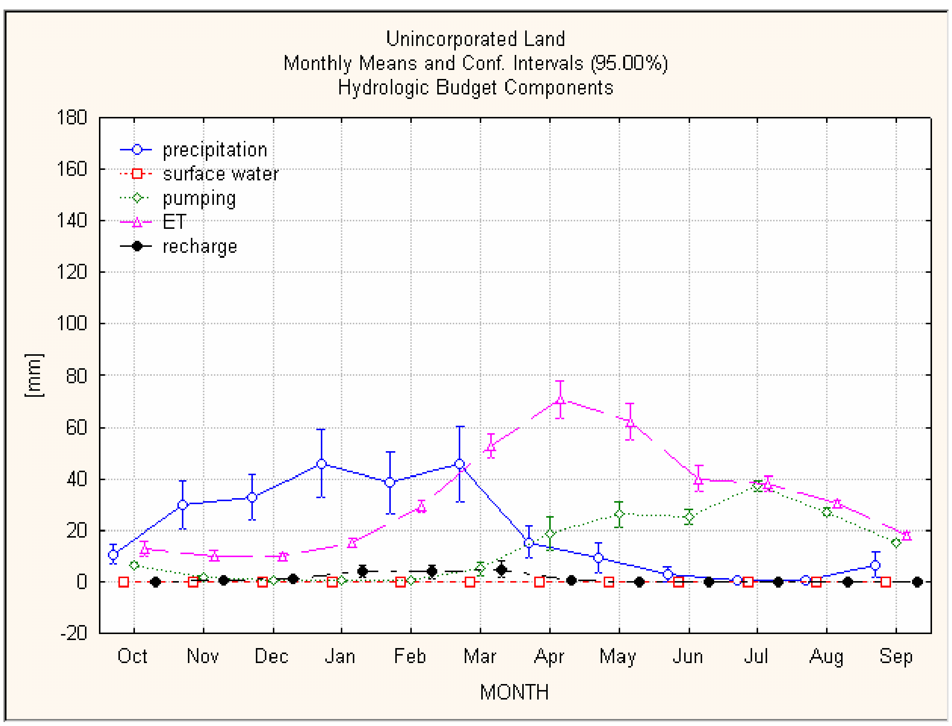

Figure 49: Average monthly water balance components (mm) for all unincorporated areas from 1970-99.

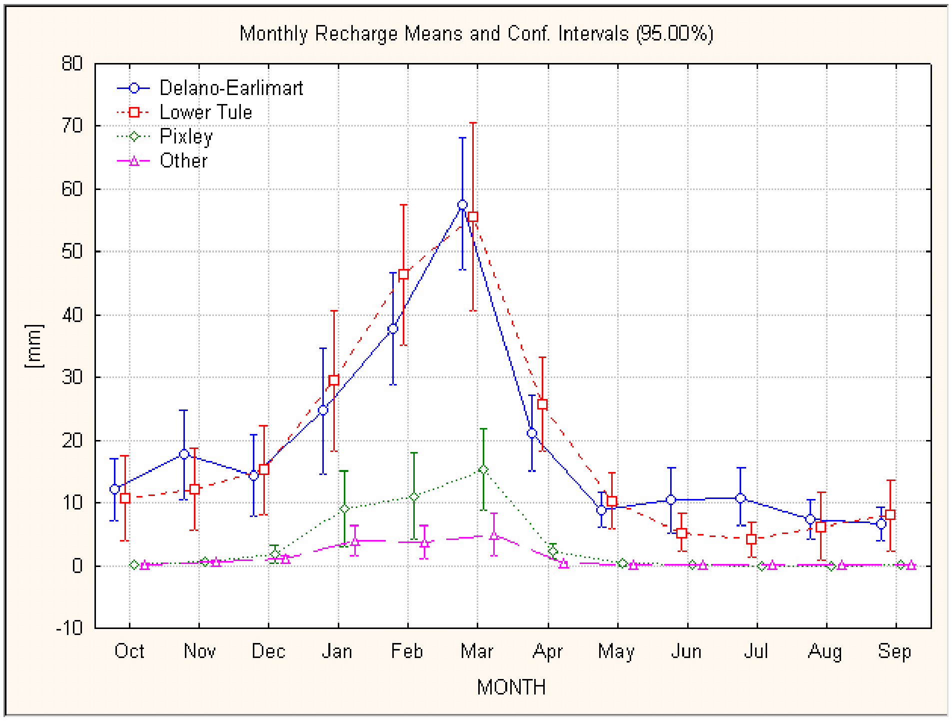

Figure 50: Comparison of average monthly diffuse recharge (mm) between Delano-Earlimart ID, Lower Tule River ID, Pixley ID, and unincorporated areas from 1970-99.

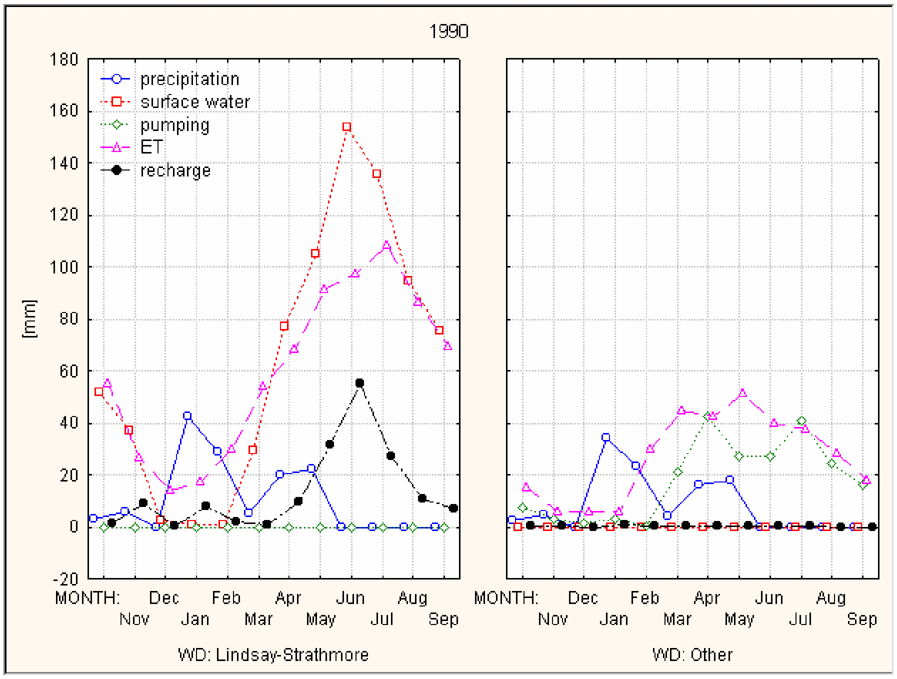

Figure 51: Average monthly water balance components (mm) for citrus crops grown in Lindsay-Strathmore Irrigation District versus citrus grown in unincorporated areas for 1990 (a dry year).

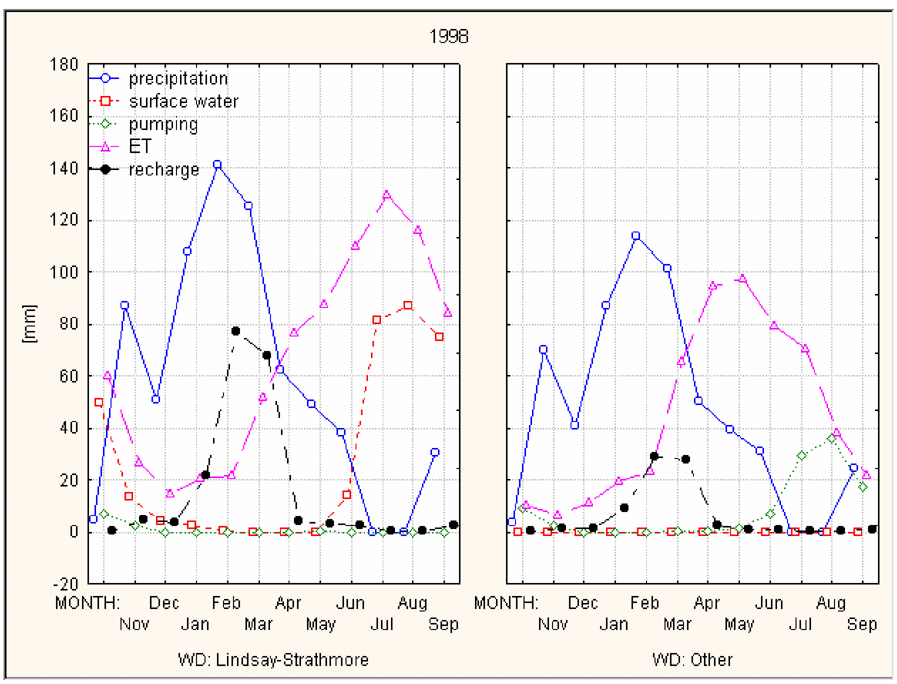

Figure 52: Average monthly water balance components (mm) for citrus crops grown in Lindsay-Strathmore Irrigation District versus citrus grown in unincorporated areas for 1998 (a wet year).

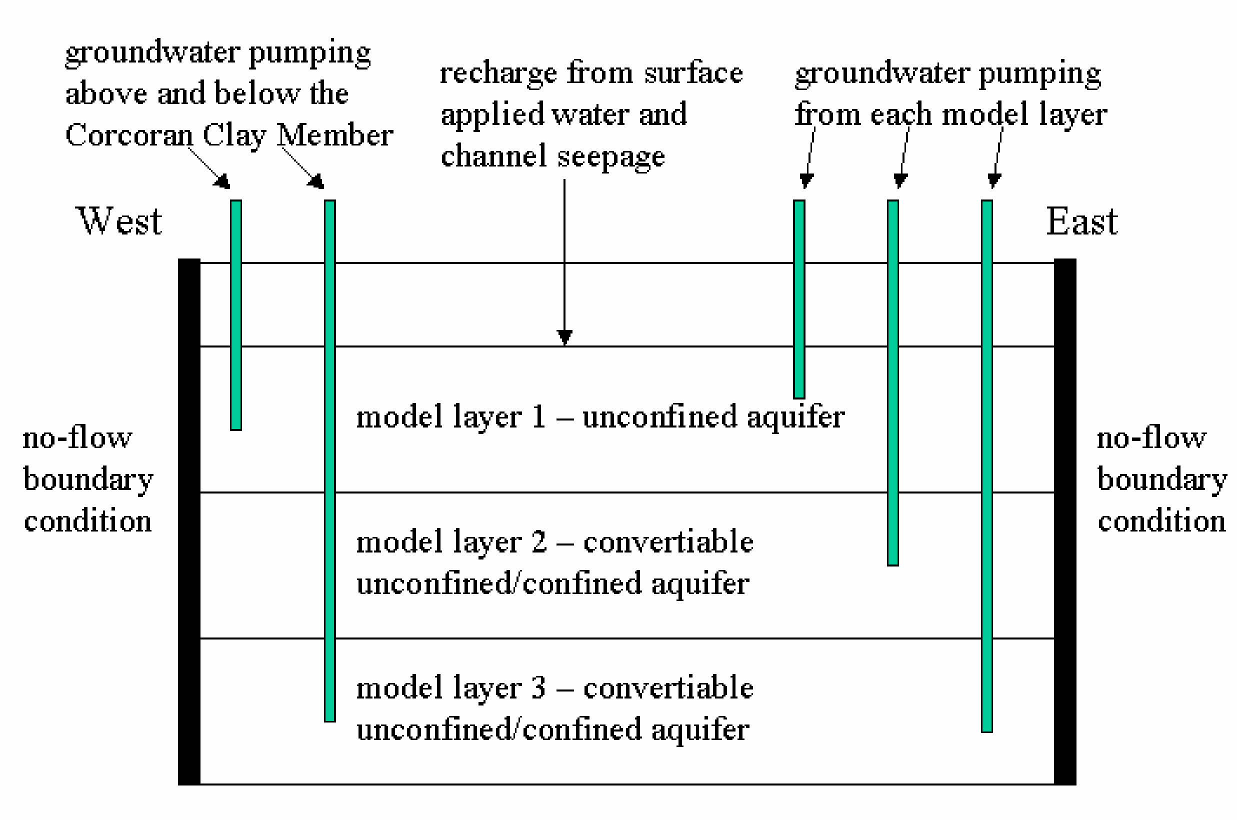

Figure 53: MODFLOW model layers of aquifer system hydrogeologic units.

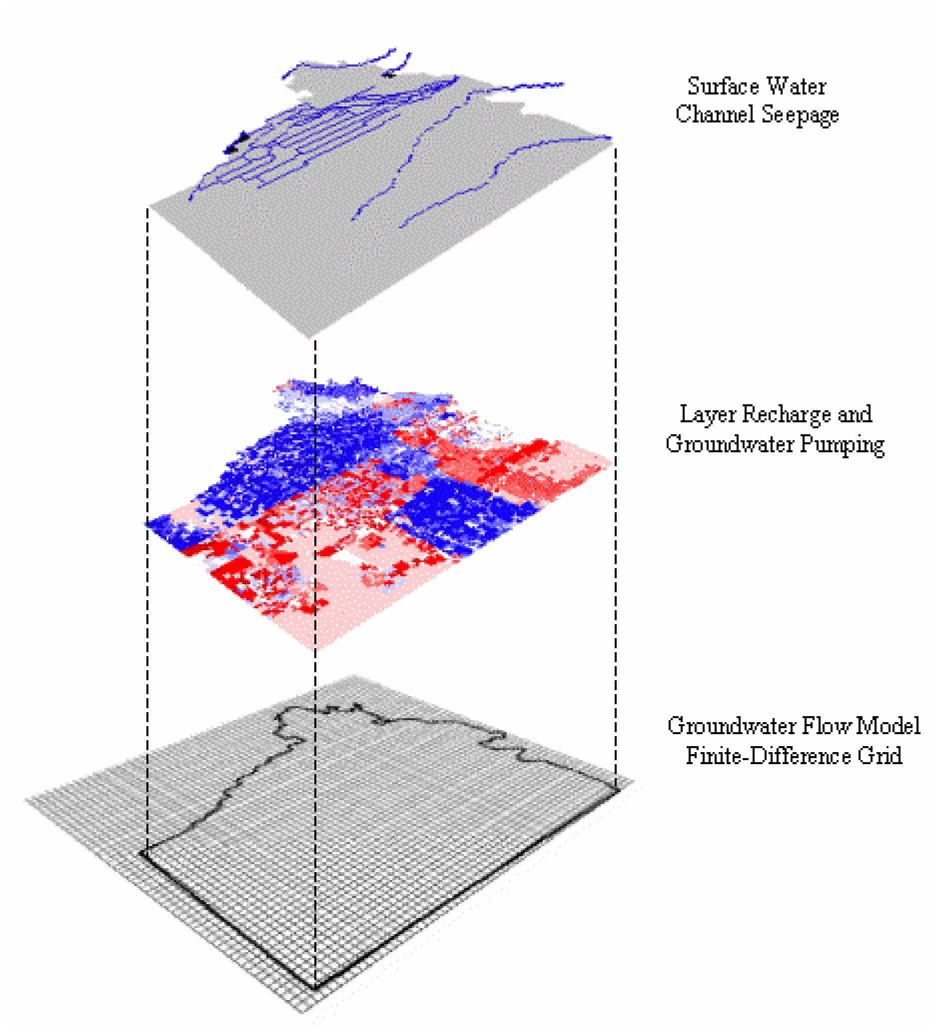

Figure 54: Overlay of channel seepage and land unit recharge and pumping GIS coverages onto MODFLOW finite-difference grid via Argus ONE™.

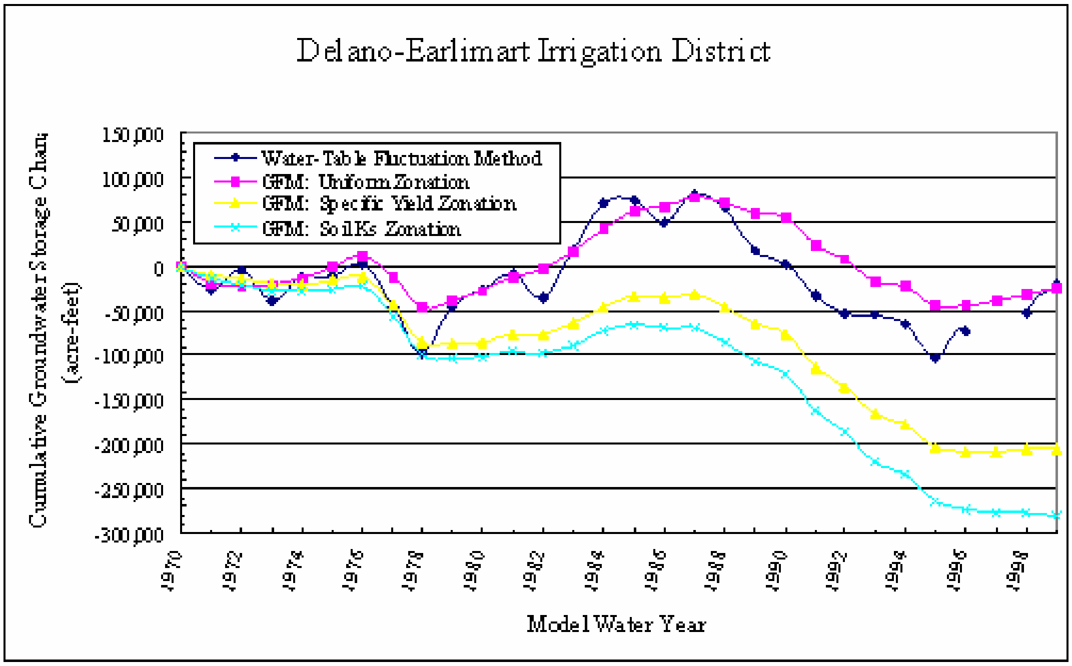

Figure 55: Water-table fluctuation method versus calibrated groundwater flow model: cumulative annual unconfined aquifer storage changes from 1970-99 for Delano-Earlimart ID from the three conceptual models of K_h structure.

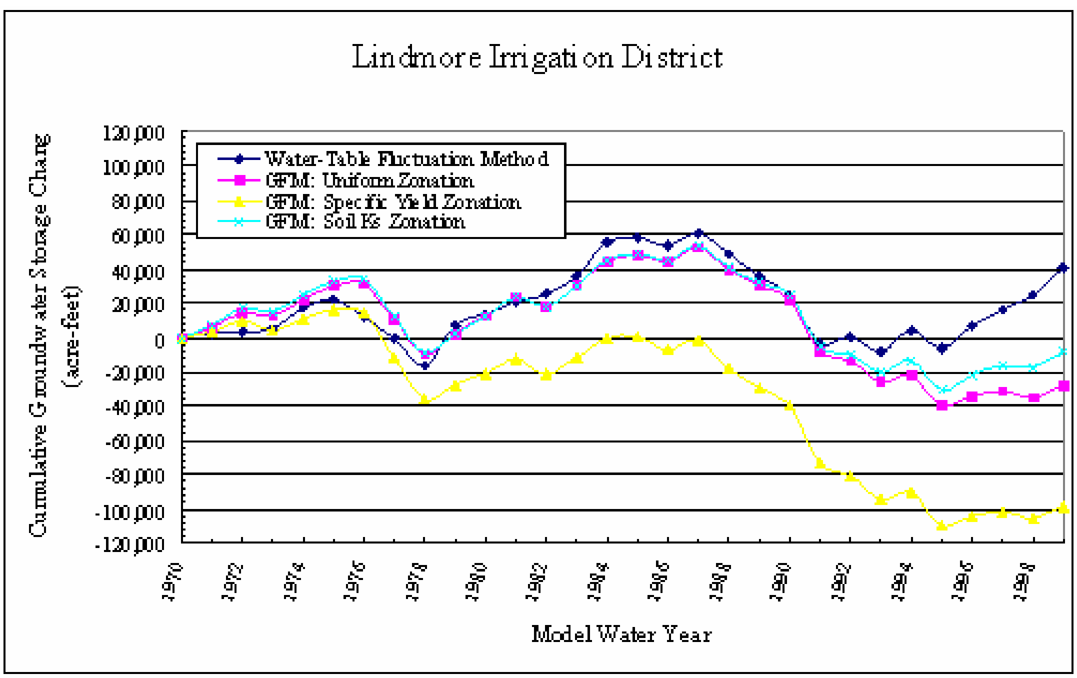

Figure 56: Water-table fluctuation method versus calibrated groundwater flow model: cumulative annual unconfined aquifer storage changes from 1970-99 for Lindmore ID from the three conceptual models of K_h structure.

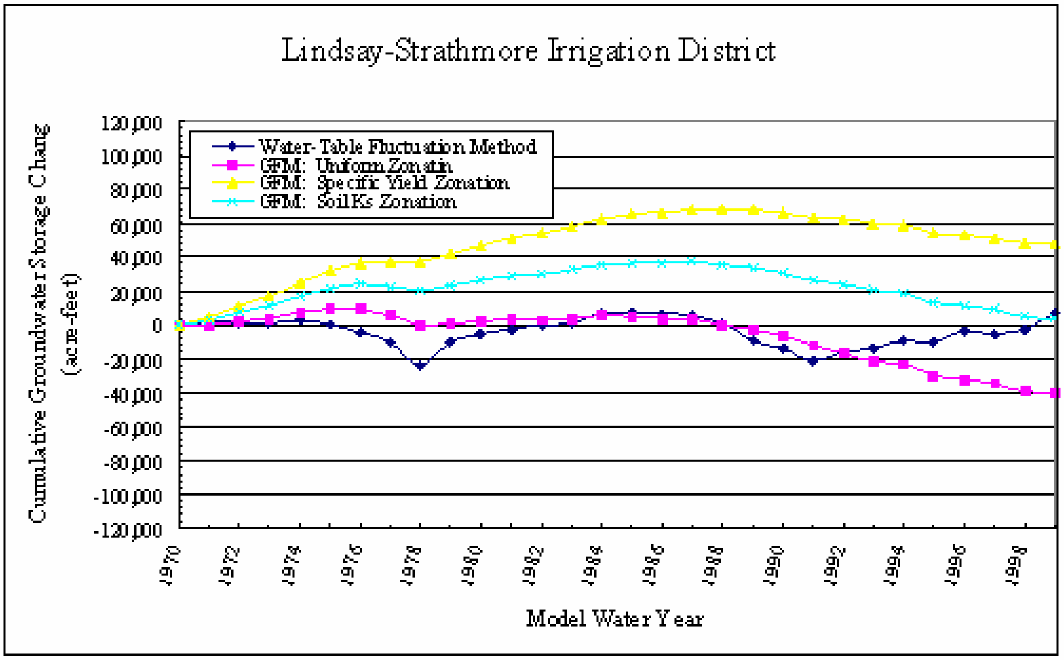

Figure 57: Water-table fluctuation method versus calibrated groundwater flow model: cumulative annual unconfined aquifer storage changes from 1970-99 for Lindsay-Strathmore ID from the three conceptual models of K_h structure.

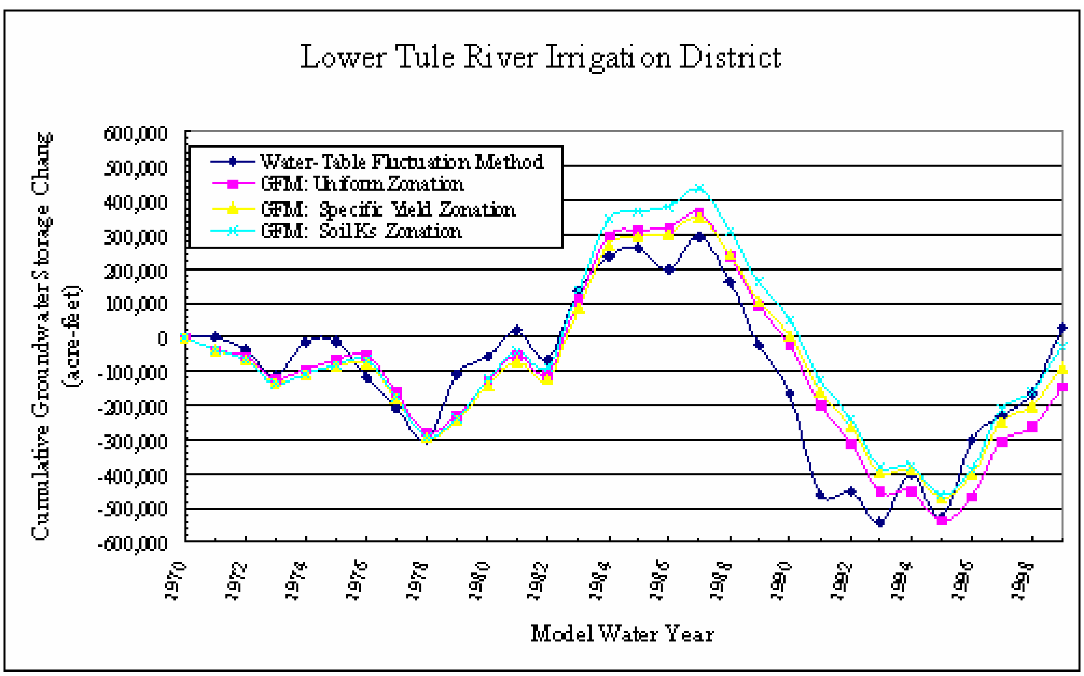

Figure 58: Water-table fluctuation method versus calibrated groundwater flow model: cumulative annual unconfined aquifer storage changes from 1970-99 for Lower Tule River ID from the three conceptual models of K_h structure.

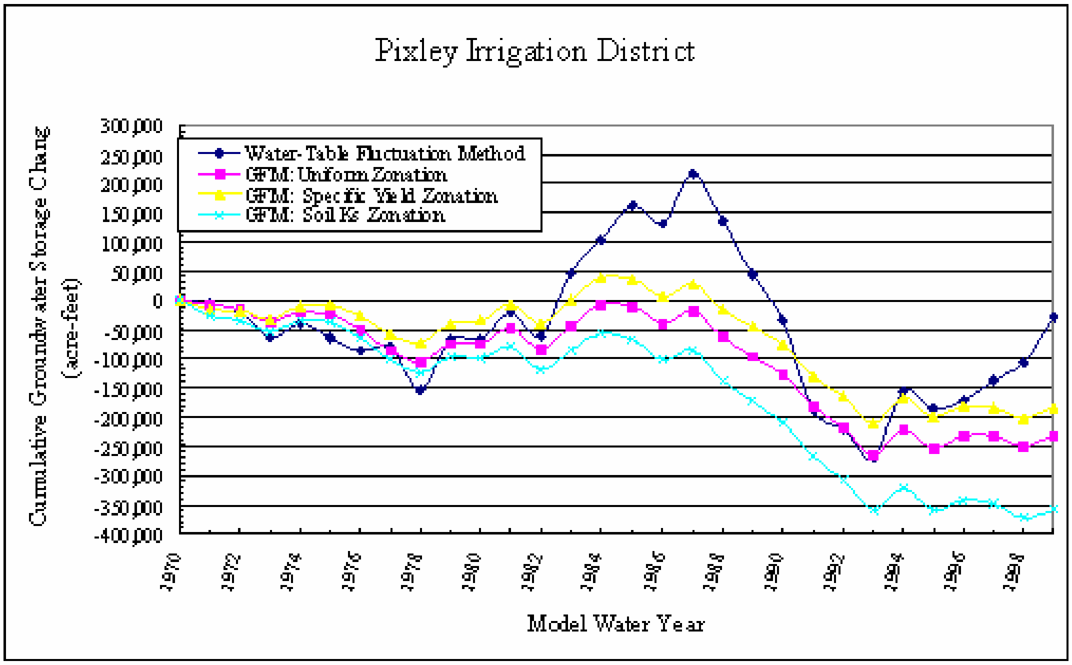

Figure 59: Water-table fluctuation method versus calibrated groundwater flow model: cumulative annual unconfined aquifer storage changes from 1970-99 for Pixley ID from the three conceptual models of K_h structure.

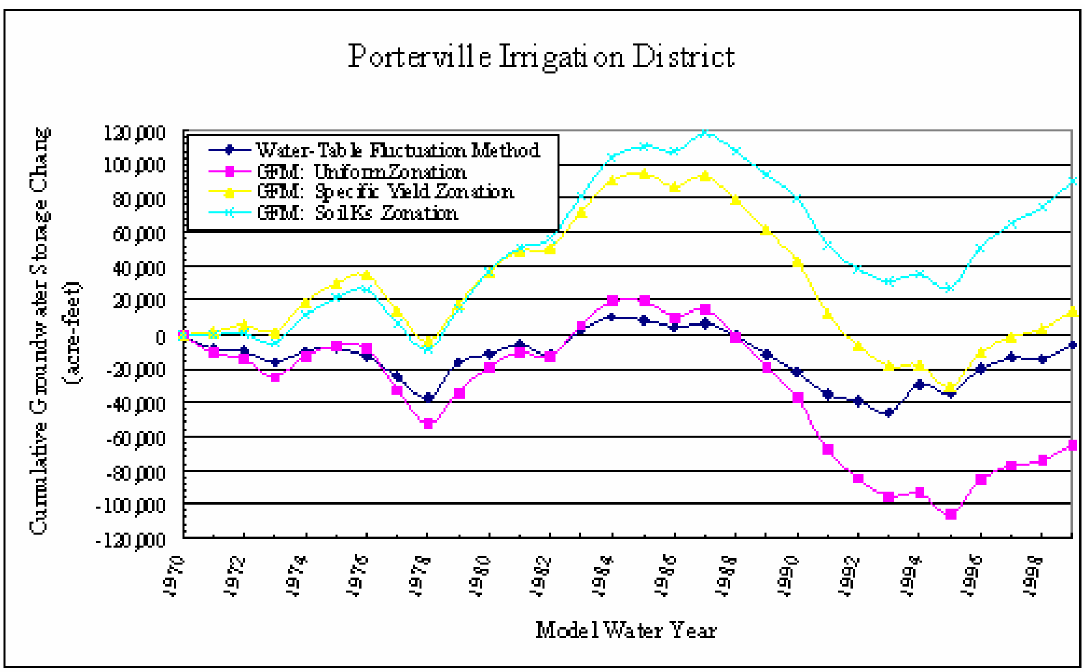

Figure 60: Water-table fluctuation method versus calibrated groundwater flow model: cumulative annual unconfined aquifer storage changes from 1970-99 for Porterville ID from the three conceptual models of K_h structure.

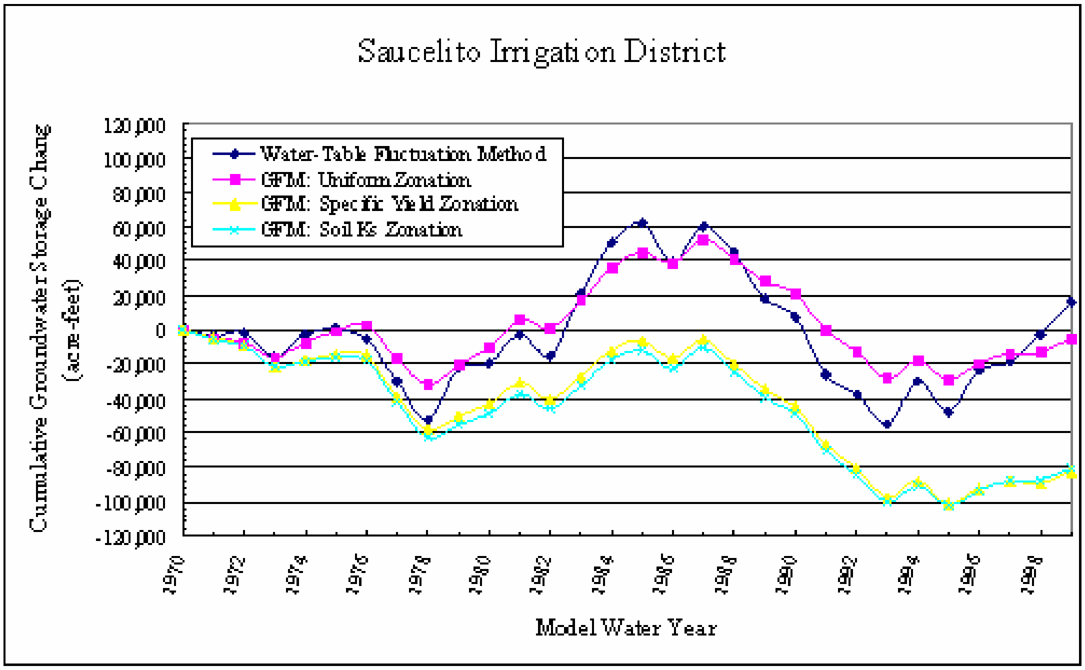

Figure 61: Water-table fluctuation method versus calibrated groundwater flow model: cumulative annual unconfined aquifer storage changes from 1970-99 for Saucelito ID from the three conceptual models of K_h structure.

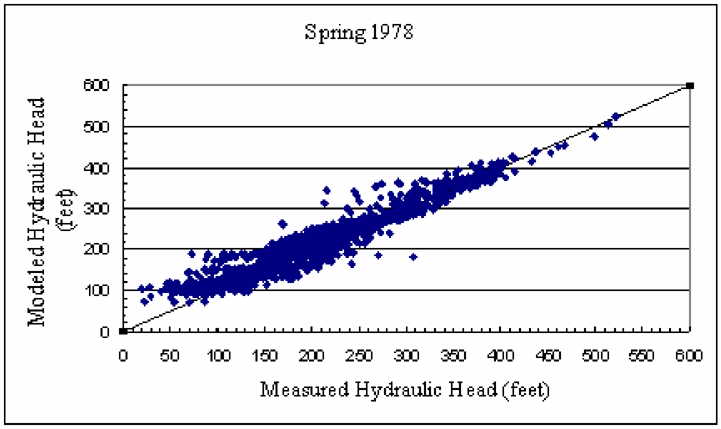

Figure 62: Measured versus modeled hydraulic heads (feet) for 1978 from the uniform zonation conceptual model.

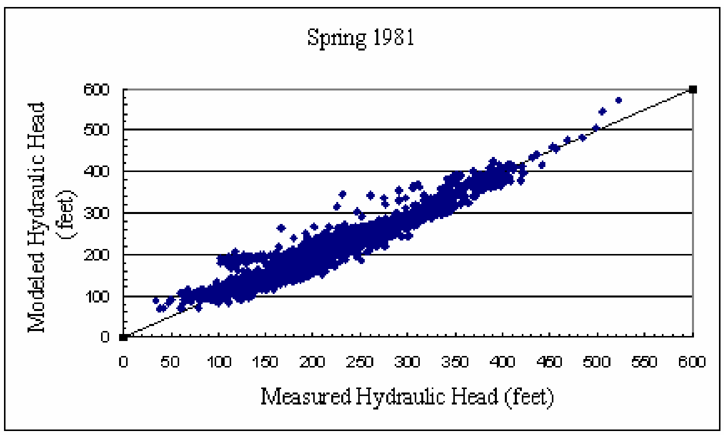

Figure 63: Measured versus modeled hydraulic heads (feet) for 1981 from the uniform zonation conceptual model.

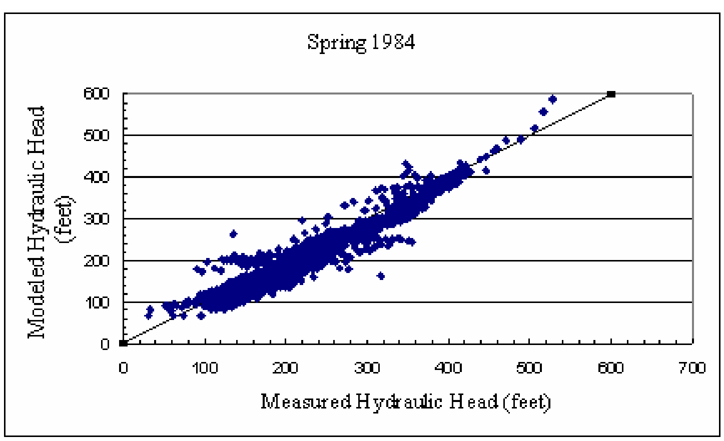

Figure 64: Measured versus modeled hydraulic heads (feet) for 1984 from the uniform zonation conceptual model.

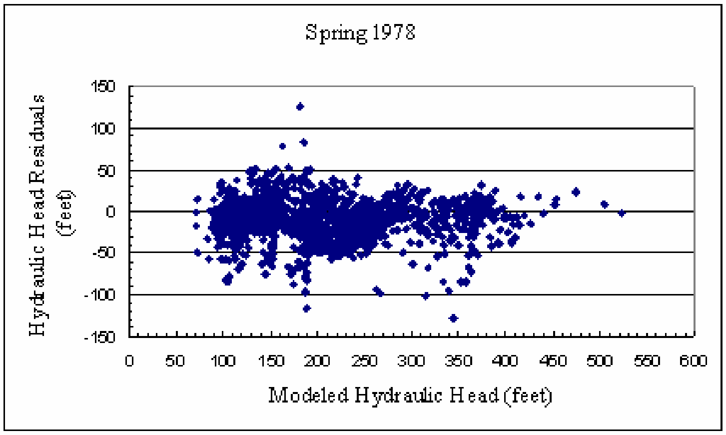

Figure 65: Modeled hydraulic heads (feet) versus residuals (feet) for 1978 from the uniform zonation conceptual model.

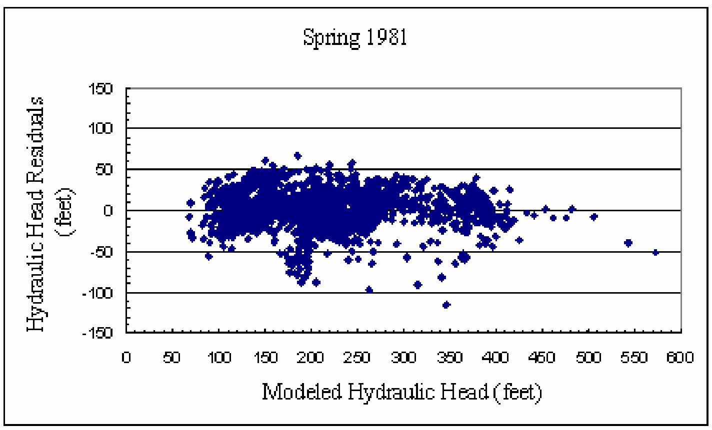

Figure 66: Modeled hydraulic heads (feet) versus residuals (feet) for 1981 from the uniform zonation conceptual model.

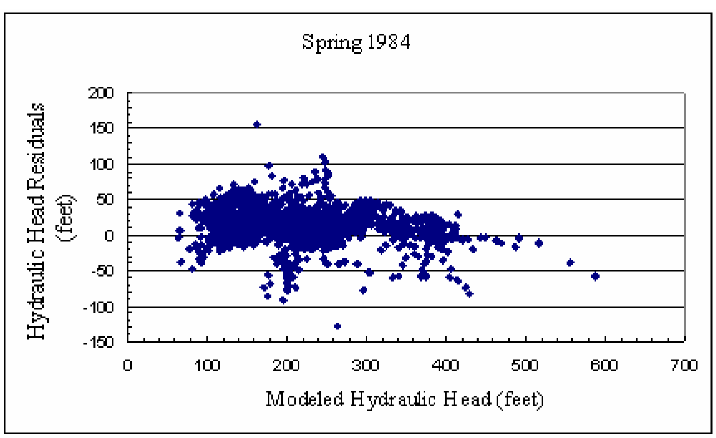

Figure 67: Modeled hydraulic heads (feet) versus residuals (feet) for 1984 from the uniform zonation conceptual model.

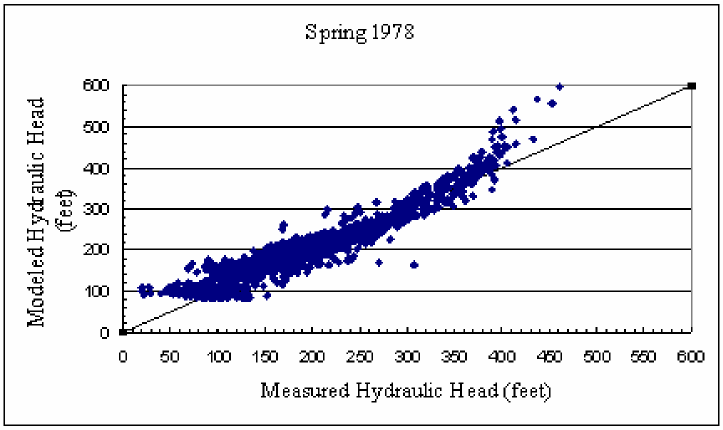

Figure 68: Measured versus modeled hydraulic heads (feet) for 1978 from the S_y-structure conceptual model.

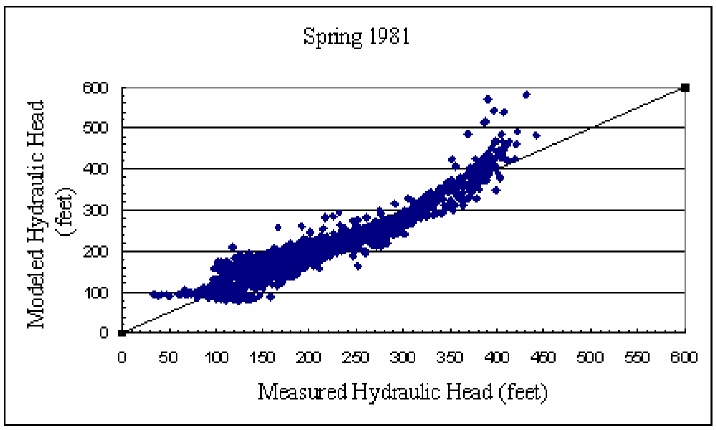

Figure 69: Measured versus modeled hydraulic heads (feet) for 1981 from the S_y-structure conceptual model.

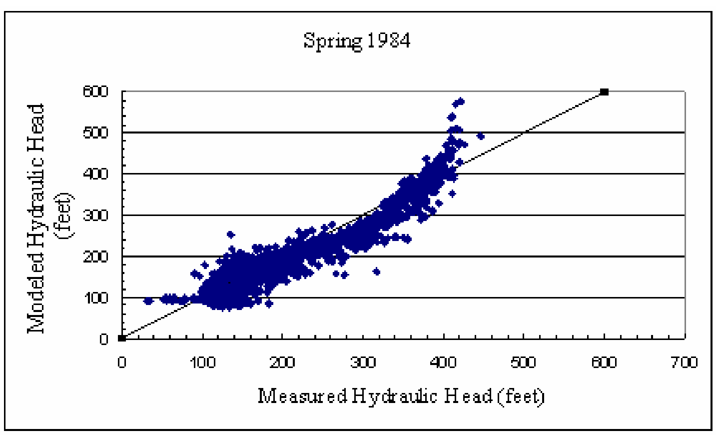

Figure 70: Measured versus modeled hydraulic heads (feet) for 1984 from the S_y-structure conceptual model.

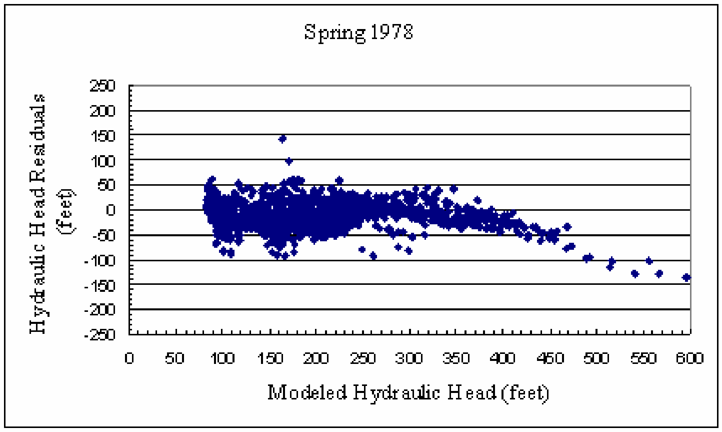

Figure 71: Modeled hydraulic heads (feet) versus residuals (feet) for 1978 from the S_y-structure conceptual model.

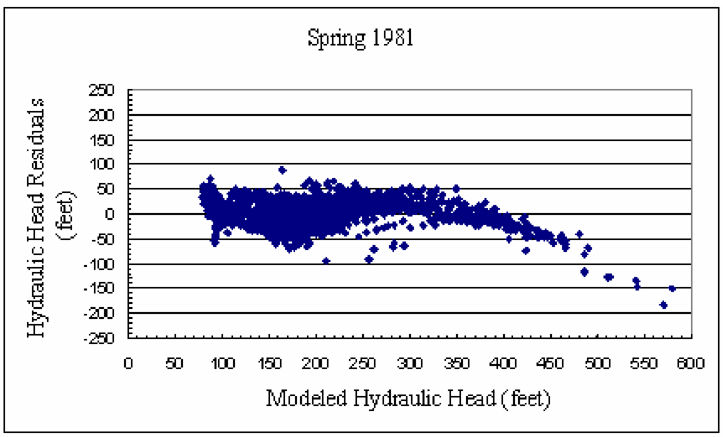

Figure 72: Modeled hydraulic heads (feet) versus residuals (feet) for 1981 from the S_y-structure conceptual model.

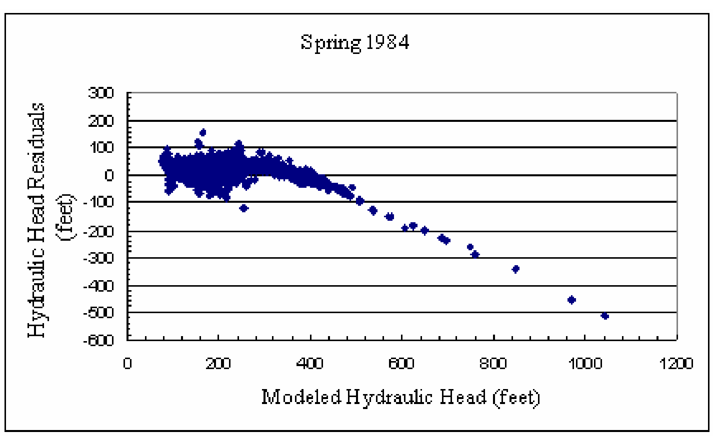

Figure 73: Modeled hydraulic heads (feet) versus residuals (feet) for 1984 from the S_y-structure conceptual model.

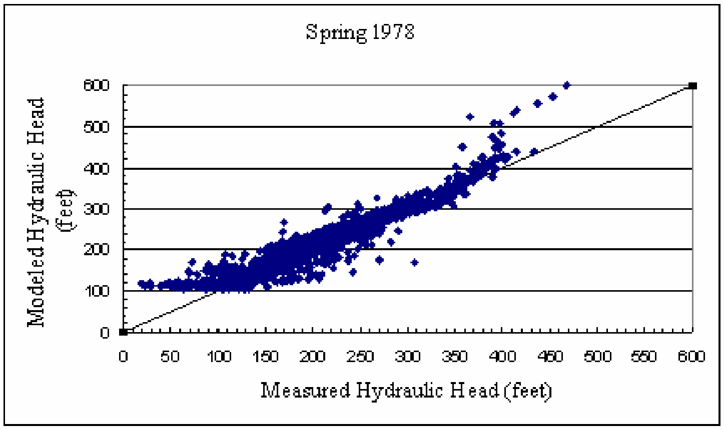

Figure 74: Measured versus modeled hydraulic heads (feet) for 1978 from the K_s-structure conceptual model.

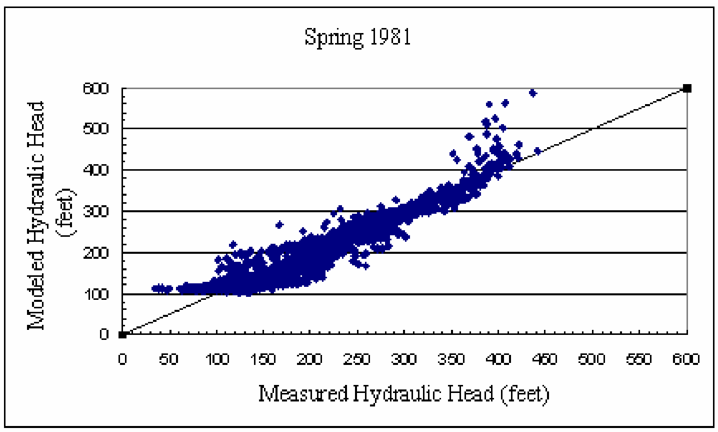

Figure 75: Measured versus modeled hydraulic heads (feet) for 1981 from the K_s-structure conceptual model.

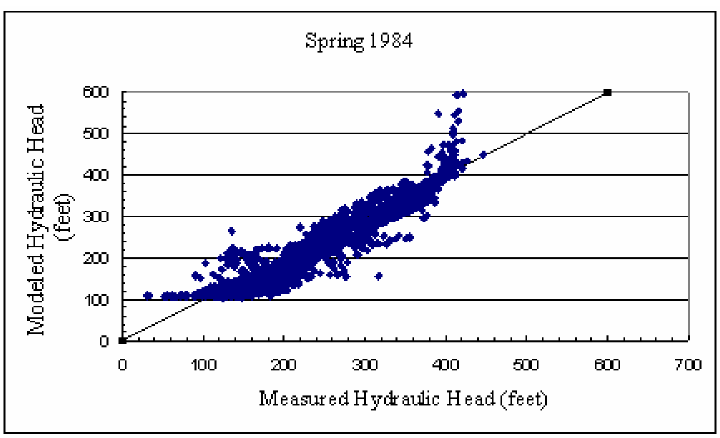

Figure 76: Measured versus modeled hydraulic heads (feet) for 1984 from the K_s-structure conceptual model.

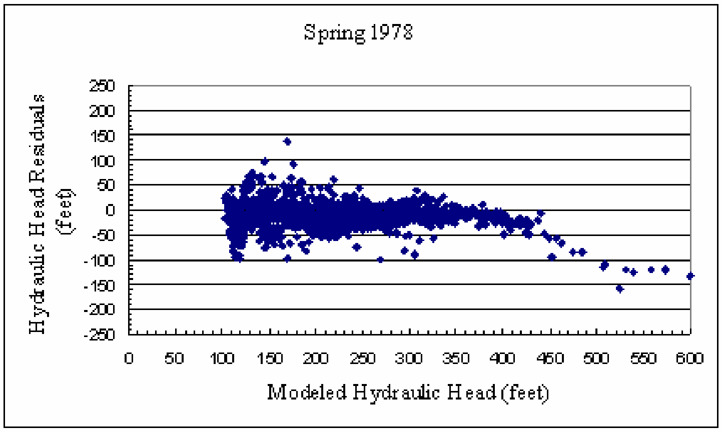

Figure 77: Modeled hydraulic heads (feet) versus residuals (feet) for 1978 from the K_s-structure conceptual model.

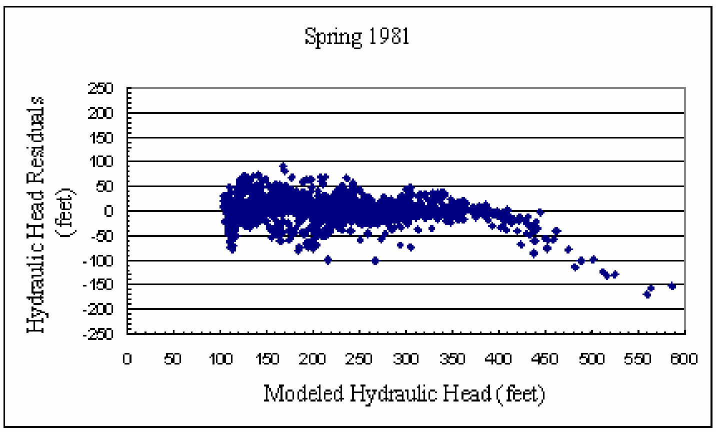

Figure 78: Modeled hydraulic heads (feet) versus residuals (feet) for 1981 from the K_s-structure conceptual model.

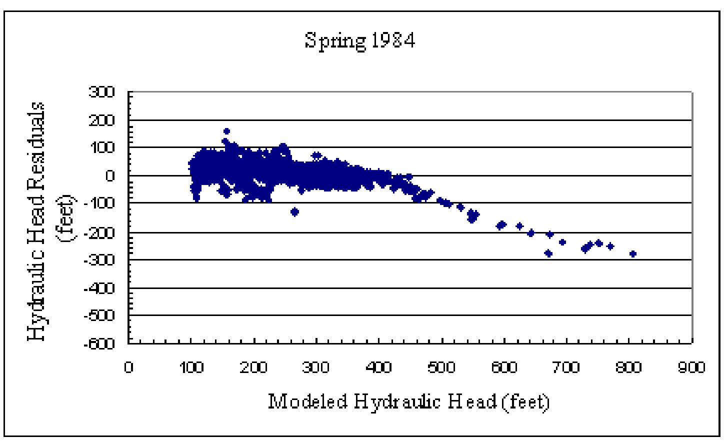

Figure 79: Modeled hydraulic heads (feet) versus residuals (feet) for 1984 from the K_s-structure conceptual model.

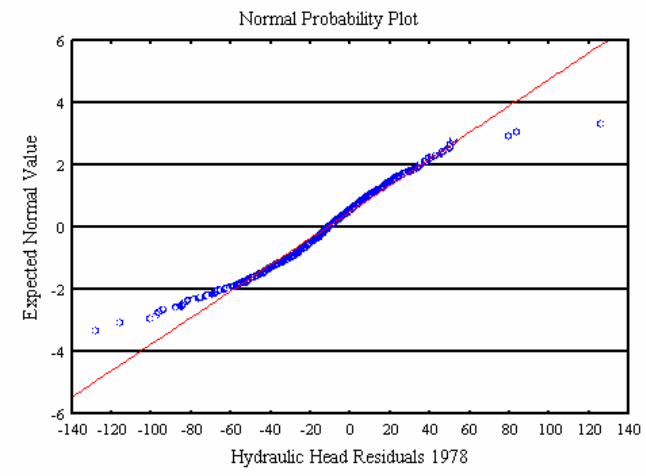

Figure 80: Normal probability plot of hydraulic head residuals for 1978 from the uniform zonation conceptual model.

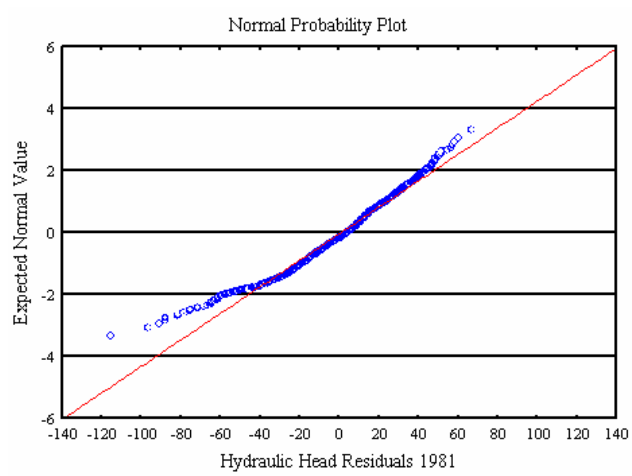

Figure 81: Normal probability plot of hydraulic head residuals for 1981 from the uniform zonation conceptual model.

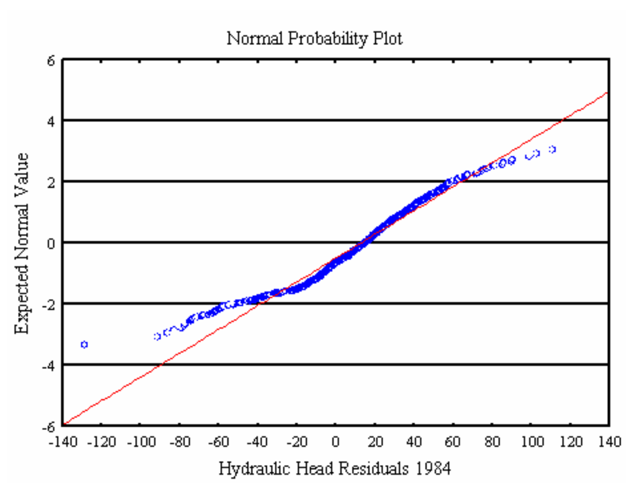

Figure 82: Normal probability plot of hydraulic head residuals for 1984 from the uniform zonation conceptual model.

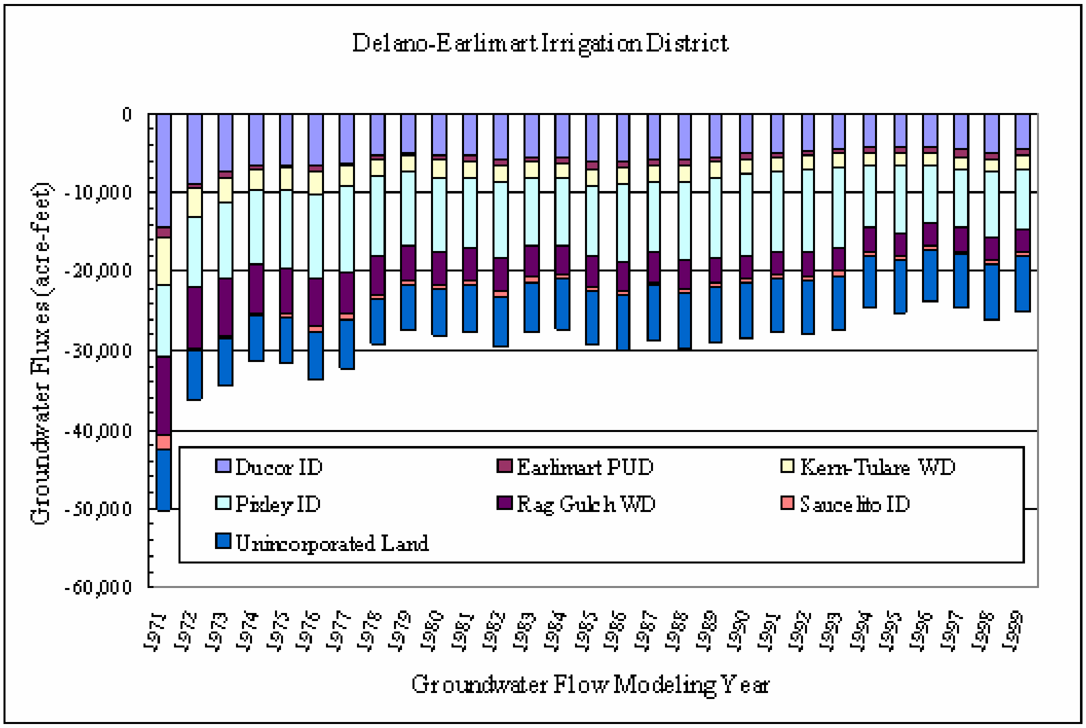

Figure 83: Computed groundwater fluxes from Delano-Earlimart ID to neighboring districts for the modeling years of 1970-99.

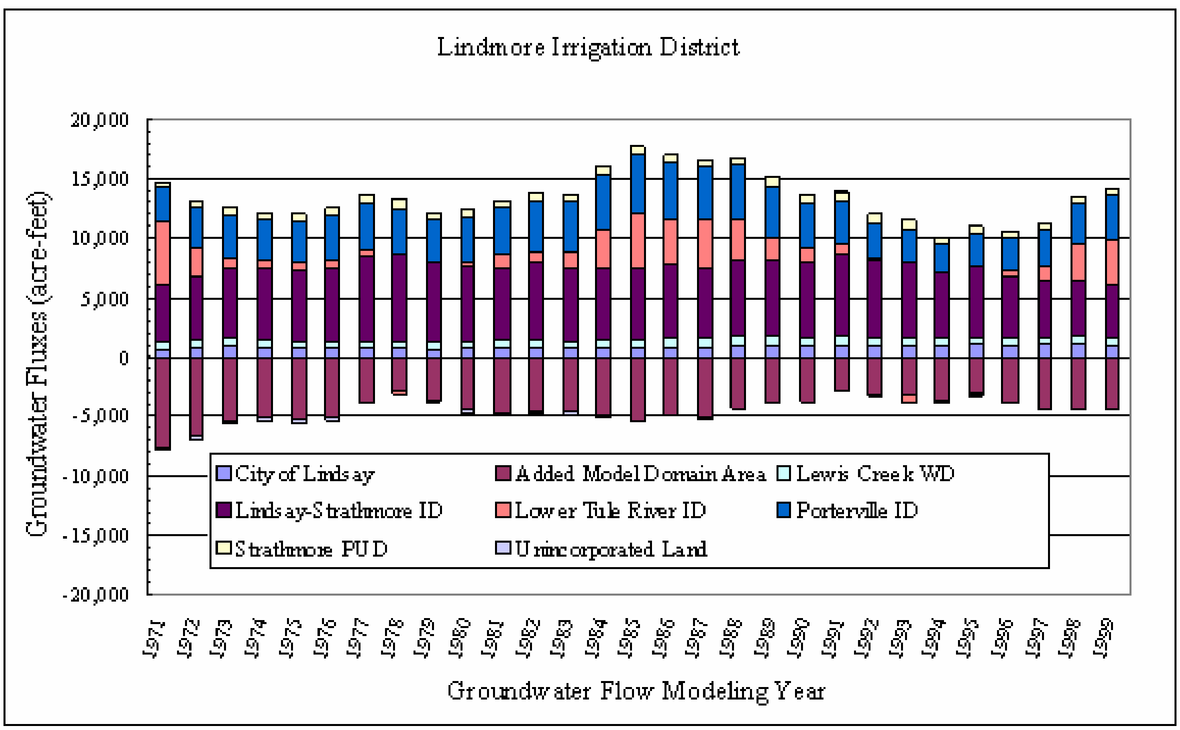

Figure 84: Computed groundwater fluxes from Lindmore ID to neighboring districts for the modeling years of 1970-99.

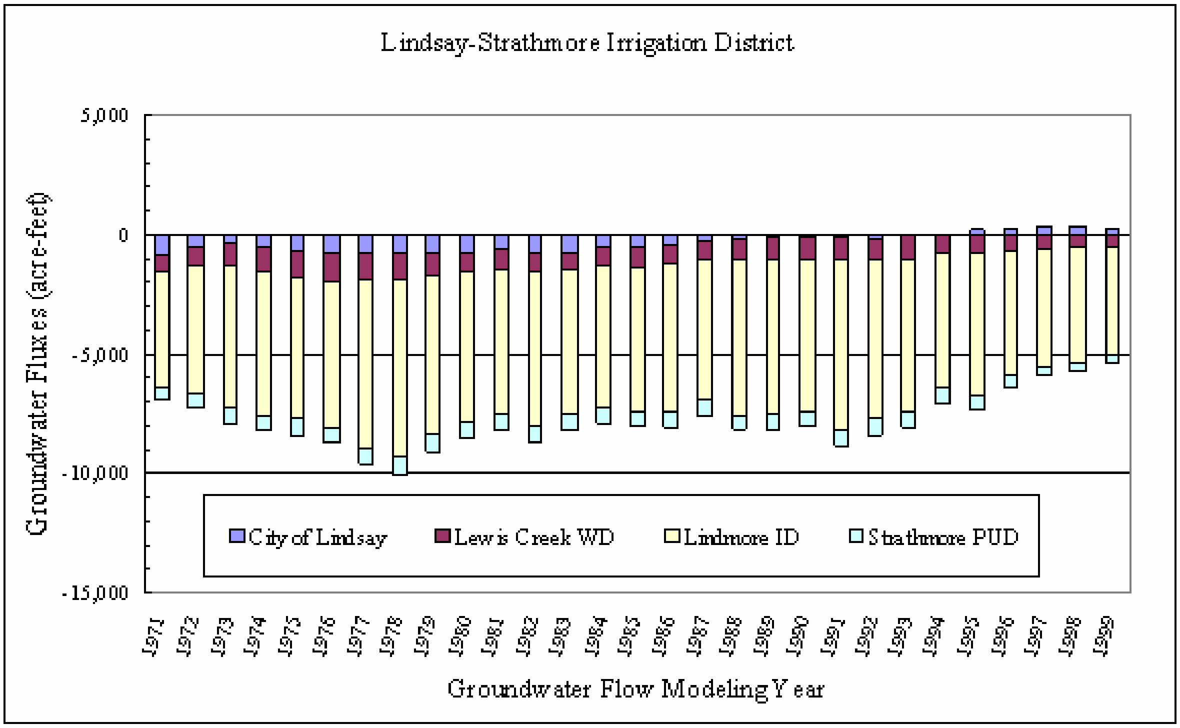

Figure 85: Computed groundwater fluxes from Lindsay-Strathmore ID to neighboring districts for the modeling years of 1970-99.

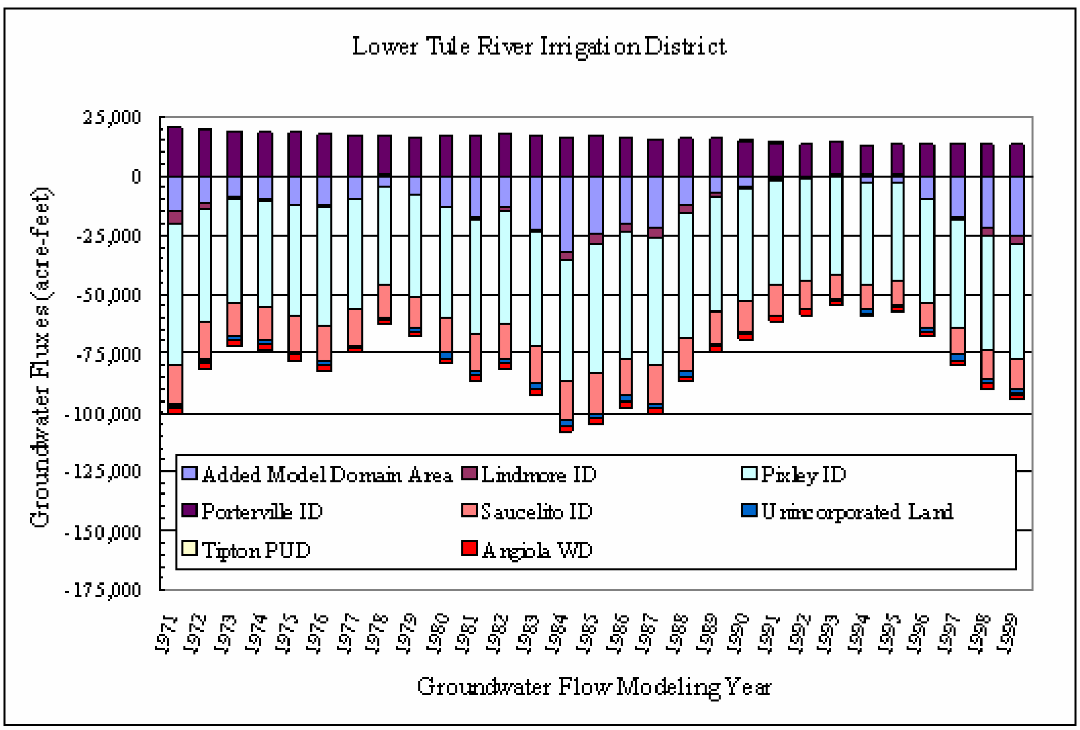

Figure 86: Computed groundwater fluxes from Lower Tule River ID to neighboring districts for the modeling years of 1970-99.

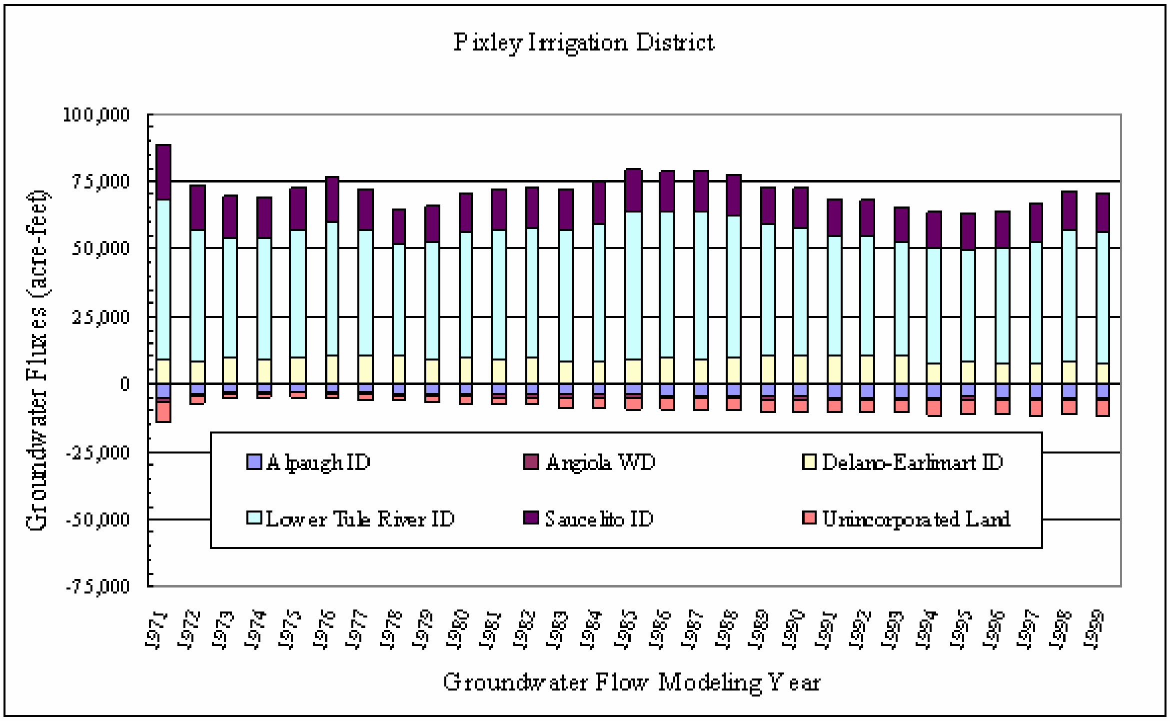

Figure 87: Computed groundwater fluxes from Pixley ID to neighboring districts for the modeling years of 1970-99.

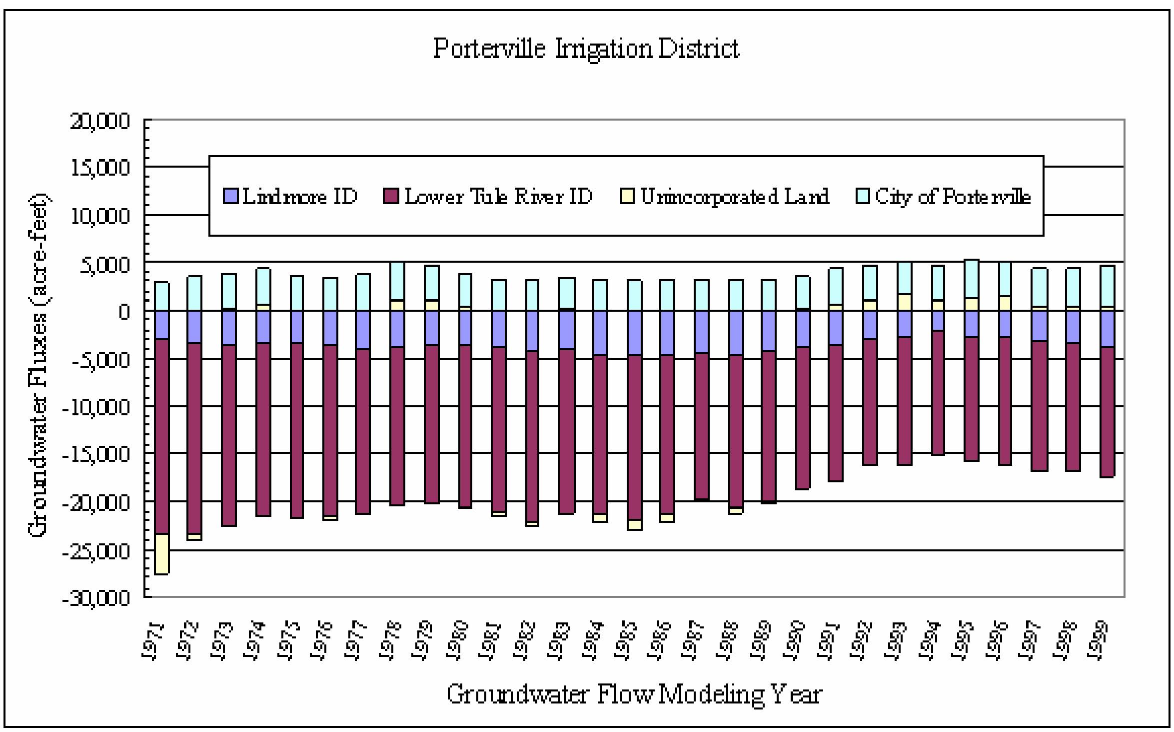

Figure 88: Computed groundwater fluxes from Porterville ID to neighboring districts for the modeling years of 1970-99.

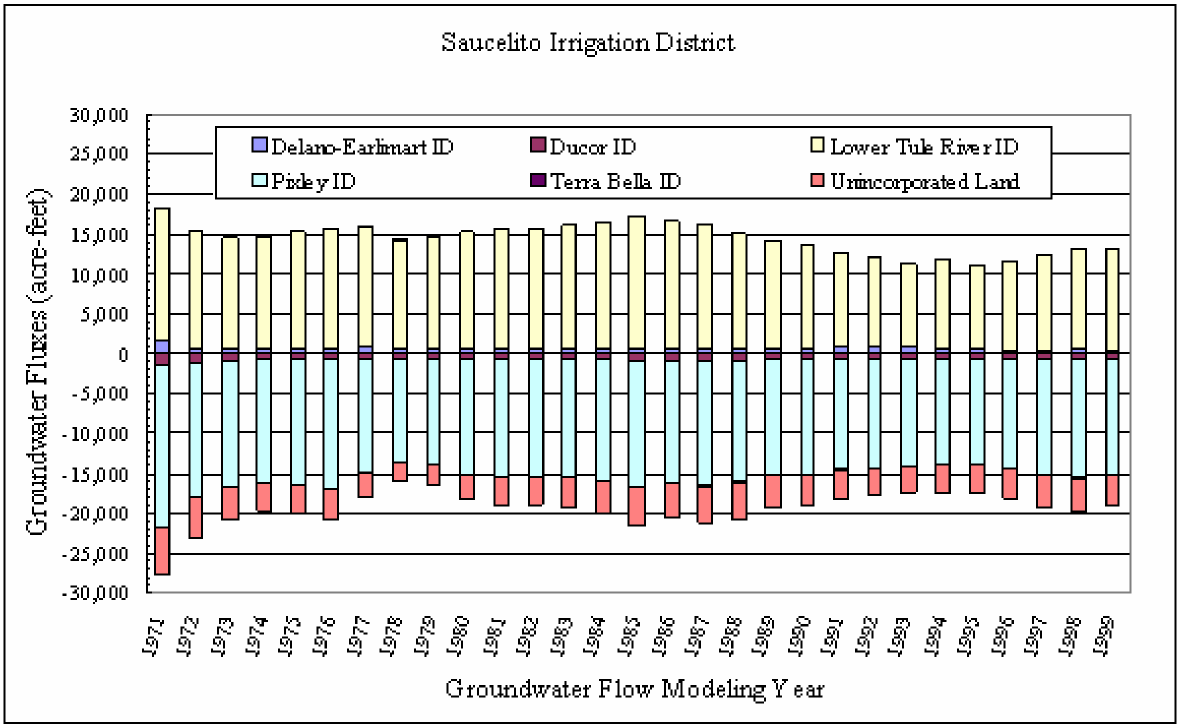

Figure 89: Computed groundwater fluxes from Saucelito ID to neighboring districts for the modeling years of 1970-99.

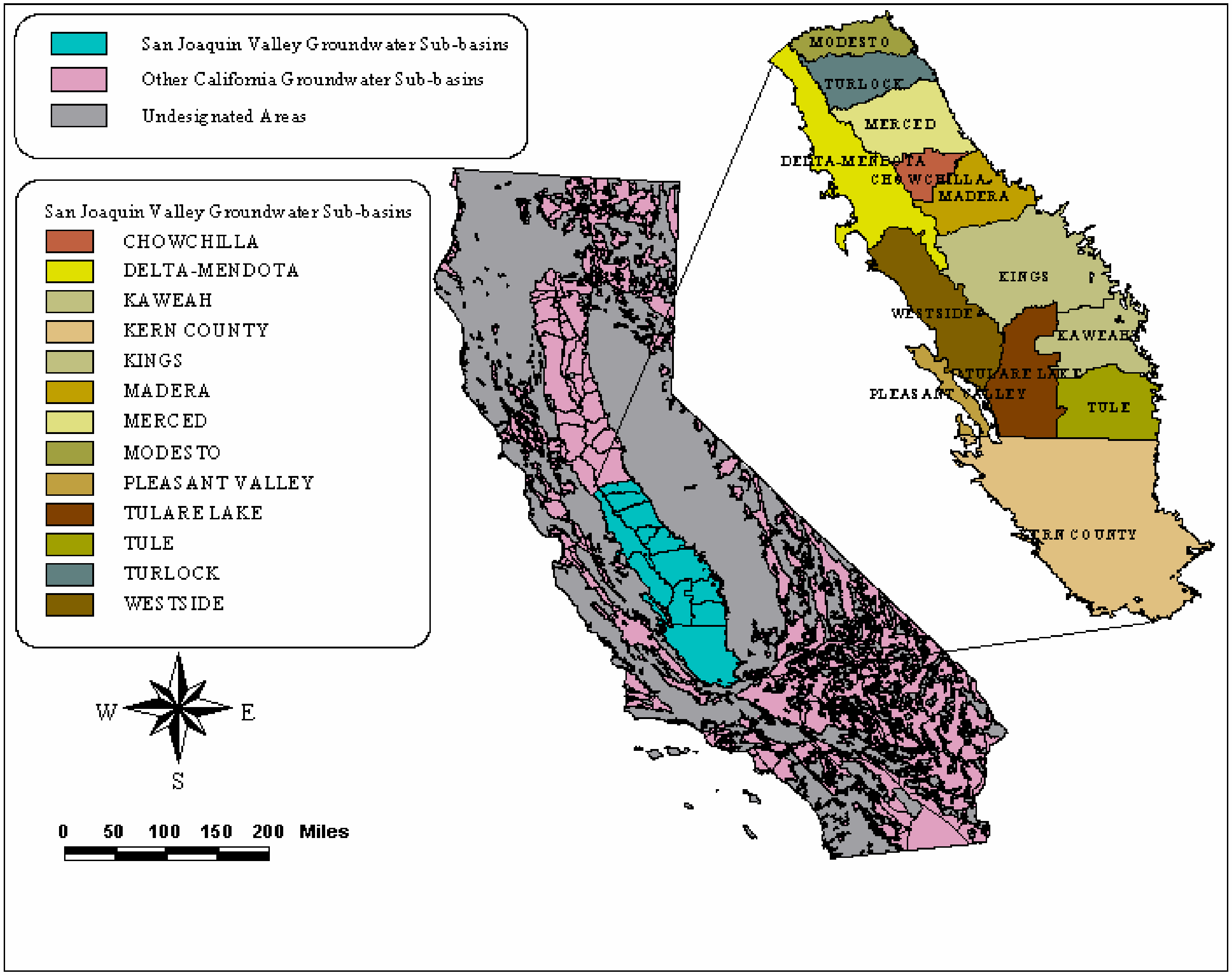

Plate 1: Groundwater sub-basins in the San Joaquin Valley, California.

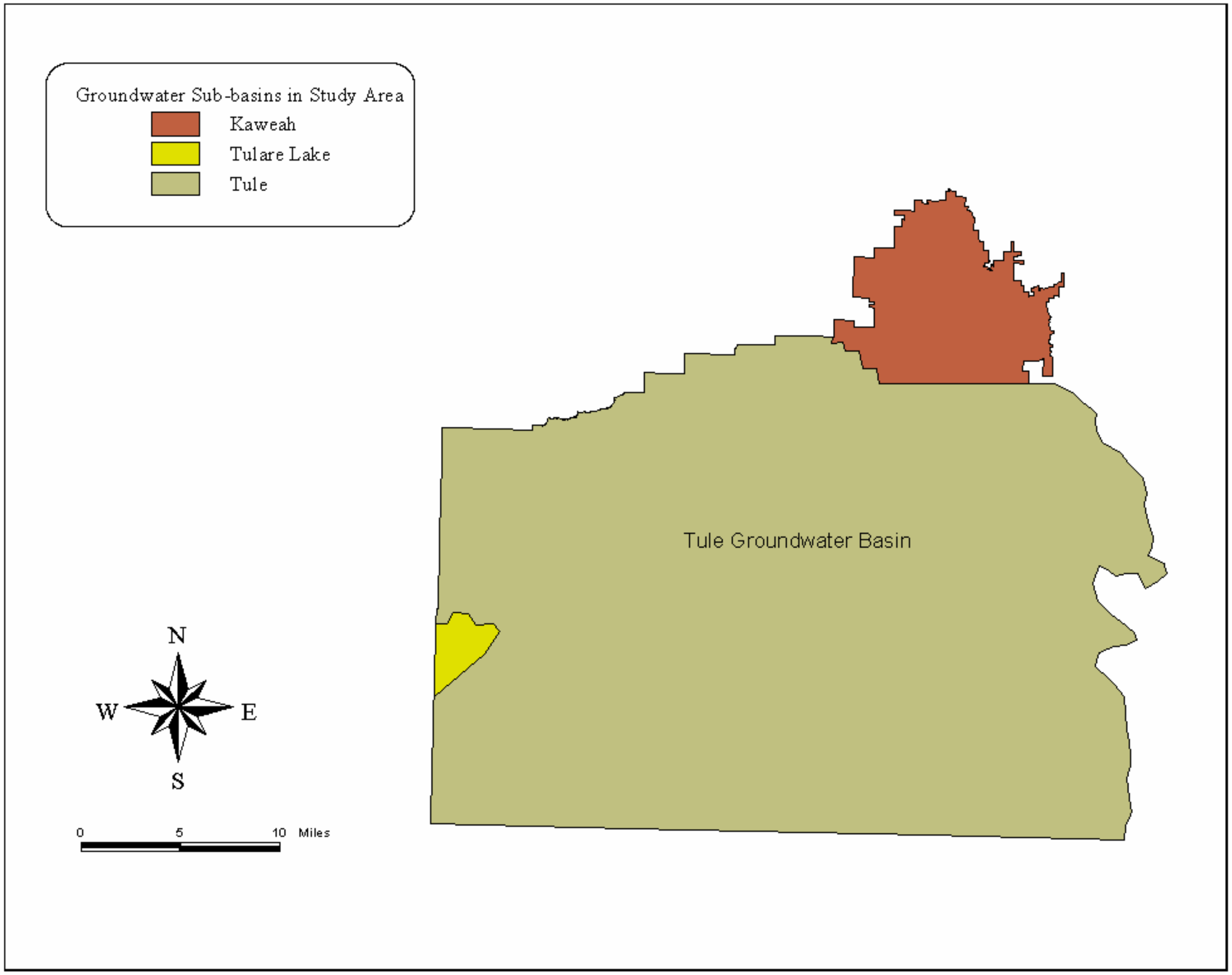

Plate 2: Study area location within the Tule, Kaweah, and Tulare Lake groundwater sub-basins.

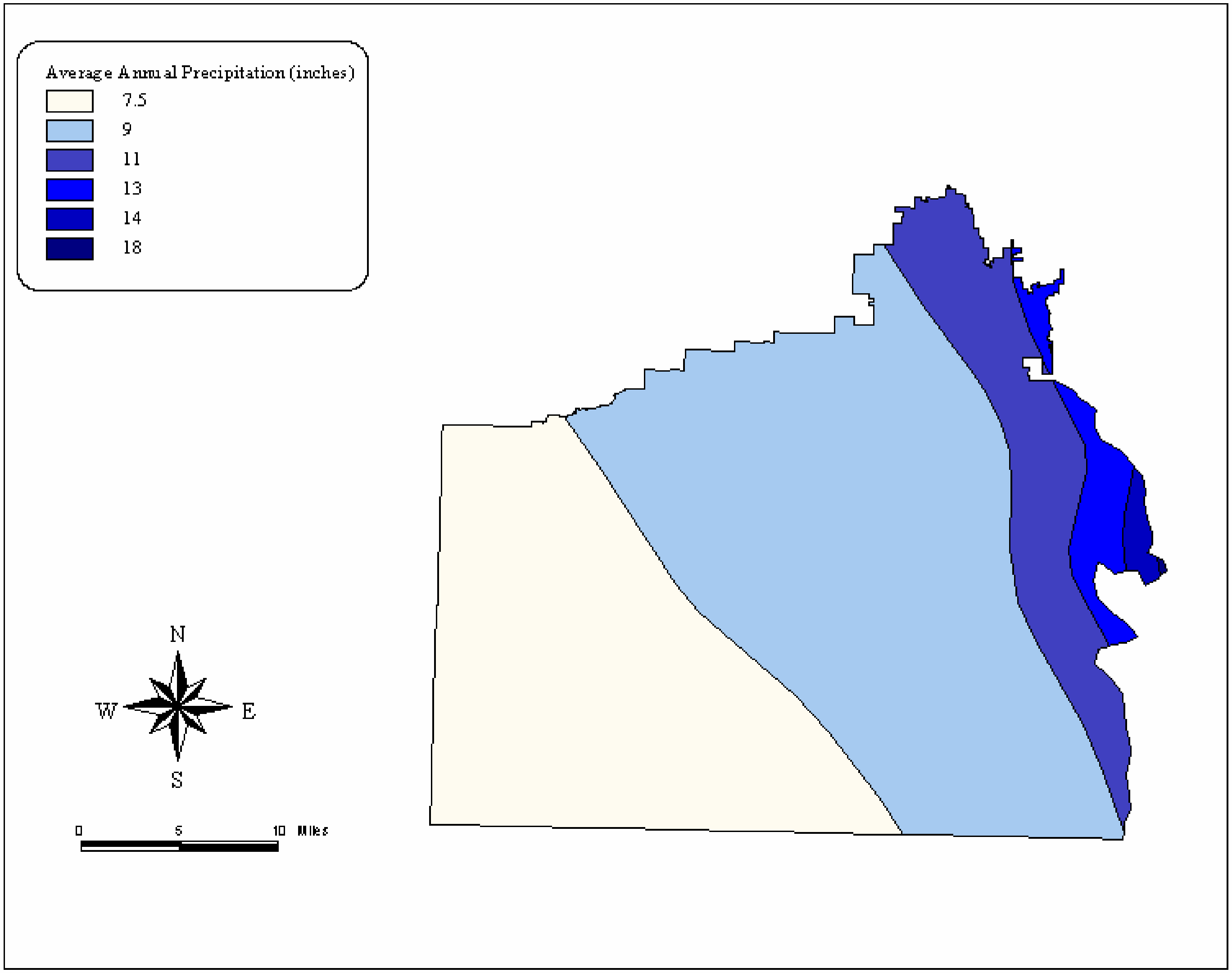

Plate 3: Isohyet of the average annual precipitation.

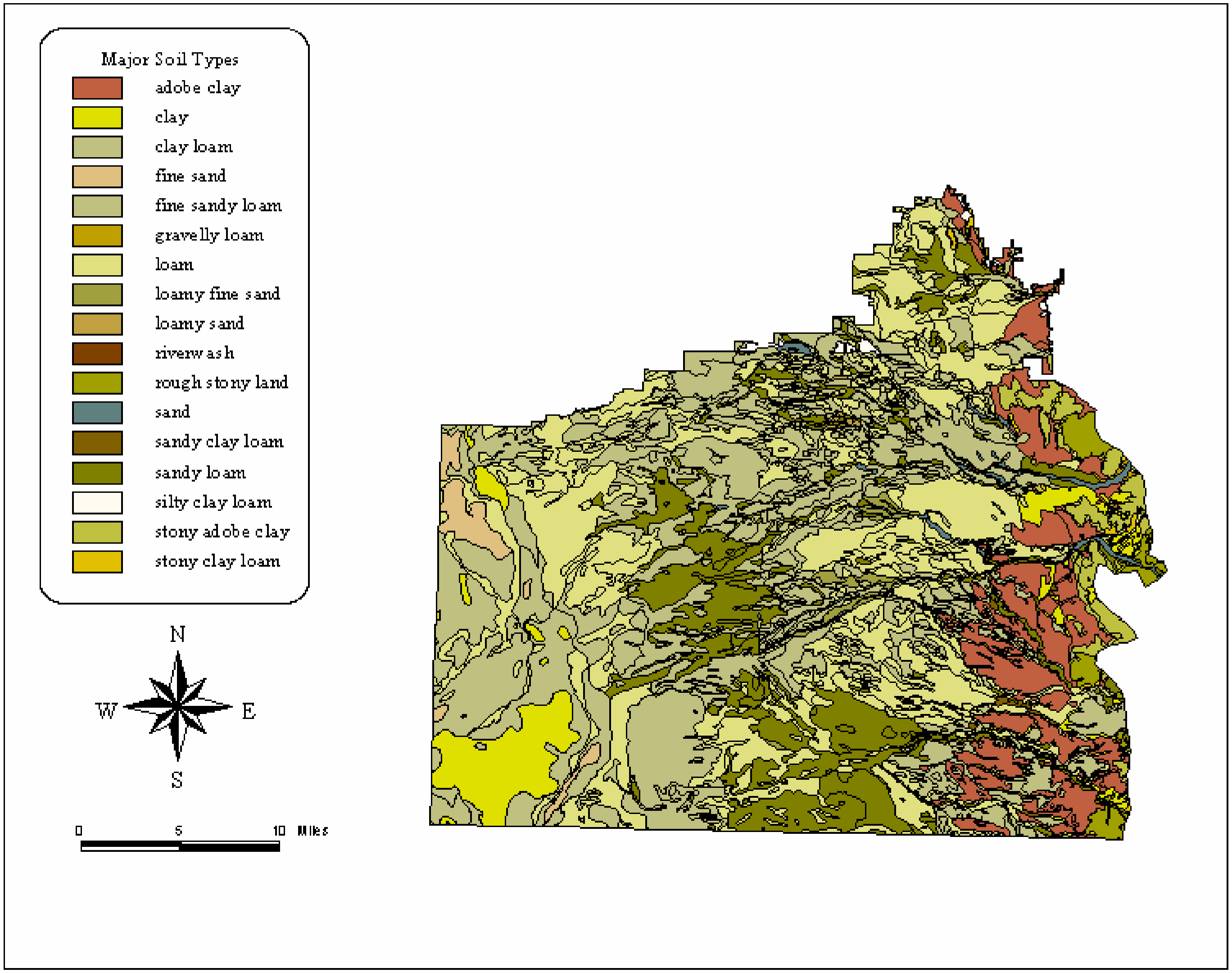

Plate 4: Major soil types from a 1935 soils survey.

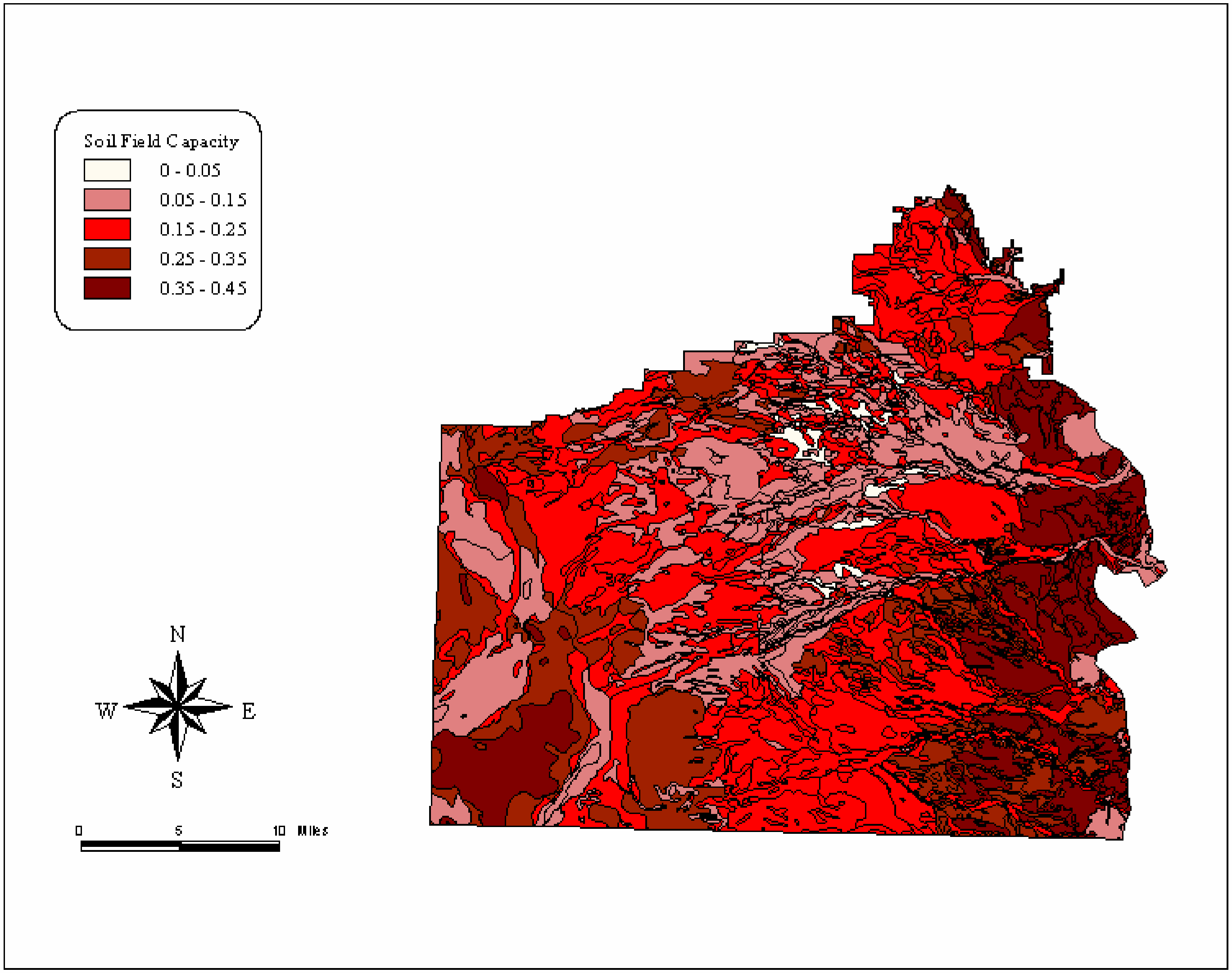

Plate 5: Field capacity of major soil types.

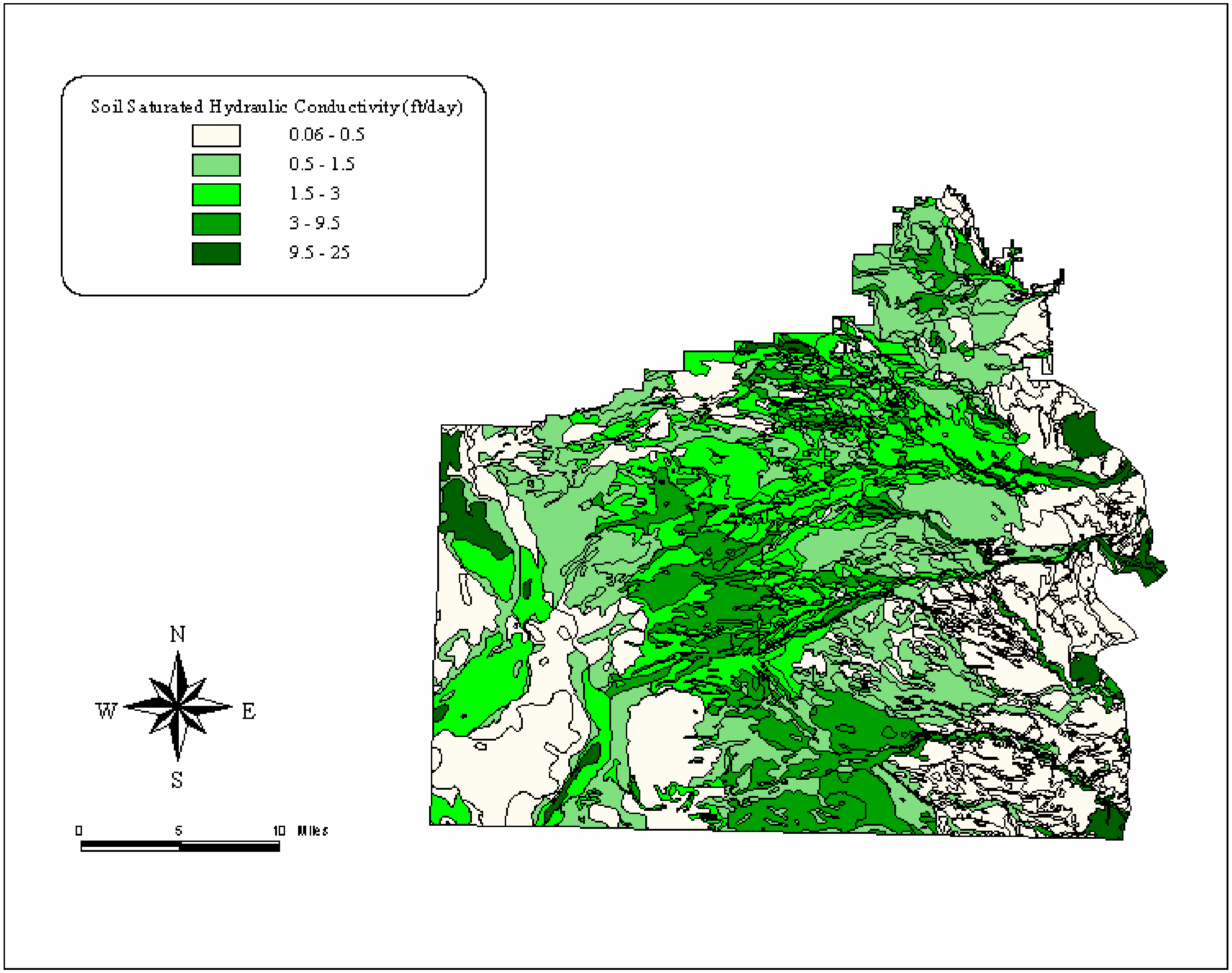

Plate 6: Saturated hydraulic conductivity (ft/day) of major soil types.

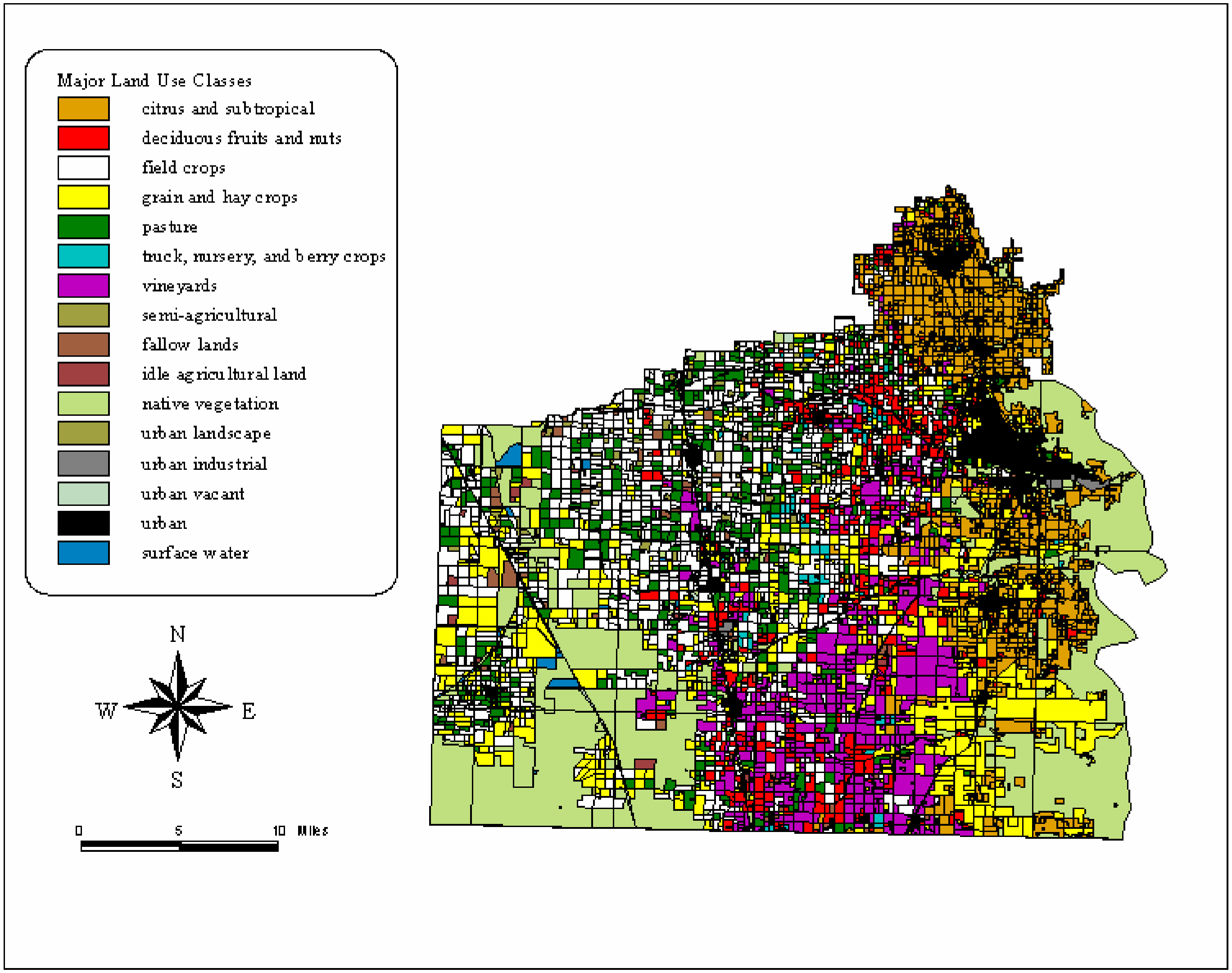

Plate 7: Major land-use classifications of land units from a 1985 land-use survey.

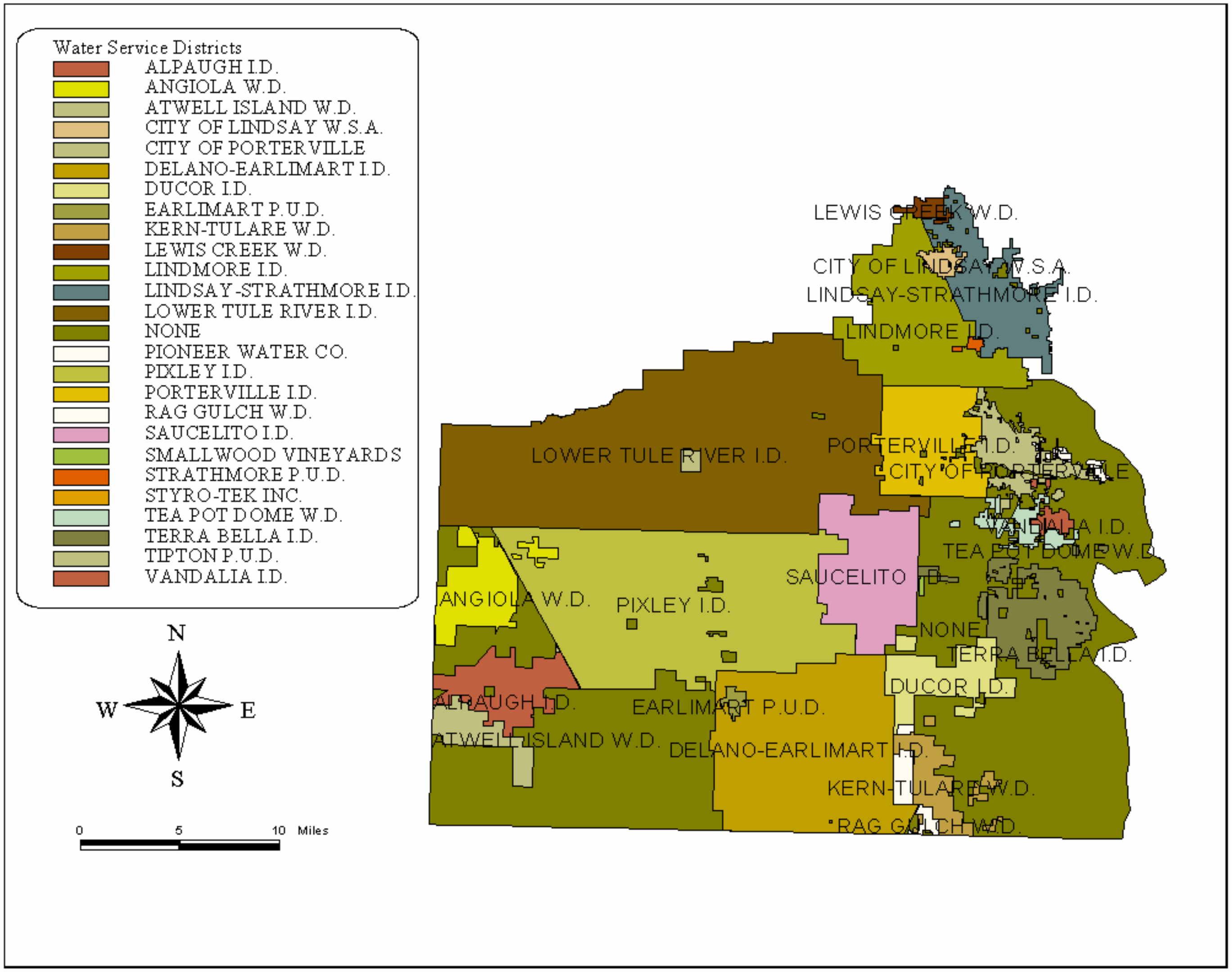

Plate 8: Water service districts.

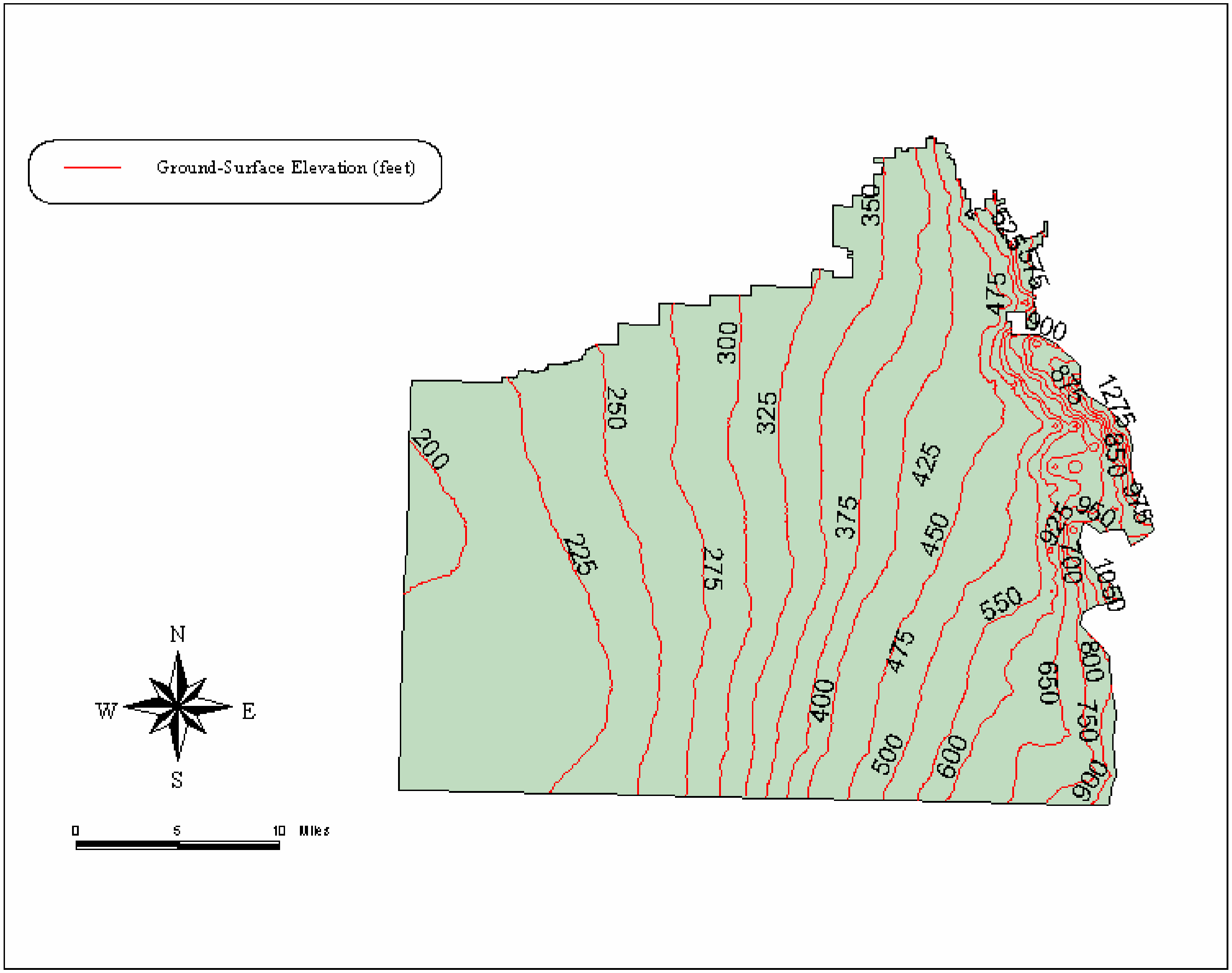

Plate 9: Ground surface elevations above sea level (feet).

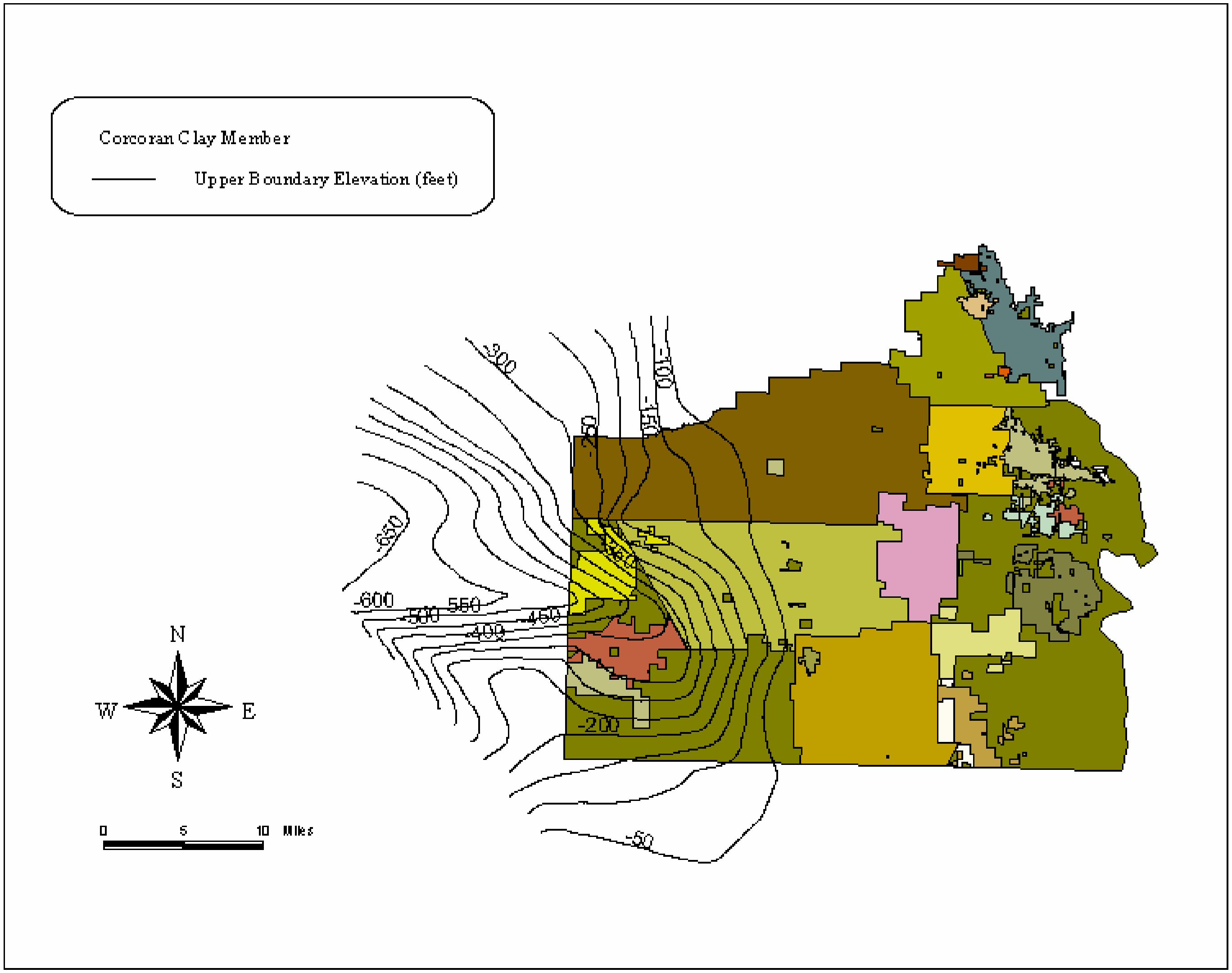

Plate 10: Lateral extent and top elevation contour map of the Corcoran Clay Member of the Tulare Formation.

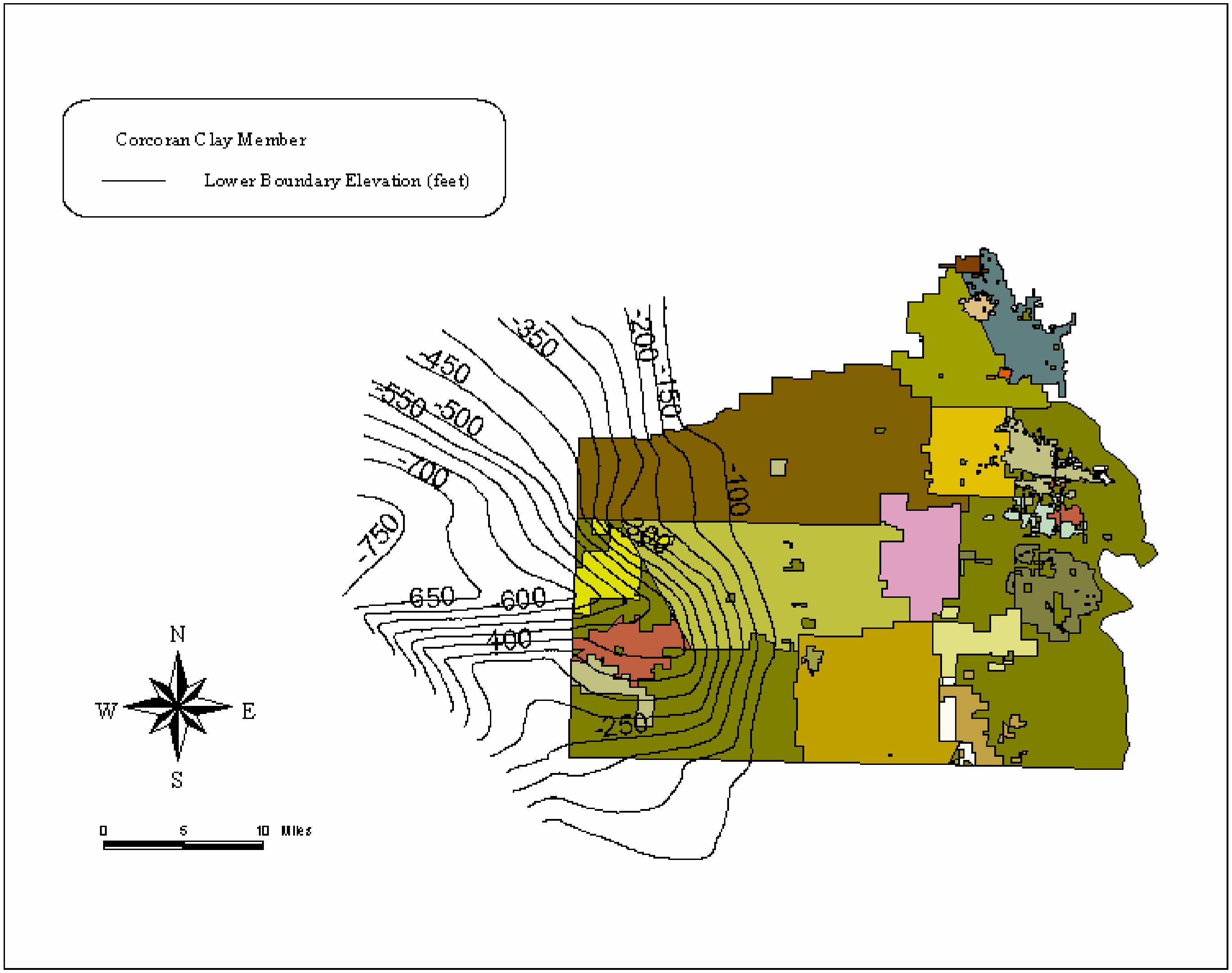

Plate 11: Lateral extent and base elevation contour map of the Corcoran Clay Member of the Tulare Formation.

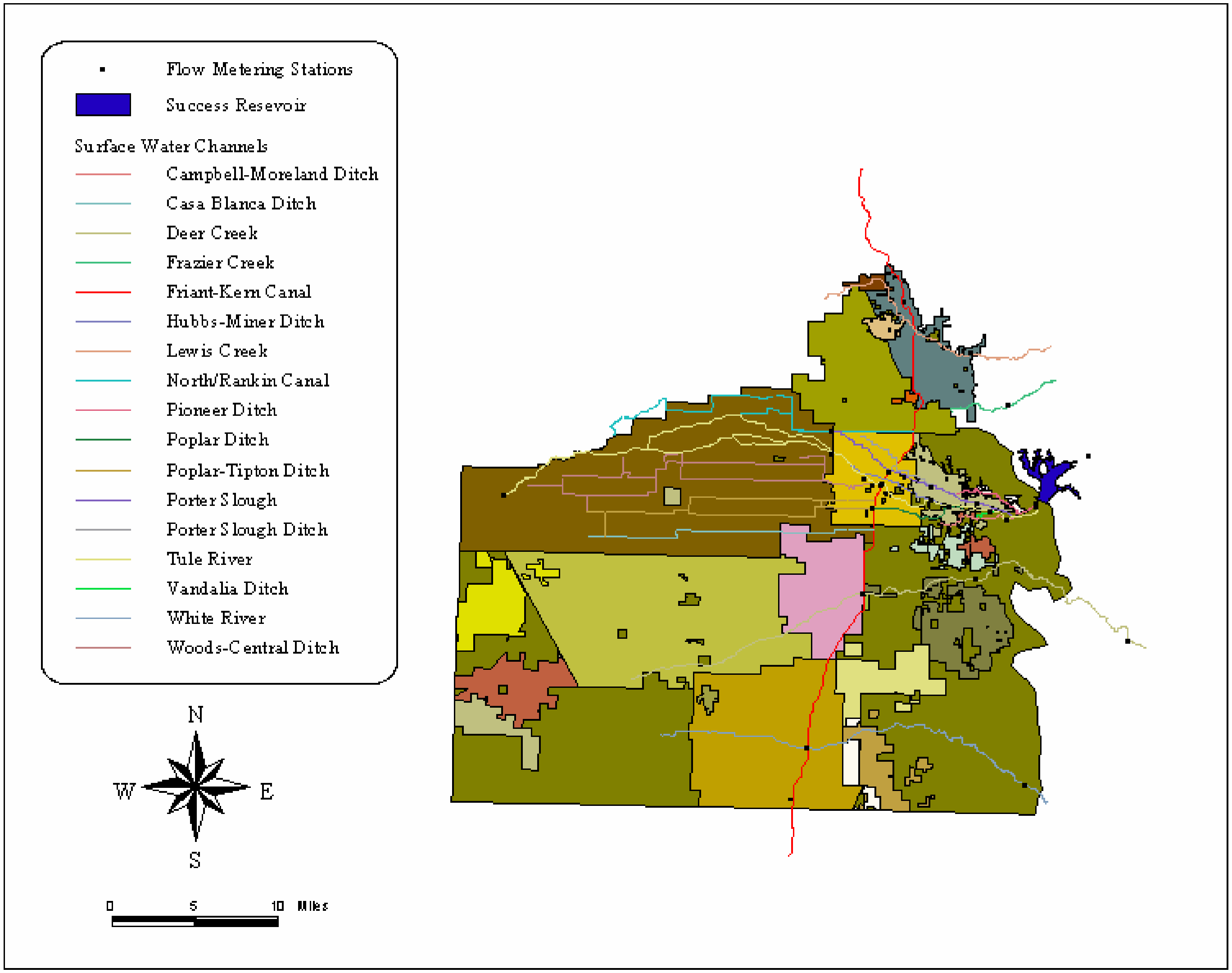

Plate 12: Major natural and constructed surface water channels in the study area.

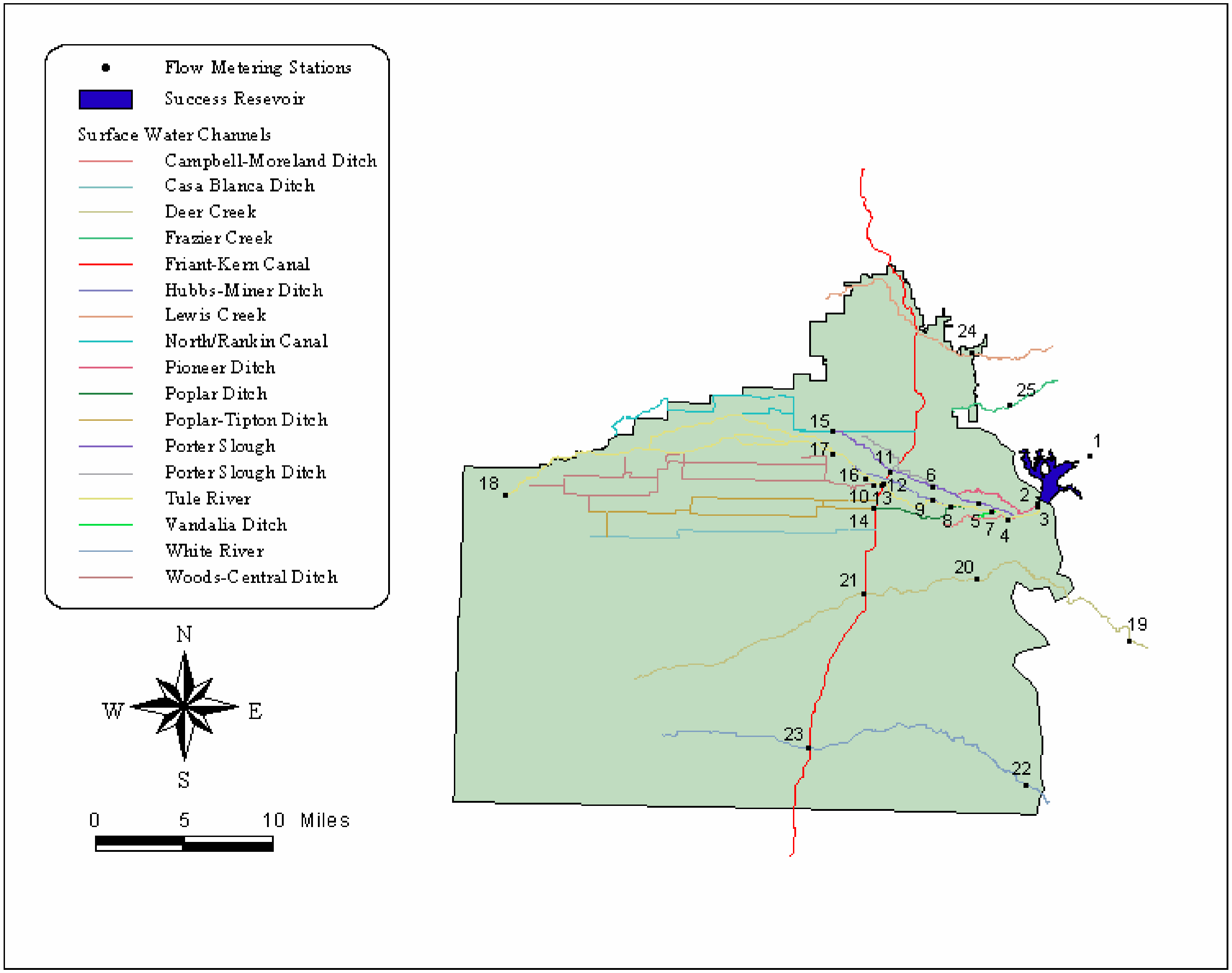

Plate 13: Locations of metering stations (Table 8) along the major natural and constructed surface water channels.

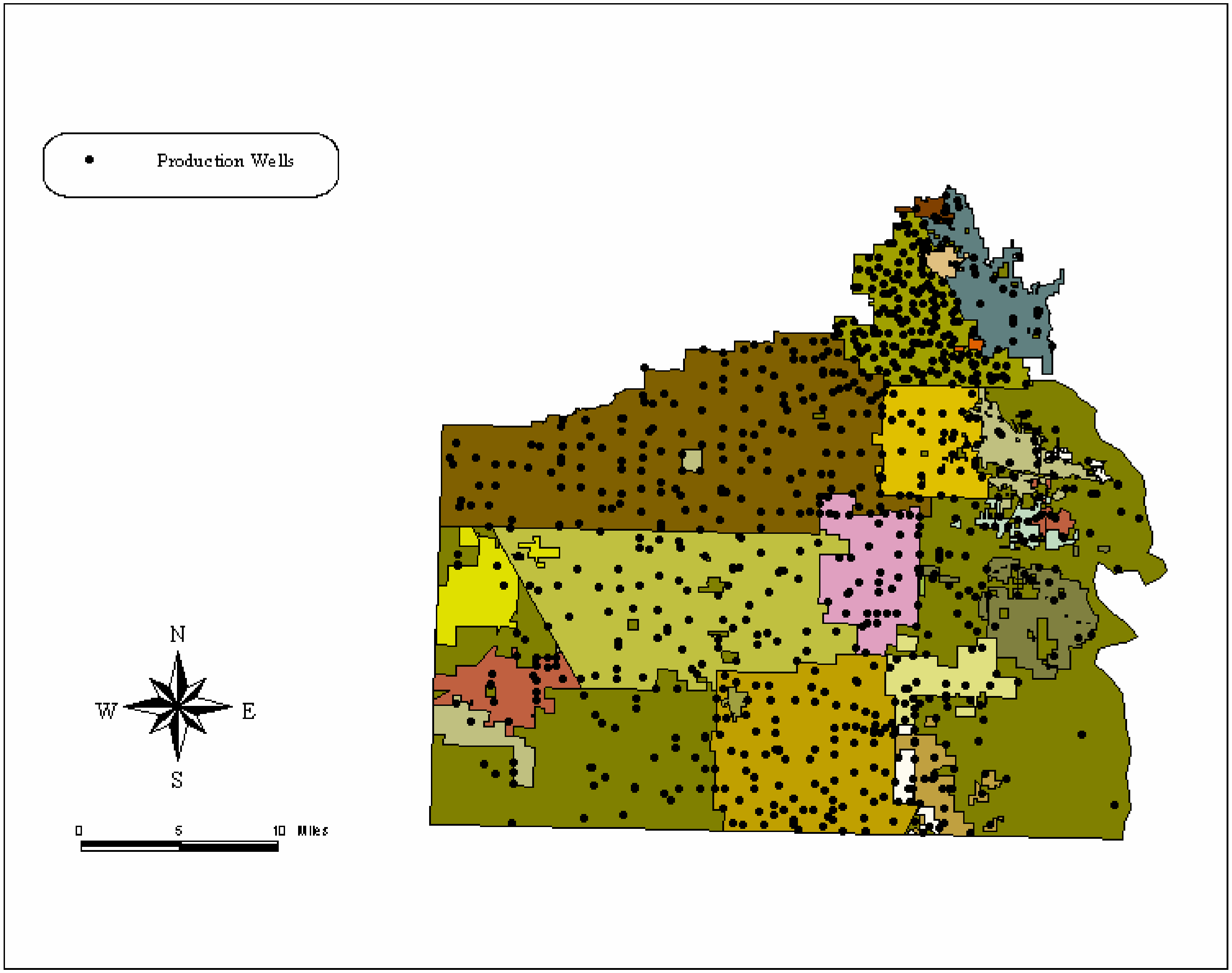

Plate 14: Locations of observation production wells in study area.

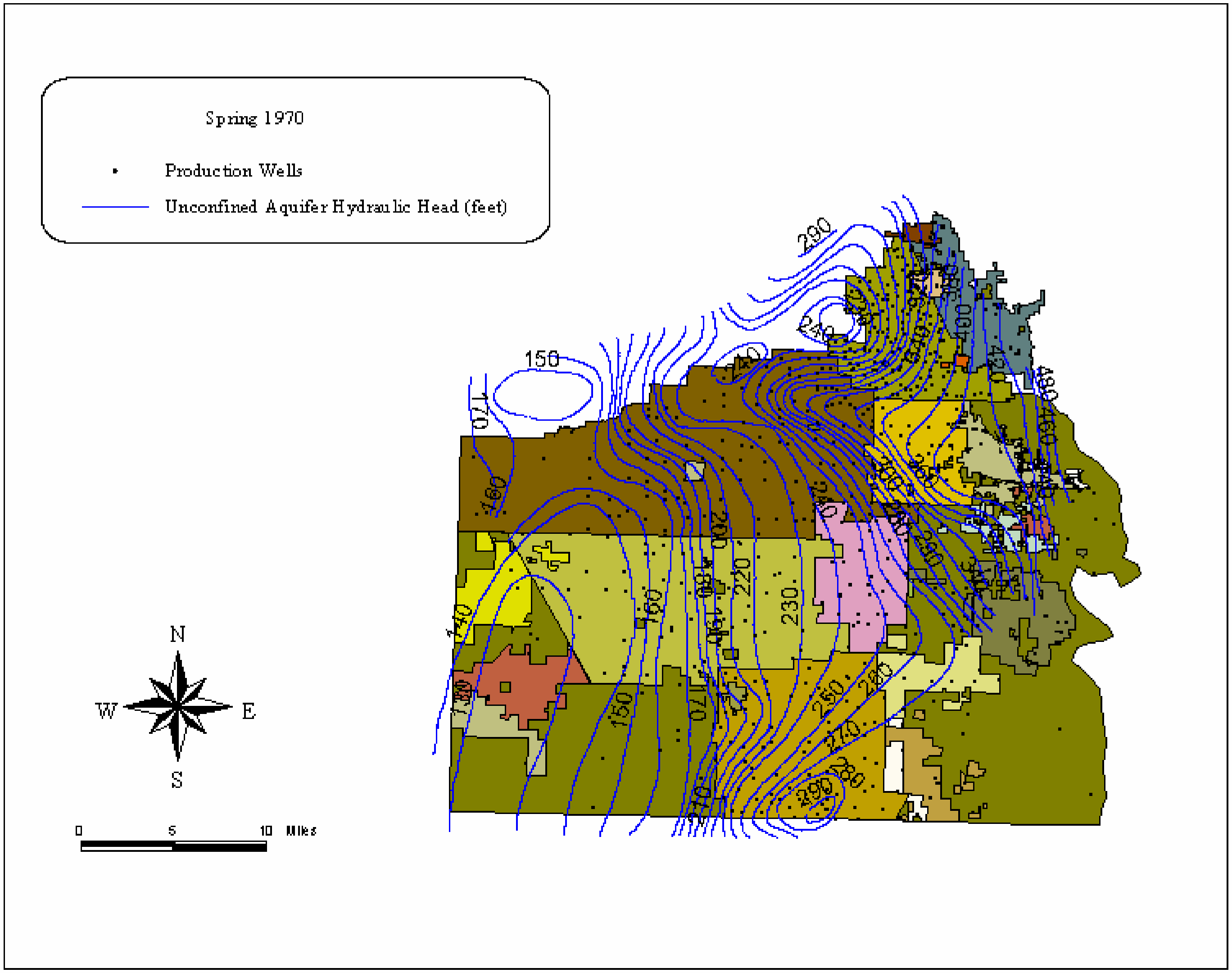

Plate 15: Contour lines of equal hydraulic head in the unconfined aquifer and locations of measured production wells for the spring of 1970.

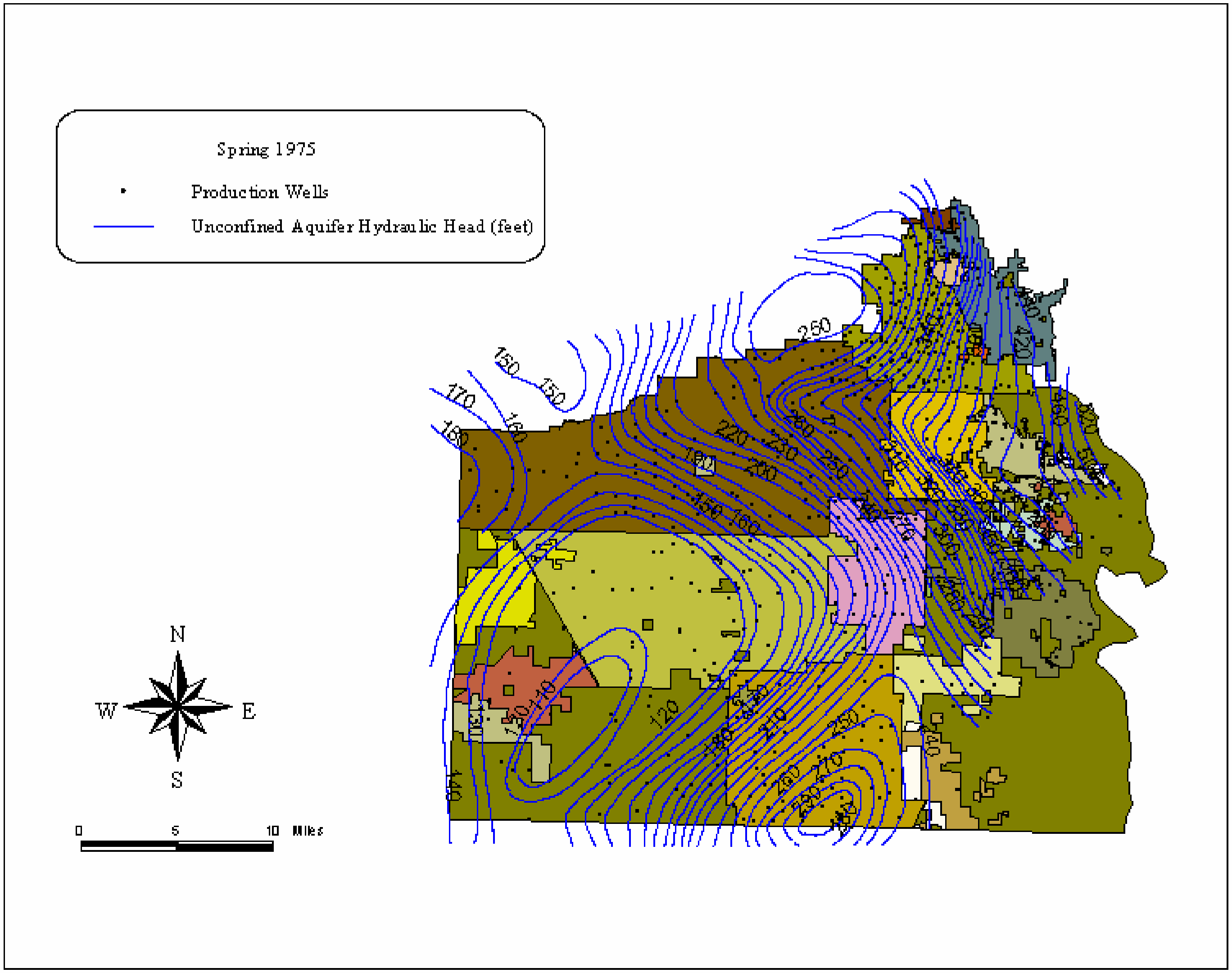

Plate 16: Contour lines of equal hydraulic head in the unconfined aquifer and locations of measured production wells for the spring of 1975.

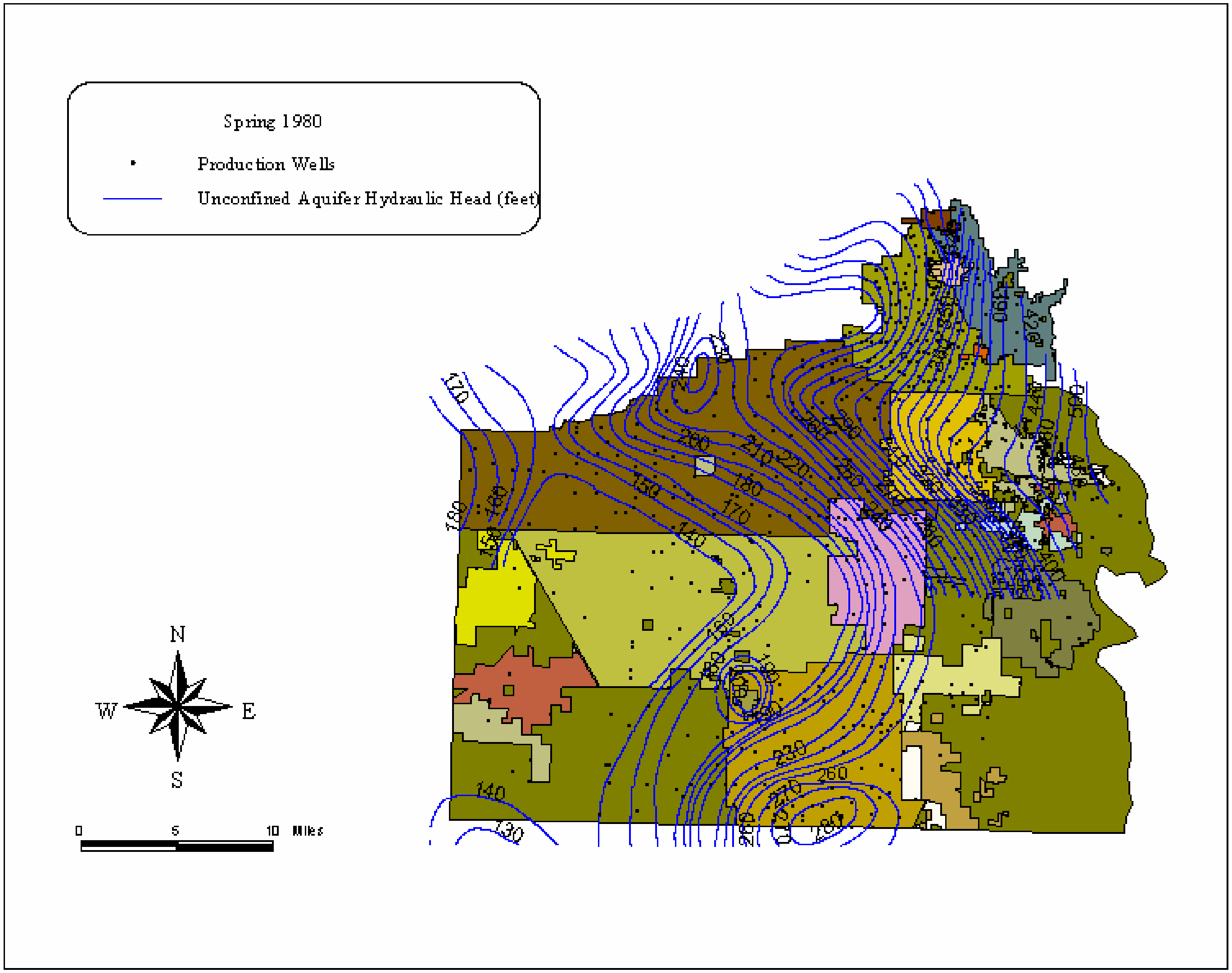

Plate 17: Contour lines of equal hydraulic head in the unconfined aquifer and locations of measured production wells for the spring of 1980.

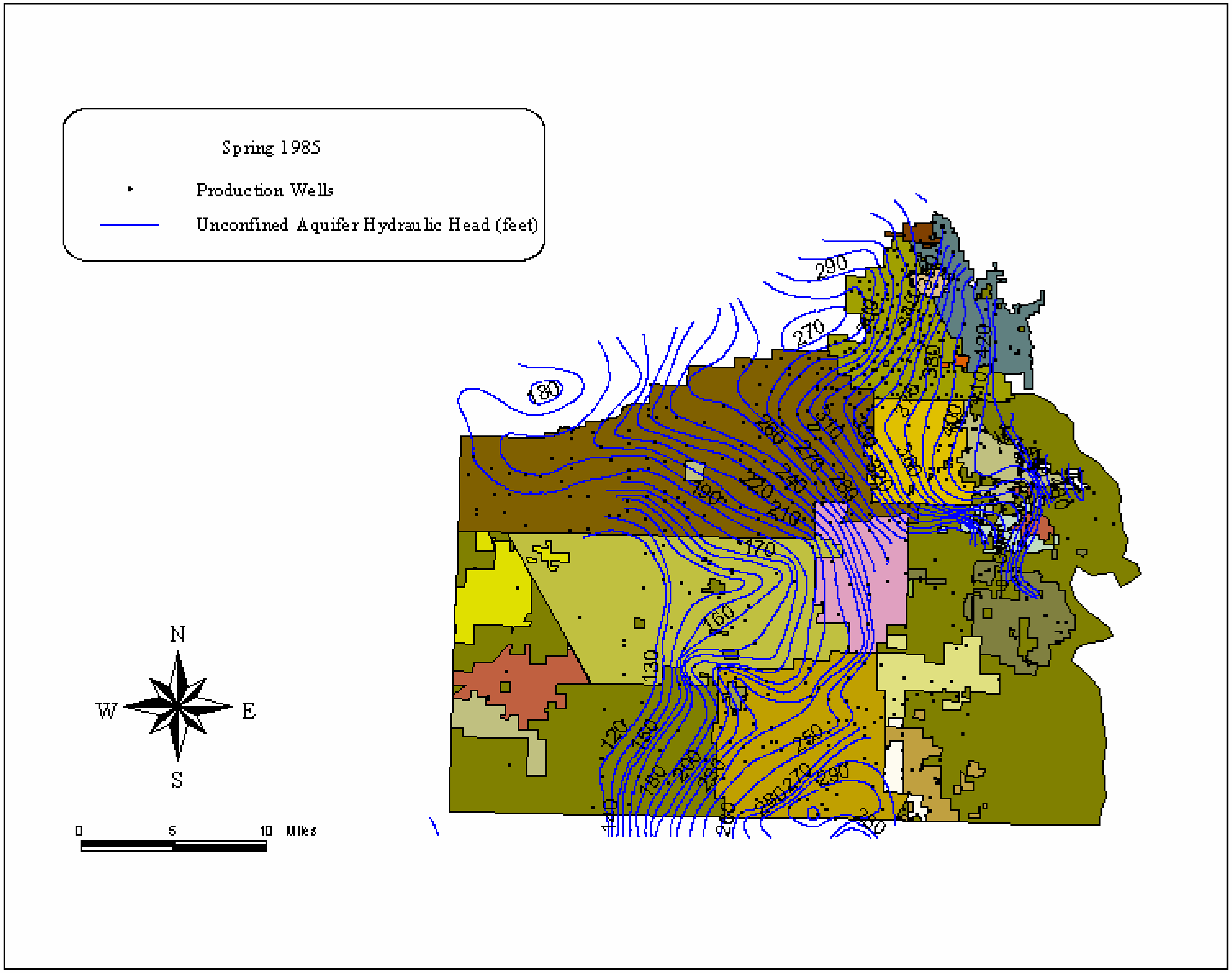

Plate 18: Contour lines of equal hydraulic head in the unconfined aquifer and locations of measured production wells for the spring of 1985.

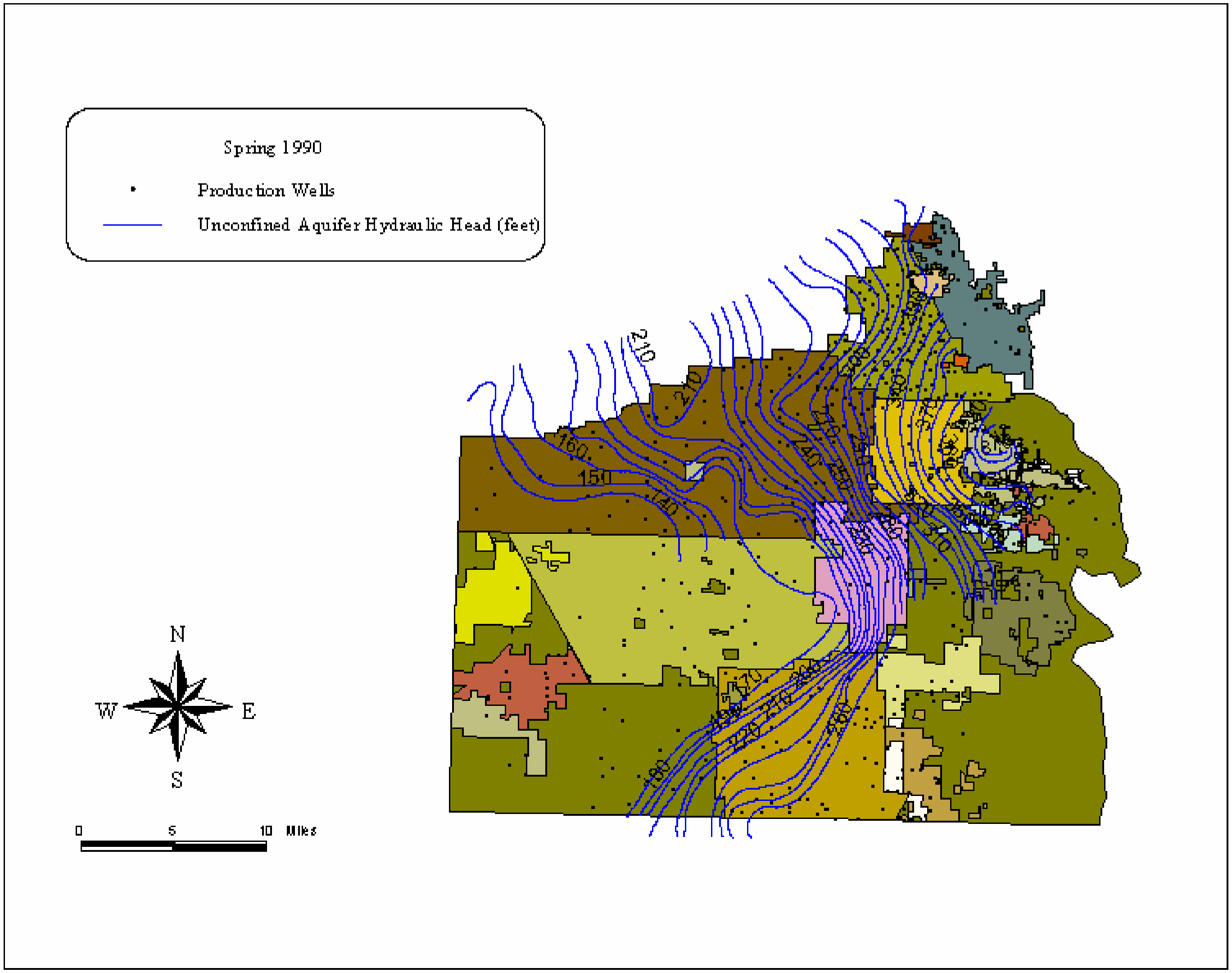

Plate 19: Contour lines of equal hydraulic head in the unconfined aquifer and locations of measured production wells for the spring of 1990.

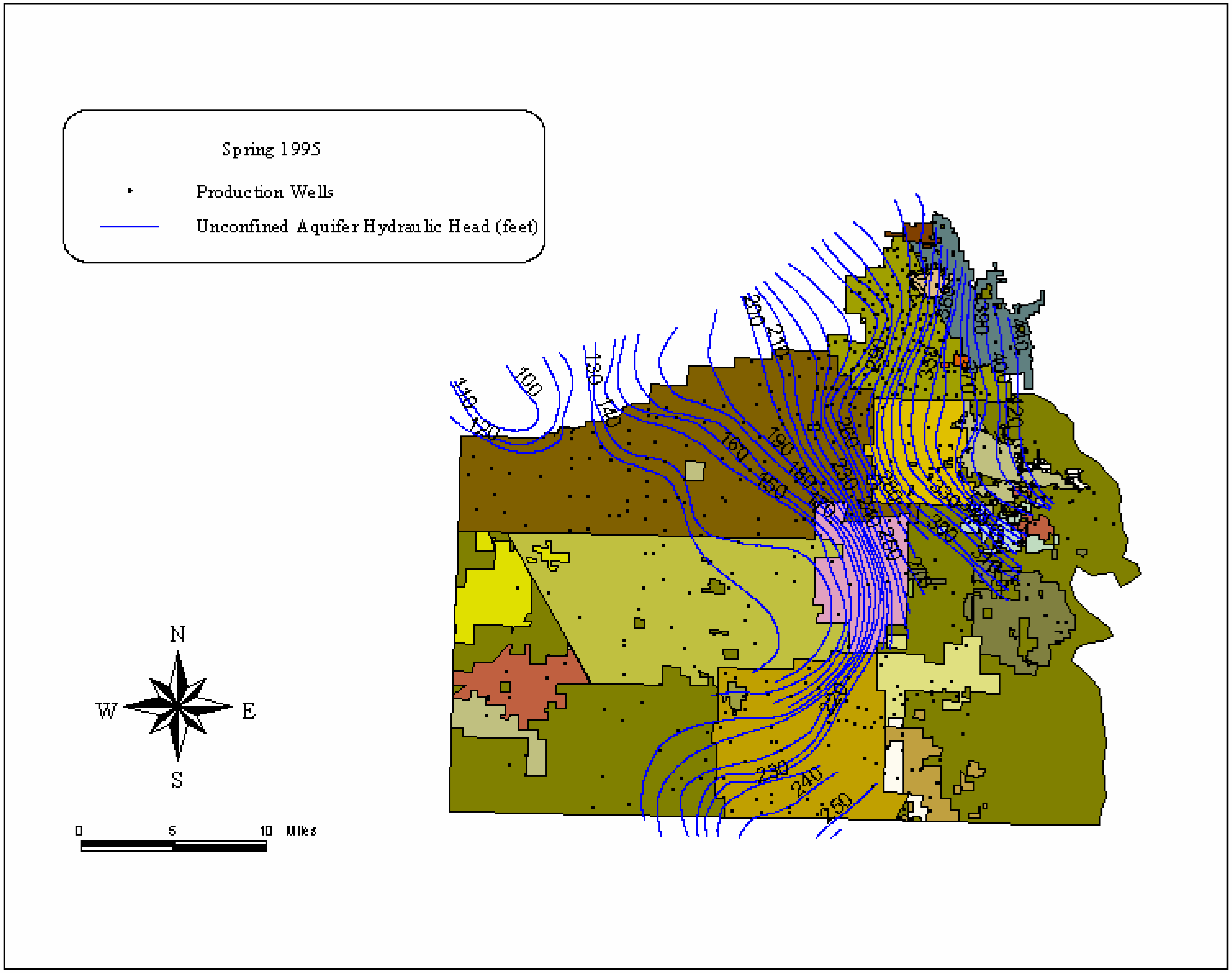

Plate 20: Contour lines of equal hydraulic head in the unconfined aquifer and locations of measured production wells for the spring of 1995.

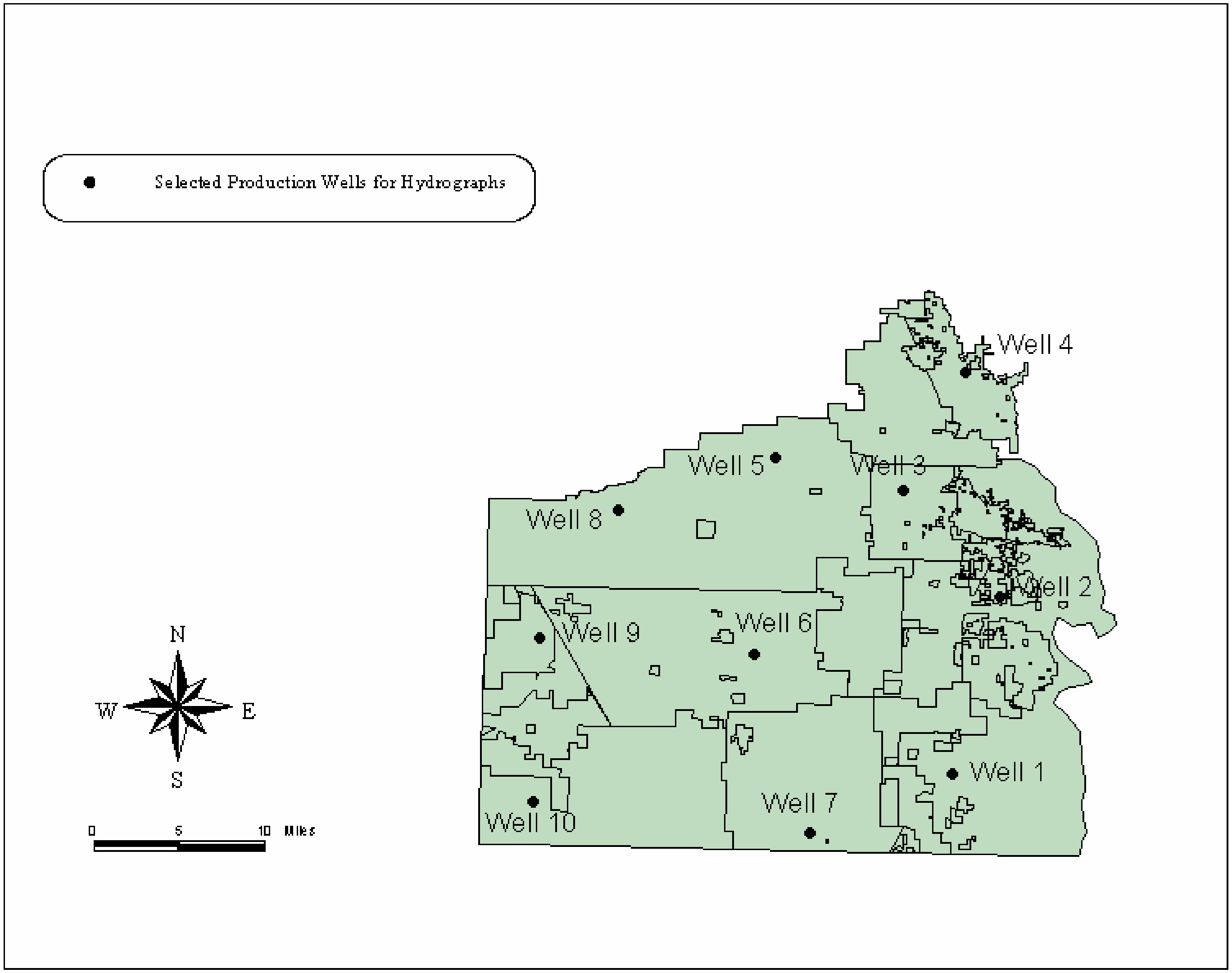

Plate 21: Locations of selected production wells used for generating hydraulic head hydrographs.

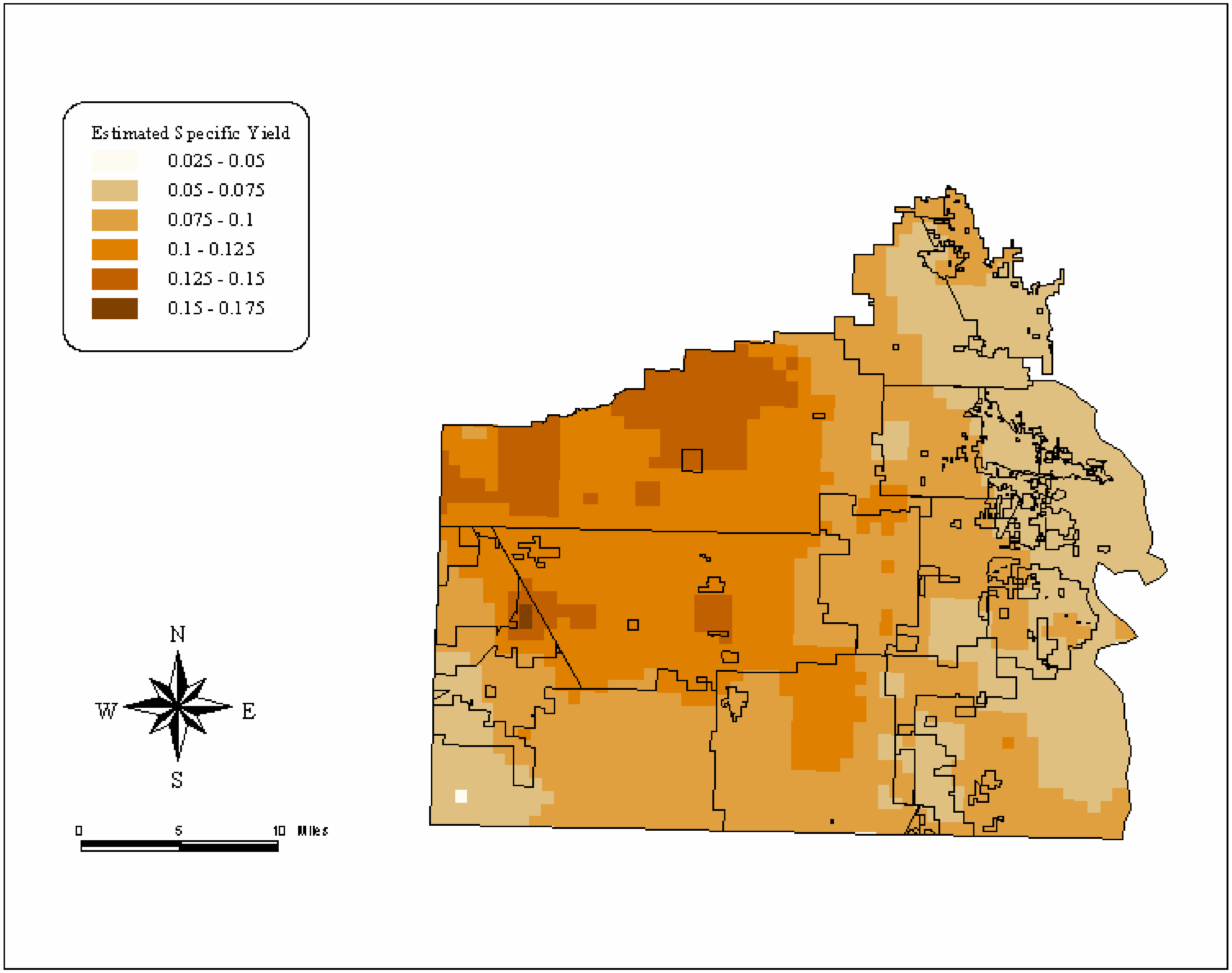

Plate 22: Estimated specific yield distribution in the unconfined aquifer.

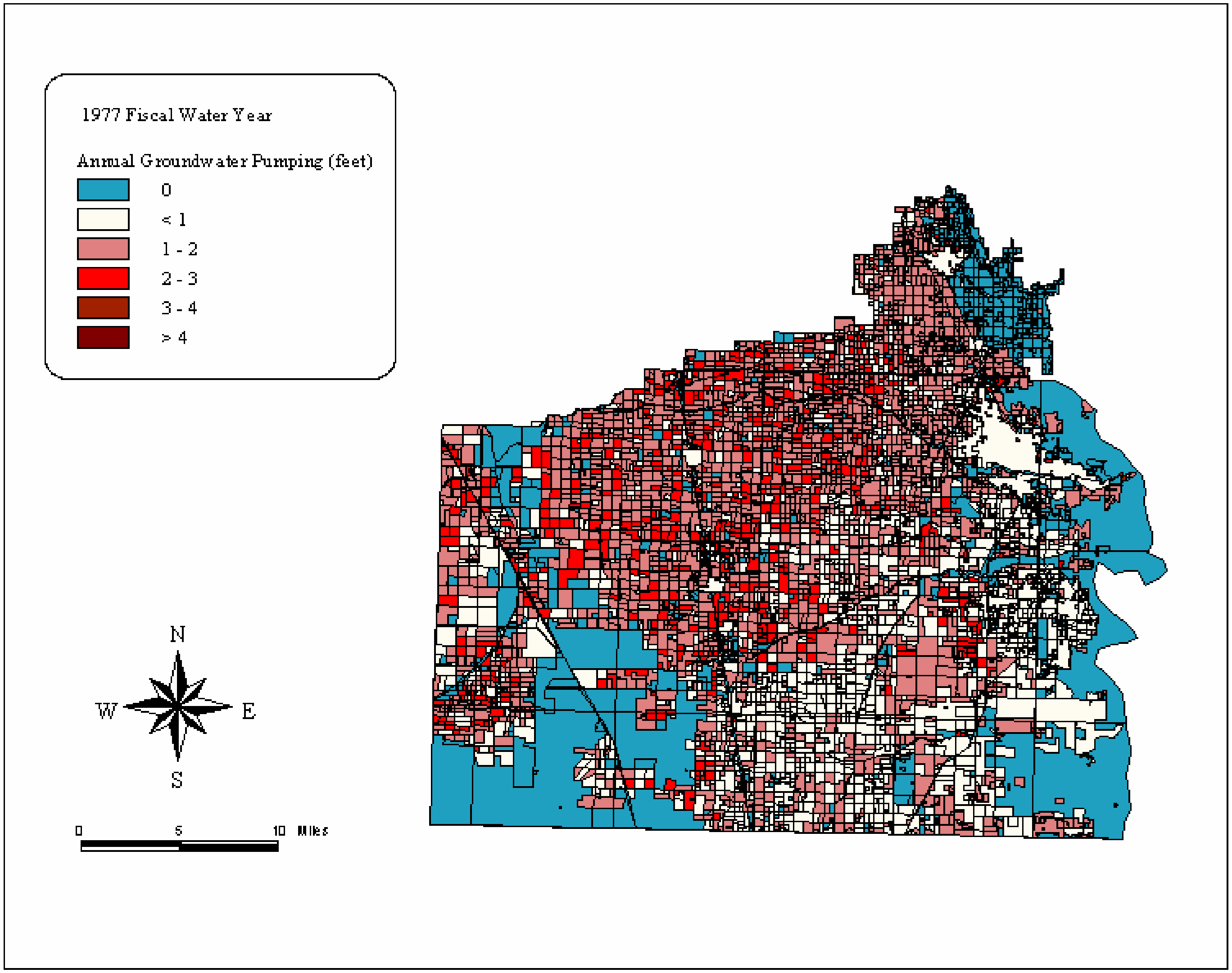

Plate 23: Spatial distribution of total groundwater pumping demand (feet) for the 1977 fiscal water year.

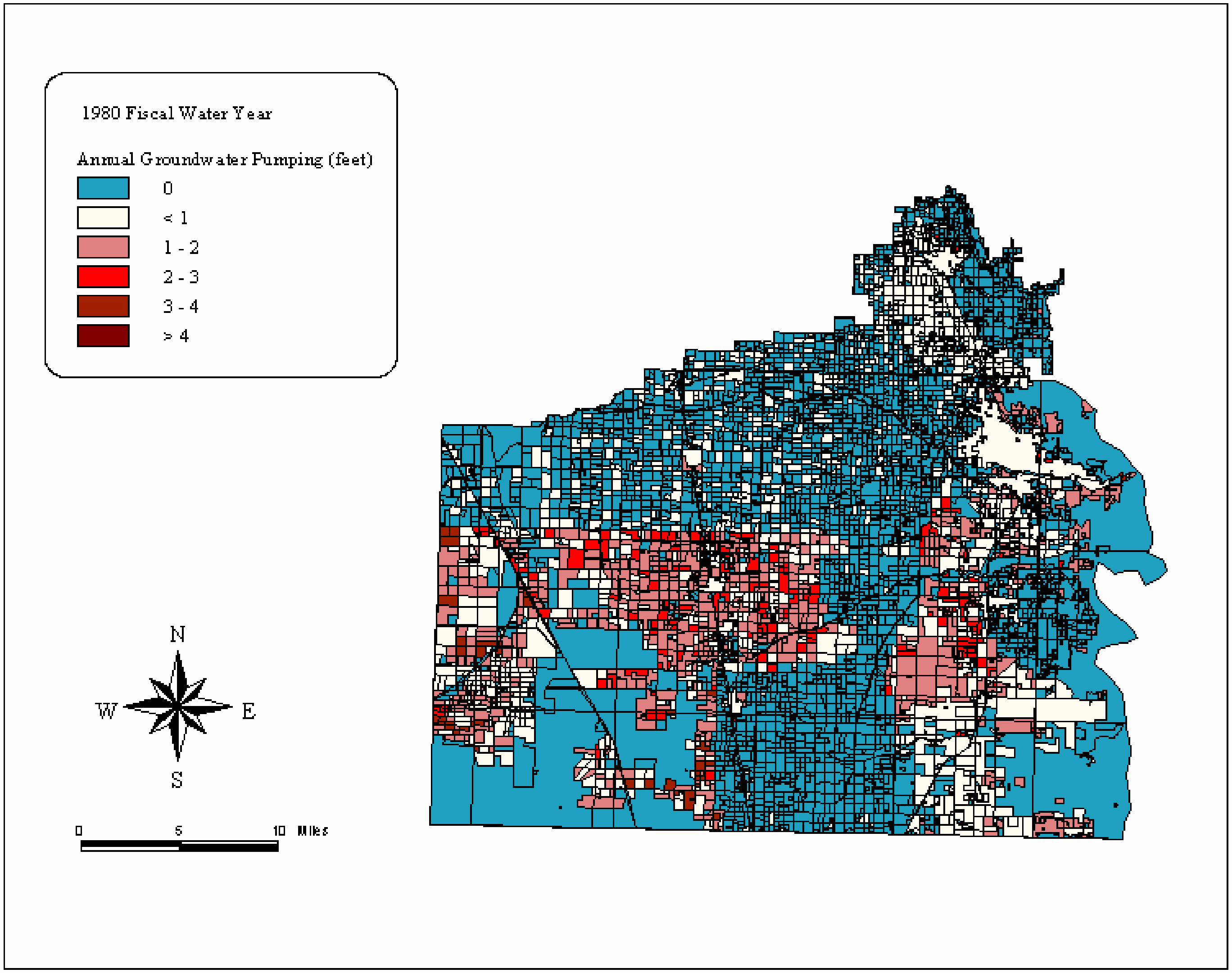

Plate 24: Spatial distribution of total groundwater pumping demand (feet) for the 1980 fiscal water year.

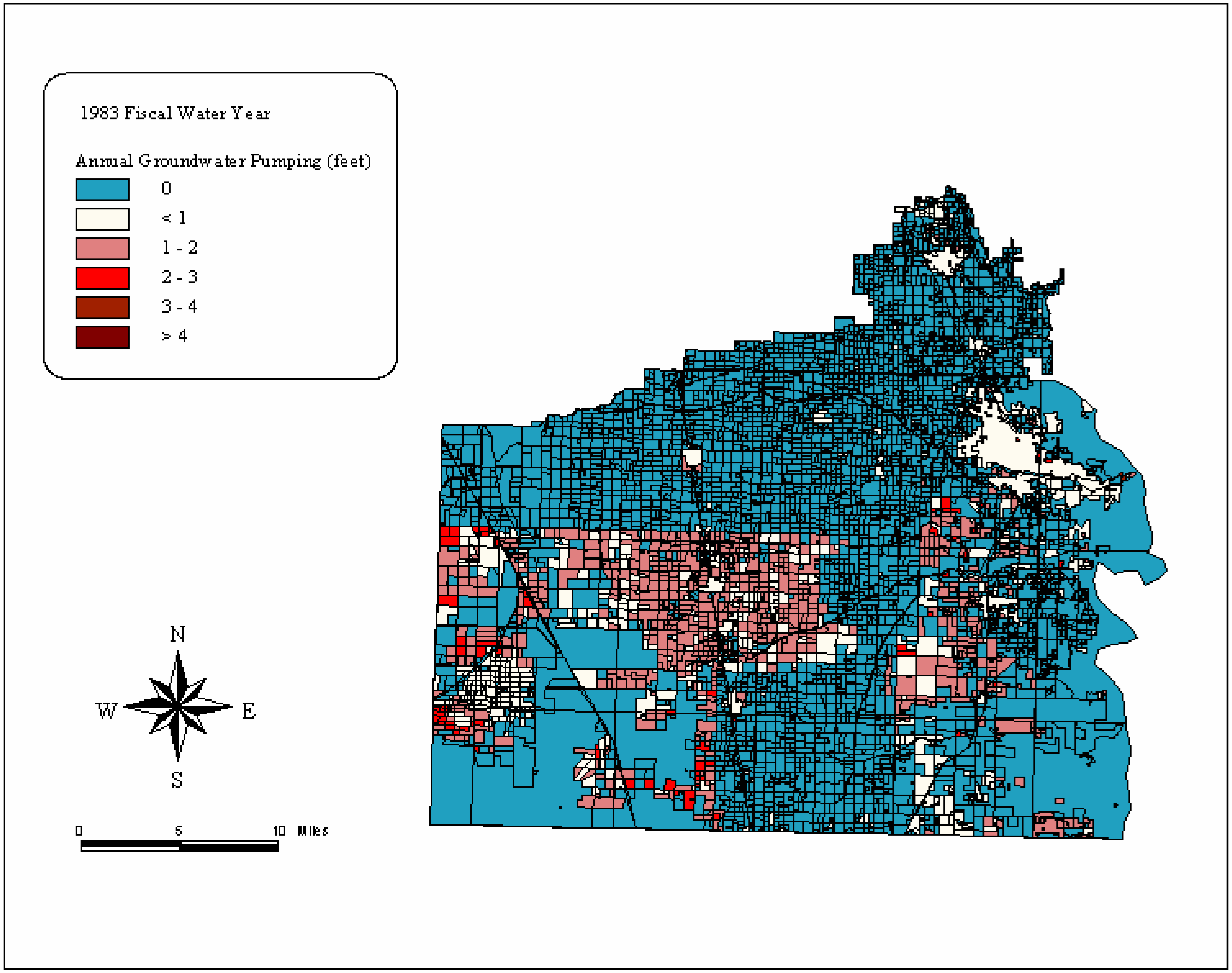

Plate 25: Spatial distribution of total groundwater pumping demand (feet) for the 1983 fiscal water year.

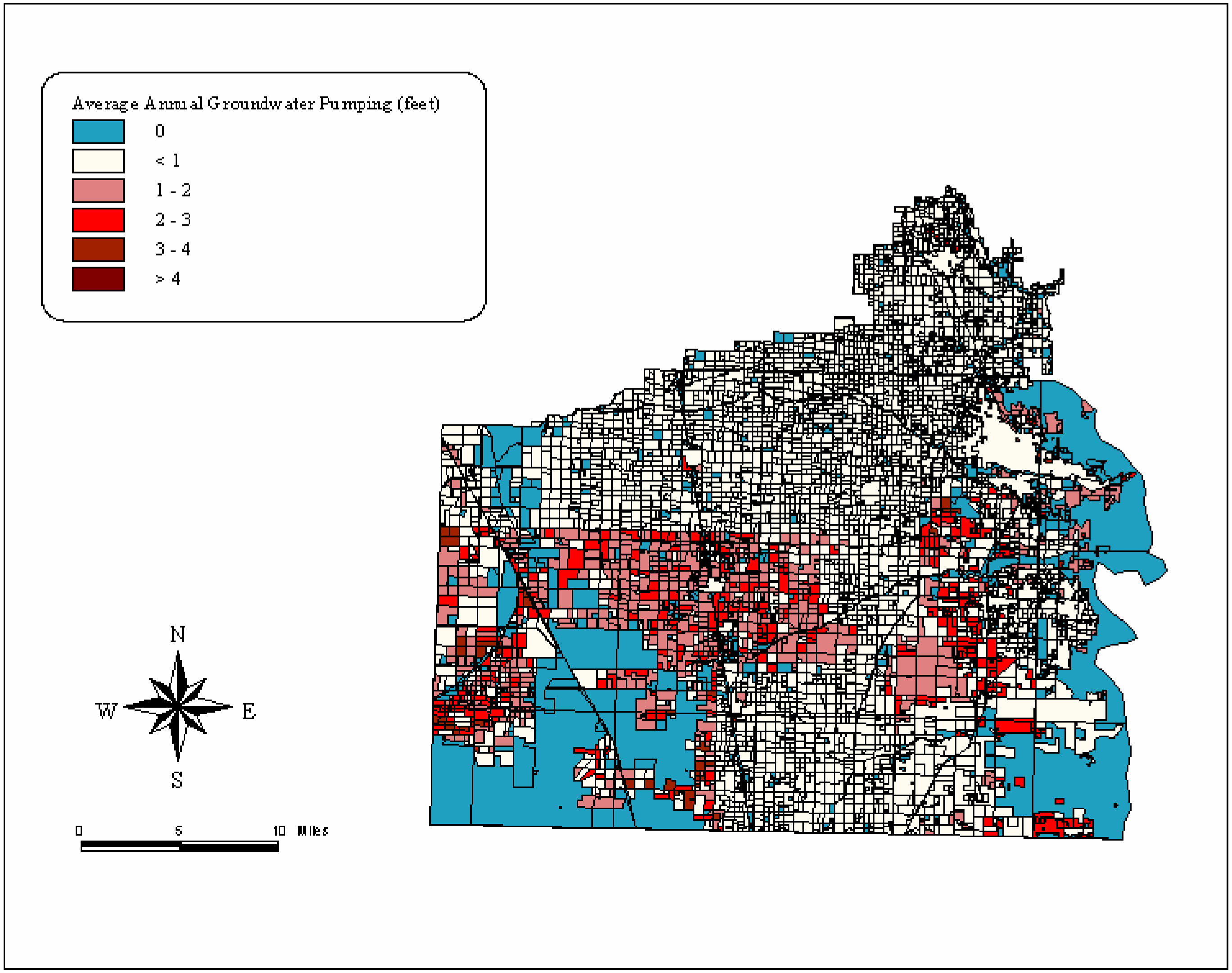

Plate 26: Spatial distribution of average annual groundwater pumping demand (feet) from 1970-99.

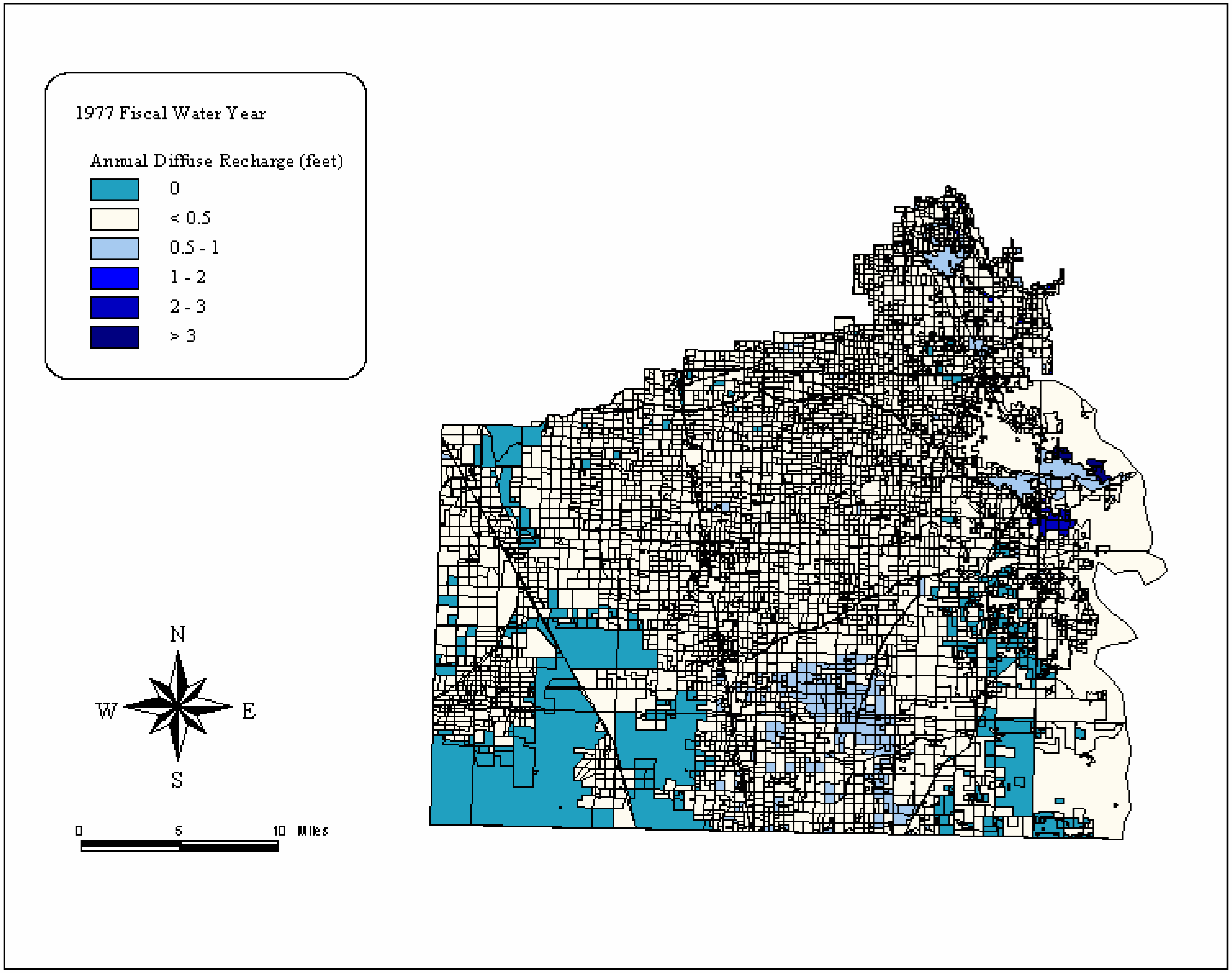

Plate 27: Spatial distribution of total diffuse recharge (feet) for the 1977 fiscal water year.

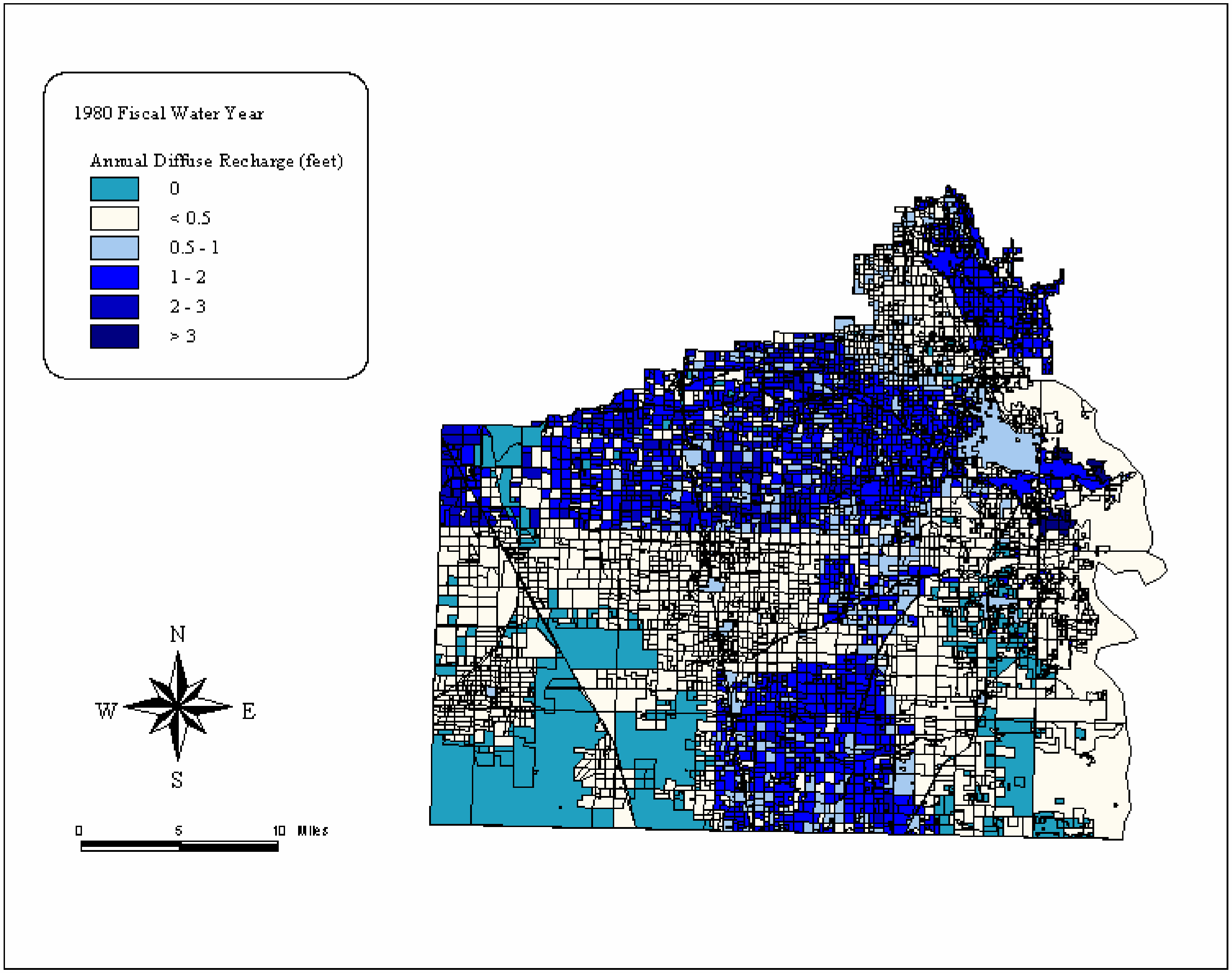

Plate 28: Spatial distribution of total diffuse recharge (feet) for the 1980 fiscal water year.

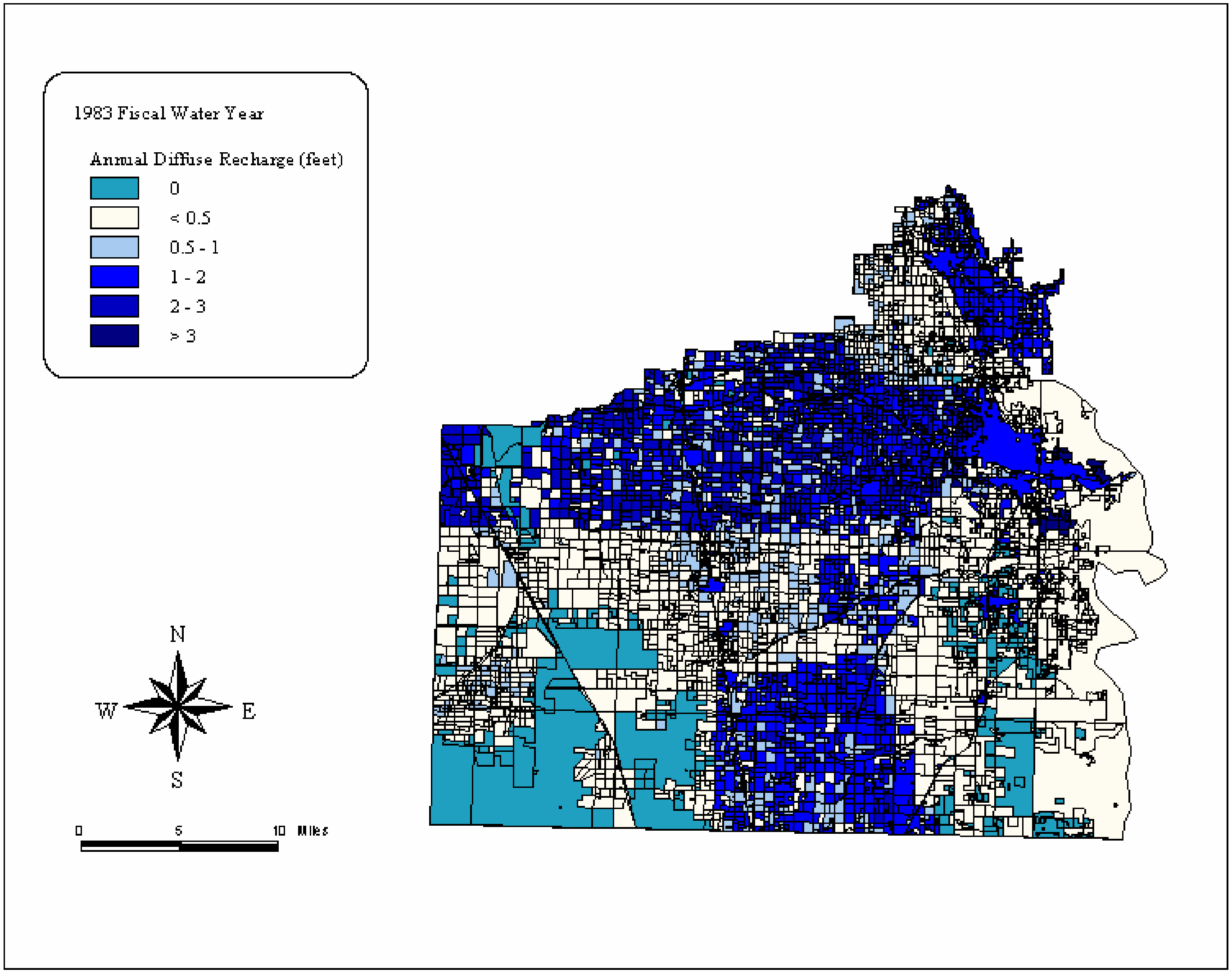

Plate 29: Spatial distribution of total diffuse recharge (feet) for the 1983 fiscal water year.

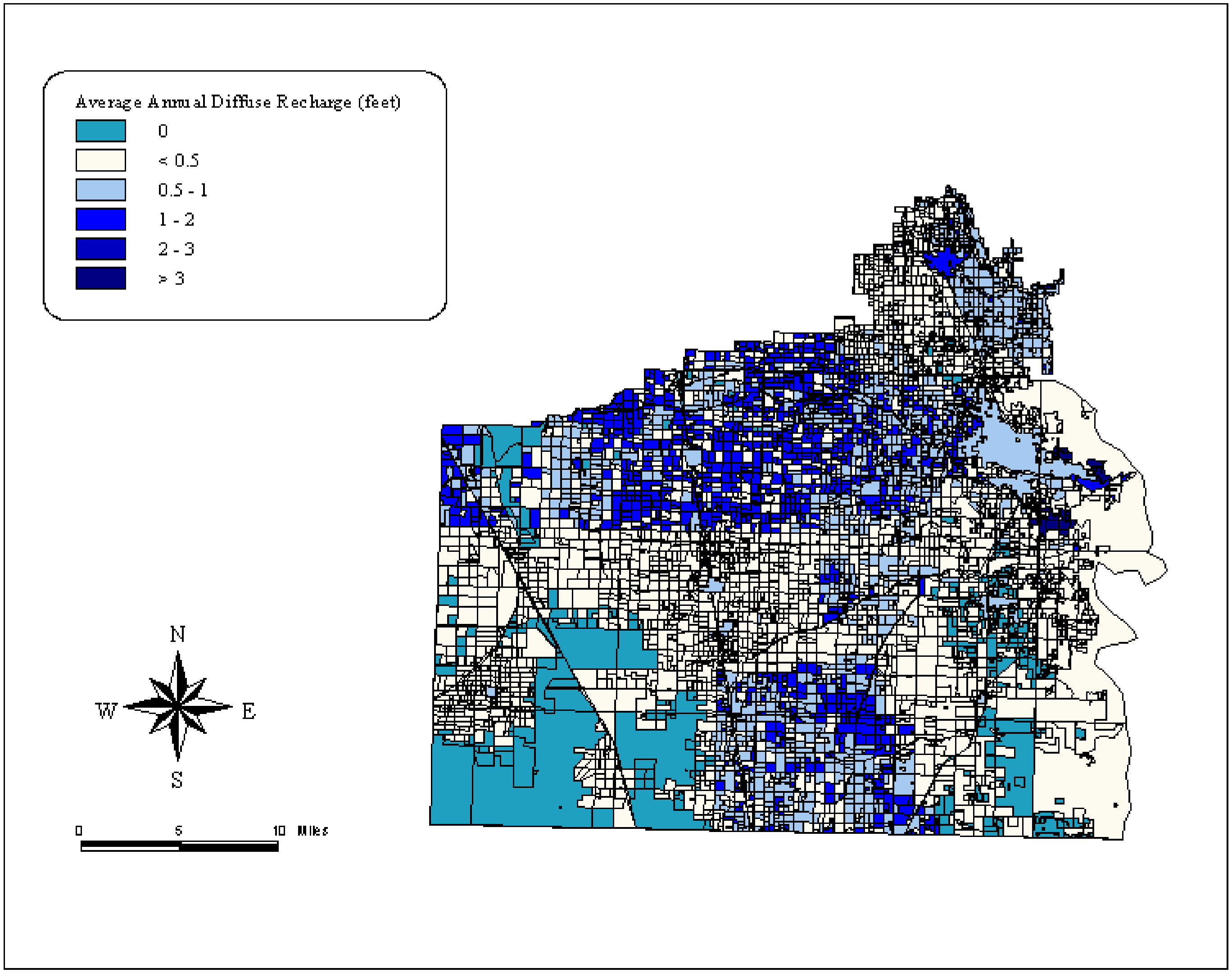

Plate 30: Spatial distribution of average annual diffuse recharge (feet) from 1970-99.

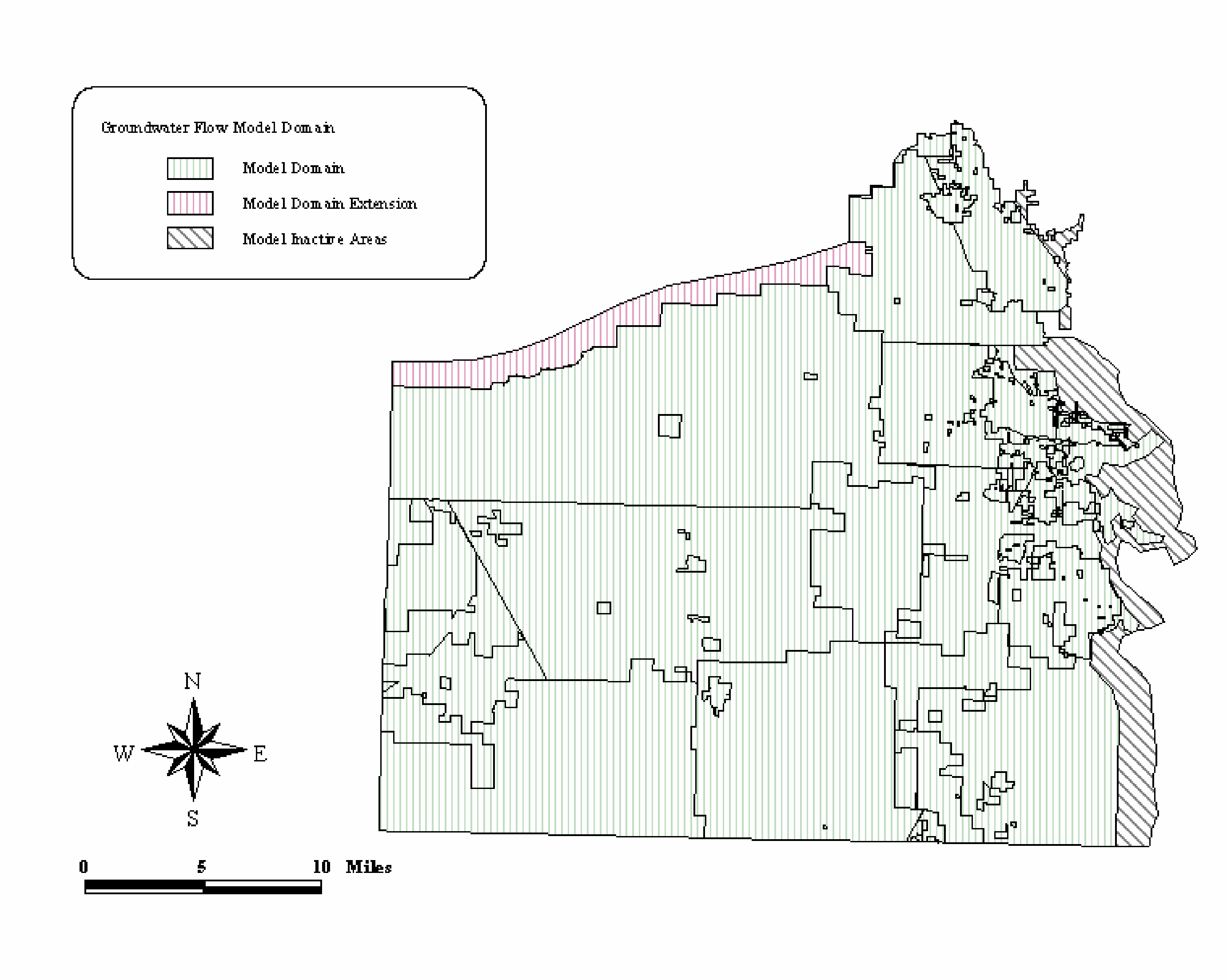

Plate 31: Groundwater flow model domain and added inactive areas.

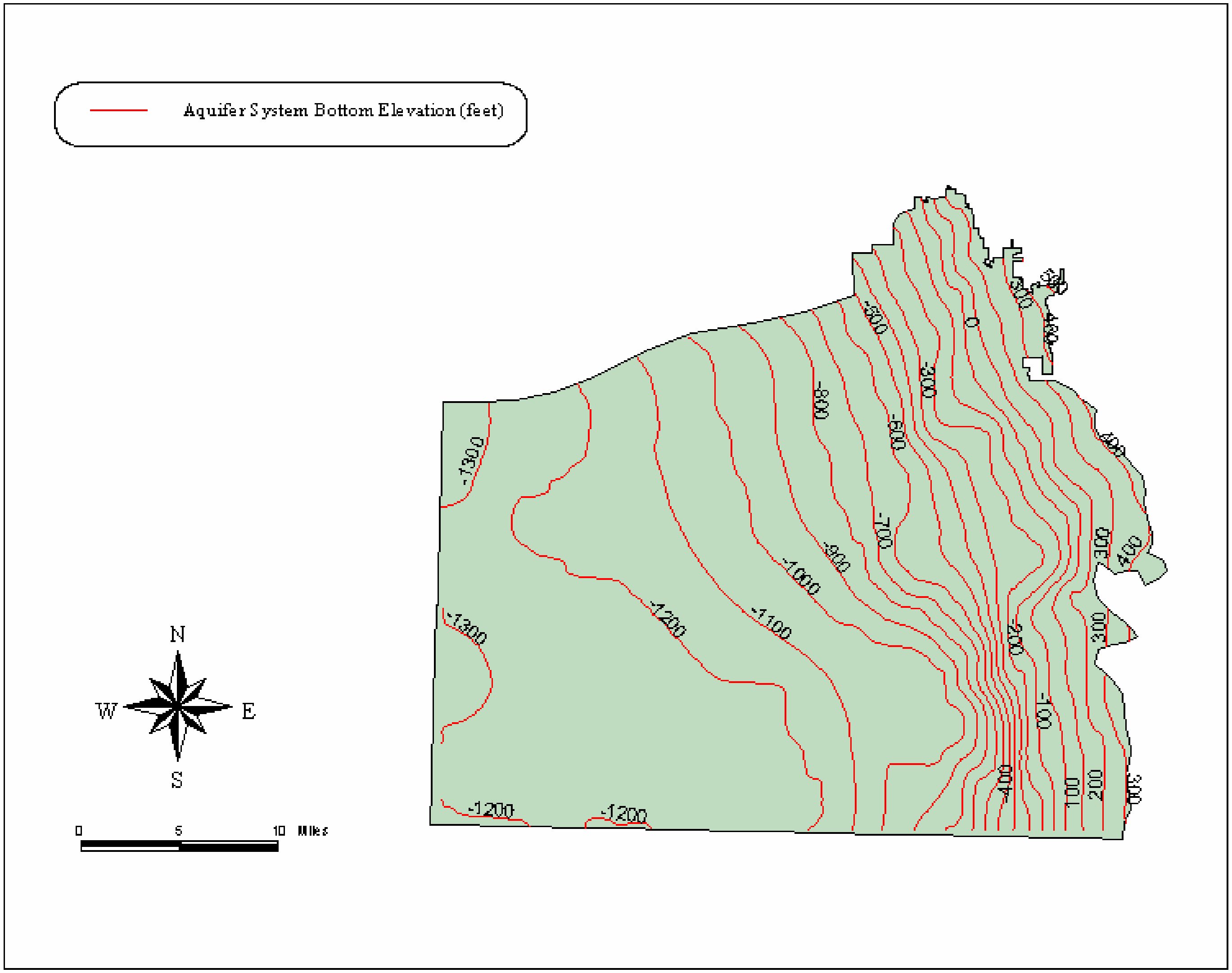

Plate 32: Aquifer system bottom boundary elevation (feet).

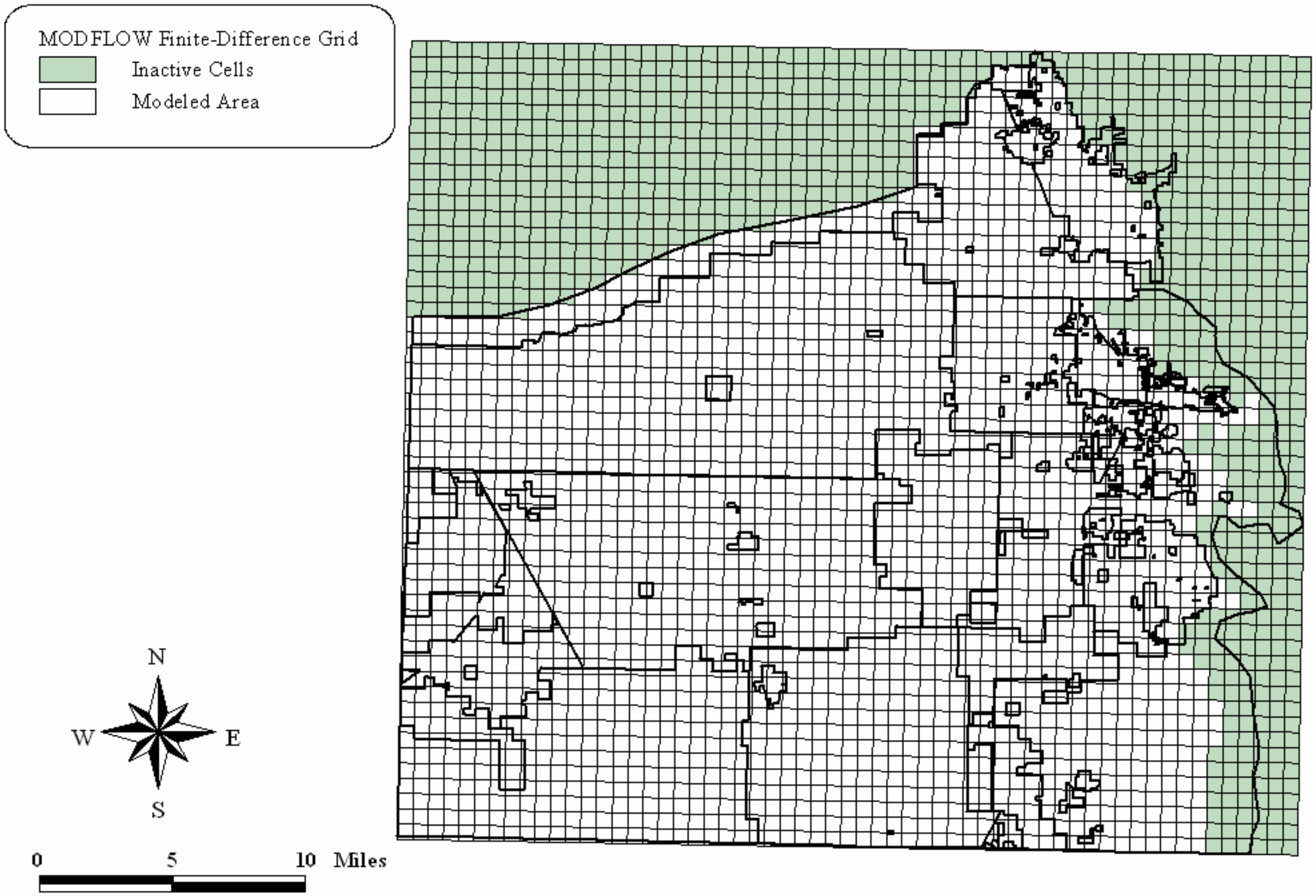

Plate 33: Groundwater flow model domain and MODFLOW finite-difference grid.

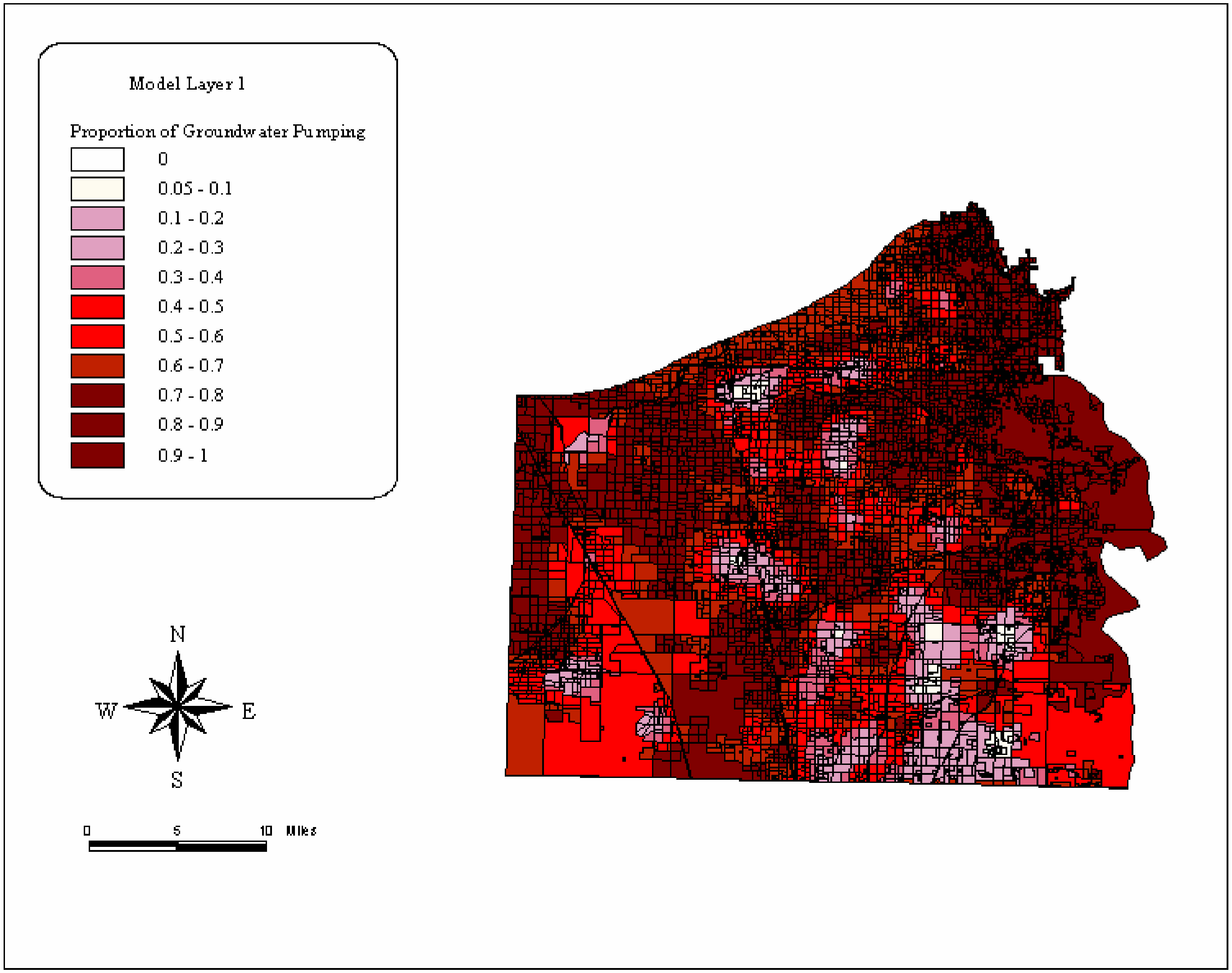

Plate 34: Proportion of total groundwater pumping demand for each land unit from model layer 1.

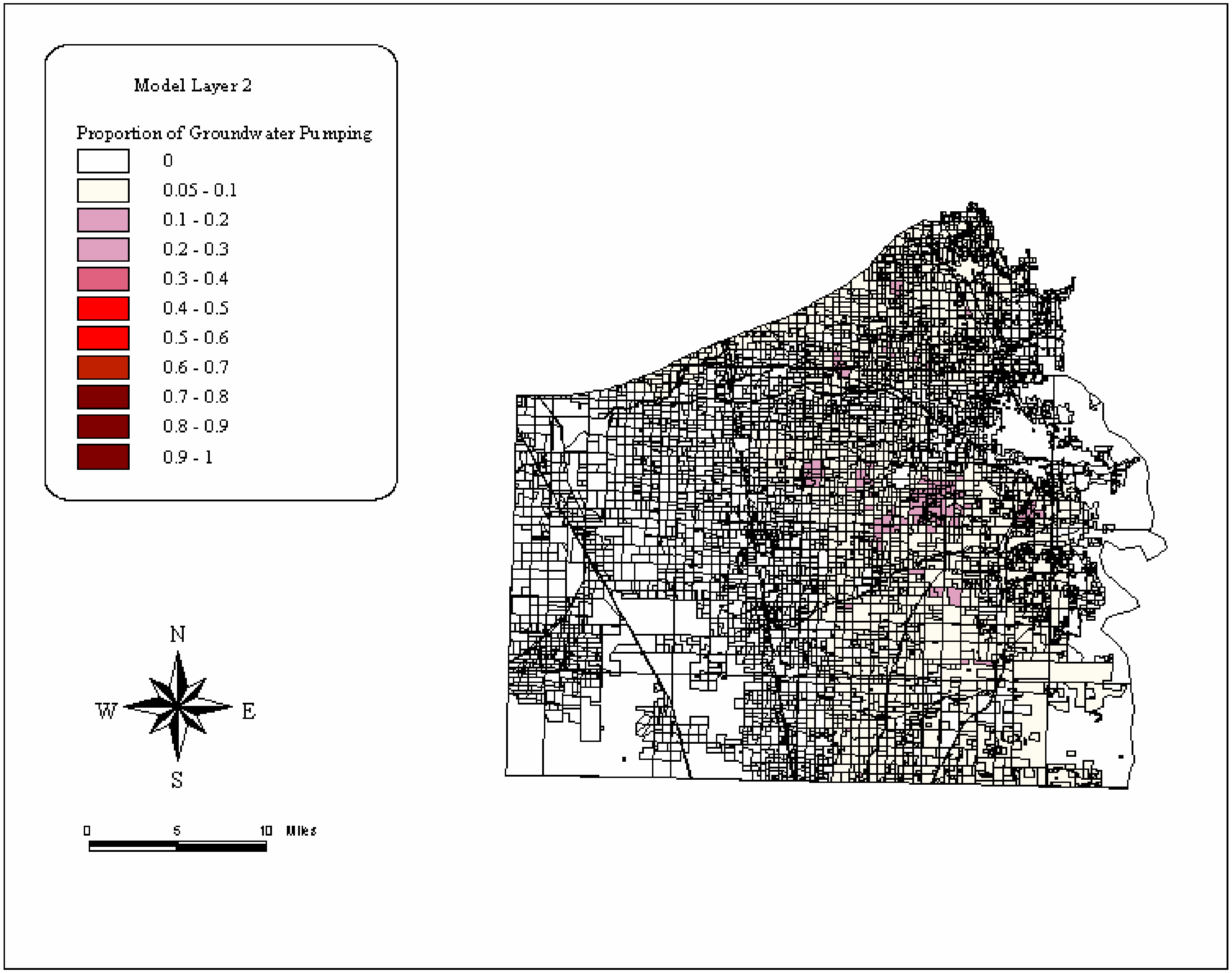

Plate 35: Proportion of total groundwater pumping demand for each land unit from model layer 2.

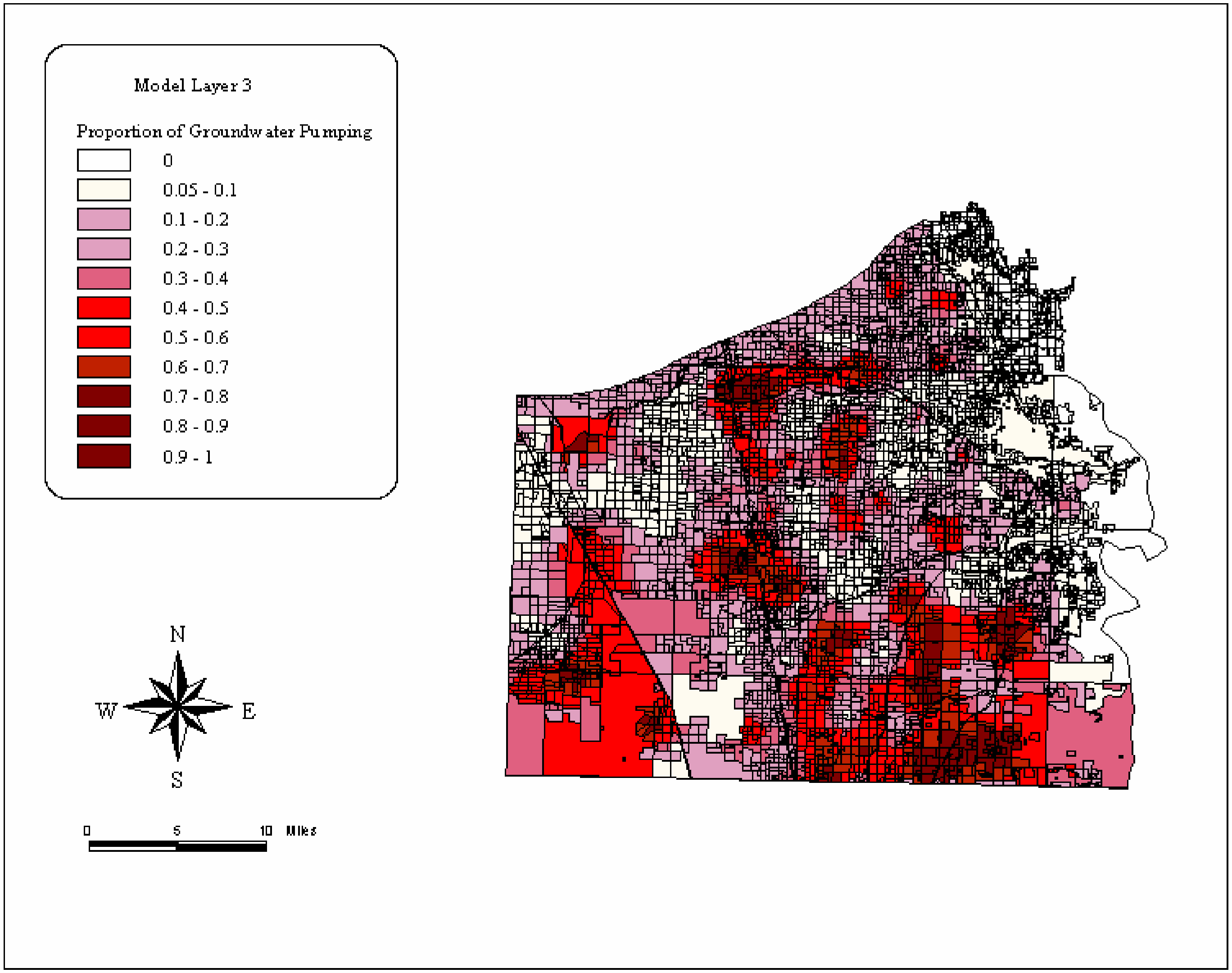

Plate 36: Proportion of total groundwater pumping demand for each land unit from model layer 3.

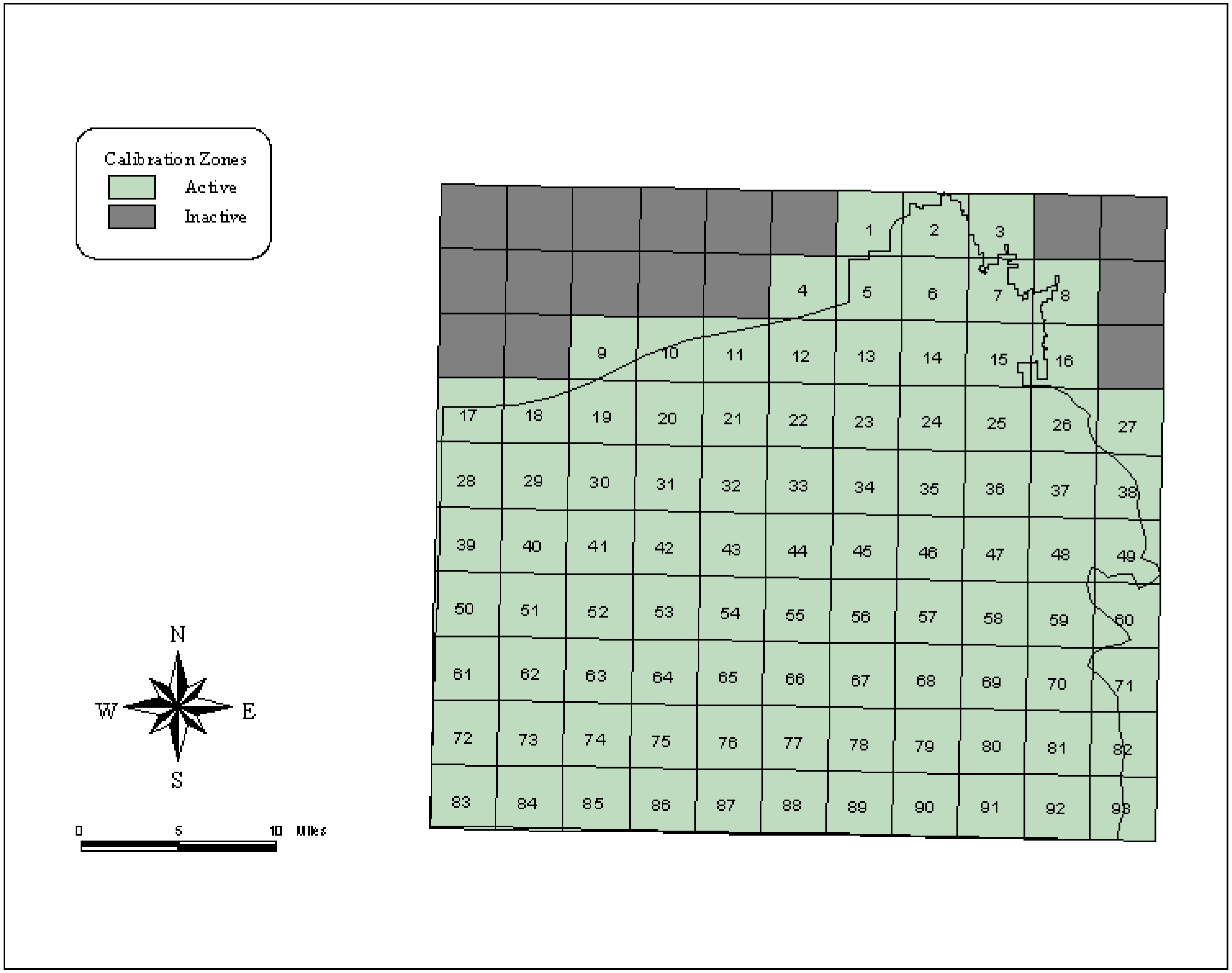

Plate 37: Unconfined aquifer horizontal hydraulic conductivity zonation.

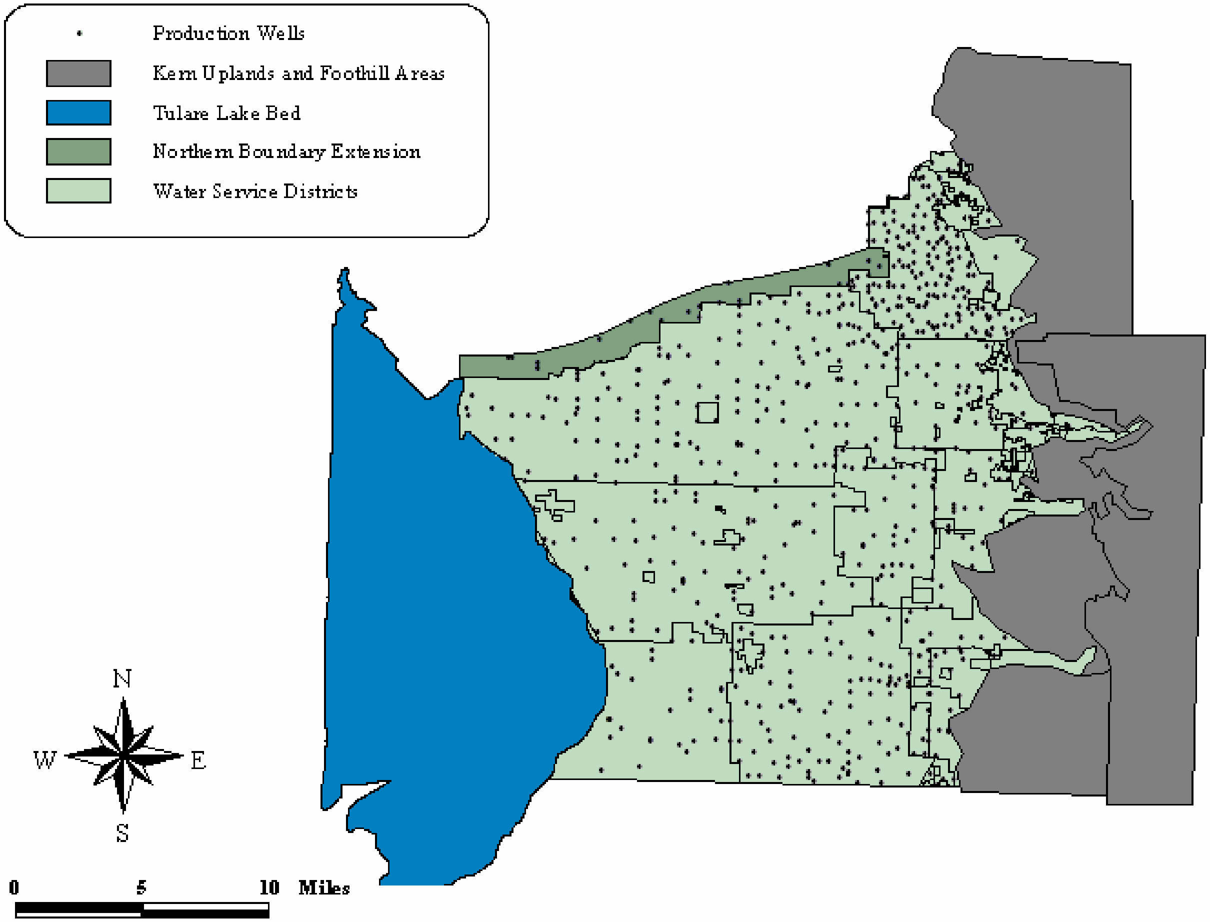

Plate 38: Production wells used for generating hydraulic head calibration targets.

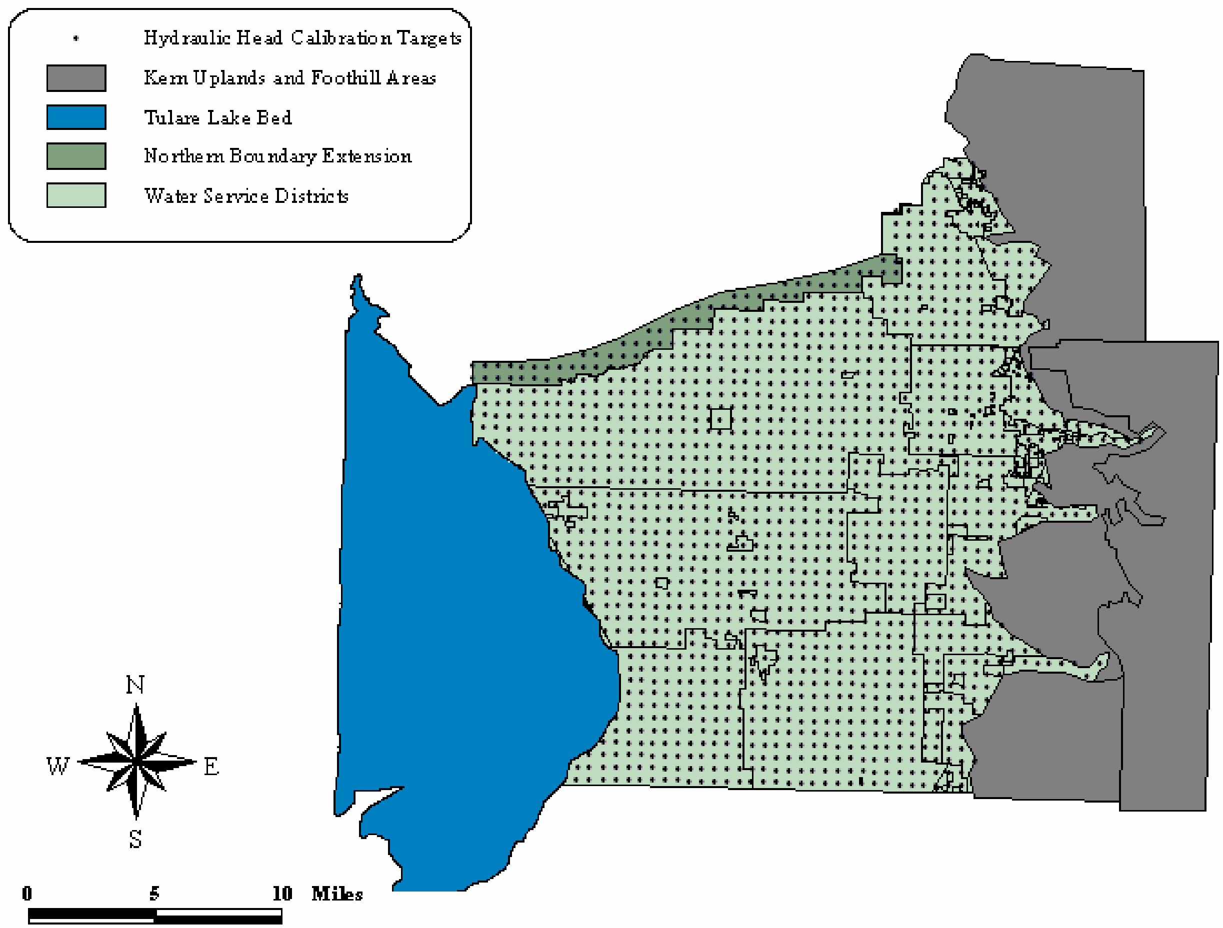

Plate 39: Block-centered hydraulic head calibration targets, generated by interpolating the production well observations to the centers of the finite-difference grid cells.

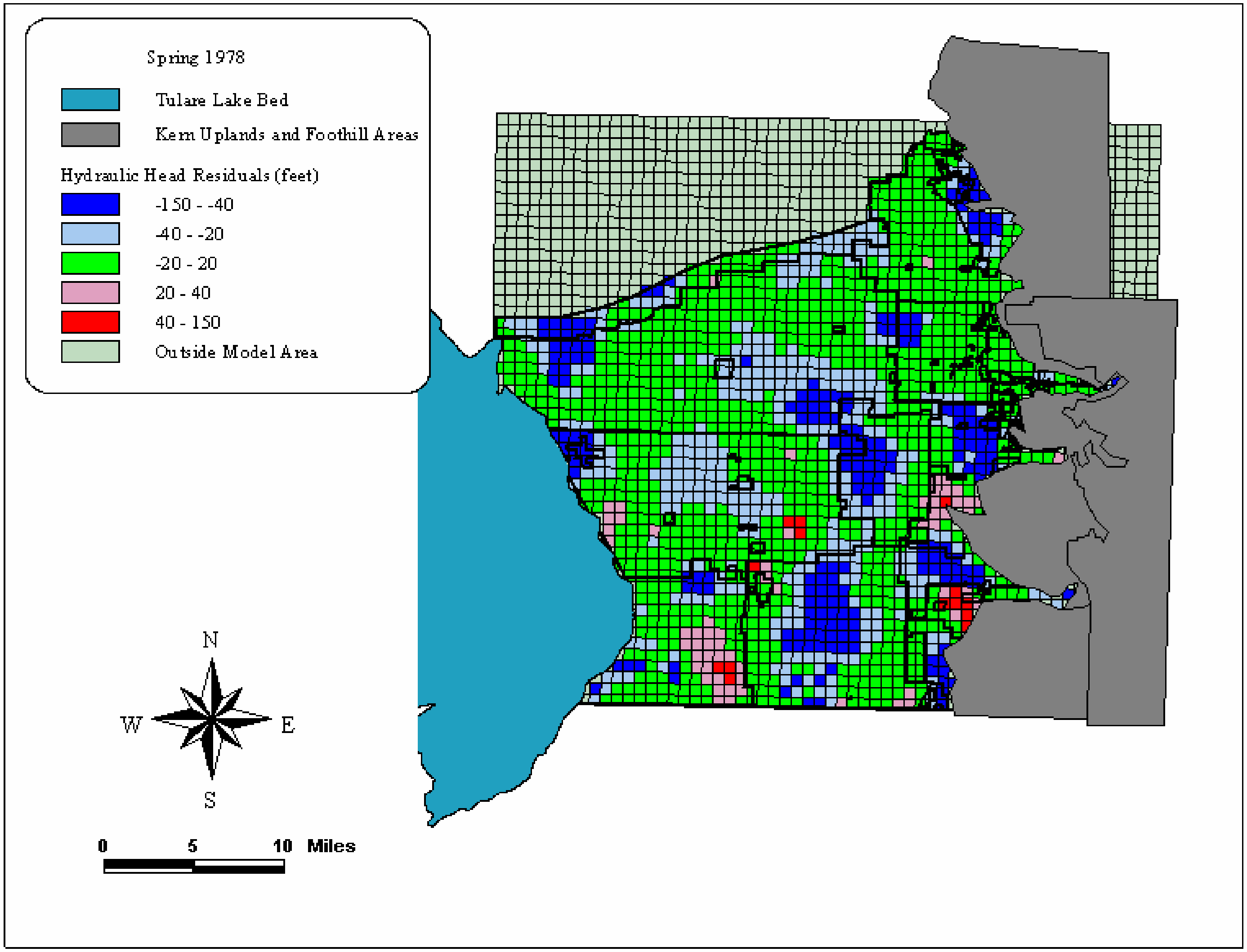

Plate 40: Unconfined aquifer (model layer 1) hydraulic head residuals (feet) for Spring 1978 from the uniform zonation conceptual model.

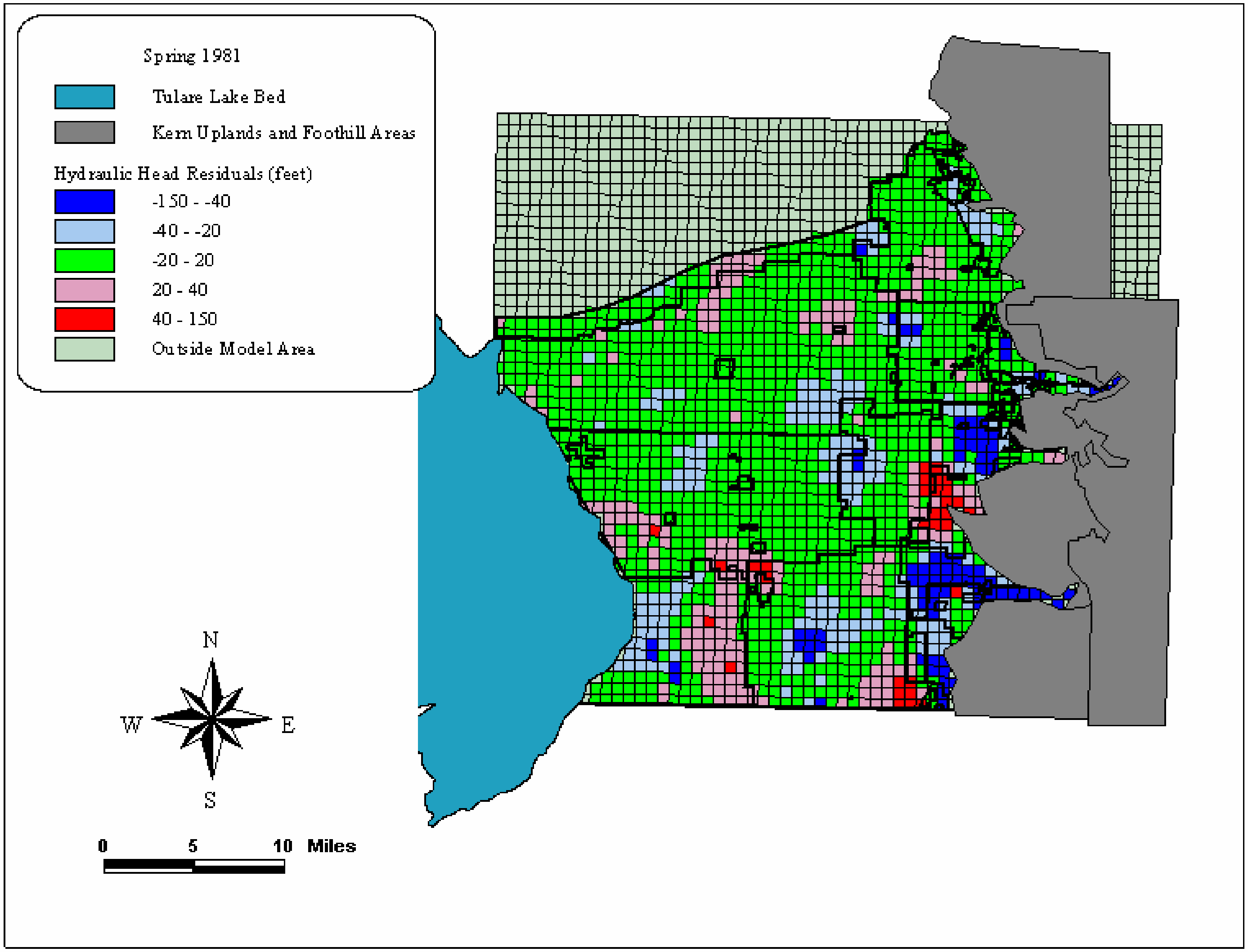

Plate 41: Unconfined aquifer (model layer 1) hydraulic head residuals (feet) for Spring 1981 from the uniform zonation conceptual model.

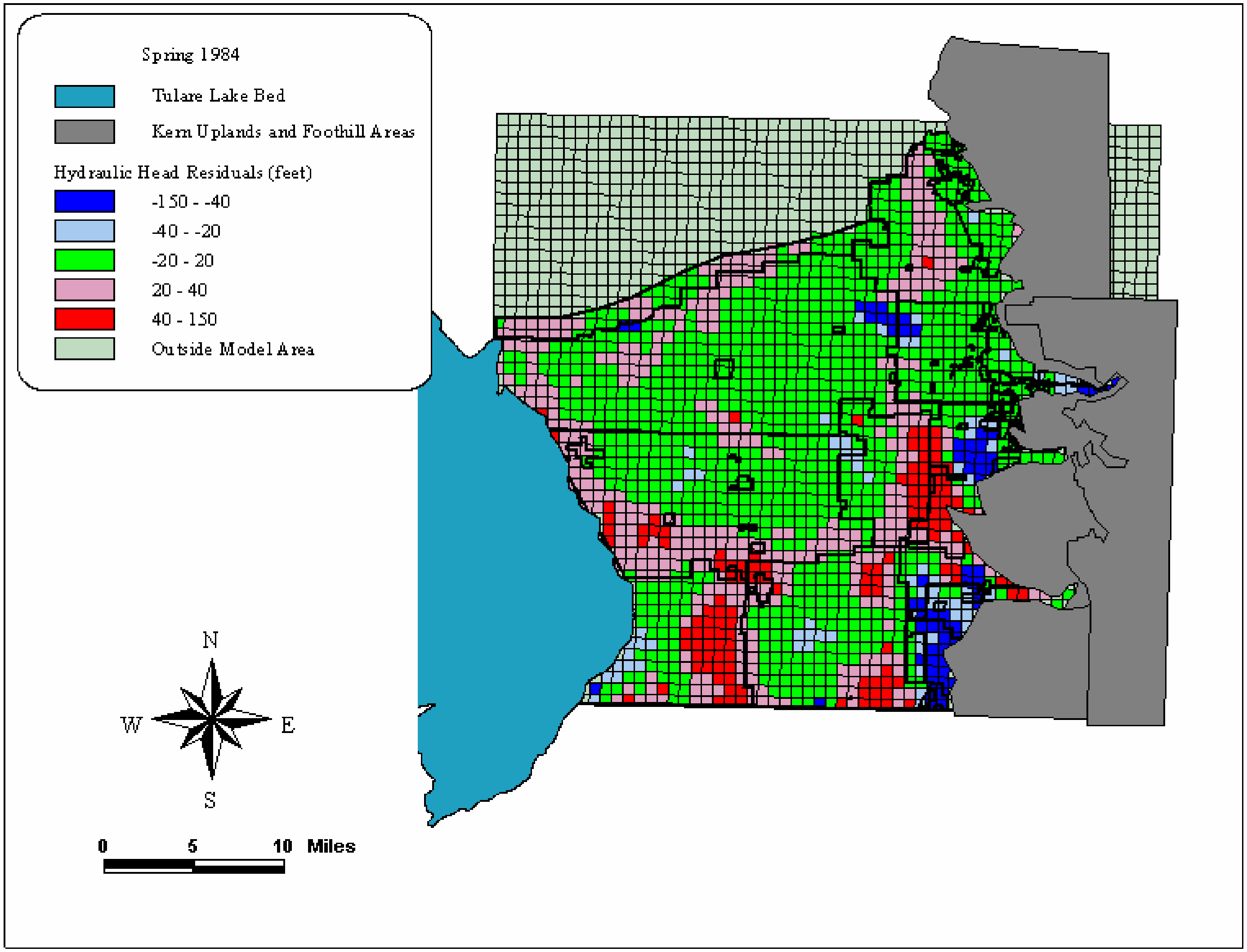

Plate 42: Unconfined aquifer (model layer 1) hydraulic head residuals (feet) for Spring 1984 from the uniform zonation conceptual model.

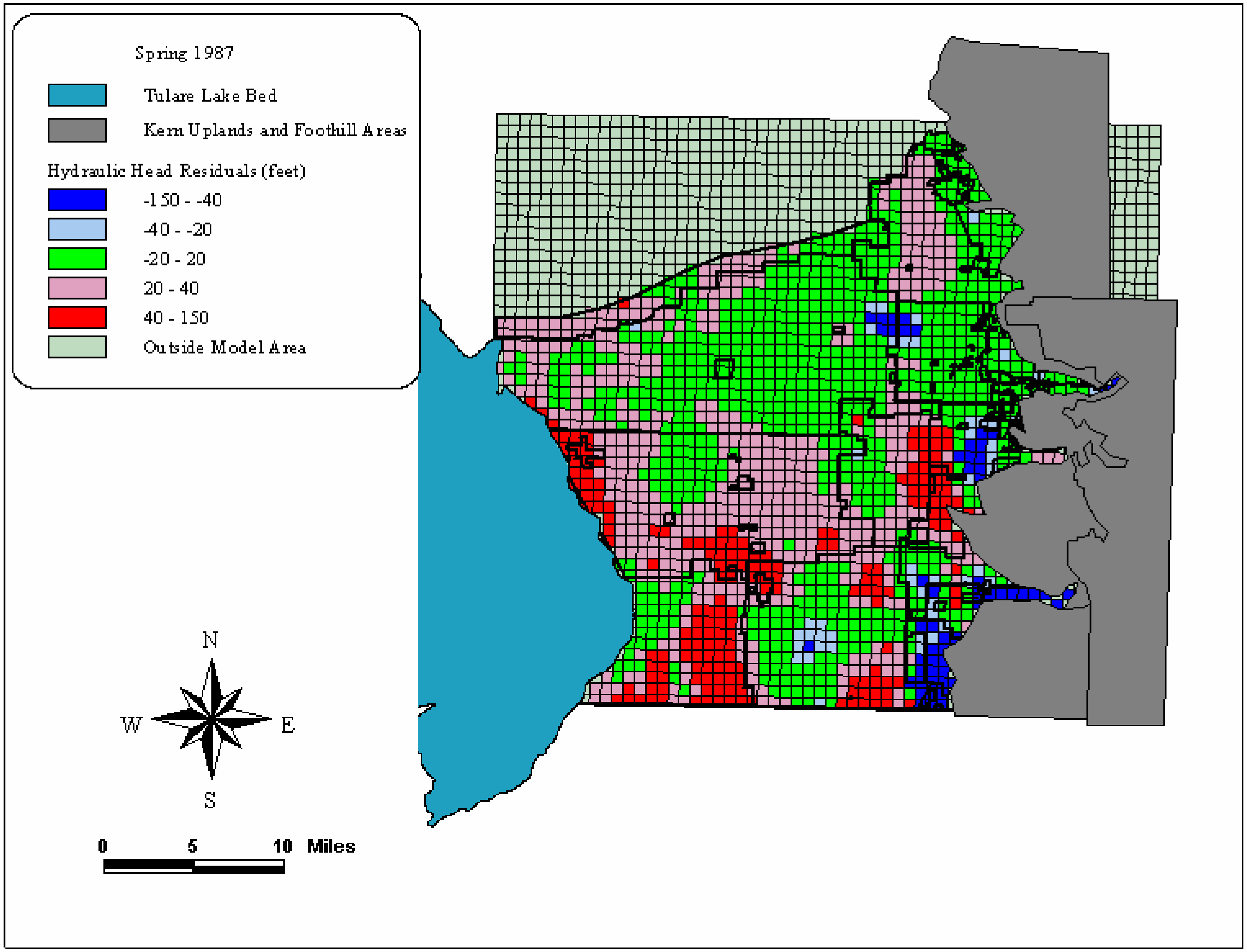

Plate 43: Unconfined aquifer (model layer 1) hydraulic head residuals (feet) for Spring 1987 from the uniform zonation conceptual model.

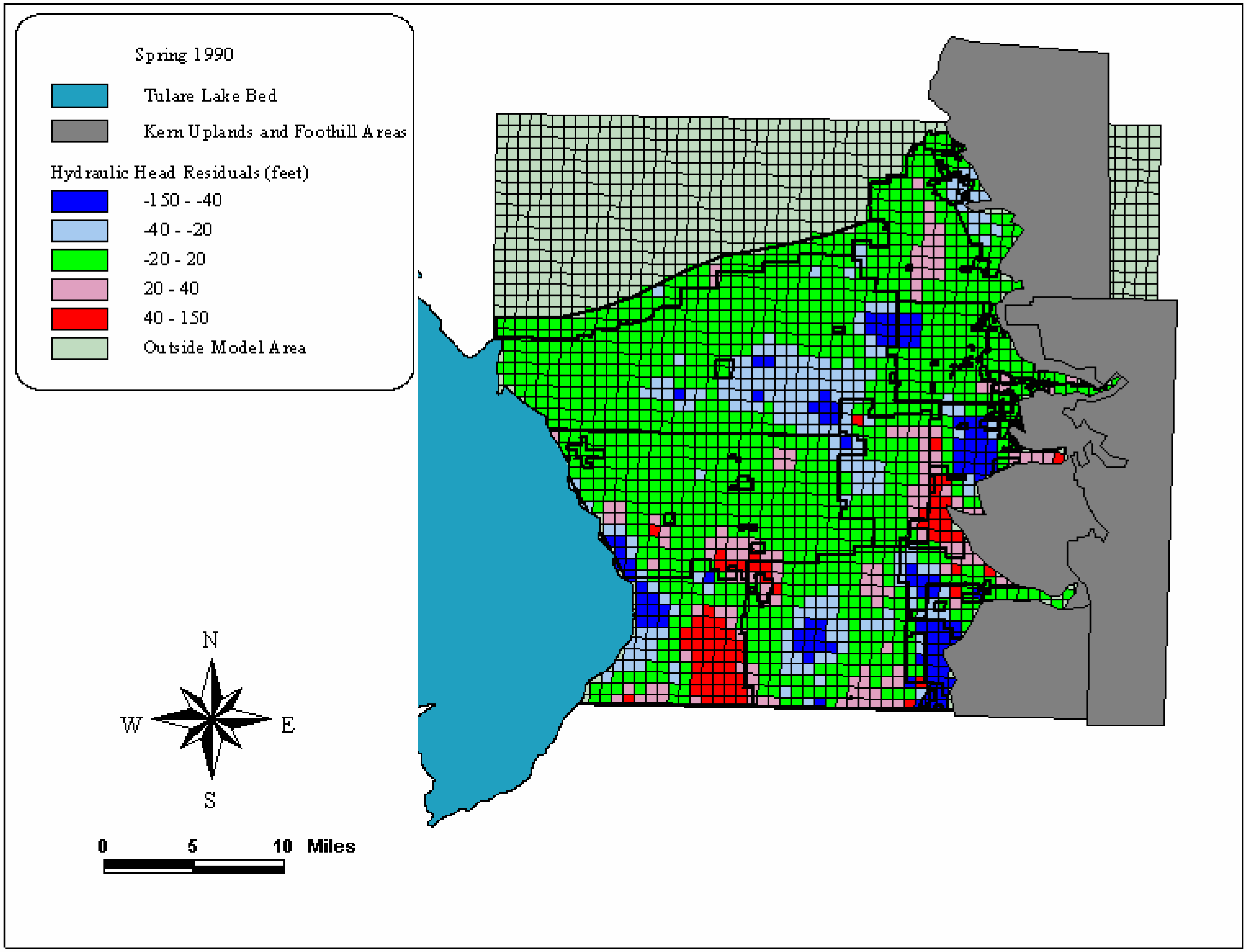

Plate 44: Unconfined aquifer (model layer 1) hydraulic head residuals (feet) for Spring 1990 from the uniform zonation conceptual model.

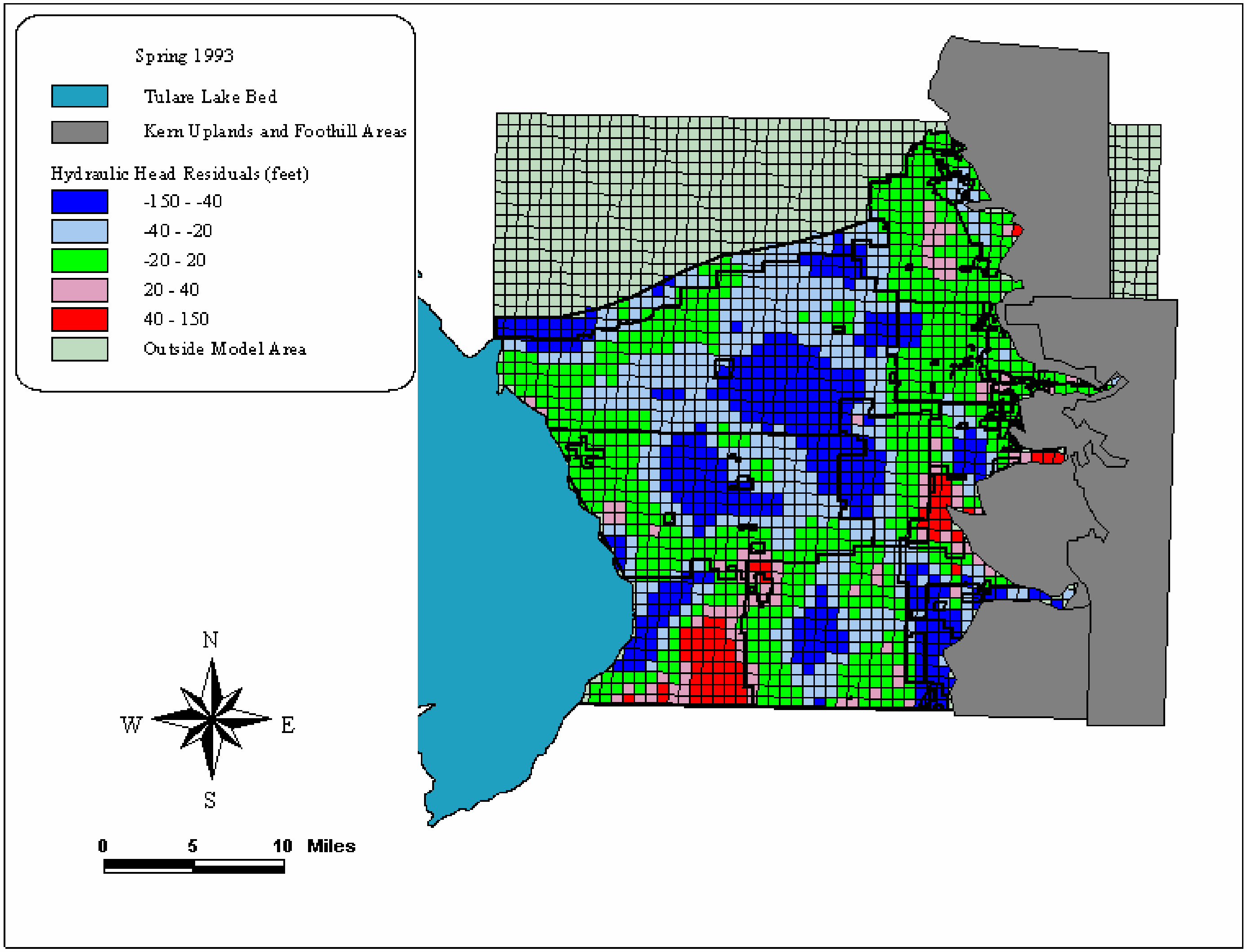

Plate 45: Unconfined aquifer (model layer 1) hydraulic head residuals (feet) for Spring 1993 from the uniform zonation conceptual model.

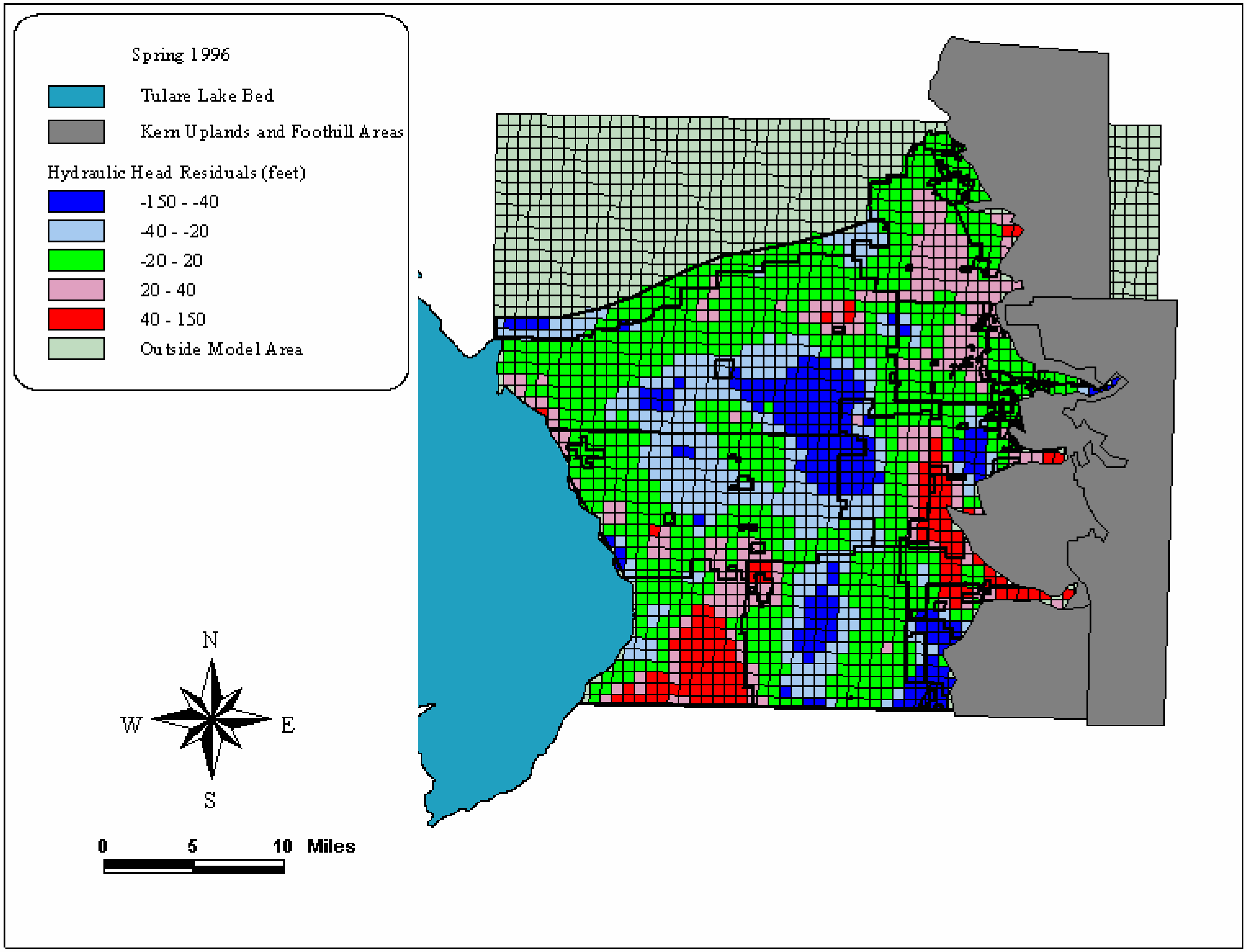

Plate 46: Unconfined aquifer (model layer 1) hydraulic head residuals (feet) for Spring 1996 from the uniform zonation conceptual model.

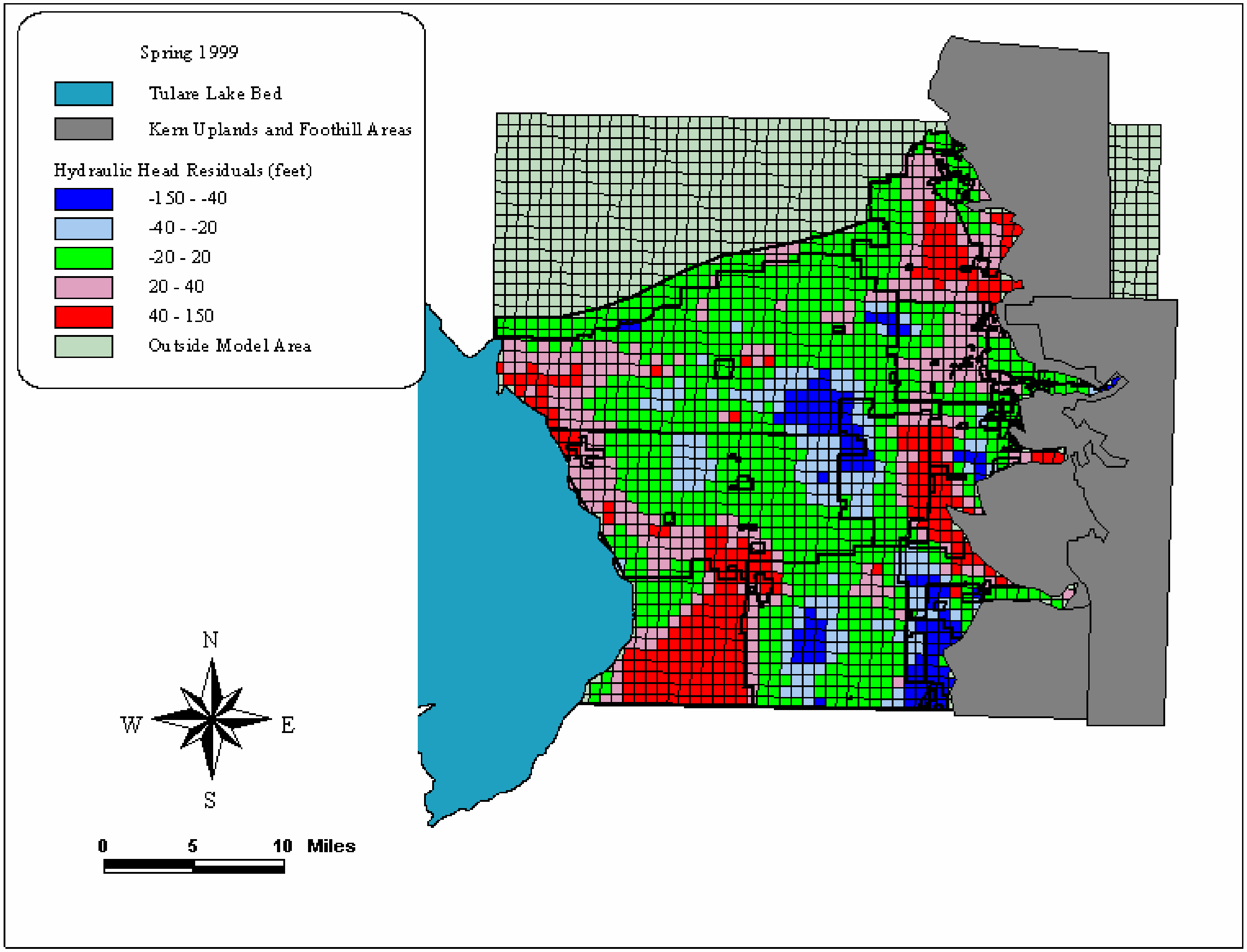

Plate 47: Unconfined aquifer (model layer 1) hydraulic head residuals (feet) for Spring 1999 from the uniform zonation conceptual model.

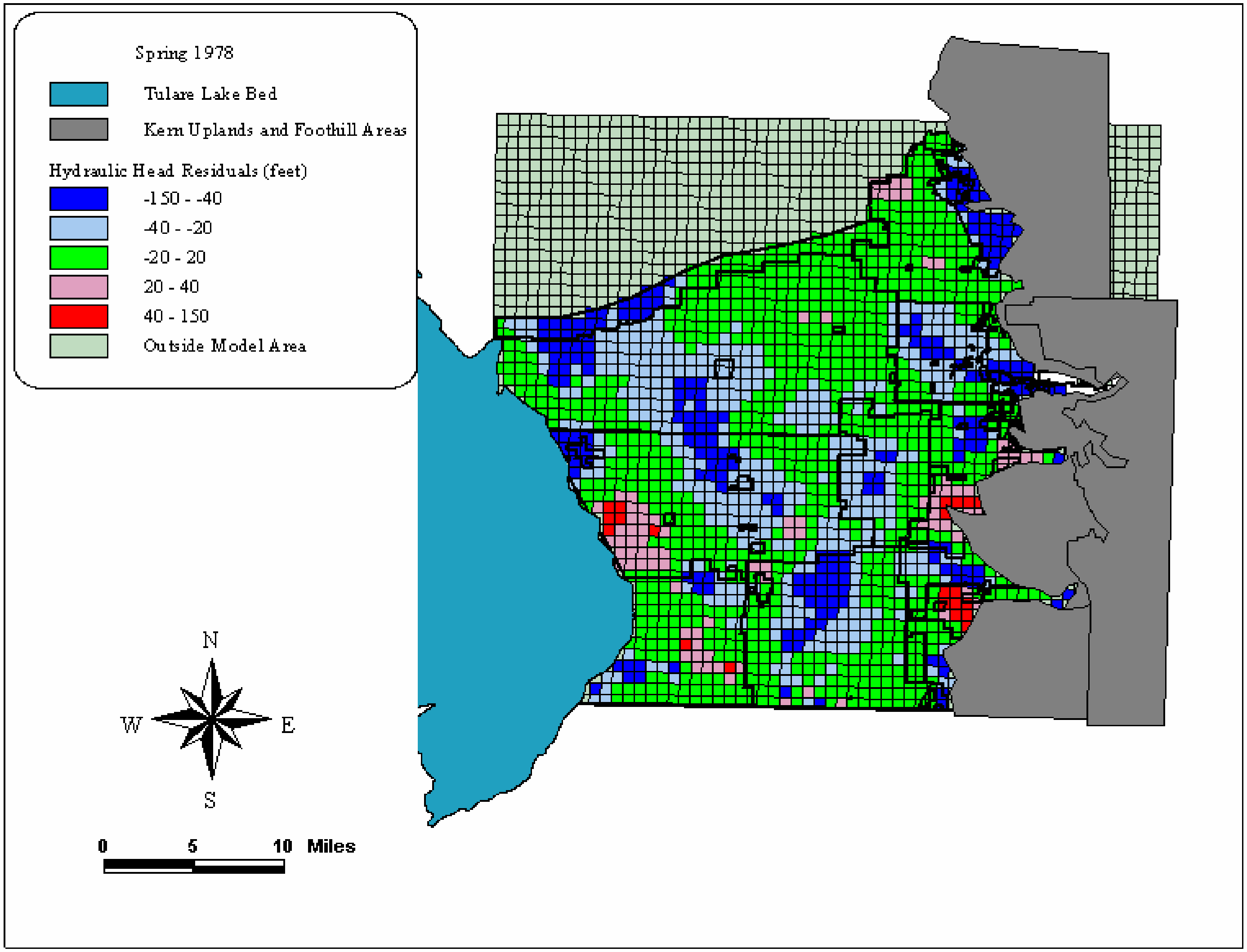

Plate 48: Unconfined aquifer (model layer 1) hydraulic head residuals (feet) for Spring 1978 from the *S*y-structure conceptual model.

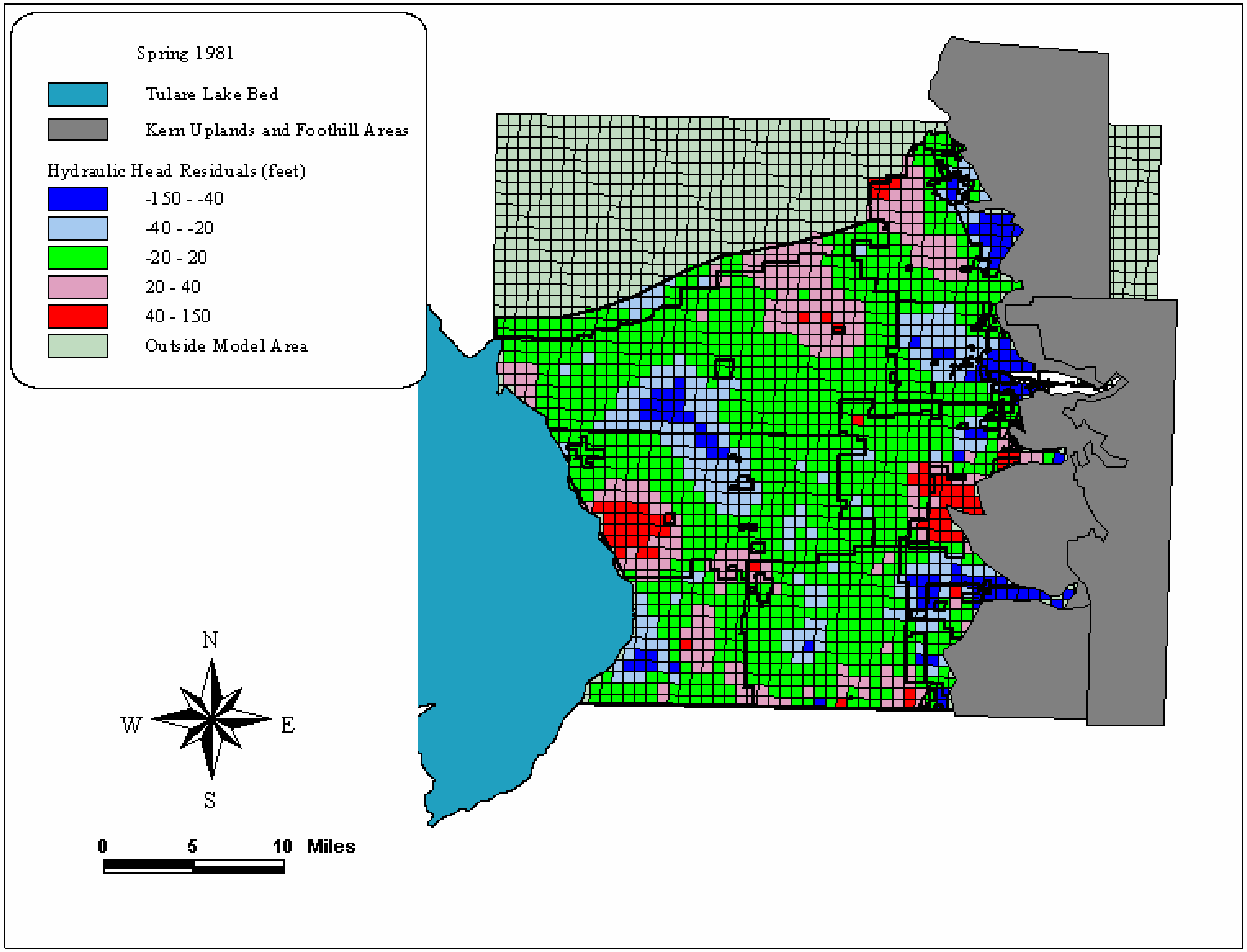

.

Plate 49: Unconfined aquifer (model layer 1) hydraulic head residuals (feet) for Spring 1981 from the *S*y-structure conceptual model.

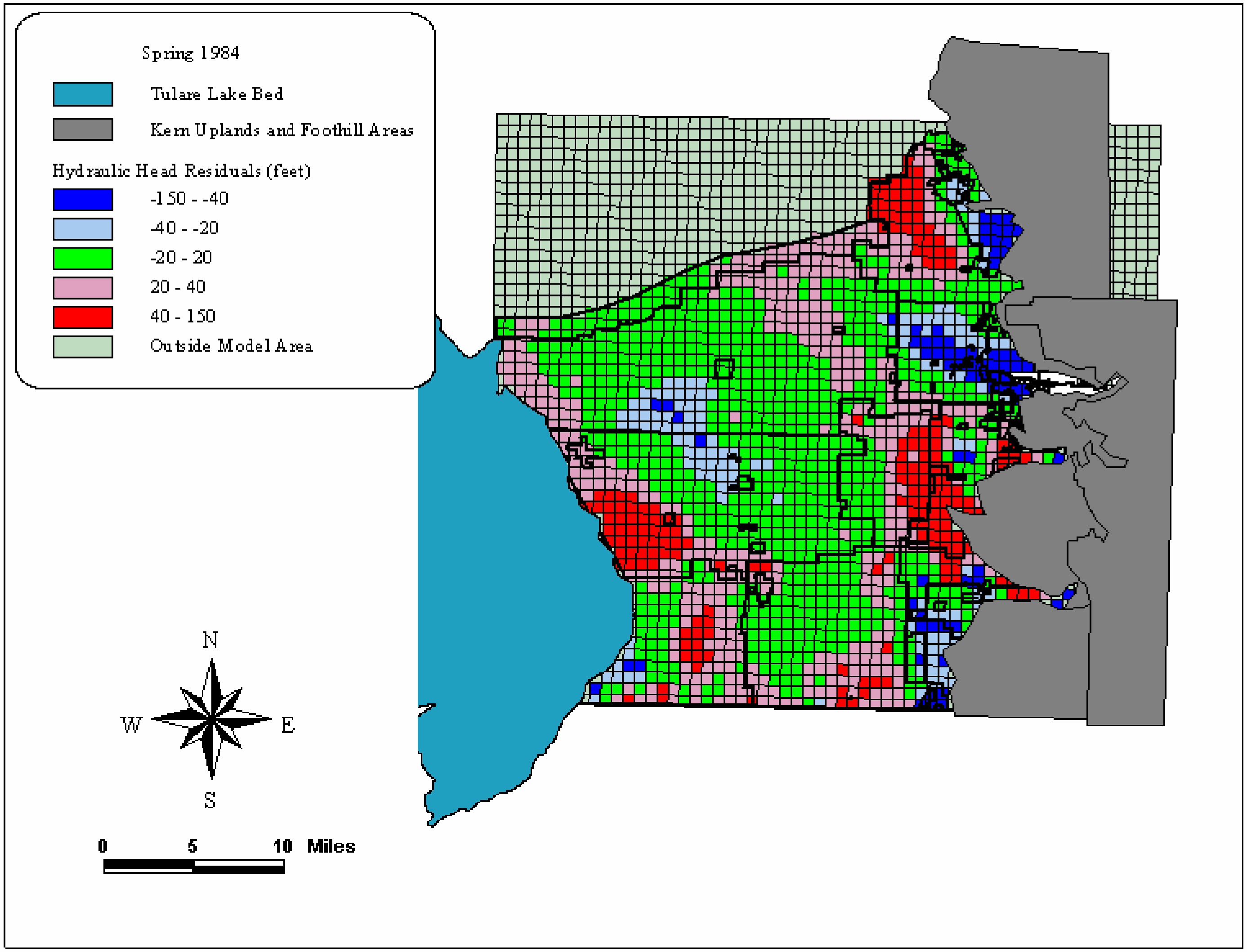

Plate 50: Unconfined aquifer (model layer 1) hydraulic head residuals (feet) for Spring 1984 from the *S*y-structure conceptual model.

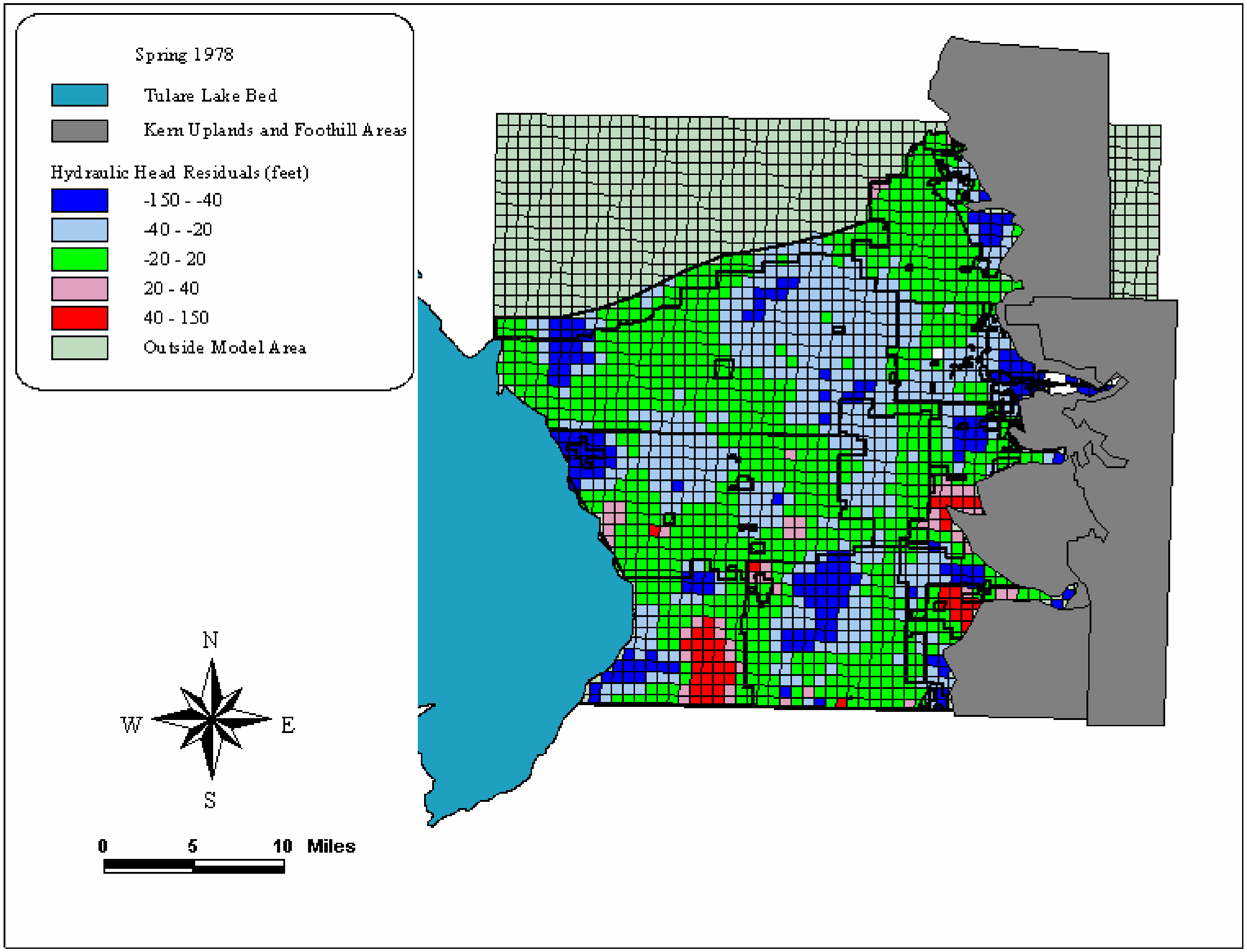

Plate 51: Unconfined aquifer (model layer 1) hydraulic head residuals (feet) for Spring 1978 from the soil *K*s-structure conceptual model.

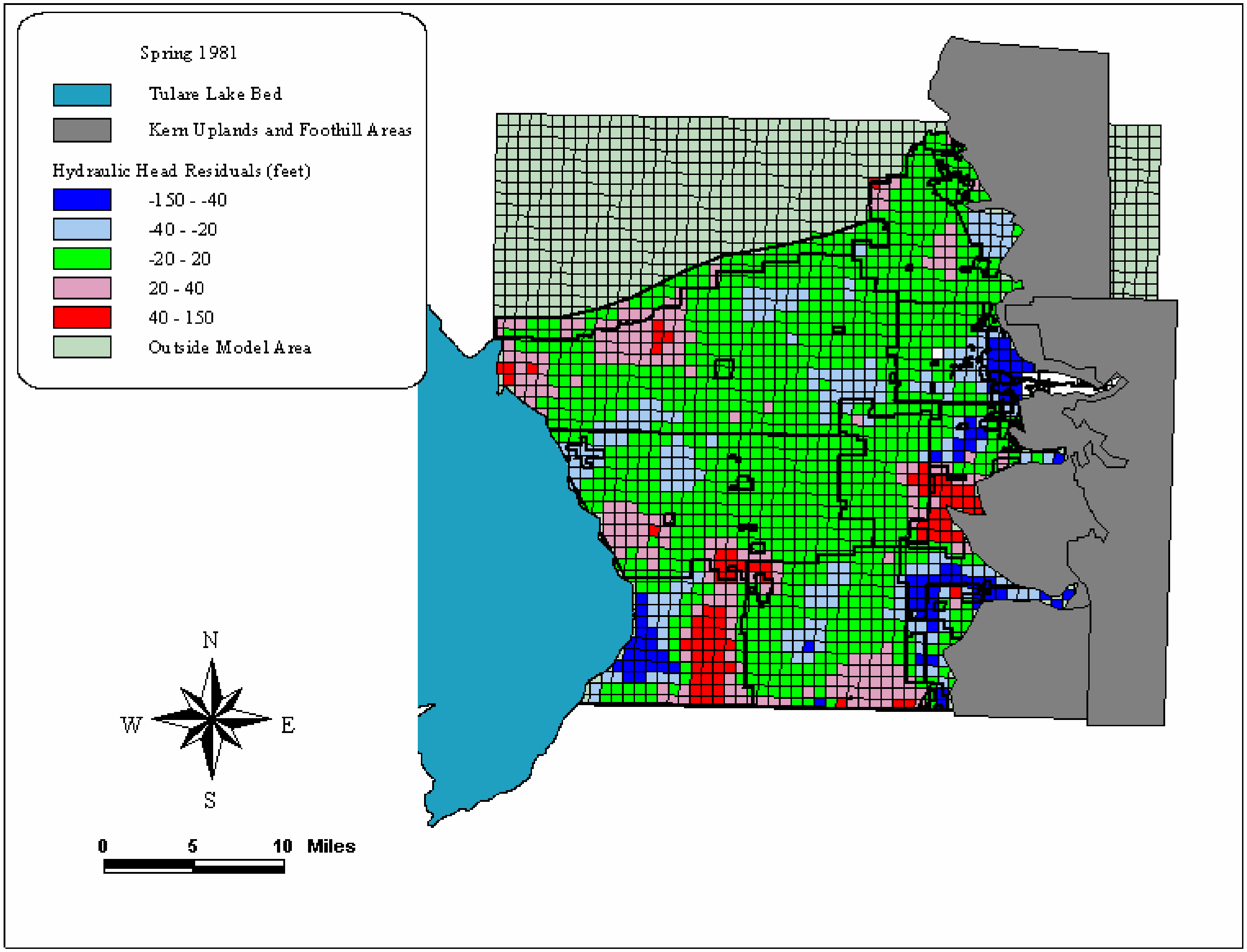

Plate 52: Unconfined aquifer (model layer 1) hydraulic head residuals (feet) for Spring 1981 from the soil *K*s-structure conceptual model.

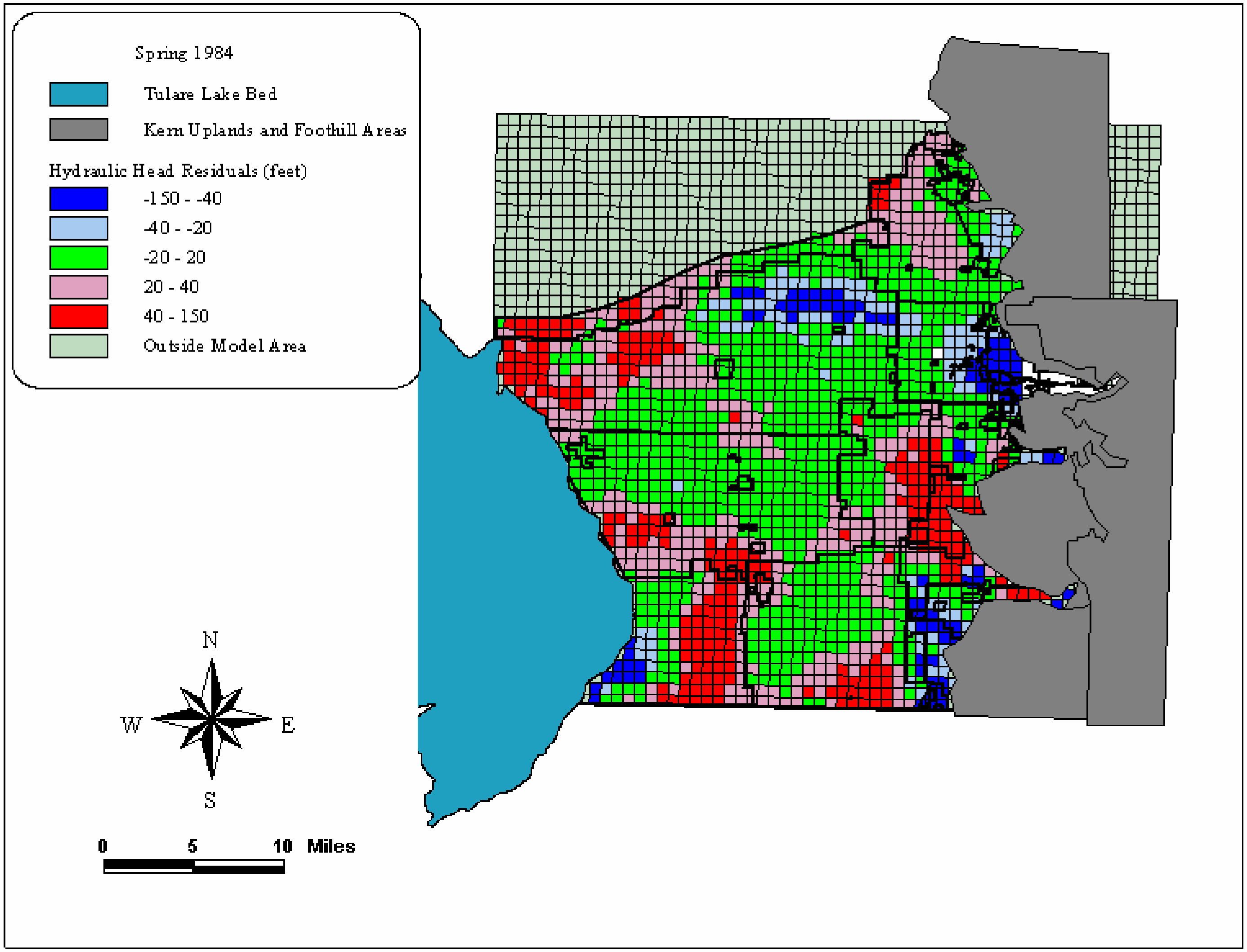

Plate 53: Unconfined aquifer (model layer 1) hydraulic head residuals (feet) for Spring 1984 from the soil *K*s-structure conceptual model.

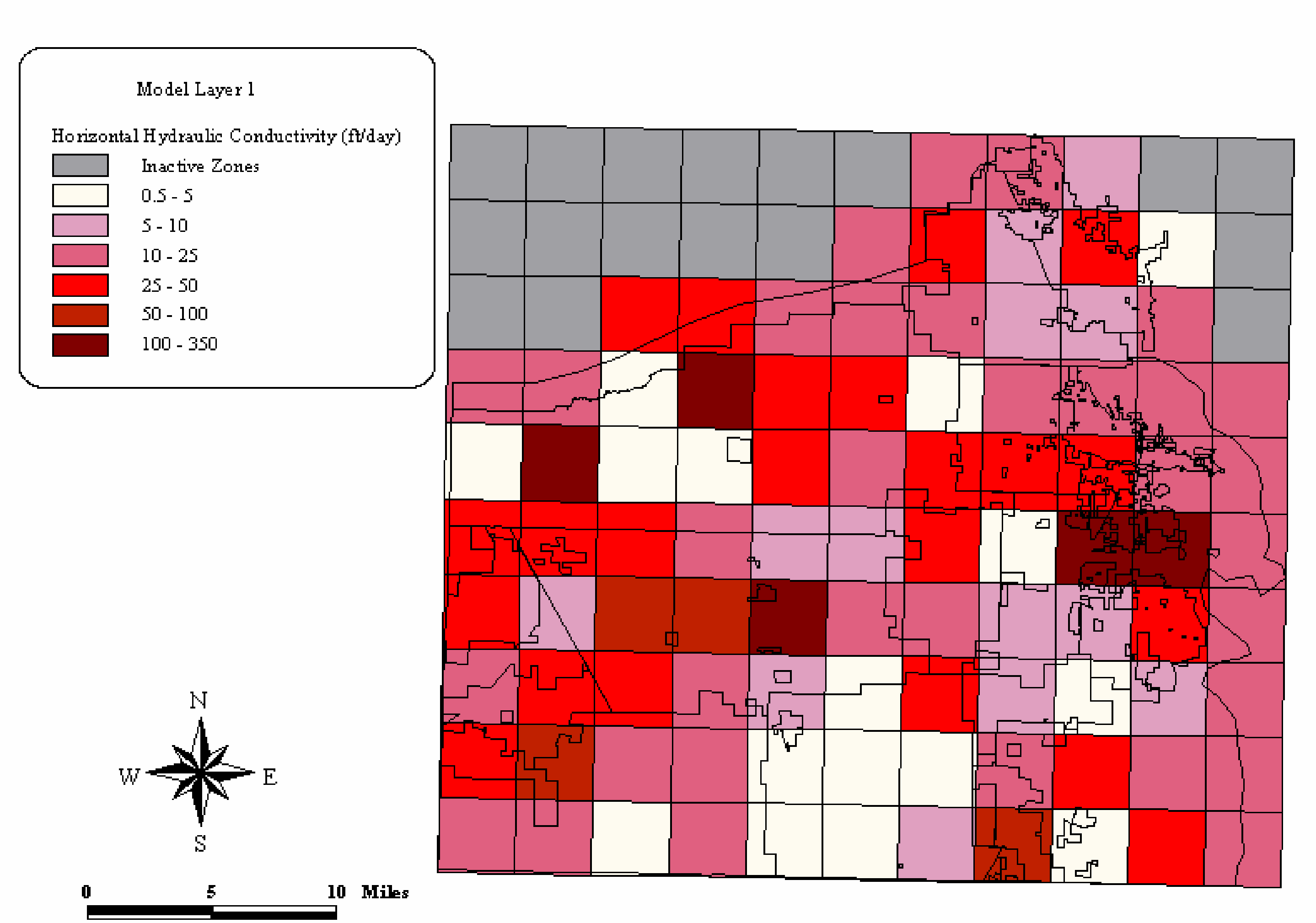

Plate 54: Estimated K_h distribution (ft/day) for model layer 1 from the uniform zonation conceptual model.

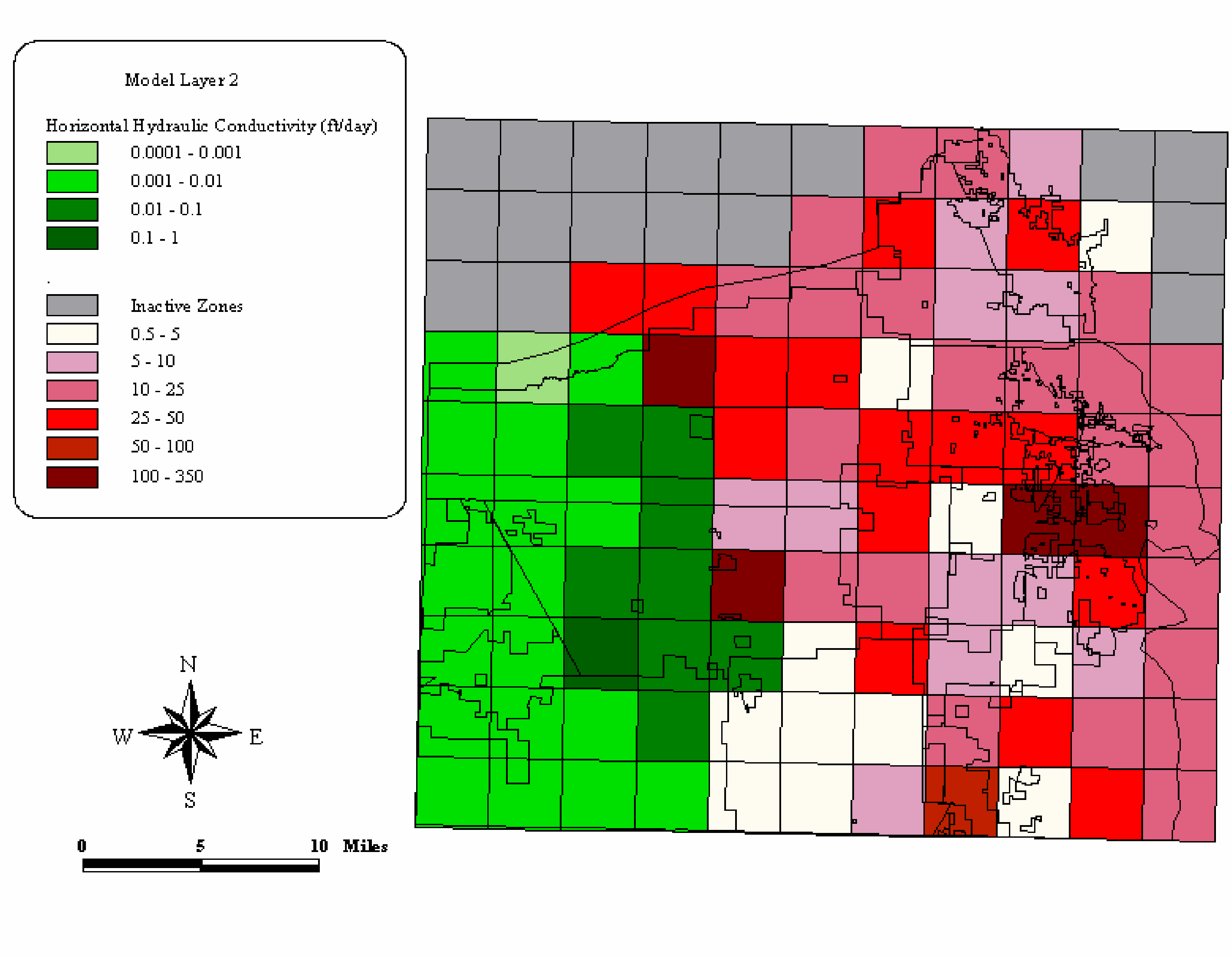

Plate 55: Estimated K_h distribution (ft/day) for model layer 2 from the uniform zonation conceptual model.

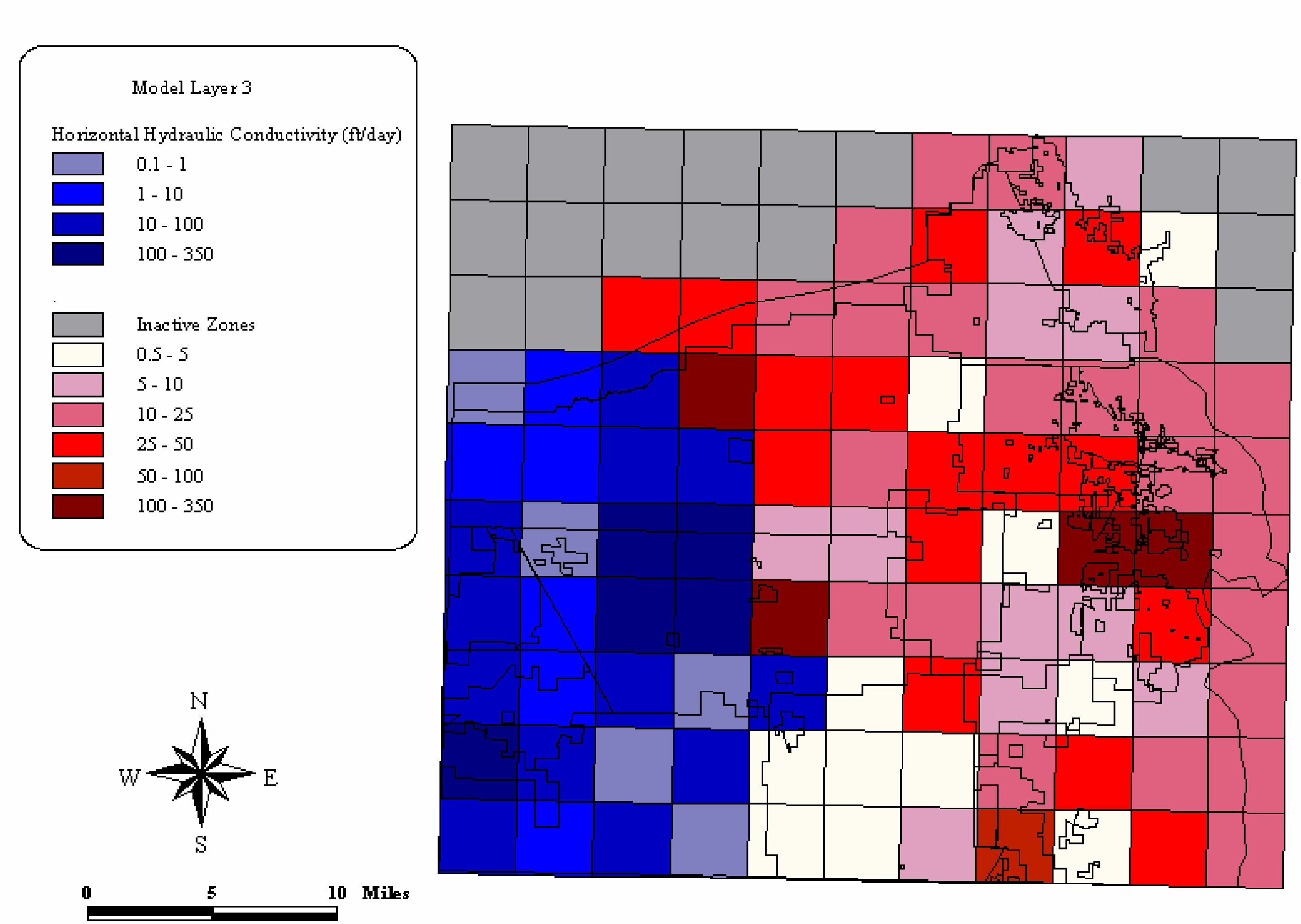

Plate 56: Estimated K_h distribution (ft/day) for model layer 3 from the uniform zonation conceptual model.

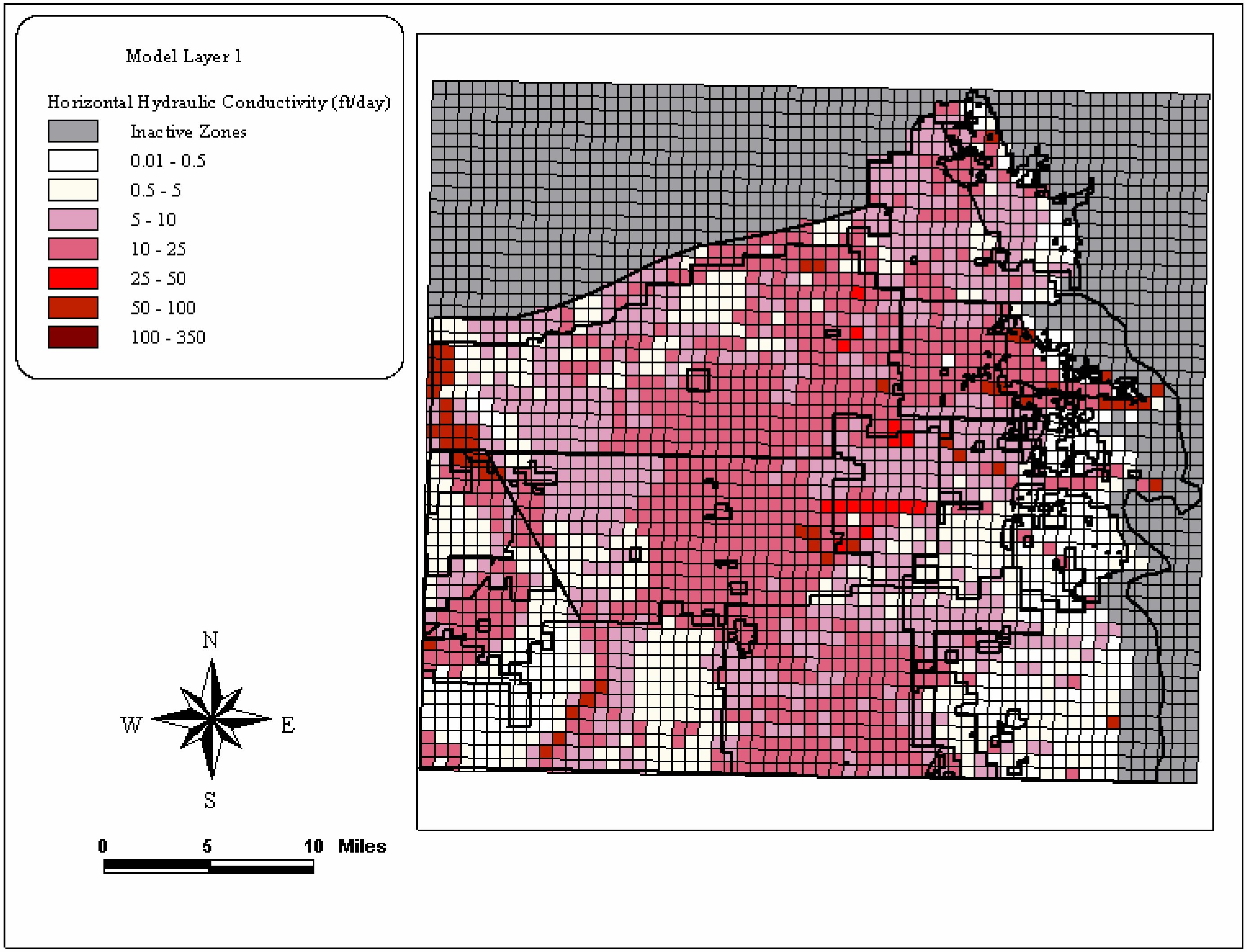

Plate 57: Estimated K_h distribution (ft/day) for model layer 1 from the soil *K*s structure conceptual model.

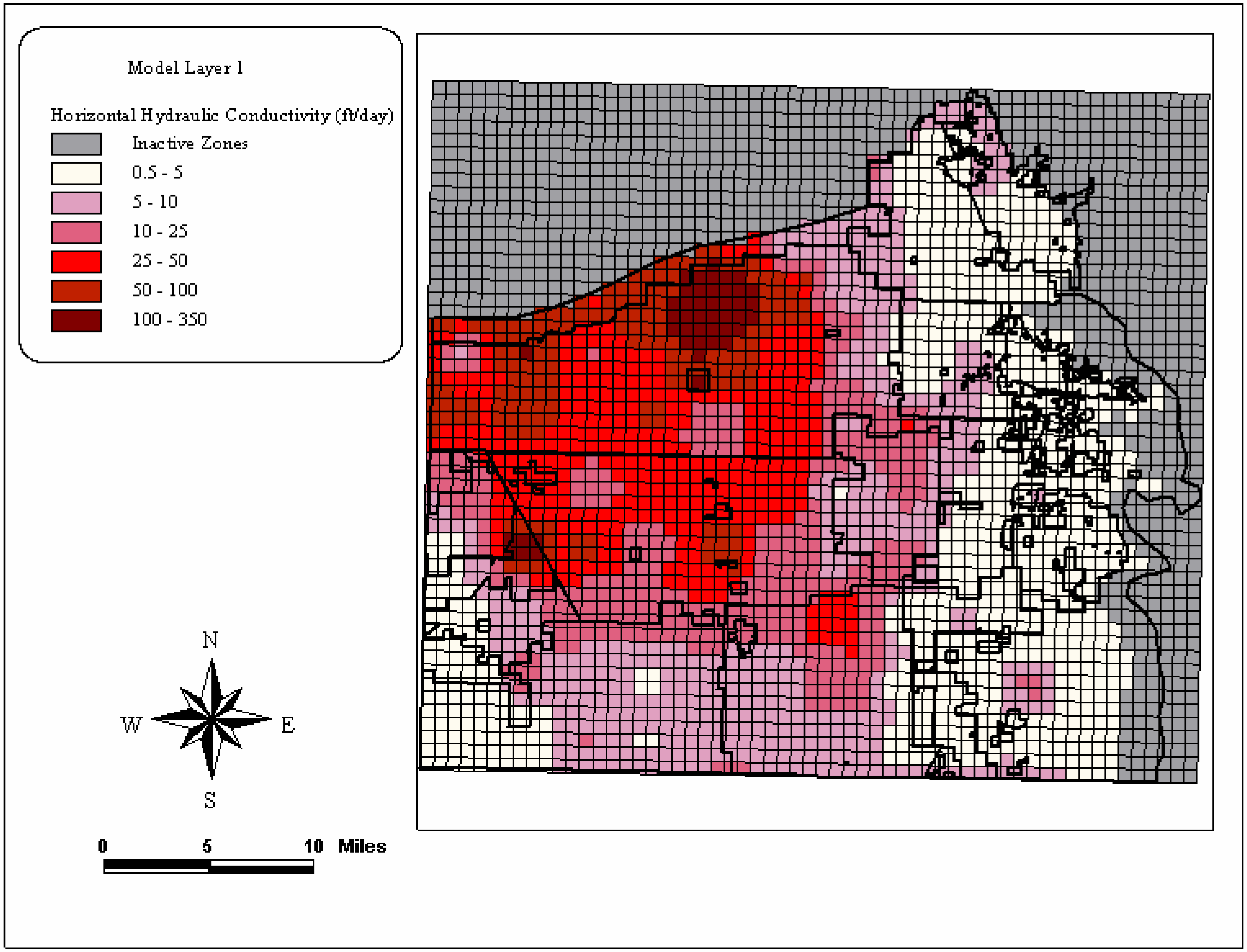

Plate 58: Estimated K_h distribution (ft/day) for model layer 1 from the specific yield structure conceptual model.

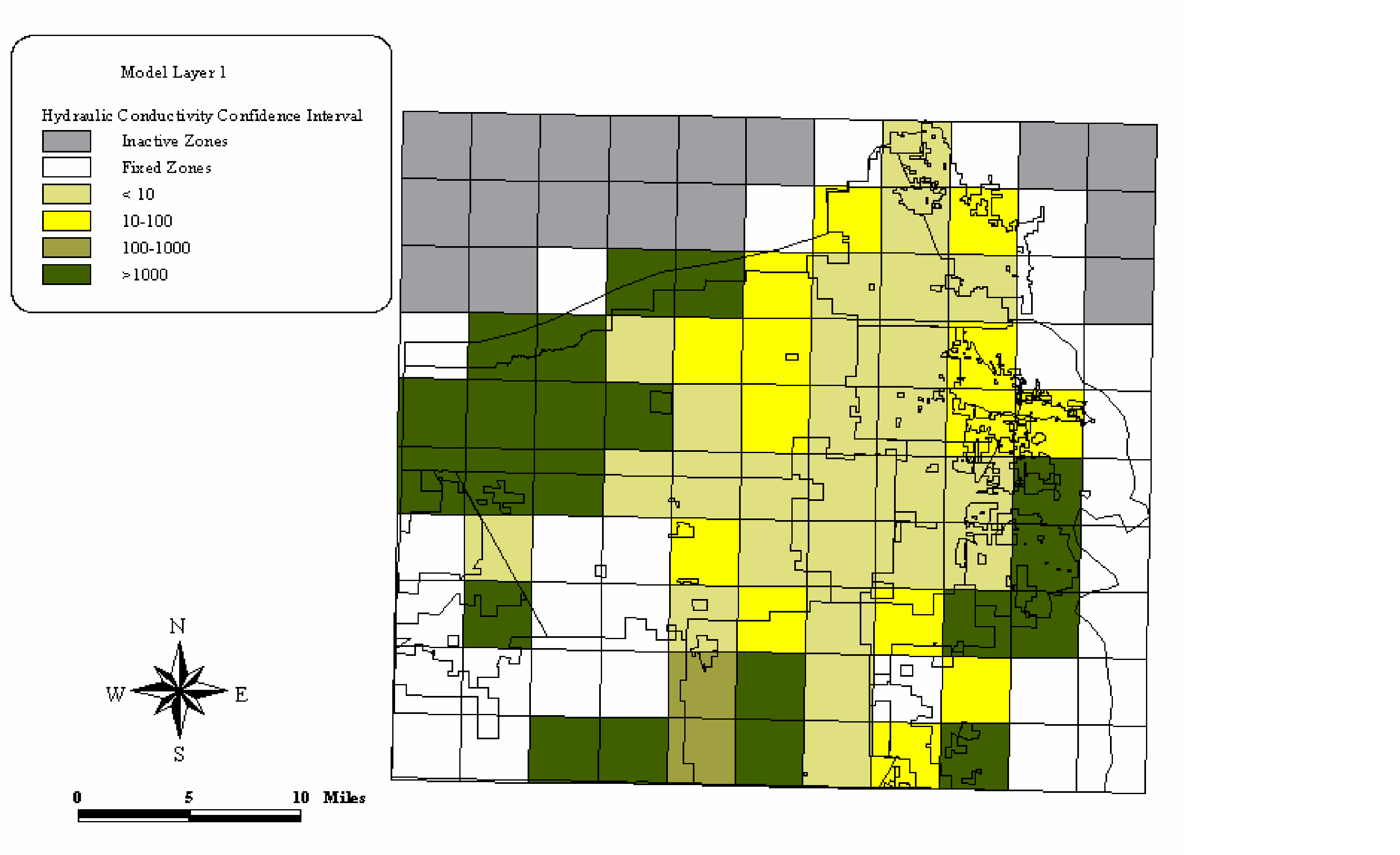

Plate 59: The ratio of the upper limit to the lower limit of the computed 95% linear confidence intervals for estimated K_h in model layer 1.

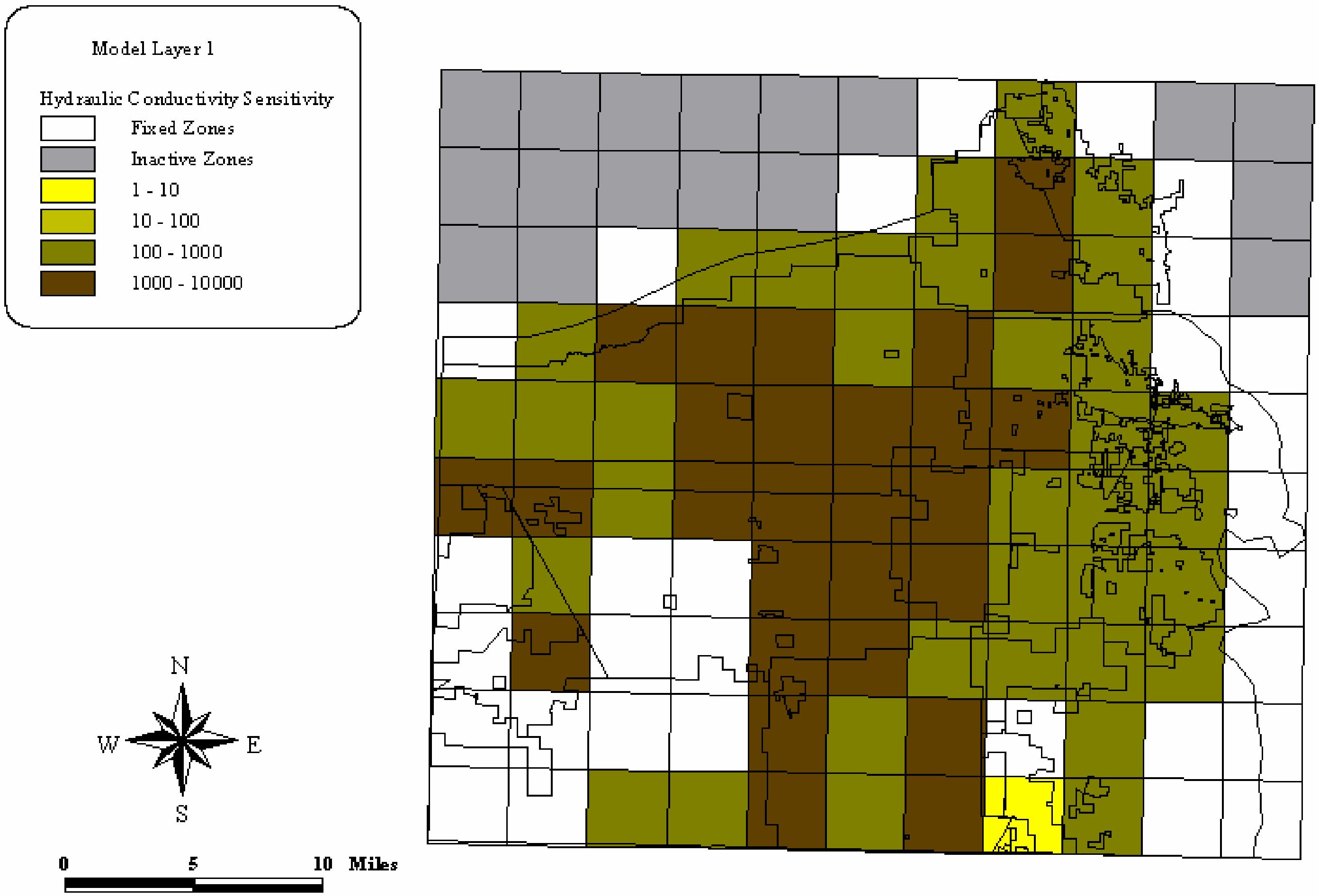

Plate 60: Composite sensitivities of model layer 1 calibrated K_h.

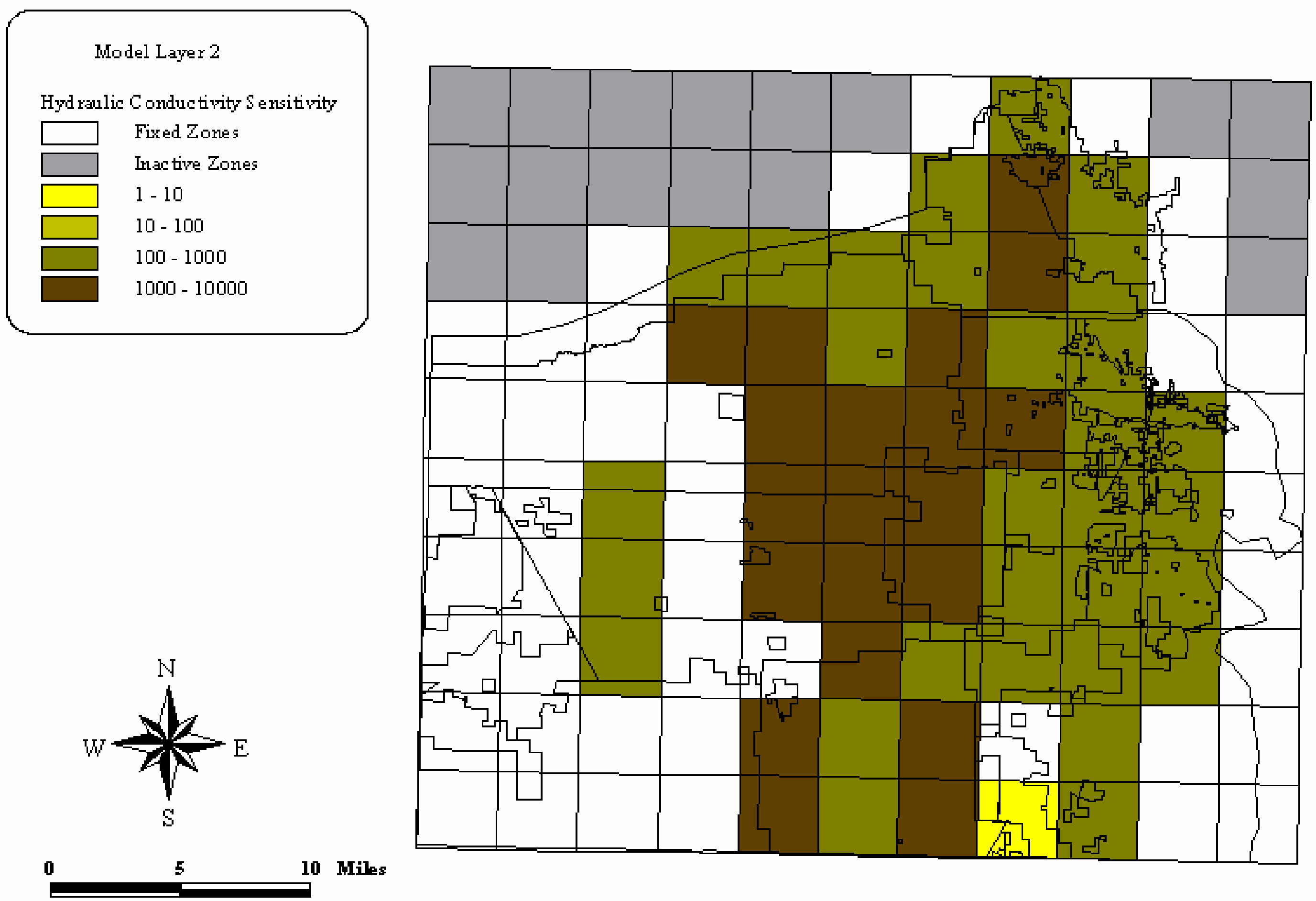

Plate 61: Composite sensitivities of model layer 2 calibrated K_h.

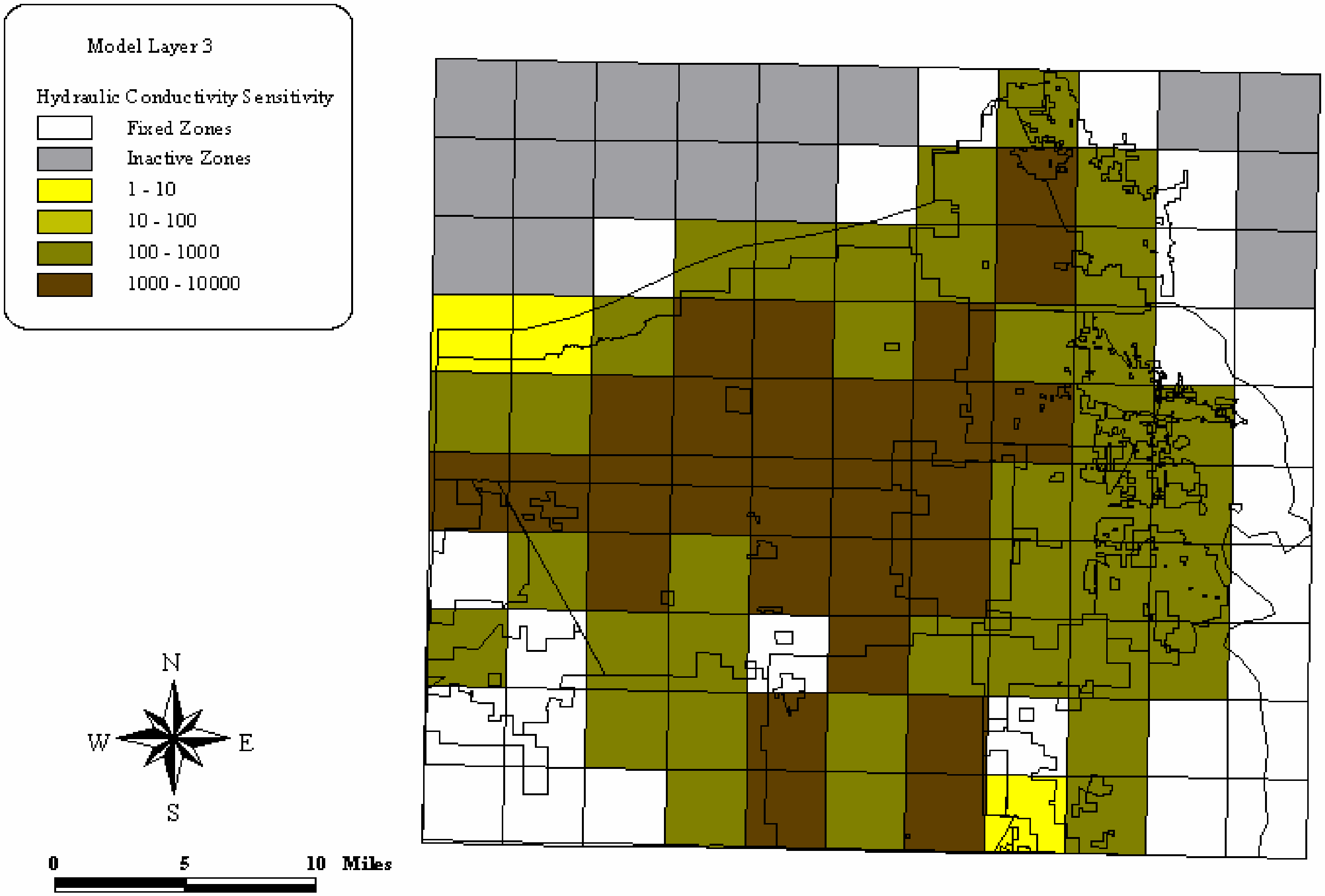

Plate 62: Composite sensitivities of model layer 3 calibrated K_h.

INSERT SLIP SHEET (P1) INSTEAD OF THIS PAGE

ATTACHMENT 2

Development of a GIS database for a Conjunctive Use Model for the combined Tule and Kaweah Groundwater Sub-Basins Area in the Southern-Eastern San Joaquin Valley, California

Nels Ruud and Thomas Harter
Department of Land, Air, and Water Resources, University of California, Davis

Prepared for:
United States Bureau of Reclamation
Submitted: September 30, 2003

List of Plates

1 Introduction

A conjunctive use model has been developed for the Tule groundwater sub-basin area and is described in Task 1 of this final report. The original intention was to expand the Tule sub-basin model north to include the Kaweah groundwater sub-basin. The combined Tule and Kaweah sub-basins model would be conceptually similar to the original Tule sub-basin model and would require similar types of data to be developed. The most significant difference between the two sub-basins, however, is that the inter-district surface water network in the Kaweah sub-basin is more complicated than that of the Tule sub-basin. When developing the Tule sub-basin model, most of the surface water diversion data was obtained from the USBR and from past Tule River Association annual reports. This data was sufficient to develop a reasonable surface water supply model for the service districts in the Tule sub-basin. To develop an analogous model for the Kaweah sub-basin would require the cooperation of the Kaweah Delta Water Conservation District (KDWCD) to provide more detailed seepage and service district delivery data.

Concurrent with our model development, KDWCD was conducting their own district-wide groundwater and surface water reconnaissance study with the assistance of a private engineering firm. As part of the study, the engineering firm in close cooperation with KDWCD planned to develop the surface water supply data. Thomas Harter and Nels Ruud were participating on the technical advisory committee formed by KDWCD to provide technical advice to the district and the engineering firm for their study. It was agreed that KDWCD would share the service district surface water delivery and channel seepage data for use in the development of the combined Tule and Kaweah sub-basins model once those tasks were completed by the engineering firm. Unfortunately, this data (anticipated to be released in the fall of 2002) did not become available before the post-doctoral assignment of Nels Ruud expired on March 31, 2003. As a result, the model extension into the Kaweah sub-basin could not be completed within the second funding year.

Nevertheless, a considerable amount of data was collected towards the goal of extending the model into the Kaweah sub-basin area. In Task 2 of this final report, we present the data which was gathered and describes relevant modeling features of the Kaweah sub-basin area, including setting, climate, hydrology, and hydrogeology. The report also includes a discussion of the remaining data to be collected to complete the combined Tule and Kaweah sub-basin model.

2 Hydrologic and Hydrogeologic Data

2.1 Setting

The expanded study area is displayed in Plate 1. The northern area represents the expansion and the southern area is the original study area of the Tule sub-basin conjunctive use model

Groundwater Sub-basins The study area includes the entire Tule and Kaweah groundwater sub-basins and parts of the Tulare Lake and Kings sub-basins (Plate 2). The areas of the Tule, Kaweah, Tulare Lake, and Kings sub-basins within the study area are 468430, 430597, 113910, and 164180 acres, respectively.

Water Service Areas The water service areas of the expansion are displayed in Plate 3. Units 1-6 are not actual service areas but are designated as hydrologic units; each of which includes parts or entireties of several service areas. The hydrologic units each receive the surface water diversions of the service areas within their boundaries. For this reason, the hydrologic units are treated as composite service areas in the conjunctive use model. The boundaries of the hydrologic units were specified by the KDWCD in their aforementioned groundwater study. The service districts in the Tule sub-basin are the same as those described in the Task 1 report.

Land Units and Land Use The land units and associated major land use are displayed in Plate 4. The associated irrigation efficiencies and crop coefficients for the different land uses will be the same as that used for the Tule sub-basin model.

Soils Composites of the major soil textural classes are shown in Plate 5. The soils survey coverage also includes assigned saturated soil hydraulic conductivity and field capacity.

2.2 Climate

Precipitation Monthly precipitation data were gathered from 13 gauging stations located in and around the study area (Plate 6). This data would be used to generate an isohyet map similar to that developed for the Tule sub-basin area.

Evapotranspiration The time-series of reference crop evapotranspiration will be the same as that used for the Tule sub-basin model.

2.3 Geology and Hydrogeology

Geomorphology The major geomorphological units in the study area are illustrated in Plate 7. The geomorphology is divided into uplands, upper terrace, lower terrace, alluvial plain, and lake bed units. The geormorphic units would have potentially been used to delineate hydraulic property zones in the calibration of the groundwater flow model.

Corcoran Clay Member Aquitard Contours delineating the position of the upper and lower boundaries of the Corcoran Clay Member aquitard are displayed in Plates 8 and 9.

Specific Yield and Hydraulic Conductivity Points values of specific yield (not shown) have been collected from DWR and can be used to generate a continuous distribution as done with the Tule sub-basin model. Preliminary values of hydraulic conductivity can be inferred from the map of the regional geomorphology (Plate 7); however, hydraulic conductivity would be a calibrated parameter in the groundwater flow model.

Historical Hydraulic Head Spring-measured unconfined aquifer water levels have been collected from DWR for the period of 1970-1999 (Plate 10). This data would be used to estimate cumulative groundwater storage changes in the unconfined aquifer and will also be used as calibration targets for the groundwater flow model.

3 Data Needs

3.1 Surface Water Supply Model

A surface water supply (SWS) model conceptually similar to that developed for the Tule sub-basin needs to be developed for the Kaweah sub-basin area. Data necessary to achieve this would include: 1) a GIS shapefile of the inter-district surface water network, 2) monthly seepage losses in the inter-district channels, 3) monthly surface water diversions to the service areas, and 4) monthly surface water deliveries to the service areas. These data can potentially be acquired from the KDWCD groundwater study.

3.2 Unsaturated Zone Water Budget Model

Excluding the output from the SWS model, sufficient data has been collected to develop the input for the unsaturated zone water budget model.

3.3 Groundwater Flow Model

Excluding the output from the UZWB model, the following data is needed to develop the groundwater flow model: 1) a GIS shapefile of the ground surface elevation, and 2) a GIS shapefile of the aquifer system bottom elevation. In addition, an estimate of the vertical distribution of groundwater pumping among aquifer layers could be determined from well log analysis or from information provided by districts.

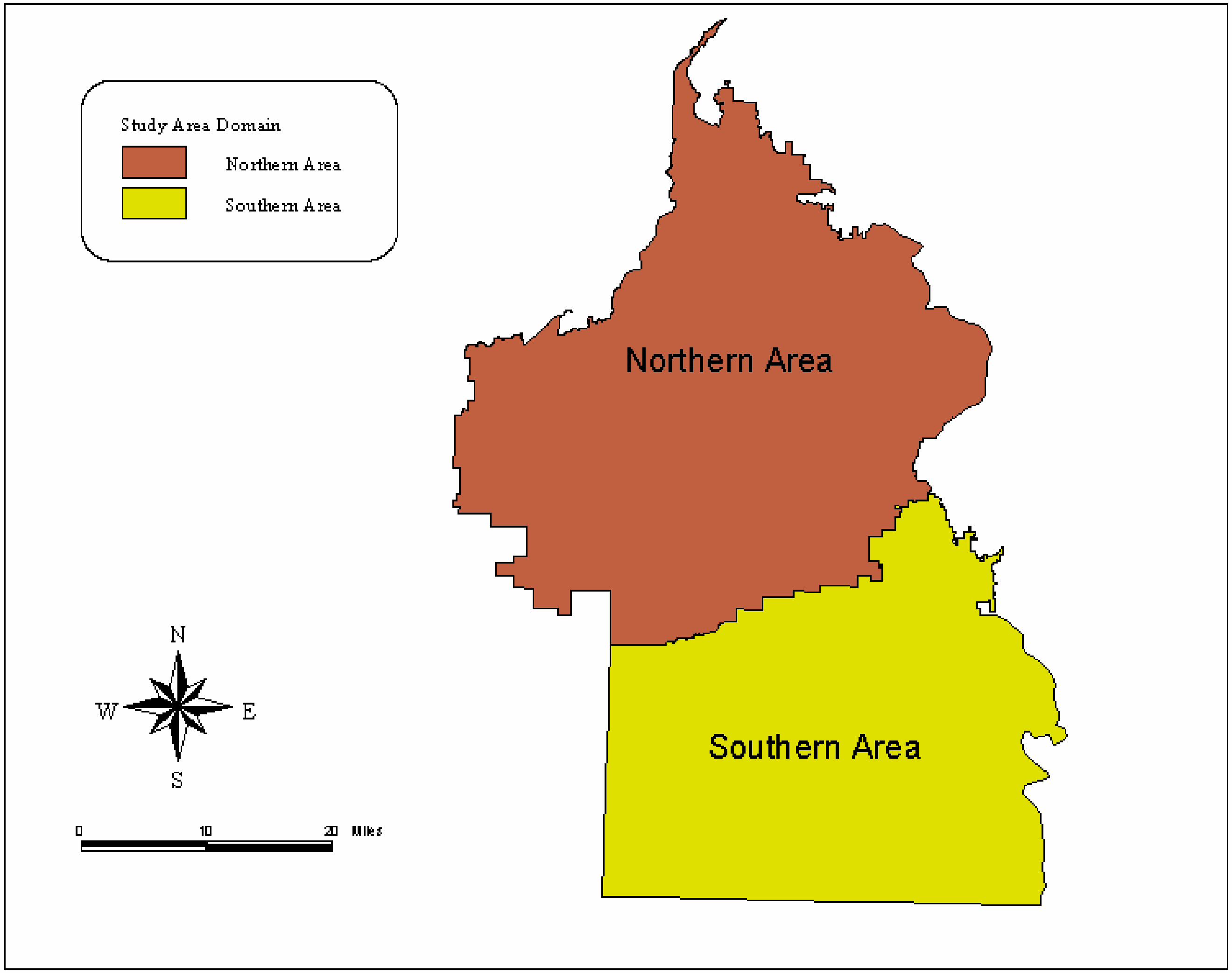

Plate 1: Northern and southern areas of the expanded study area.

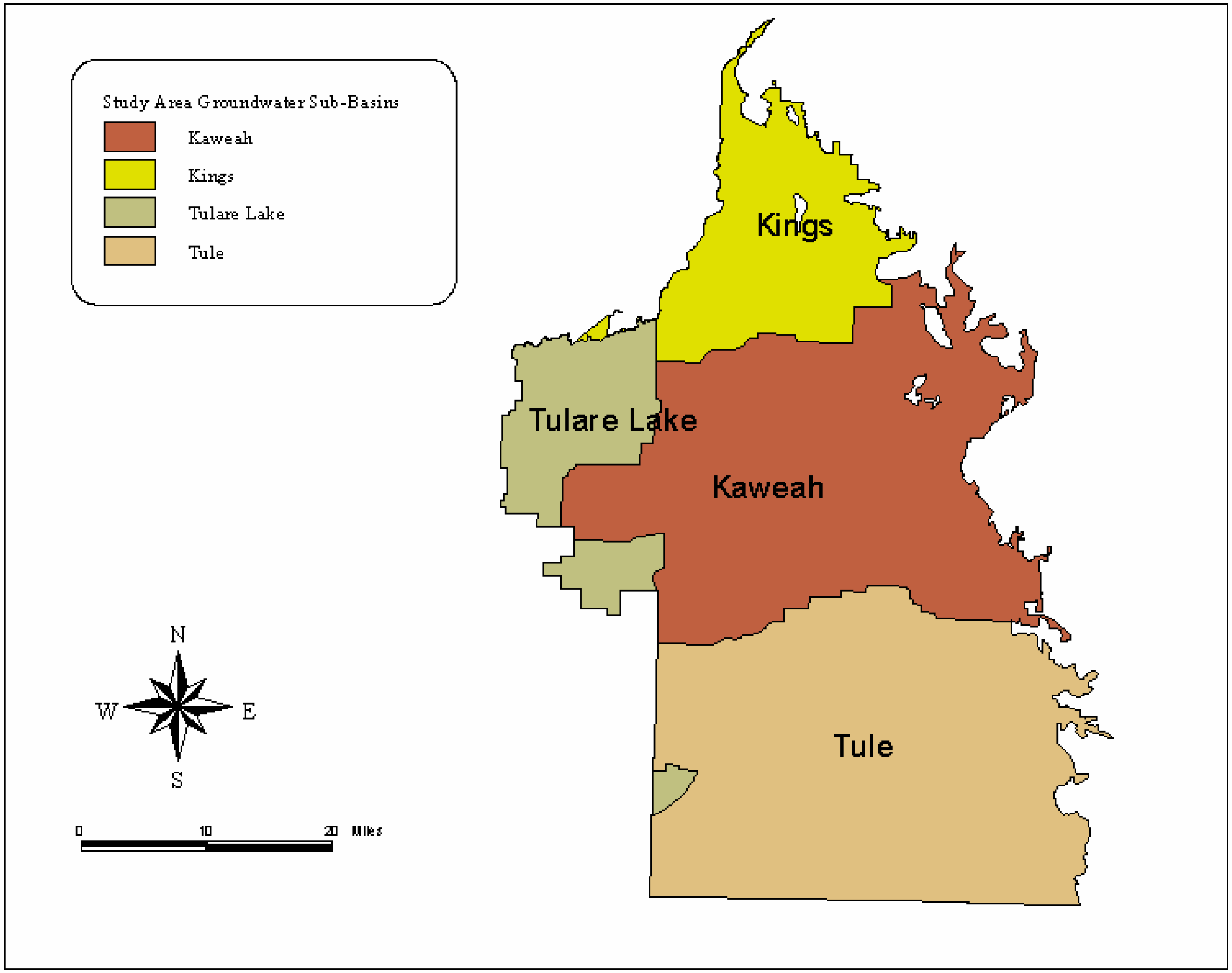

Plate 2: Groundwater sub-basins in the expanded study area.

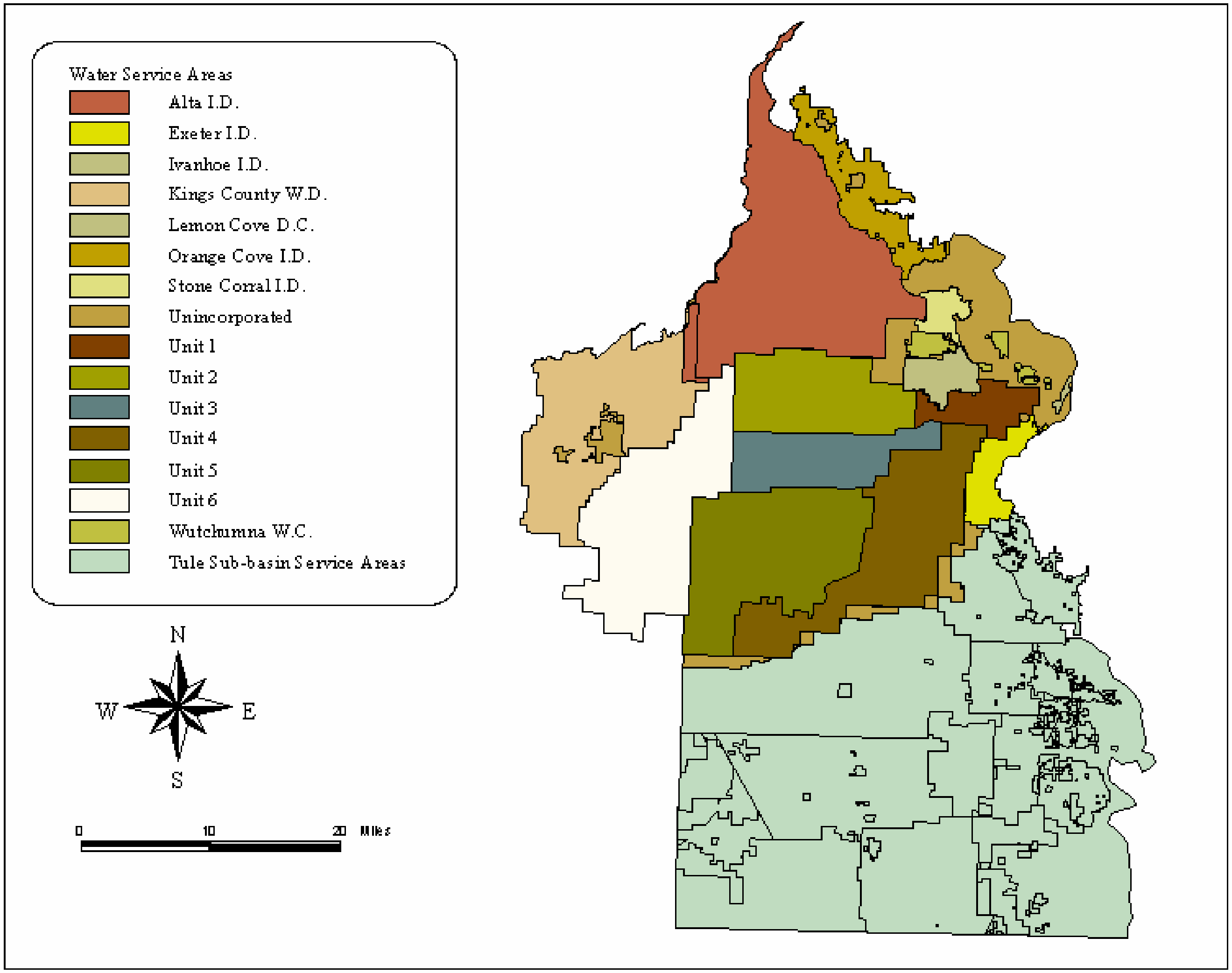

Plate 3: Water service areas in the northern expansion area.

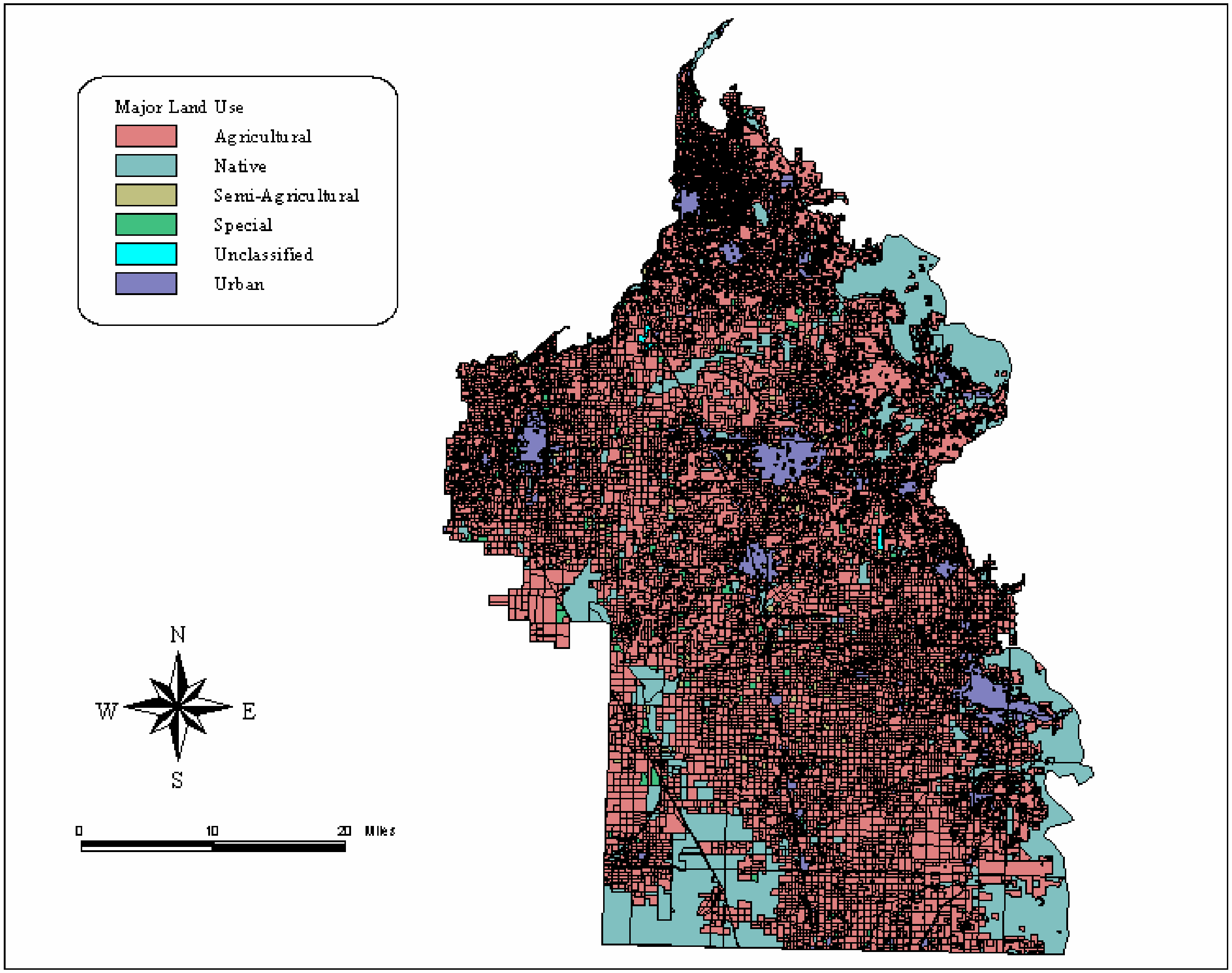

Plate 4: Major land uses in the expanded study area.

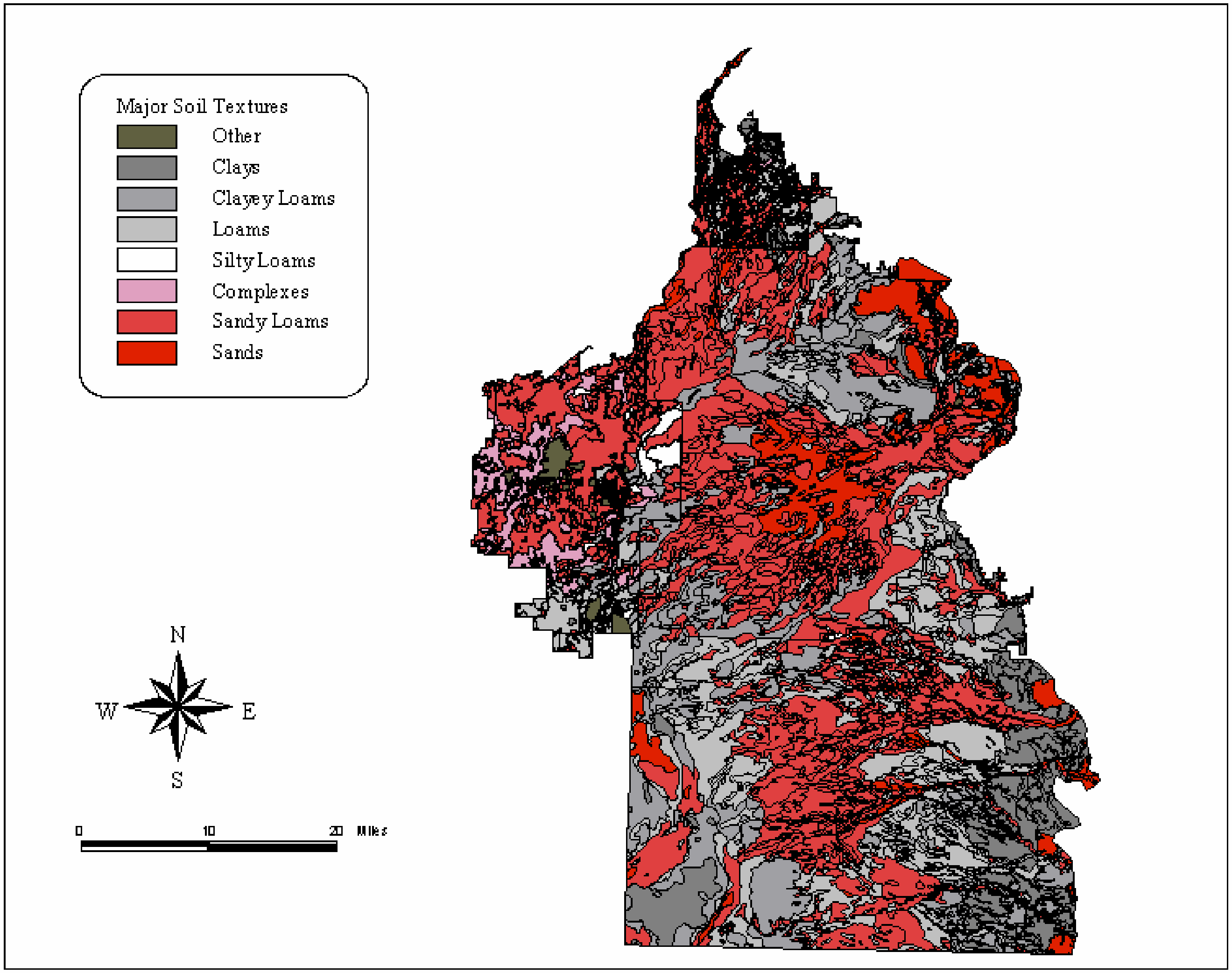

Plate 5: Major composite soil textures in the expanded study area.

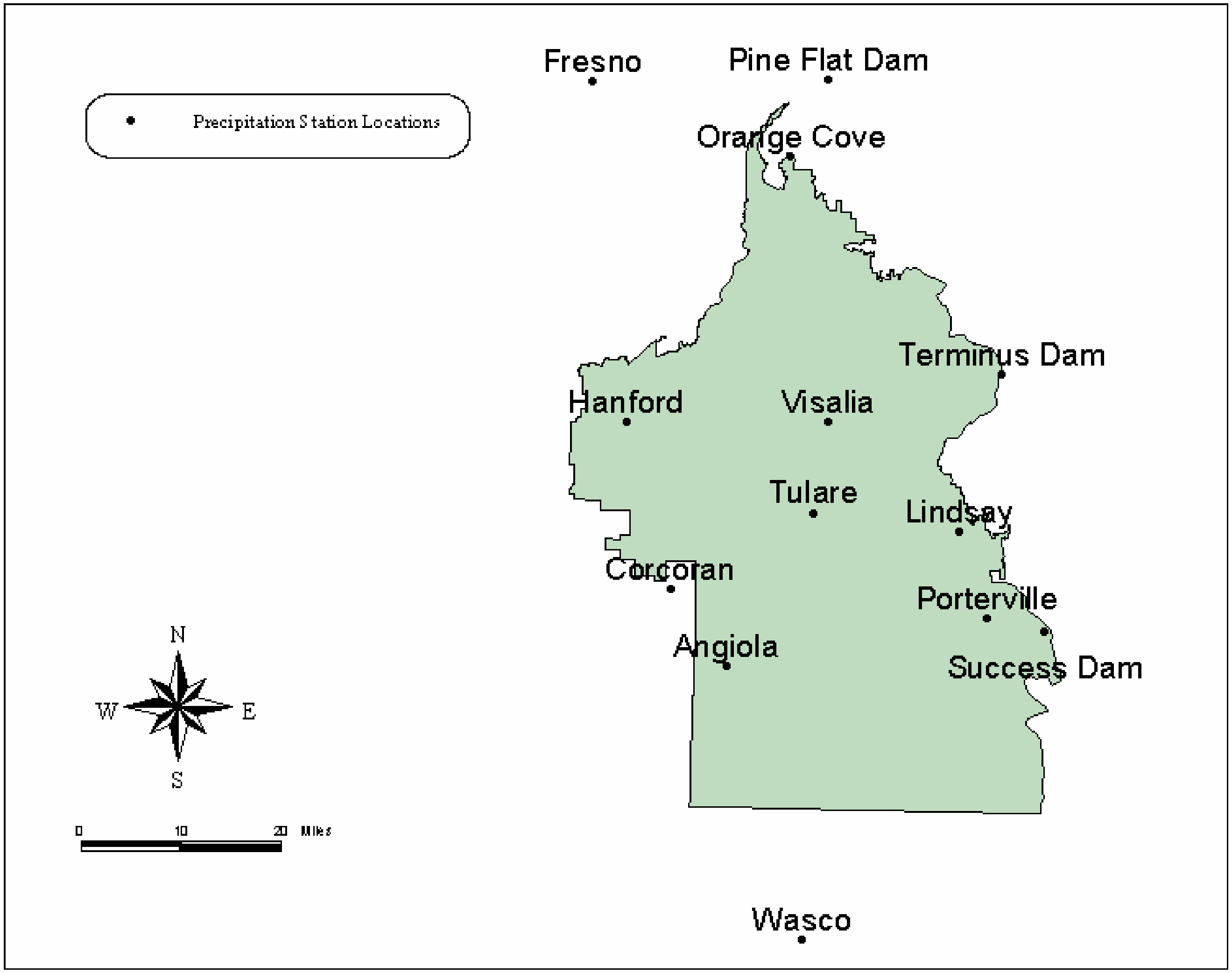

Plate 6: Locations of precipitation stations in and around the expanded study area.

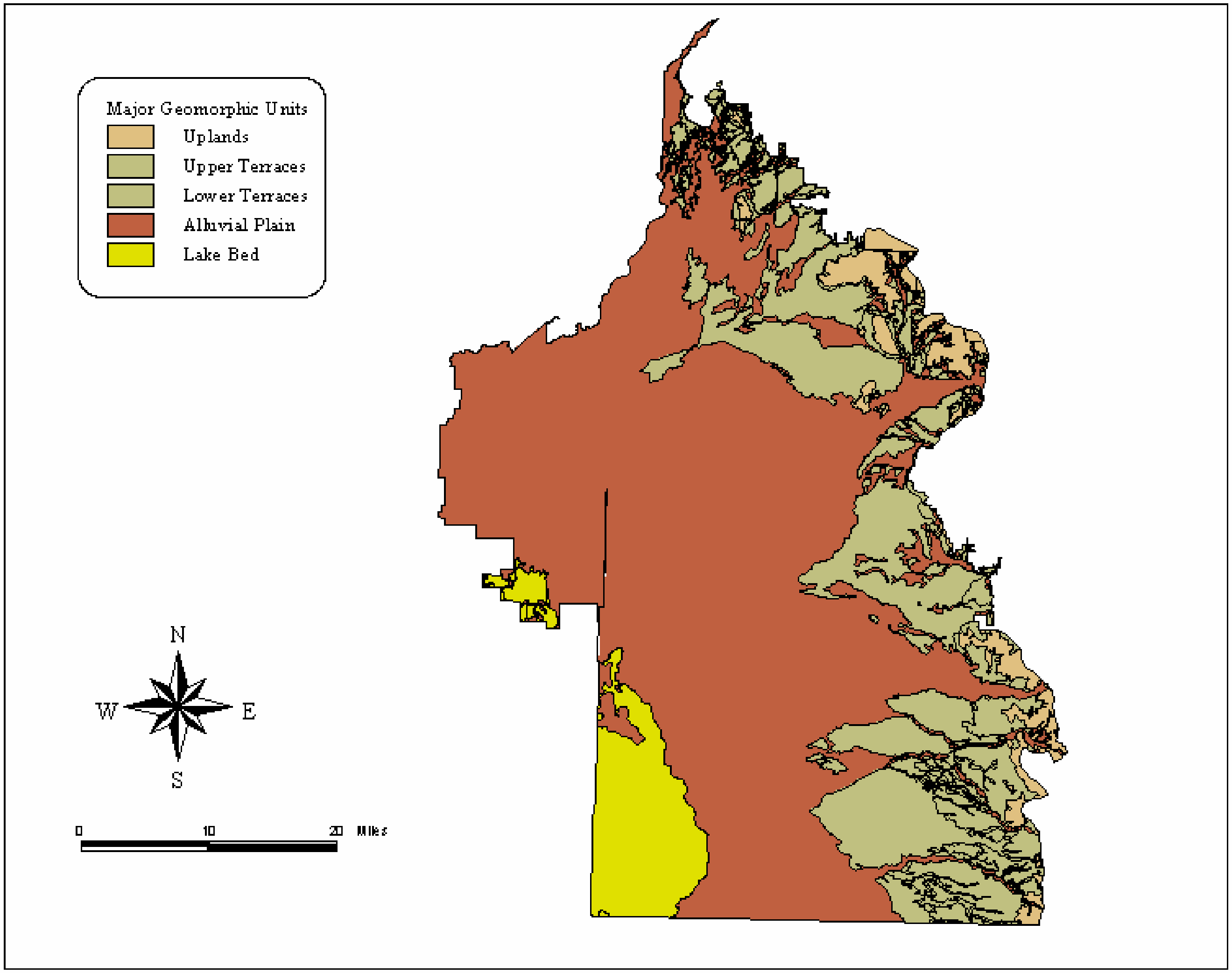

Plate 7: Major geomorphological units in the expanded study area.

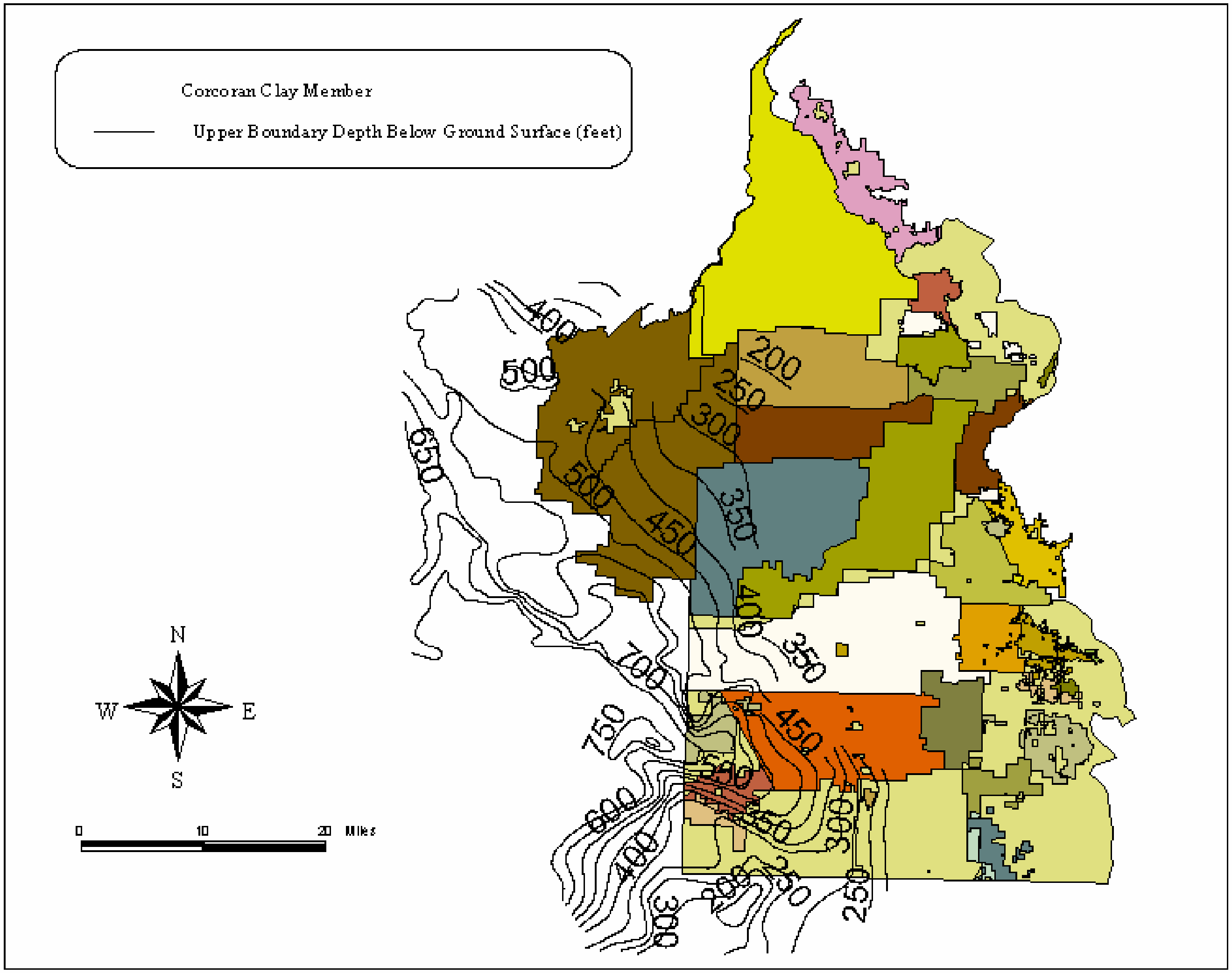

Plate 8: Depth below ground surface (feet) of upper boundary of the Corcoran Clay Member.

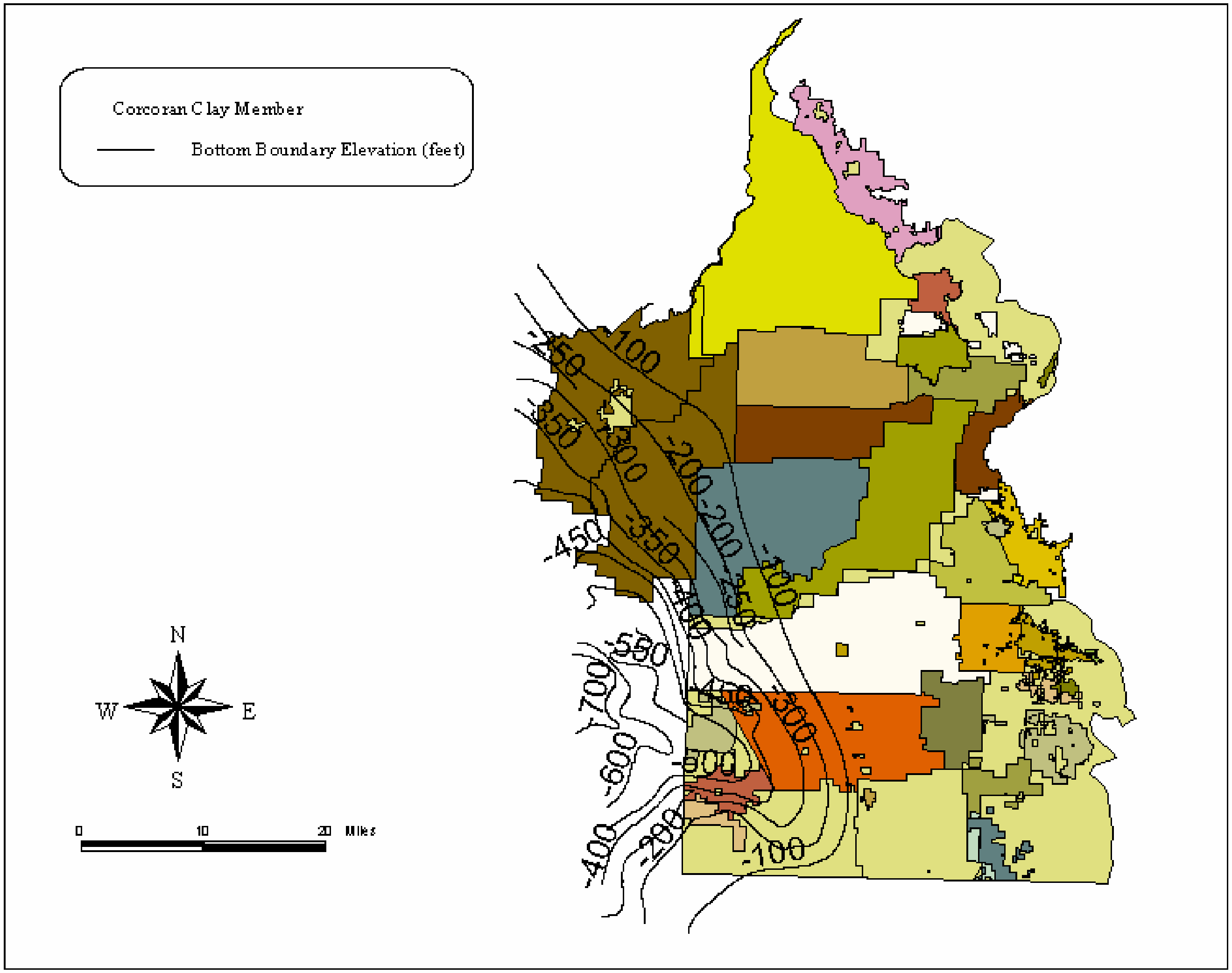

Plate 9: Elevation (feet) of lower boundary of the Corcoran Clay Member.

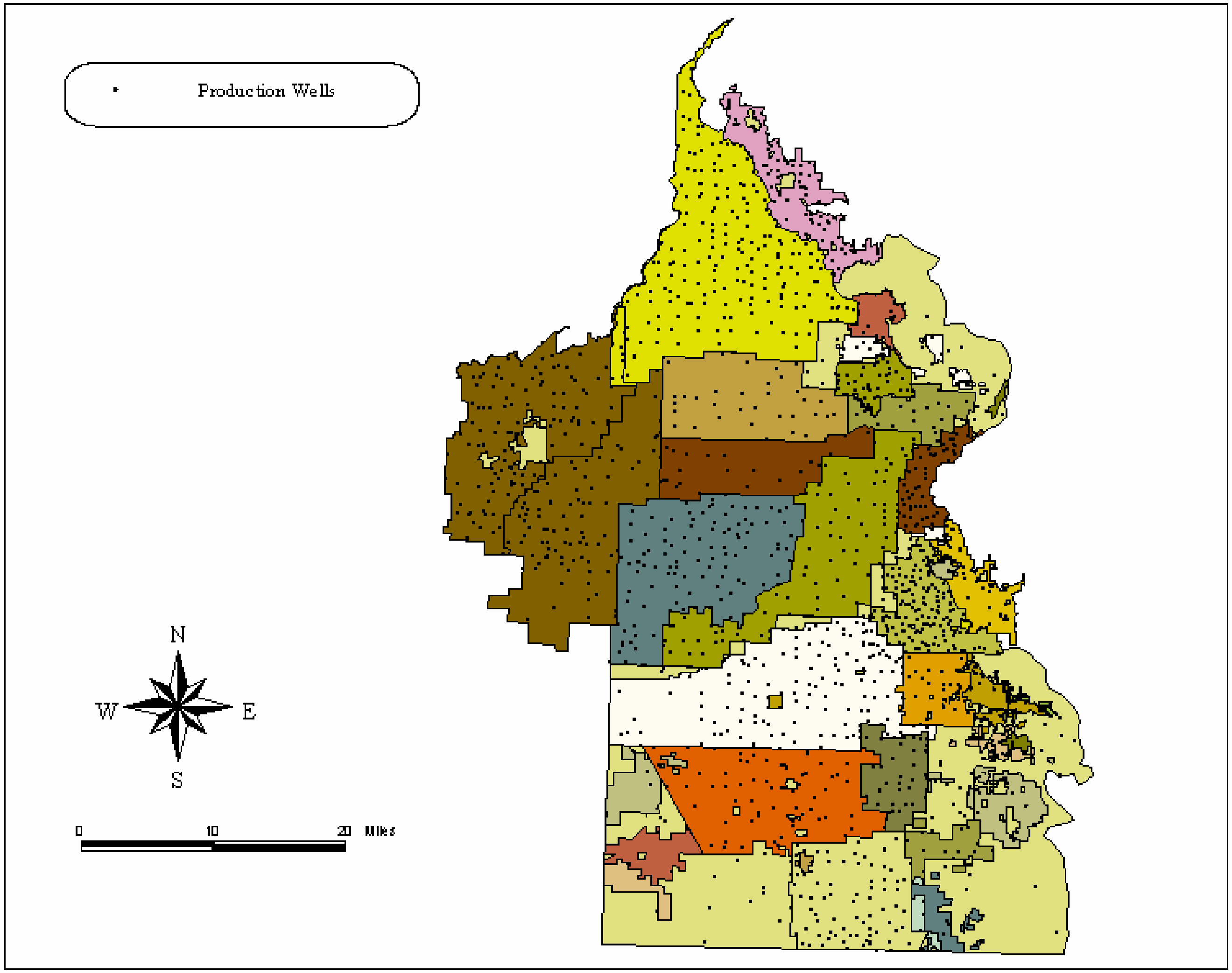

Plate 10: Locations of production wells used for measuring hydraulic head.

INSERT SLIP SHEET (P1) INSTEAD OF THIS PAGE

ATTACHMENT 3

MODELING OF FRIANT WATER MANAGEMENT AND GROUNDWATER

Guilherme F. Marques
Marion W. Jenkins
Jay R. Lund

Department of Civil and Environmental Engineering
Department of Land, Air and Water Resources
University of California, Davis, 95616

A report for the United States Bureau of Reclamation

AKNOWLEDGEMENTS

Valuable contribution to this work was provided by Thomas Harter (LAWR/UCDavis), Nels Ruud (LAWR/UCDavis), Randi Fields (USBR), Mark Leu (CH2MHILL), Marc Baldo (Colorado State Univ.), Mark Jensen (HEC), Susan Burke, Steve Hatchett and Mike Tansey (USBR).

TABLE OF CONTENTS

LIST OF FIGURES

LIST OF TABLES

ABSTRACT

Improvements to FREDSIM model are presented here and include variable groundwater pumping costs calculation, development of economic performance functions at the irrigation district level and improvement in the physical and operational representation of groundwater for conjunctive use modeling. FREDSIM is a network-flow simulation model driven by irrigation district economic. Groundwater is represented by a system of individual zones with subsurface flow modeled by Darcy law and conductance data used to represent response to hydraulic gradients. The simulation model updates the groundwater heads at each time step and recalculates the pumping cost based on energy requirements. Preliminary results indicate consistent behavior of the approach with adjustments necessary in the lag representation of groundwater flows. Results show that users change supply sources and quantities, and transfer water reacting to variations in water price, economic value and water availability. For higher changes in surface and groundwater prices, significant operations change may compromise current conjunctive use operations. The historical overdraft pattern is still occurring despite the increase in groundwater prices. Reduction of this overdraft requires reduction of groundwater pumping. In terms of surface water this is equivalent to 33% of contract surface supplies that would be required as non-local transfers. Without additional surface supplies, a 49% reduction in overdraft (9.8 maf) would cost an additional $5 million/yr average in scarcity costs, a 26% increase.

INTRODUCTION

Model Development

This report presents new developments made in the FREDSIM model (FRiant Economics-Driven SIMulation model). Initial FREDSIM development is found in Leu (2001). Major new developments include updating economic functions with new functions developed at the irrigation district level, development of a scheme for variable heads and groundwater pumping costs, improving the representation of groundwater operations by including spatial and temporal pumping pattern data, updated pumping capacities based on groundwater model results and spatial information on conveyance losses and irrigation inefficiency deep percolation. The run period was extended from the initial 10 years to 73 years with preliminary data on Friant deliveries based on correlation with Millerton Lake historic inflows.

Project Area Description

The Friant Division project area includes agricultural regions supplied by the Friant Kern canal south of San Joaquin River and the Madera canal at north of San Joaquin. Approximately 1,000,000 acres of land are supplied, ranging from the community of Chowchilla to the Tehachapi Mountains in Kern County to the south. Both Friant and Madera canals are supplied with water from Millerton Lake (Friant Dam) located in the San Joaquin River, and operated by the Friant Water Users Association (FWUA) (Leu, 2001). FWUA is a group of users with water supply contracts with the United States Bureau of Reclamation (USBR). Friant Dam is operated by USBR.

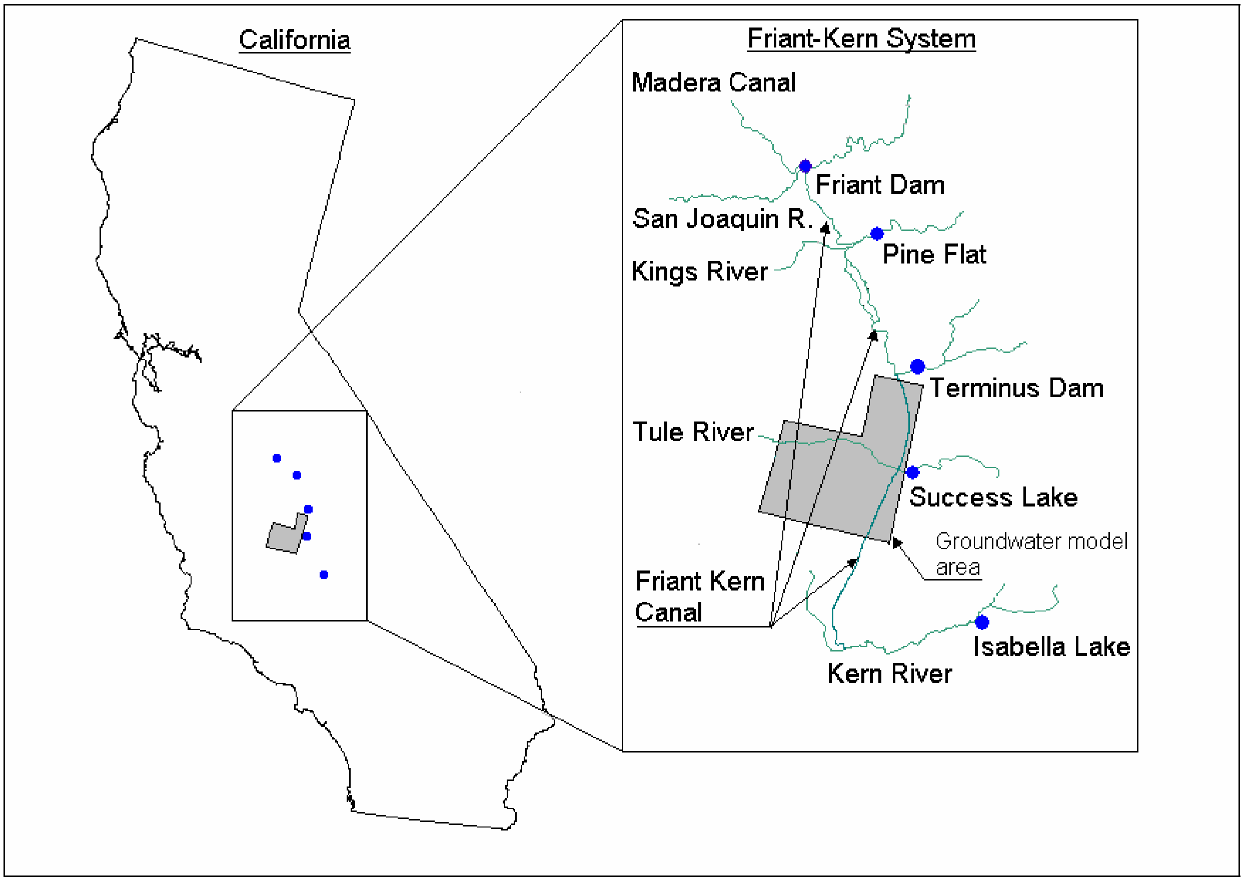

Figure 1 – Project area

METHOD

Introduction

This section presents the approach used in the development of FREDSIM (FRiant Economics-Driven SIMulation model). FREDSIM model is developed from the irrigation district level of detail using the decision support system MODSIM. Components modeled include irrigation districts, cities (as demand nodes), surface and groundwater reservoirs, the Friant and Madera canals, the Cross Valley canal, and some diversion structures connecting Friant and Madera canals to the irrigation districts and demands. The system's network is built in MODSIM with data on canal and reservoir capacities, reservoir historic inflows, seepage losses and water costs. The groundwater representation tracks head fluctuation in different portions of the aquifer and their respective pumping costs.

MODSIM Program

MODSIM is a computer based decision support system that uses a capacitated network flow approach for simulation and optimization of water resources systems. The MODSIM solver uses an out-of-kilter algorithm and has been applied with success in the simulation of diverse river basin systems (Dai and Labadie. 2001; Fredericks and Labadie, 1998). Components of a water system are represented by nodes and links. The types of nodes available are *storage nodes* (representing surface reservoirs and groundwater basins), *non-storage demand nodes* (representing demand locations such as irrigation districts and cities) and *non- storage nodes* (representing river confluences and diversion points). Nodes are connected by links representing either the physical system, i.e. rivers, artificial canals and pipelines; or the institutional/contractual elements such as water rights and delivery contracts. Nodes and links also store information on flows and storage upper and lower bounds, costs and hydrologic losses.

MODSIM finds the least cost network flows iteratively for each time step and the results are used as initial conditions for the following time step. Although it can be defined as an optimization model, MODSIM's sequential operation by optimizing individual time steps allows it to be used as an efficient simulation tool (Labadie, 1995). The linear optimization problem solved each time step is (Labadie, 1995):

$$\text{Min } Z = \sum_{l \in A} c_l q_l \qquad (1)$$

Such that

$$\sum_{j \in O_i} q_i - \sum_{k \in I_i} q_k = 0; \forall i \in N \qquad (2)$$

$$l_l \le q_l \le u_l ; \forall l \in A \qquad (3)$$

Where A is the set of network links, c_l is the cost per unit of flow rate on link *l*, q_l is the integer value flow rate in link *l*; O_i is the set of links starting at node *i*, I_i is the set of links ending at node *i*, N is the set of all nodes, l_l is the lower bound for flow on link *l* and u_l is the upper bound for flow in link l.

Mass balance is maintained in all nodes through equation (2) and upper and lower bound constraints are represented in constraint (3). Hydrologic losses along links are incorporated by an iterative algorithm.

FREDSIM concept

FREDSIM simulates water operations in the Friant Division as a system driven by economic performance at the irrigation district level. Estimates regarding the water economic value in the system are placed as costs in links and the MODSIM solver optimizes (equation 1) to find the least cost flow path to supply the system's demands.

Costs representing water economic value are built from water's *marginal economic value*, or, how much the water user would be willing to pay to have one additional unit of water. At full supply the marginal value of water is zero; as water gets scarcer users place a higher value on it. In the model, economic demand functions are expressed as economic losses relative to full supply deliveries.

The economic functions are generated by the SWAP (Statewide Agricultural Production) model as piece-wise linear functions. SWAP is a farm optimization model that maximizes economic benefit within land, water and capital constraints, based on data on crop prices, yields and elasticities. Detail on SWAP model appears in Howitt et al (1999).

The marginal value for each demand level in the function is represented in MODSIM as a benefit (negative cost) attached to an *economic link* delivering water to a given demand. The corner points in the function are entered as upper bounds on each link. The economic functions are fixed by year and vary by month. A set of 12 functions is developed for each irrigation district or water district. Each function has five segments.

As the optimization process takes place, the solver will face five pathways to deliver water to each demand. Once it is trying to minimize the total cost, the water will be delivered preferably through the link with the lower cost, in this case the one with the higher negative value. This link represents the first segment in the demand function where a higher value is placed in the first amounts of water available. As more water is available the first high value link may reach its upper bound and the next unit of water available has now a smaller marginal value. At this point the additional water will flow through the link with the second lower penalty slope. The process continues as the links reach their upper bounds and additional water available is moved to lower cost links, representing the latter segments of the demand function where the marginal value for water is lower. This configuration drives the allocation of water among the demands and defines allocation priorities and supply preferences. If different demands have access to diverse supply sources with different costs, the next unit of water will be drawn from a source which cost is not higher than the marginal value of the water at the present level of supply. If the marginal value of water is very low (close to full supply), and no supply sources with lower cost are available, no more water is supplied to the demand. This is a case where some level of water scarcity is considered optimal. Another important aspect is that economic functions reflect the crop values of a given demand, ensuring that scarce water is always delivered first to higher value crops. The model schematic appears in Figure 2.

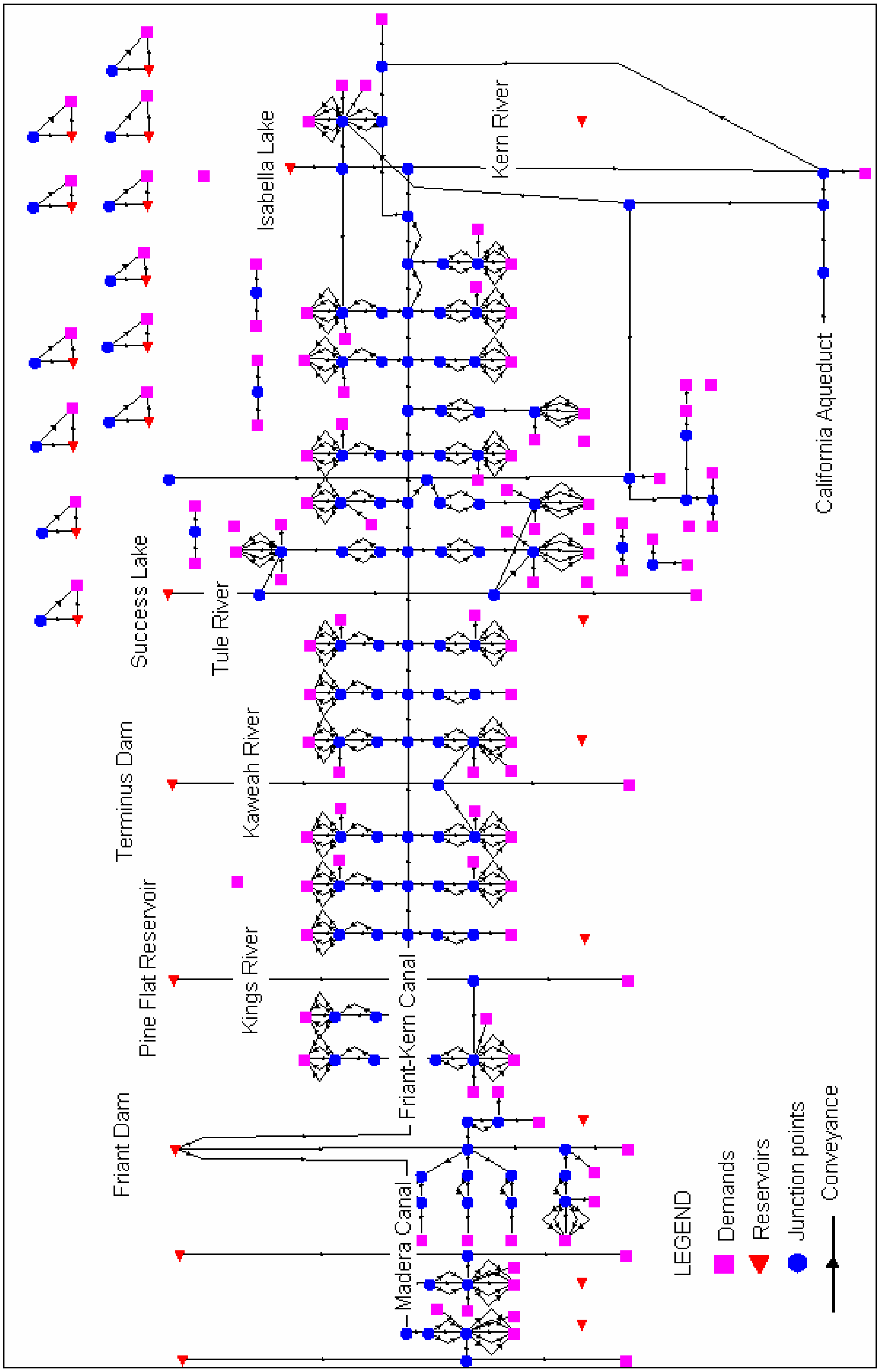

Figure 2 – FREDSIM schematic

Groundwater Operations in FREDSIM

Groundwater is an important water supply source in the Friant Division. While groundwater supply provides flexibility, intensive exploitation when surface water is unavailable or more expensive, reflects on groundwater's cost as water levels in the aquifer are lowered and more energy is required to pump it over higher heads. This dynamic affects groundwater use when one's objective is to maximize the economic value of water allocation in the system. Heavy reliance on groundwater may not be an option in the long run.

Preliminary results found in Leu (2001) in the initial development of the FREDSIM model show a constant, declining trend in groundwater storage when groundwater pumping cost is fixed. Where pumping cost is more attractive than the cost of other sources, groundwater will be continuously exploited with no awareness of further impacts. As noted by Leu (2001), over a longer period the effects of the declining groundwater levels may increase pumping cost reducing the groundwater's appeal as a lower cost supply.

The approach presented here takes a further step in modeling groundwater in the Friant system by representing variable heads as function of storage in the groundwater aquifers. Additionally, subsurface flows are estimated as responses to spatial variation in pumping and/or recharge. Additional information to model the groundwater behavior is provided by Ruud et al (2002). In Ruud et al (2002), part of the project region is modeled with MODFLOW in order to simulate subsurface flows as response to external stresses of pumping and deep percolation.

Groundwater zones concept

The primary objective of the groundwater representation in FREDSIM at this point is to track and update pumping heads with temporal and spatial variation, so that pumping costs can also be estimated. The aquifers are subject to external spatially variable stresses that add or subtract stored water. Some irrigation districts pump more water or have higher deep percolation losses. The aquifer geologic characteristics also vary spatially, meaning that the same stress may cause different responses in different places.

In an unconfined porous media, one way to link the water table to storage is through the s*pecific yield* or drainage porosity. Specific yield is the ratio of the volume of water that is drained by gravity forces over the bulk media volume Charbeneau (2000). This means that by lowering the water table by an amount Δh over an area A, the volume of water drained from an unconfined porous media is given by:

$$V_{drained} = Sy * A * \Delta h \qquad (4)$$

Equation (4) allows estimation of a variation in head when water is removed or added to an unconfined aquifer, provided that the section considered is small enough so that the specific yield can be assumed as homogeneous. Specific yield information is available for part of the project area based on GIS maps developed in Ruud et al (2002).

Another important aspect is the presence of subsurface fluxes that occur as heads variy spatially and hydraulic gradients are established. Darcy law is applied to establish a linear relationship between flux and the hydraulic gradient defined by the difference in head between two adjacent cells. This relationship is presented in equation (5).

$$Q_{ij} = C_{ij}^{eff} * \Delta h_{ij} \quad (5)$$

Where Q_{ij} is the flux between sections j and j, Δh_{ij} is the difference in head and C_{ij}^{eff} is the *effective conductance* between cells i and j. Areas with homogeneous specific yield define the boundaries of the sections and the conductance parameter can be estimated running the modeled area in MODFLOW and observing the paired data Q_{ij} vs. Δh_{ij} (further detail in Ruud et al, 2002). Homogeneous specific yield values are obtained by averaging the specific yield data for a given cell. By fitting the paired data with a linear regression curve we can estimate the slope, which is the conductance parameter searched. The goodness of fit will depend ultimately on how the cell boundaries and specific yield values were devised and if those boundaries and values can capture the aquifer's behavior acceptably. If the cells are too large, the cell average specific yield value may become a meaningless representation of the aquifer's characteristics or, if it is too small, a given cell may suffer significative influence of other non-adjacent cells and the linear relationship among two adjacent cells described in equation (5) may not hold. Both situations result in poor fit. A few attempts were made with different sizes, boundaries, and specific yield values for the cells until acceptable fits for equation (5) were obtained. The cells are also referred to as groundwater *zones* and are treated as individual, interconnected, groundwater reservoirs. The final configuration of the groundwater zones appears in Figure 3

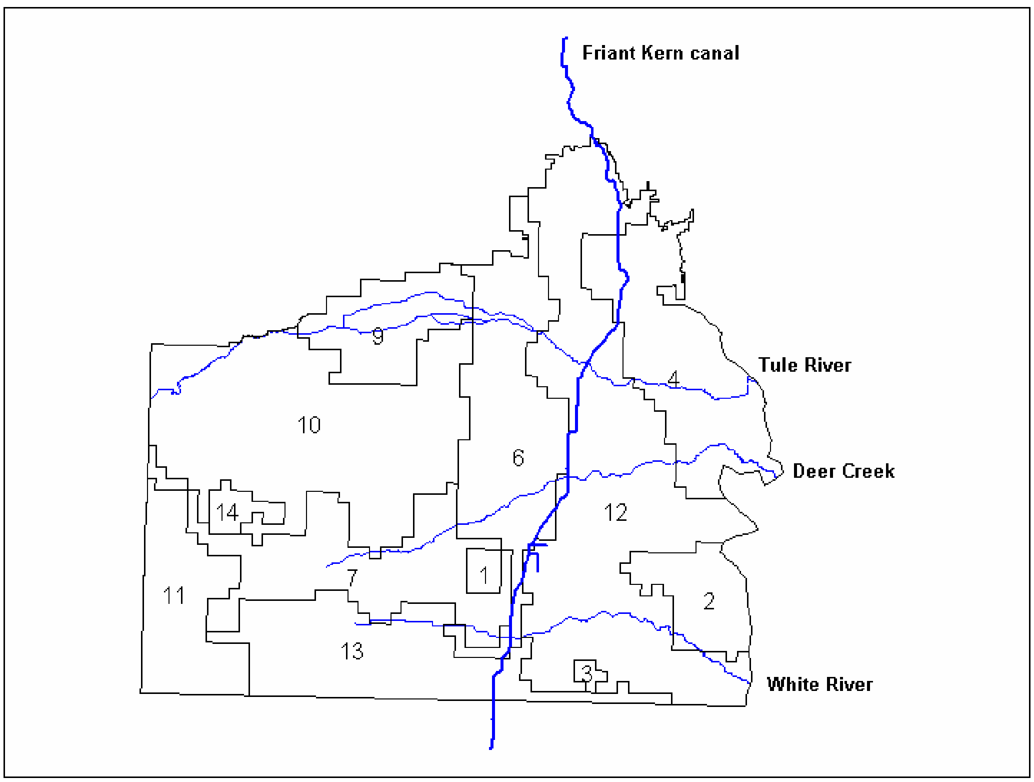

Figure 3 - Groundwater zone definitions

There are 12 groundwater zones[*] identified by the numbers in Figure 3. Their areas and specific yield values are presented in Table 1, and the conductance values and correlation coefficient R^2 of the linear fit appear in Table 2.

Table 1 - Groundwater zones definition

GW zone	Specific Yield	Area (acres)
1	0.1200	2,986.5
2	0.0630	19,554.3
3	0.0630	1,493.3
4	0.0630	54,288.9
6	0.0970	59,059.8
7	0.1030	52,026.2
9	0.1365	26,619.0
10	0.1200	104,023.3
11	0.0785	33,095.4
12	0.0760	130,030.1
13	0.0880	52,962.7
14	0.1340	5,226.3

After testing different configurations, some zones still did not present a satisfactory correlation with adjacent zones and in this case no linear correlation and flux estimation can be drawn. Some zones presented a high degree of correlation, with R^2 values as high as 0.94 indicating that boundaries defined and specific yield values are suitable to describe a linear relationship between hydraulic gradient and flux.

[*] Identification numbers range from 1 to 14. Groundwater zones #5 and #8 were merged with other zones at the end and are not present. The original numbers were maintained.

Table 2 - Effective conductance values

GW zone "i"	GW zone adjacent "j"	R^2 coefficient	Conductance (acres-foot/month)
1	7	0.55	8.19
2	12	0.96	13.60
3	12	0.91	6.41
4	12	0.44	55.14
6	7	0.48	6.84
	9	0.81	7.56
	10	-	
	12	0.81	36.16
	13	0.49	4.09
7	11	-	-
	13	0.51	26.73
	1	0.71	8.82
	10	0.85	126.92
	14	-	
	6	0.48	6.84
9	10	0.49	45.18
	6	0.81	7.56
10	6	-	
	9	0.49	45.18
	7	0.85	126.92
	14	0.86	6.19
11	7	-	-
	13	-	
12	2	0.96	13.60
	3	0.91	6.41
	4	0.44	55.14
	6	0.81	36.16
	13	-	
13	6	0.49	4.09
	7	0.51	26.73
	11	-	
	12	-	

The Irrigation districts that overlap the groundwater modeled area are presented in Figure 4. The list of districts appears in Table 3.

Table 3 - Demands with variable pumping cost

Irrigation District/Demand	MODSIM name
Delano-Earlimart ID	DEID
Kern-Tulare WD	KTWD
Lindmore ID	LIID
Lindsay-Strathmore ID	LSID
Lower Tule River ID	LTID
Pixley ID	PXID
Porterville ID	POID
Rag Gulch WD	RGWD
Saucelito ID	SAID
Tea Pot Dome WD	TPWD
Terra Bella ID	TBID

Groundwater supply for those districts is modeled with variable head/cost. A district will have access to the groundwater in the zones it overlays and the amount pumped from each zone is defined according to pump pattern data, processed from GIS maps developed in (Ruud et al, 2002). The pump pattern provides the percentage of total groundwater use that a district extracts from each of the groundwater zones it has access to. See appendix Table 17 for details. The pumping pattern varies by month and by year type*. The other two stresses affecting the groundwater zones are deep percolation from conveyance seepage losses and irrigation inefficiency. The amount of water that deep percolates from a given district due to irrigation inefficiency is distributed among the groundwater zones underneath it according to the area occupied by each one. Conveyance losses are distributed among groundwater zones according to the percentage of the main delivery structure length that overlays each groundwater zone.

* Year types considered are based on a dry year (1977), a wet year (1983) and a normal year (1982)

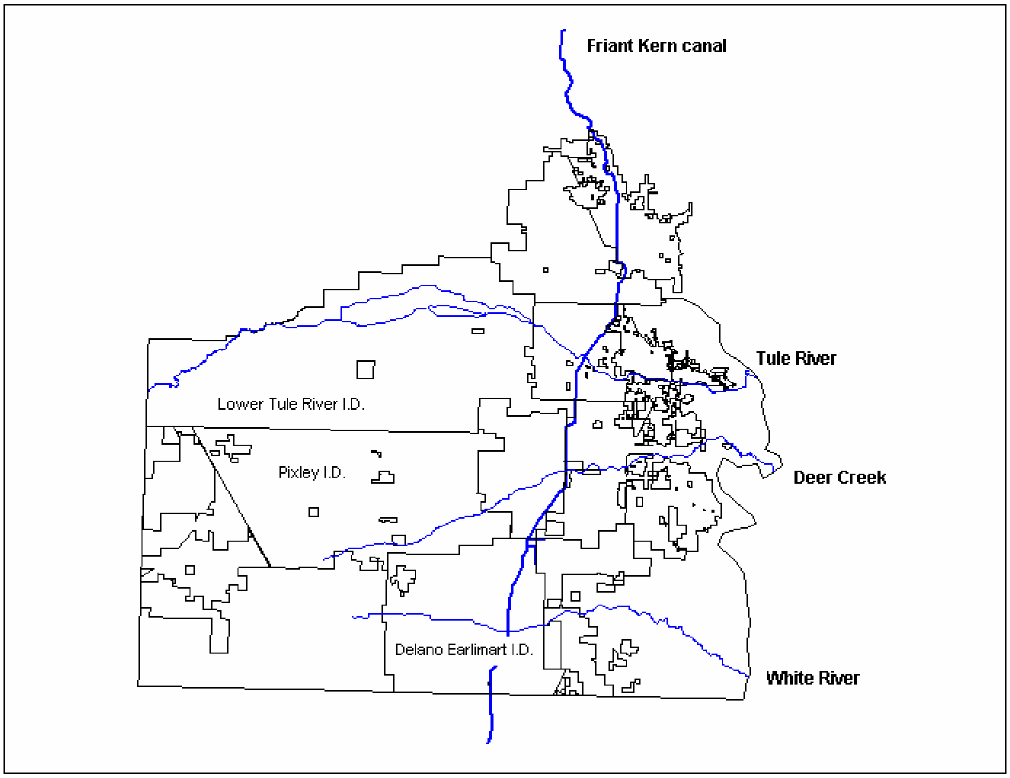

Figure 4 - Irrigation districts on modeled area

Regional water table level (head) calculation

Water table level for each groundwater zone is updated every time step based on storage variations of each zone. The groundwater zones are set in MODSIM's network as storage nodes. Storage will change as water is pumped, deep percolates, or flows from/to adjacent zones. Head calculations are made in a *Perl script* subroutine that runs parallel to the MODSIM run. At each time step, heads are re-calculated and their value used to calculate the new pumping cost, which is used by MODSIM to solve flows the current period. The Perl script subroutine accesses the necessary variables from MODSIM after each time step, performing the required calculations and sending the updated values (pumping costs) back. Variations in storage due to pumping and deep percolation are managed directly by MODSIM with the pump pattern percentages and deep percolation distribution set in the model's interface. Subsurface Darcy fluxes are calculated separately in the Perl subroutine using equation (5), the conductance parameters and the difference in head between the zones. The operation is repeated for all adjacent zones and the fluxes are accumulated to obtain the final net volume that a given groundwater zone will exchange with the adjacent zones in the present time step. The net volumes are added to the groundwater zones node through a set of artificial inflow and demand nodes.

After MODSIM solver converges to the optimal solution, the heads are updated in the perl subroutine based on the difference between the optimal storage and the previous storage (equation 6)

$$h_i^{t+1} = h_i^t + \frac{\Delta S_i}{Sy_i * A_i} \qquad (6)$$

Where h_i^{t+1} is the updated head at groundwater zone i, h_i^t is the initial head, ΔS_i is the storage change, Sy_i and A_i are respectively the specific yield and area of groundwater zone i.

Pumping cost calculation

Pumping cost is calculated based on the energy required to pump water over the total head, considering head losses due to well and pump inefficiencies. The term "total head" includes the regional water table level *h*, plus the local drawdown *s* generated during pumping. Calculation of drawdown is based on aquifer transmissivity and storage coefficient data and can be made using the *Thiem* equation, for confined aquifers, or *Theis* equation, for unconfined aquifers. Thiem equation (7) estimates steady-state drawdown for confined and semi-confined aquifers and is used here as an initial approach. Necessary assumption to use this equation is small drawdown relative to the aquifer saturated thickness.

$$s = \frac{Q_{well}}{2\pi T} \ln \frac{r_{eff}}{r_{well}} \qquad (7)$$

Q_{well} is the well pumping rate, based on typical well flow capacity T is the aquifer transmissivity, defined as the integral of the hydraulic conductivity over the aquifer saturated thickness, r_{eff} is the effective radius, and defines the distance from the well bore at which there is no drawdown effect, and r_{well} is the well bore radius.

The *input power* IP_j [kw] required to pump water over the total head $(s + h)$ [ft] in a given groundwater site and at a given pumping rate Q_{well} [gpm] can be calculated through the expression (8) (Harter, 2001).

$$IP_j = \frac{Q_{well} * (2 * s + h_{reg\,j}^{\,t}) * 0.735}{3{,}960 * e_o} \text{ [kw]} \qquad (8)$$

A 50% efficiency for both well and pump is assumed. The *energy consumed* E_{well} [kw-hr] by a well operating at these conditions during a period of time t_p [hr] is then (9):

$$E_{well\,j} = IP_j * t_p \text{ [kw-hr]} \qquad (9)$$

The volume of water V_{well} [gal] extracted after time t_p is given by (10)

$$V_{well} = Q_{well} * t_p * 60 \text{ [gal]} \qquad (10)$$

The energy required to pump a unit volume of water E_o [kw-hr/gal] is:

$$E_{o\,j} = \frac{E_{well\,j}}{V_{well}} = \text{ [kw-hr/gal]} \qquad (11)$$

As seen, the energy required does not depend on the pumping time, nor on the well pumping rate Q_{well}. Now, defining the energy cost as *c* [\$/kw-hr], one can finally obtain the unit pumping cost per volume PC_j [\$/af] as:

$$PC_j = \frac{E_{o\,j} * c}{n} = \frac{(2 * s + h_{reg\,j}^{\;t}) * 0.735 * c}{3{,}960 * e_o * n} \quad [\$/af] \qquad (12)$$

Where n (3.069E-06) converts US gallons to acre-feet.

Although some variations on the pumping cost may occur within a time step, they are assumed to be negligible and the pumping cost is only re-calculated at the beginning of a given time step, using the end-of-period head from the previous time step. This assumption seems reasonable since groundwater flow is rather slow and the impact of pumping on water depth may take some time to develop.

Economic Functions

New sets of economic functions were developed at the irrigation district level. Functions were developed based on the Statewide Agricultural Production Model (SWAP). The SWAP model maximizes economic returns subject to resource, production and policy constraint, and calculates the monthly *shadow value* per unit of water for each level of water supply. Based on detailed information about crop acreages for each irrigation district, demand functions were developed at the irrigation district level.

Based on the economic functions and current water supply levels, water *scarcity* and *scarcity costs* are evaluated. Scarcity is defined here as the difference between a water supply level were the marginal value for additional water is zero (full supply) and the current supply level. This represents a case where water may be available for supply, but it is not economically worthwhile to use it. The *area* below the economic function between these two points in defined as the *scarcity cost* (Figure 5), and represents the loss of economic value from deliveries being less than full supply.

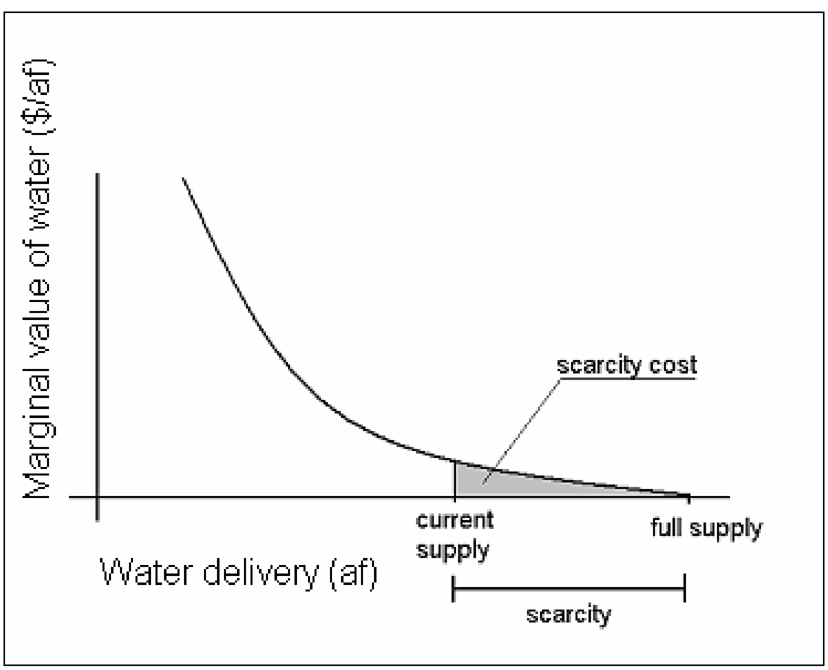

Figure 5 - Economic (demand) function and water scarcity

Surface Water Distribution Support Model

To generate water demand functions, the SWAP model requires input on applied water and evapotranspiration of applied water for all irrigation districts. The UZWB (Unsaturated Zone Water Budget) model, developed to compute water budget over the land surface and unsaturated zone, was used to provide applied water demand over each land unit of the project area. Land units are defined by their respective landuse type and were later aggregated into irrigation districts. Mass balance is performed in UZWB based on precipitation, irrigation applications, water demand, consumptive use, percolation, recharge, excess irrigation and groundwater pumping (Ruud and Harter, Attachment 1 of this Final Report; Naugle, 2001).

Evapotranspiration of applied water (ETAW) refers to the portion of ET supplied by irrigation, i.e. excluding water already present in the soil (soil moisture) and precipitation water. UZWB is originally configured to output demand for applied water based on ET. Thus some adjustments were introduced in the model to separate the required ETAW.

On the adjustments, the effective precipitation Peff is initially calculated as

$$Peff = \begin{cases} (ETa + fc - \phi), & Pe > (ETa + fc - \phi) \\ Pe, & Pe \leq (ETa + fc - \phi) \end{cases} \qquad (13)$$

Where ETa is the evapotranspiration in a given month, Pe is the precipitation; fc is the field capacity and ϕ is soil moisture content. Equation (13) sets the amount of space available in the soil to store water as the summation of evapotranspiration plus the field capacity, minus water already present (ϕ). If precipitation in a given month exceeds this amount, then the effective precipitation is (ETa + fc - ϕ), otherwise the effective precipitation Peff equals the precipitation. Effective precipitation may increase the amount of water stored in the soil and this effect is carried to the next month with an accounting storage variable Speff0. The evapotranspiration of applied water ETAW is then calculated as (14)

$$ETAW = \begin{cases} 0, & ETA < (Speff\,0 + Peff) \\ (ETa - Speff\,0 - Peff), & ETA > (Speff\,0 + Peff) \end{cases} \qquad (14)$$

Equation 14 adds soil water content from the previous month (Speff0) to the effective precipitation on the present month and compares the total with the evapotranspiration ETa in the present month. If ETa is smaller, all water used by crops is being provided by effective precipitation and soil moisture and in this case ETAW is zero. If ETa exceeds (Speff0 + Peff) then a portion of the ETa will be provided by irrigation applied water. This portion is the ETAW and it is calculated in equation (14) as (ETa – Speff – Peff). Whenever ETAW is zero, the amount of water over ETa is carried to the next month in the variable Speff0.

One important aspect that limits this approach is the temporal distribution of ETa and precipitation. The calculations are performed monthly and all ETa is lumped at the end of the month. In a more detailed temporal scale, precipitation and evapotranspiration can vary and the actual amount of water stored in the soil as effective precipitation will not be same as the monthly total calculated in (13). Sequences of days with low evapotranspiration, paired with a higher precipitation, may result in monthly totals of effective precipitation considerably lower than the lumped monthly sum of equation (13), for the same monthly totals of precipitation and evapotranspiration. Overestimated effective precipitation will result in underestimates for ETAW. This limitation may be one reason why ETAW estimates from UZWB are consistently lower than ETAW present in other data sources (Table 5). A more detailed model is required at this point to account for proper temporal variations in evapotranspiration and precipitation.

Crop categories

Land use categories from the UZWB database originally included 61 types. The land use categories related to agricultural use present in the project area were grouped into the SWAP crop categories (Table 4). Land acreages are based on DWR land survey, year of 1985 (Zhang, 1993)

Table 4 - Crop categories

UZWB crop group	SWAP crop	SWAP crop abbreviation
orange	citrus	CITR
olive(avg)	olives	OLVS
peaches(avg)	peaches	PEAC
prunes(avg)	prunes	PRUN
almonds(avg)	almonds	ALMD
walnuts(avg)	walnuts	WALN
cotton	cotton	COTT
corn	corn	CORN
misc. field crops(avg)	miscelaneous	MISC
grain and hay crops	wheat, miscelaneous grains, miscelaneous hay	WHET, MGRN, MHAY
alfafa &alfafa mixtures	alfafa	ALFH
tomatoes	miscelaneous vegetables	MVEG
vineyard	grapes	GRPE
mixed pasture	pasture	PAST

ETAW data

ETAW data output from UZWB is presented by crop type and by month. For comparison, annual totals of ETAW for each crop type are compared to other sources of data and the percent variation is calculated (Table 5).

Table 5 - ETAW comparison table

UZWB crop	UZWB ETAW (ft/yr)	**Bulletin 160-93 Tulare** (ft/yr)	% UZWB difference	**CU model cvpm 18** (ft/yr)	% UZWB difference	**cvpm model cvpm 18** (ft/yr)	% UZWB difference	**Bulletin 160-98 cvpm 18** (ft/yr)	% UZWB difference
Alfalfa &alfalfa mixt.	2.79	3.00	-7.0%	3.12	-10.6%	3.14	-11.1%	3.10	-10.0%
Almonds (avg)	2.37	-	-	2.34	1.3%	-	-	2.30	3.0%
Orange	1.88	1.90	-1.1%	1.90	-1.1%	1.92	-2.1%	1.90	-1.1%
Corn	1.98	2.00	-1.0%	1.71	15.8%	2.02	-2.0%	2.00	-1.0%
Cotton	2.27	2.50	-9.2%	2.34	-3.0%	2.53	-10.3%	2.50	-9.2%
Vineyard	1.84	2.10	-12.4%	2.00	-8.0%	2.13	-13.6%	2.10	-12.4%
misc. field crops(avg)	1.98	2.00	-1.0%	1.71	15.8%	2.02	-2.0%	1.97	0.5%
Tomatoes	1.97	2.30	-14.3%	2.01	-2.0%	2.23	-11.7%	2.00	-1.5%
Olive(avg)	2.2	2.60	-15.4%	1.90	15.8%	1.92	14.6%	1.90	15.8%

Mixed pasture	2.47	3.20	-22.8%	3.36	-26.5%	3.34	-26.0%	3.30	-25.2%
Peaches(avg)	2.3	2.50	-8.0%	2.34	-1.7%	2.74	-16.1%	2.69	-14.5%
Prunes (avg)	2.3	2.50	-8.0%	2.34	-1.7%	2.74	-16.1%	2.69	-14.5%
Walnuts(avg)	2.66	2.50	6.4%	2.34	13.7%	2.74	-2.9%	2.69	-1.1%
Grain and hay crops	0.45	1.00	-55.0%	0.38	18.4%	0.91	-50.5%	0.90	-50.0%

Differences are around 15% with some cases over 20% or as low as 1%. Comparing to bulletins 160-93, 160-98 and CVPM model, the LAIUIZ ETAW values are consistently lower, while comparison with CU model ETAW presents more balanced differences. Consistently lower ETAW values are a concern since they will result in lower demand for water from the SWAP model and may cause FREDSIM to underestimate potential water scarcities which drive the model.

MODEL RUNS

Three runs were made with the economic functions generated by SWAP for each irrigation district. All runs include the subsurface flows based on estimated conductance values. The first run, FPlow (fixed original lower groundwater pumping cost), maintains the original groundwater pumping costs based on Leu (2001) (table 3.1, second column) regardless of variations on water table level. Some of the original groundwater pumping costs were adjusted so the model prioritizes the use of contract water over groundwater when enough surface water is available for supply. During dry periods, the scarce surface supply is complemented with groundwater. These operations are verified in URS (2002).

The second run, FPhigh (fixed updated, higher groundwater pumping cost), updates the groundwater pumping cost based on detailed water table data and equation (12). The pumping cost is calculated based on the initial head and maintained through the 73 years run period.

The third run, VP (variable groundwater pumping cost) updates the pumping cost every month based on water table fluctuation. Since the groundwater model does not cover the entire project area, only the irrigation districts included in the groundwater model (Table 3) have variable pumping costs. The remaining districts (representing 73 % of total water demand) are modeled with the original FREDSIM pumping cost (Table 6, first column).
The run period was extended from the original 10 years to 73 years based on historical inflow data to the surface reservoirs. The forecast for class 1 and class 2 deliveries to Friant was correlated with annual inflows at Millerton and the correlation function was used to extend the class 1 and class 2 forecasts for the entire historical inflow record. Although the correlation coefficient was acceptable, the ten years of class 1 and class 2 deliveries used in the correlation are a short period of time for this sort of statistical analysis; a longer record of class 1 and class 2 deliveries should be used in future model improvements.

The purpose of the runs comparison is to evaluate possible changes in operations driven by the region's economics as the groundwater cost varies.

Table 6 - Groundwater pumping costs

Irrigation District	Original pumping Cost[1,2] ($/af)	Adjusted pumping cost FPlow run[2] ($/af)	Updated pumping cost FPhigh run[2,3] ($/af)	Variable pumping cost VP run average[4] ($/af)	Variable pumping cost VP run minimum[4] ($/af)	Variable pumping cost VP run maximum[4] ($/af)
AEWD	80	80	80	-	-	-
CHWD	36	45	45	-	-	-
DEID	40	45	59*	75	58	97
EXID	23	45	45	-	-	-
FC18	0	0	0	-	-	-
FRCO	0	0	0	-	-	-
FRID	23	45	45	-	-	-
FRCY	0	0	0	-	-	-
GAWD	33	45	45	-	-	-
GFWD	31	45	45	-	-	-
HVID	19	45	45	-	-	-
INWD	19	45	45	-	-	-
IVID	25	45	45	-	-	-

KTWD	45	45	96*	96	60	119
LCWD	20	45	45	-	-	-
LIID	22	45	122*	128	113	142
LWSA	0	0	0	-	-	-
LSID	23	45	132*	133	125	147
LTID	32	45	73*	87	52	120
MACO	0	0	0	-	-	-
MAID	31	45	45	-	-	-
OCID	19	45	45	-	-	-
OCCY	0	0	0	-	-	-
PXID	36	45	45*	81	45	112
POID	20	45	114*	127	113	139
RGWD	43	45	61*	91	60	136
SAID	40	45	78*	110	78	130
SWID	64	64	64	-	-	-
SSMD	45	45	45	-	-	-
SCID	17	45	45	-	-	-
TPWD	39	45	117*	130	117	143
TBID	43	45	117*	130	117	142
TVWD	0	0	0	-	-	-
TUCO	0	0	0	-	-	-
TUID	32	45	45	-	-	-

[1] Source: Leu, 2001
[2] Zero costs indicate no GW use in that irrigation district
[3] Only costs marked (*) were updated due to data availability
[4] average, max and min values for 73 years run period

Demands for Irrigation Water

Maximum annual demands based on the new economic functions appear in Table 7. Original economic functions were based on scaled down values from CVPM regions calculated by SWAP model (Leu, 2001). The new functions are based on irrigation district data run on SWAP model. Where additional data sources were available, values were checked for consistency. For example, Arwin Edison's 2000 water year summary report (ARVIN-EDISON, 2000) reports 262,634 af of deliveries including Cross Valley Canal exchanges, Friant water, Kern river supply and groundwater pumping.

Table 7 - Economic Demands

Irrigation District abreviation	Irrigation District name	Maximum Economic Demand – Original Economic Functions(af/yr)	Maximum Economic Demand – New Economic Functions(af/yr)	Estimated crop Consumptive use based on FWUA / MWDSC (2001)(af/yr)
AEWD	Arvin-Edison Water Storage District	408,389	269,809	303,857
CHWD	Chowchilla Water District	224,915	208,100	150,357
DEID	Delano-Earlimart Irrigation District	174,992	145,328	115,110
EXID	Exeter Irrigation District	46,221	34,600	31,140
FC18	Fresno County #18	138	150	n/a
FRCO	Fresno County	2,989	3,001	n/a
FRCY	Fresno, City of	59,989	60,001	n/a
FRID	Fresno Irrigation District	714,862	566,934	438,187

GAWD	Garfield Water District	3,492	4,330	n/a
GFWD	Gravelly Ford Water District	30,027	23,709	n/a
HVID	Hills Valley Irrigation District	10,757	6,310	8,086
INWD	International Irrigation District	1,293	1,301	n/a
IVID	Ivanhoe Irrigation District	38,353	34,400	26,600
KTWD	Kern-Tulare Water District	45,650	10,839	28,363
LCWD	Lewis Creek Water District	1,442	1,451	n/a
LIID	Lindmore Irrigation District	76,990	61,124	158,551
LSID	Lindsay-Strathmore Irrigation District	29,991	34,899	77,004
LTID	Lower Tule River Irrigation District	404,555	302,365	310,029
LWSA	Lindsay, City of	2,487	2,499	n/a
MACO	Madera County	187	199	n/a
MAID	Madera Irrigation District	380,510	309,578	238,838
OCCY	Orange Cove City	1,386	1,398	n/a
OCID	Orange Cove Irrigation District	89,886	79,300	68,352
POID	Porterville Irrigation District	48,337	38,917	33,131
PXID	Pixley Irrigation District	245,990	114,191	204,609
RGWD	Rag Gulch Water District	18,858	6,626	10,376
SAID	Saucelito Irrigation District	55,993	45,207	44,681
SCID	Stone Corral Irrigation District	18,829	17,534	13,057
SSMD	So. San Joaquin Municipal Utility District	184,992	164,070	365,936
SWID	Shafter-Wasco Irrigation District	126,992	108,600	n/a
TBID	Terra Bella Irrigation District	36,728	24,853	62,206
TPWD	Tea Pot Dome Water District	7,993	9,366	7,844
TUCO	Tulare County	38,052	38,061	n/a
TUID	Tulare Irrigation District	206,990	248,800	175,721
TVWD	Tri-Valley Water District	5,783	5,792	n/a

RESULTS

Fixed Groundwater Pumping Costs vs. Variable Groundwater Pumping Cost – Overall results

The results analysis compares the FPlow run (original groundwater pumping costs) to FPhigh (updated groundwater pumping costs based on new head data and equation 12, and then FPhigh to VP (variable groundwater pumping cost). A significant difference in pumping cost is found by comparing FPlow to FPhigh (Table 8) and the results analysis look at the impact of this difference in water supply operations. The second comparison looks at the results differences between maintaining the updated pumping cost fixed through the whole run time (FPhigh) and letting it vary according to fluctuations in head (VP)

Supply mix comparison between both runs appear in Tables 8 and 9. Supply sources available include contract water (Friant Kern canal deliveries class 1 and class 2) groundwater and other surface supplies (EXT). EXT is used for supply or groundwater recharge in wet periods. Values are in acre-feet/year, 73 year average.

Table 8 - Supply mix: Original pumping cost (FPLOW) vs. updated pumping cost (FPHIGH)

	FPLOW				FPHIGH			
	Class 1 (af/yr avg.)	Class 2 (af/yr avg.)	EXT (af/yr avg.)	GW (af/yr avg.)	Class 1 (af/yr avg.)	Class 2 (af/yr avg.)	EXT (af/yr avg.)	GW (af/yr avg.)
AEWD	0	98,467	39,461	139,725	0	98,467	39,461	139,725
CHWD	7,936	56,321	36,828	107,016	7,854	56,196	36,828	107,190
DEID	62,822	26,118	0	55,507	93,056	26,118	0	19,880
EXID	4,147	6,869	0	23,581	3,962	6,869	0	23,766
FC18	144	0	0	0	144	0	0	0
FRCO	925	0	0	0	925	0	0	0
FRCY	57,499	0	0	0	57,499	0	0	0
FRID	1,144	27,045	345,738	204,700	452	27,045	345,738	204,700
GAWD	3,357	0	0	0	3,357	0	0	0
GFWD	0	4,484	0	13,511	0	4,484	0	13,511
HVID	0	0	0	6,310	3	0	0	6,307
INWD	1,151	0	0	0	1,151	0	0	0
IVID	0	2,858	4,800	26,742	19	2,858	4,800	26,723
KTWD	0	0	9,509	0	0	0	9,509	0
LCWD	1,386	0	0	0	1,386	0	0	0
LIID	6,563	7,960	0	46,601	31,624	7,960	0	20,252
LSID	26,366	0	0	3,096	26,371	0	0	1,245
LTID	23,225	80,502	65,579	144,208	54,659	80,502	67,721	97,434
LWSA	2,351	0	0	0	2,351	0	0	0
MACO	199	0	0	0	199	0	0	0
MAID	4,077	67,073	45,686	200,420	3,526	67,073	45,686	200,971
OCCY	1,340	0	0	0	1,340	0	0	0
OCID	4,000	0	0	75,300	4,049	0	0	75,251
POID	1,091	7,052	18,957	14,639	7,952	7,052	21,162	6,478
PXID	0	0	17,267	101,400	3	0	12,857	103,801
RGWD	3,472	0	0	3,084	4,091	0	0	1,542
SAID	2,707	11,843	0	30,656	19,014	11,843	0	13,396
SCID	2,900	0	0	14,634	2,907	0	0	14,627
SSMD	46,009	18,088	0	99,896	46,061	18,088	0	99,844
SWID	47,916	14,313	0	38,107	47,916	14,313	0	38,217
TBID	8,368	0	0	16,480	24,312	0	0	454
TPWD	3,664	0	0	5,696	7,192	0	0	1,998
TUCO	933	0	0	0	933	0	0	0
TUID	24,266	50,845	109,333	39,709	24,266	50,845	109,333	39,709
TVWD	304	0	0	0	304	0	0	0
Total	**350,262**	**479,838**	**693,158**	**1,411,018**	**478,878**	**479,713**	**693,095**	**1,257,021**

The increase in groundwater cost from FPlow to FPhigh reduces the groundwater supply as seen in Table 4.1 (irrigation districts in red are the ones modeled with updated groundwater cost from FPlow to FPhigh). All modeled districts reduce groundwater pumping over 50% (with the exception of LTID, 32%). Terra Bella irrigation district (TBID) presents a reduction of 97% in groundwater pumping as the cost is updated from $45/af in FPlow to $117/af in FPhigh. This operation is followed by an increase in Class 1 TBID water supply from 8.4 kaf/yr to 24.3 kaf/yr, on average, to make up for the difference.

The effects of groundwater cost changes ripple over other surface operations. The next least expensive supply source is other surface, non-contract water (EXT). Irrigation districts with higher crop values will switch to other surface supplies reducing their availability to other districts. For example, Porterville Irrigation District (POID) and Lower Tule River Irrigation District (LTID) reduce groundwater pumping by 56% and 32% respectively and increase Class 1 and other surface supplies (in this case, from Tule River) to compensate. This increase in withdrawals from Tule River affects Pixley Irrigation District (PXID), which has its supply from Tule River reduced from 17.3 kaf/yr to 12.8 kaf/yr, average.

Table 9 - Supply mix: updated pumping cost (FPhigh) vs. variable pumping cost (VP)

	FPhigh				**VP**			
	Class 1 (af/yr avg.)	**Class 2** (af/yr avg.)	**EXT** (af/yr avg.)	**GW** (af/yr avg.)	**Class 1** (af/yr avg.)	**Class 2** (af/yr avg.)	**EXT** (af/yr avg.)	**GW** (af/yr avg.)
AEWD	0	98,467	39,461	139,725	0	98,467	39,461	139,725
CHWD	7,854	56,196	36,828	107,190	7,670	56,131	36,828	107,343
DEID	93,056	26,118	0	19,880	93,262	26,118	0	19,673
EXID	3,962	6,869	0	23,766	3,939	6,869	0	23,773
FC18	144	0	0	0	144	0	0	0
FRCO	925	0	0	0	925	0	0	0
FRCY	57,499	0	0	0	57,499	0	0	0
FRID	452	27,045	345,738	204,700	452	27,045	345,738	204,700
GAWD	3,357	0	0	0	3,357	0	0	0
GFWD	0	4,484	0	13,511	0	4,484	0	13,511
HVID	3	0	0	6,307	3	0	0	6,307
INWD	1,151	0	0	0	1,151	0	0	0
IVID	19	2,858	4,800	26,723	10	2,858	4,800	26,732
KTWD	0	0	9,509	0	0	0	9,509	0
LCWD	1,386	0	0	0	1,385	0	0	0
LIID	31,624	7,960	0	20,252	31,624	7,960	0	20,252
LSID	26,371	0	0	1,245	26,371	0	0	1,245
LTID	54,659	80,502	67,721	97,434	53,926	80,504	64,260	99,657
LWSA	2,351	0	0	0	2,351	0	0	0
MACO	199	0	0	0	199	0	0	0
MAID	3,526	67,073	45,686	200,971	3,529	67,073	45,686	200,934
OCCY	1,340	0	0	0	1,340	0	0	0
OCID	4,049	0	0	75,251	4,020	0	0	75,251
POID	7,952	7,052	21,162	6,478	7,965	7,050	21,699	6,707
PXID	3	0	12,857	103,801	9,102	0	15,883	92,334
RGWD	4,091	0	0	1,542	4,091	0	0	1,542
SAID	19,014	11,843	0	13,396	19,014	11,843	0	13,396
SCID	2,907	0	0	14,627	2,884	0	0	14,627
SSMD	46,061	18,088	0	99,844	45,940	18,088	0	99,844
SWID	47,916	14,313	0	38,217	47,916	14,313	0	38,217
TBID	24,312	0	0	454	24,312	0	0	454
TPWD	7,192	0	0	1,998	7,192	0	0	1,998
TUCO	933	0	0	0	933	0	0	0
TUID	24,266	50,845	109,333	39,709	24,240	50,845	109,333	39,734
TVWD	304	0	0	0	304	0	0	0
Total	**478,878**	**479,713**	**693,095**	**1,257,021**	**487,050**	**479,648**	**693,197**	**1,247,956**

Some small changes are verified by comparing run FPhigh to variable pumping cost VP (Table 9), mostly on irrigation districts with intense groundwater use (e.g. PXID). Groundwater pumping cost for Pixley increases from $45/af in the first month to $111/af in the last month of the 73 years run, resulting in reduction of amount pumped of approximately 11%. Class 1 and other surface supplies are increased to substitute the groundwater.

As groundwater costs increase, irrigation districts switch to other cheaper supply sources to maximize revenue and avoid scarcity. When groundwater costs start at a higher value than other surface supply sources, further increase will have little effect on pumping until the pumping cost exceeds that the district's willingness to pay for additional water. Since class 1 and class 2 water are limited by contract amounts (i.e. the districts can not trade water among themselves) the system's flexibility to cope with increase in groundwater costs by switching to other surface water supplies is also limited. Tables 10 and 11 present overall results for the whole project area and for the districts subject to variable groundwater pumping cost respectively. The results compared are from the FPlow run (original groundwater pumping costs) and VP (variable pumping costs). Numbers presented are 73-year averages.

Table 10 - Overall average results – all FRIANT contractors

	Variable pmp cost **FPlow run**		Fixed pmp cost **VP run**	
Totals (taf/yr avg)		% Total		% Total
Demand	2,984	100.0%	2,984	100.0%
Total Supply	2,891	96.9%	2,865	96.0%
Scarcity	93	3.1%	119	4.0%
Total Supply	2,891	100.0%	2,865	100.0%
Surface contract supply	867	30.0%	1,004	35.0%
Surface other supply[1]	613	21.2%	613	21.4%
GW supply	1,411	48.8%	1,248	43.6%

[1]Excluding artificial recharge

Effects of increased groundwater pumping costs include substitution of groundwater for contract water and increase in scarcity in VP run. Of the 163 taf/yr average reduction in groundwater supply, 137 taf is replaced by contract water (Table 10), the remaining 26 taf accounting for increase in scarcity. This reflects the region's capability in accommodating for some changes in operating policy. Economic penalties associated with the supply change are investigated in the scarcity costs section. Advantages of the groundwater/surface water operating policy in run VP includes less aquifer overdraft and related problems. Groundwater storage is analyzed is further detail in the next section.

Table 11 - Overall results – GW modeled FRIANT contractors[1]

	Fixed pmp cost **FPlow run**		Variable pmp cost **VP run**	
Totals (taf/yr avg)		% Total		% Total
Demand	794	100.0%	794	100.0%
Total Supply	786	99.0%	760	95.7%
Scarcity	9	1.1%	34	4.3%
Total Supply (taf/yr avg)	786	100.0%	760	100.0%
Surface contract supply	272	34.6%	410	53.9%
Surface other supply[2]	93	11.8%	93	12.2%
GW supply	421	53.6%	257	33.8%

[1]See table 2.3
[2]Excluding artificial recharge

Groundwater operations

Most irrigation districts face increasing groundwater pumping costs, once groundwater is a significant portion of the supply and intensive groundwater pumping is present during the 73 years run period.

Differences in groundwater pumping from FPlow run (fixed original groundwater pumping costs) to FPhigh (fixed updated groundwater pumping costs) are significant due to the difference in cost but as we move from FPhigh to the variable pumping cost run VP differences in pumping are limited to irrigation districts highly dependent on groundwater supply (Pixley ID). Time series of annual average pumping appear in Figure 6. In very dry years the differences among the three runs are smaller as surface supply is limited and the irrigation districts turn to groundwater to avoid scarcity costs. In wet years the higher price of groundwater in runs FPHIGH and VP results in districts switching supply to less expensive surface water available.

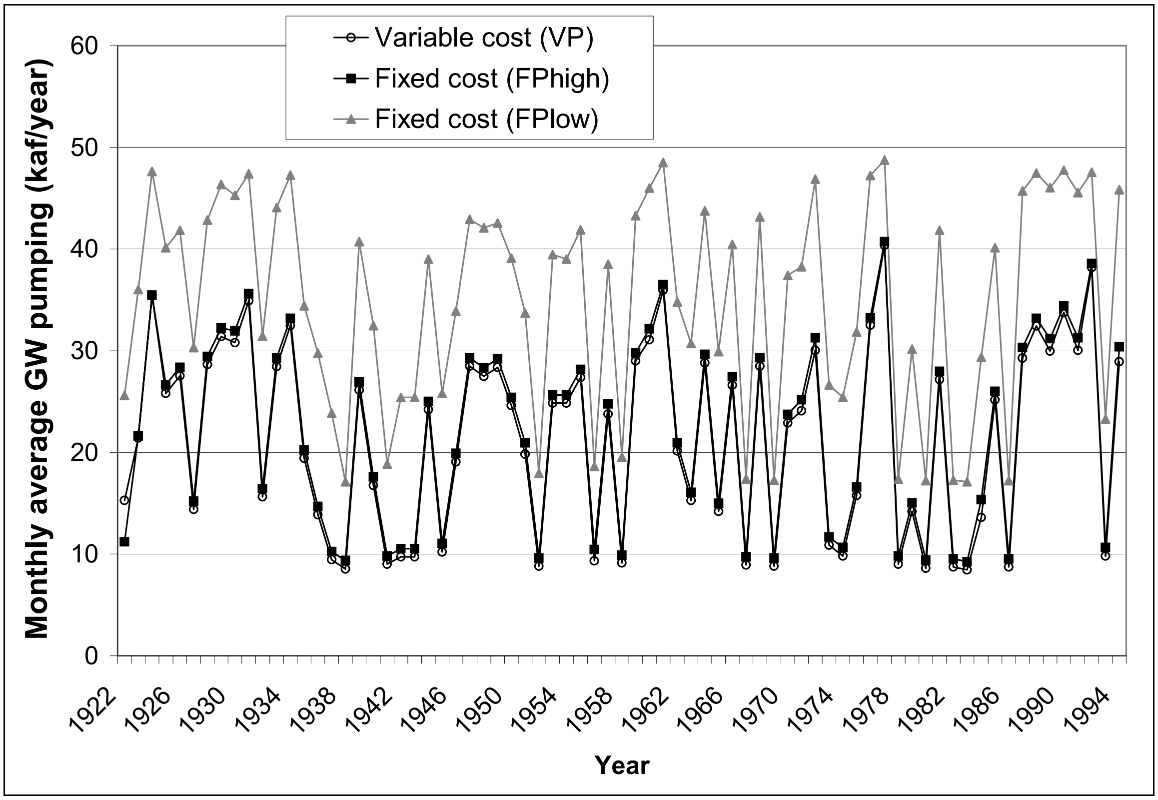

Figure 6 - Monthly average GW pumping total for modeled districts[1]

In the variable pumping cost run (VP) the gradual increase in pumping costs produces further reductions in pumping, but Pixley ID is basically the only irrigation district affected. Overall, short period, seasonal, variations in pumping cost do not affect pumping.

Groundwater pumping in Pixley is reduced in the months of March and April and replaced by class 1 water. As the months get drier (i.e., May, June, July) class 1 water availability is reduced and Pixley resorts to groundwater pumping to match demand. With fixed pumping cost, variations in groundwater pumping are driven by surface water availability. With pumping cost varying, a second factor is introduced and some change is perceived in the pumping pattern (Figure 7). Faster increases in cost during dry years reduces pumping in VP, as opposed to a more variable pumping pattern in the fixed pumping cost run FPhigh.

Since Pixley is willing to pay $125/af of water for the last portion of supply, according to its economic function, and pumping costs increase up to $109/af there is no cutback in GW pumping due to scarcity in VP run compared to FPhigh run. Although the irrigation district faces decreases in net revenue as the water cost increases, it is still economically attractive to use groundwater supply at the margin. This explains partially the relative unresponsive pattern of groundwater pumping to fluctuations in pumping cost. The other factor leading to the lack of response to pumping costs is surface water operations. The limited availability of surface water (at a lower cost than groundwater) and the non-representation of inter-district transfers limits districts to resort to groundwater pumping when surface water (contract water plus local sources) is not enough, while in practice surface water could be purchased from other districts.

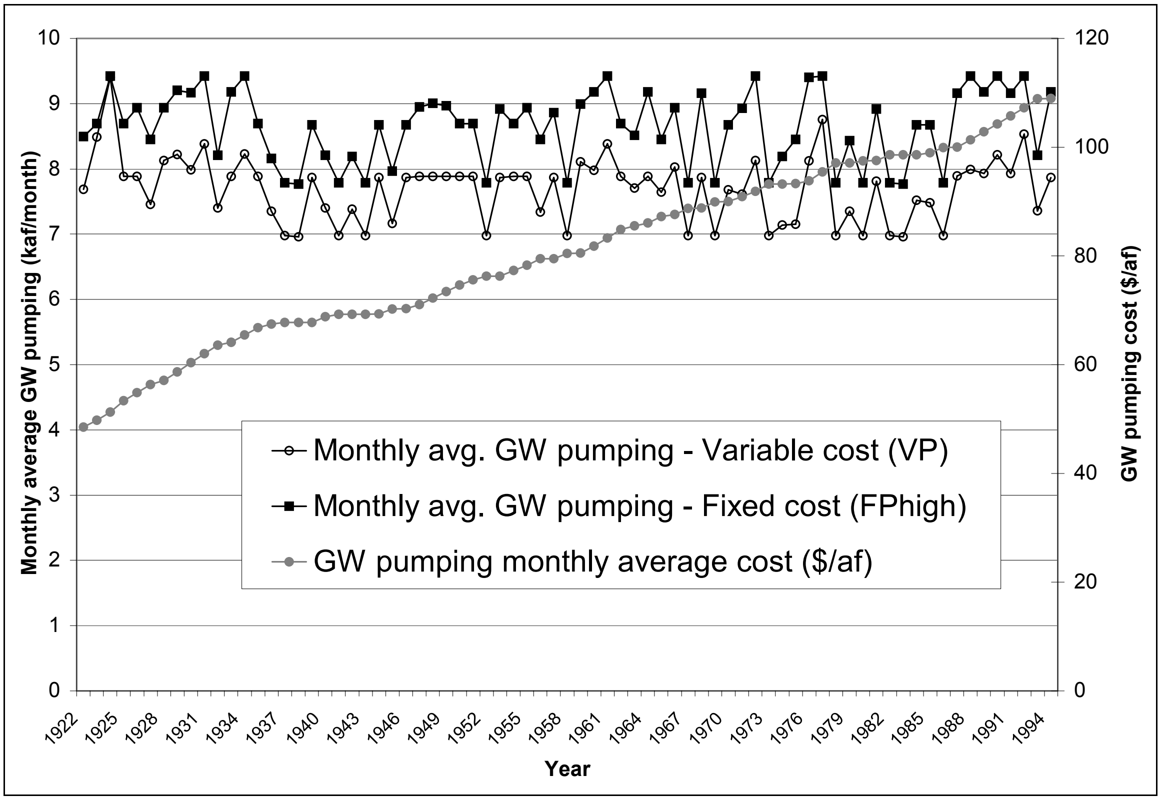

Figure 7 - Groundwater pumping in Pixley (PXID) irrigation district

Groundwater heads and pumping cost

In the first 20 years of simulation groundwater heads are mostly dominated by subsurface flows moving towards equilibrium from the initial heads. This is a limitation of the present approach where there is no detailed representation of lags in the system. Subsurface flows are lagged by one month. The consequence is the steeper initial portion of the pumping cost curves. Irrigation districts depending most on groundwater basins with lower initial water tables (e.g., LTID) face an initial period of declining costs as water table in their main groundwater supply basins rise to equilibrium with neighbor groundwater basins.

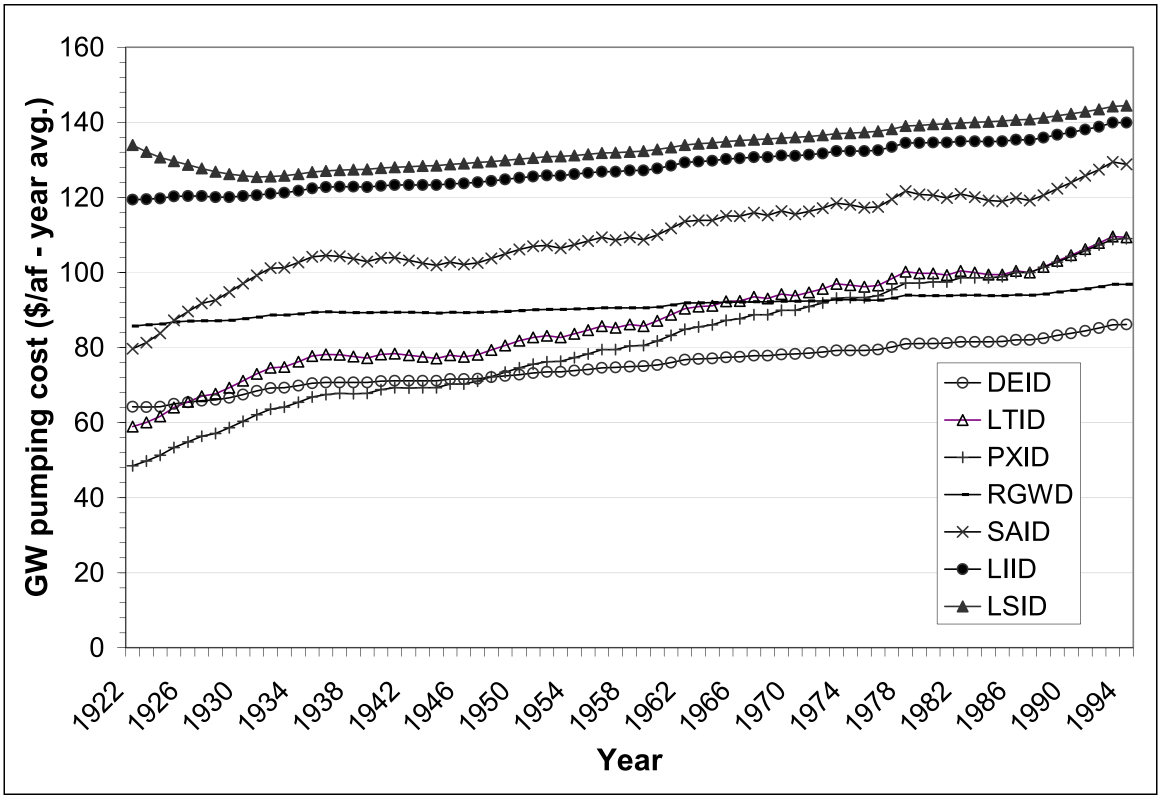

Figure 8 - Year average groundwater pumping costs

After the initial 20 years of simulation heads are mostly driven by groundwater pumping. The steep section during the drought years from 1987 to 1992 in Figure 8 for Pixley ID is paired with a sequence of years of continuous high volume pumping, driving the groundwater pumping costs up.

Irrigation districts share groundwater supply and are affected by neighbor districts operations. This is particularly true for POID where groundwater pumping accounts for a small part of the total withdrawal on its main groundwater supply, site GW12. Other irrigation districts withdrawing groundwater from GW12 are Lower Tule River ID (LTID), Lindmore ID (LIID), Lindsay Strathmore ID (LSID), Delano Earlimart ID (DEID), Kern Tulare Water District (KTWD) and Ragh Gulch Water District (RGWD). Figure 9 presents the time series of pumping heads[1] and respective pumping costs for groundwater site GW12 including the droughts of 1976-1977 and 1987-1992. The intensive pumping during 1976-1977 drives the heads from around 528 ft to 536 ft. After that, the sequence of wet years until 1988 results in a stable/slight increase in pumping heads and cost until just before 1987, where a long dry period starts. The stepwise pattern of head increase reflects the monthly pumping pattern, with the flat section from September to May, and the "jump" carrying the effect of the concentrated pumping from July through August (Figure 9).

[1] The term pumping *head* refers to the distance between the water table and the ground level, i.e., the higher the head, the higher the pumping cost.

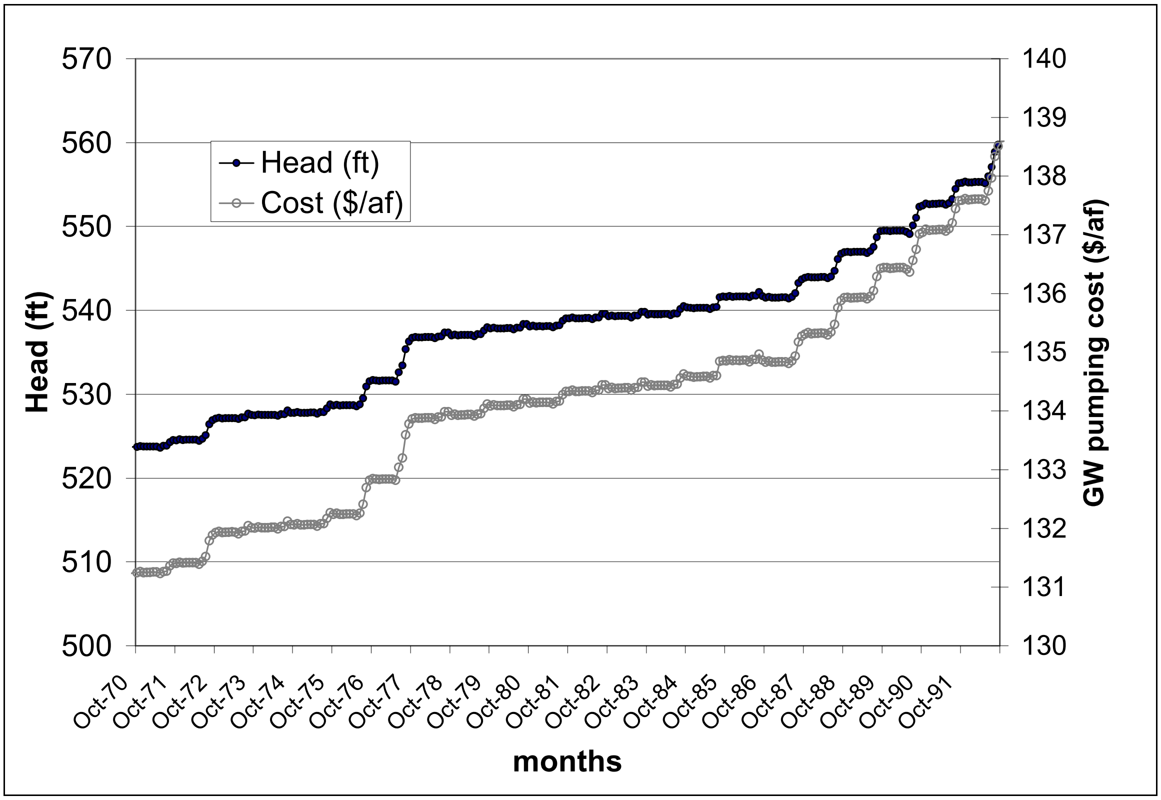

Figure 9 - Groundwater site GW12 heads and pumping costs for 1970-1991

Groundwater pumping infrastructure capacity is based on historic pumping in dry periods (1976-1977 drought). Although the escalating groundwater operating costs in the VP run reduce the pressure on the infrastructure, the upper bounds on pumping capacity are still being reached in some irrigation districts indicating there is a positive marginal value in expanding it. Irrigation districts with binding groundwater pumping capacity include Saucelito ID (SAID), Lindsay Strathmore ID (LSID), Rag Gulch WD (RGWD), Delano Earlimart ID (DEID), Lindsay ID (LIID), Terra Bela ID (TBID), Tea Pot Dome WD (TPWD) and Lower Tule River ID (LTID).

Groundwater Storage

Reduced groundwater pumping results in an end-of-period (EOP) storage increase of about 34% from FPlow to FPhigh run, and of 1.6% from FPhigh to the variable pumping VP run, over the 73-year simulation period (Figure 10). The small difference in storages between FPhigh run and VP run reflect the lack of response in groundwater pumping to variations in pumping cost, given economic conditions and the relative prices of groundwater compared to surface water.

The cost of this reduction in aquifer overdraft is an increase in the average annual scarcity from 8 taf to 34 taf for the eleven irrigation districts modeled with variable pumping cost (Table 3). Relative to the target demands (full supply), this represents an increase in scarcity from 1% to 4%.

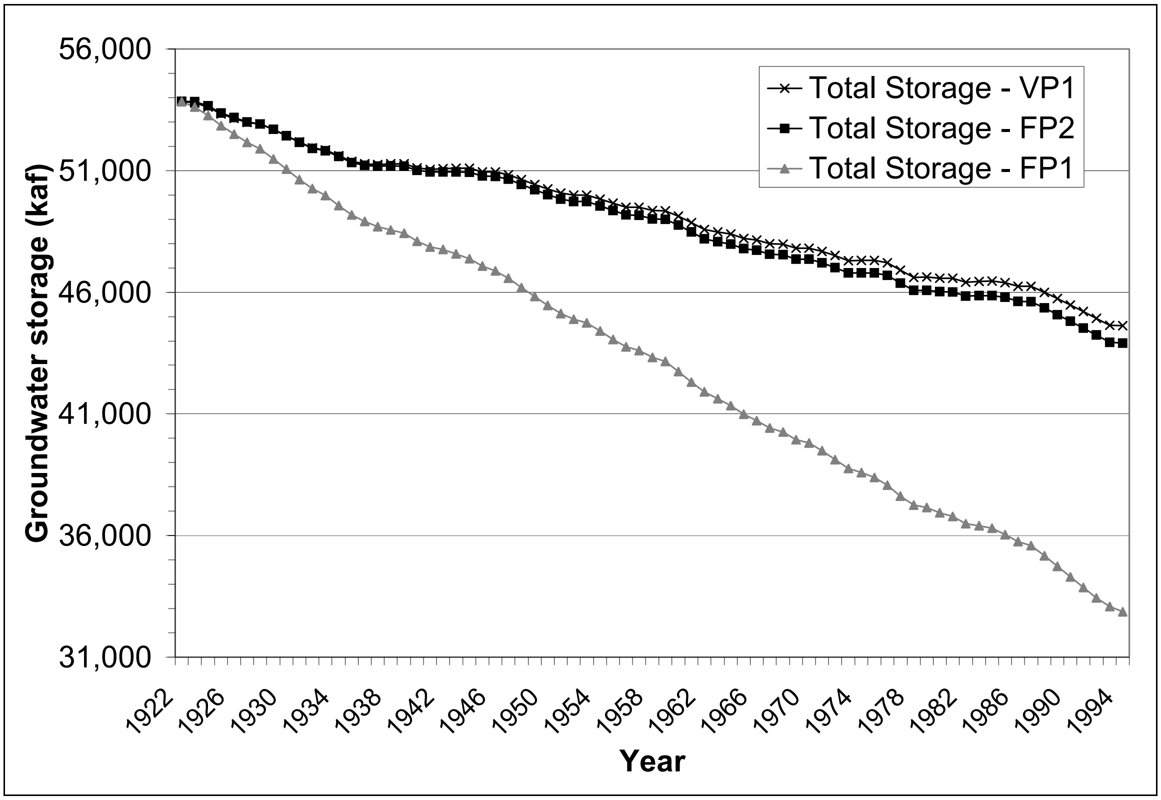

Figure 10 - Groundwater storage

Additional benefits from total operating costs also must be considered. As pumping costs increase and groundwater use is reduced the total groundwater operating cost decreases, and scarcity cost increases. When properly calibrated, model will allow examination of trade-offs in overdraft against increases in scarcity and evaluate potential for improvement in regional water management operations and policies. Groundwater and surface water operations can be changed by varying surface contract water price, or subsidizing energy costs to change groundwater pumping cost. The model will help to evaluate the costs and benefits of such changes.

<u>Surface Water Operations</u>

When groundwater pumping costs increase irrigation districts may look at alternative supplies to reduce operating and scarcity costs. Changes in external surface supply (EXT) are verified and water is reallocated based on its economic value. For example, Porterville ID (POID), Lower Tule River ID (LTID) and Pixley ID (PXID) share surface supply from the Tule River, with VP run results appearing in Figure 11 for the 1987-1992 drought. Water has the highest marginal value for Porterville ID. Whenever surface supply is available from Tule River, POID will take priority unless its target demand has already been met, or the delivery infrastructure reaches its capacity (4.6 taf/month). Due to the high pumping cost, groundwater is used only during the dry months, when there is not enough surface supply. The upper bound for Tule River delivery infrastructure is often reached for Porterville and Pixley irrigation districts, indicating potential benefits for expanding its capacity.

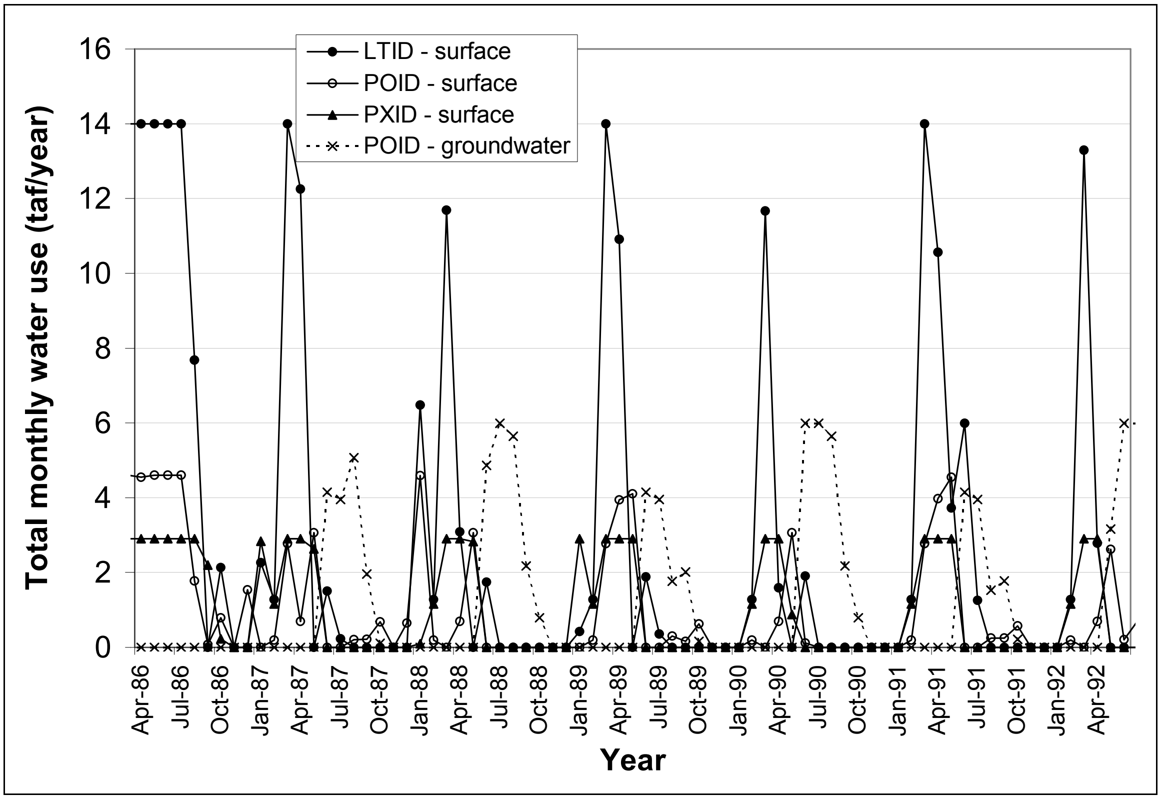

Figure 11 - Tule River supply for 1987-1992 drought – VP run

Scarcity Costs

Irrigation districts face scarcity as water costs increase beyond their willingness to pay. The economic loss associated with these scarcities is based on foregone benefits from supply cutbacks. Since willingness to pay for additional water is higher with lower supply levels, the total economic loss, or penalty, depends not only on the cutback itself, but also on the level of supply being applied.

Total annual scarcities are plotted in Figure 12 for 73-year period. During dry years the difference between FPlow and VP runs is higher, reflecting the economic impact of high pumping costs when surface water is limited. Differences from FPhigh and VP run are virtually inexistent.

The lower groundwater pumping cost run (FPlow) results in 21 maf of total overdraft over 73 years and a $19 million/yr average penalty in scarcity costs. Avoiding this overdraft would require reducing groundwater pumping by either cutting back in production or acquiring supplemental non-local surface supplies averaging 288 kaf/yr. The groundwater pumping curtailment seen in VP run could reduce the overdraft to 9.2 maf at a cost of $24 million/yr in scarcity costs, if no supplemental surface supply is available. To eliminate the 9.2 maf overdraft 126 kaf/yr average of supplemental surface supplies would be needed.

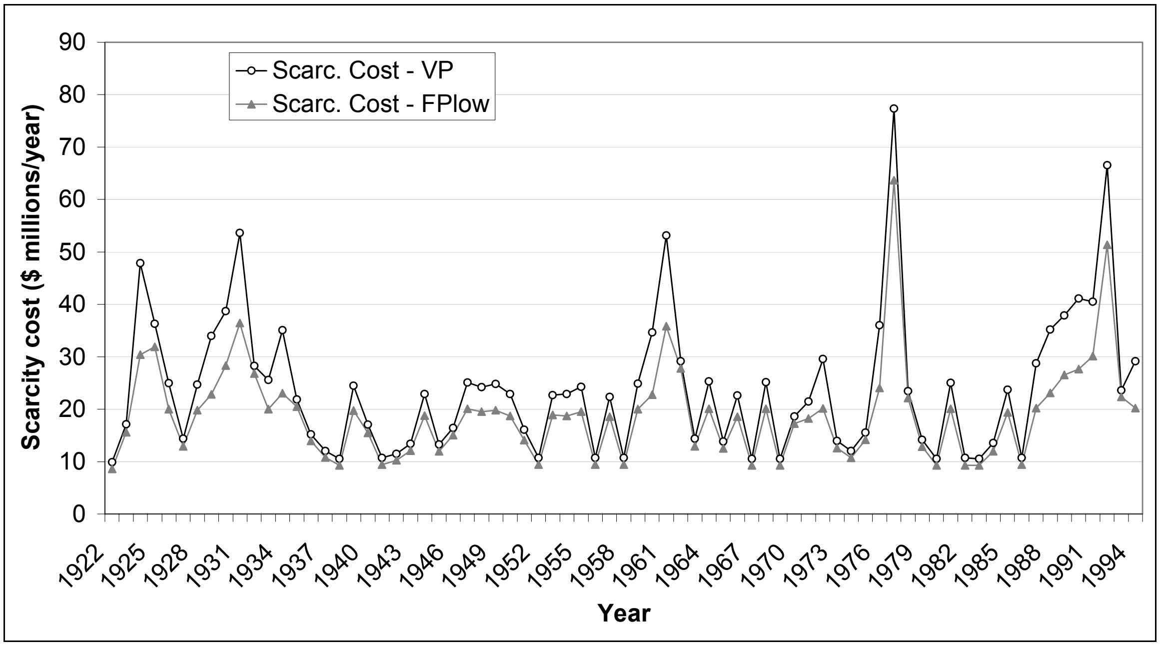

Figure 12 - Annual scarcity costs

<u>Policy study</u>

Friant users adopt conjunctive use operations extensively to increase water availability and flexibility in its use. These operations include artificial recharge through infiltration ponds and natural streams, and groundwater pumping (Naugle, 2001; ARVIN EDISON, 2000a, 2000b). Although not all of those operations are modeled in detail in the present study, some reactions of the system to possible management policies can be evaluated using the simulation model presented. Policies such as energy price changes and surface water price chances can affect conjunctive use operations by altering the balance between surface water and groundwater use. The policies analyzed here include variation of surface water prices and variation of energy cost. The model version used is the variable groundwater pumping cost and for easier understanding of the impacts, only the Friant contractors modeled with variable groundwater cost are included in the analysis.

Surface water price change

Class 1 and Class 2 water are the most important components of surface water supply to contractors and changes in their price are expected to affect the relative value of groundwater, change pumping patterns, operating costs and end-of-period groundwater storage. Contract water prices have been increased in the past due to increasing operation and maintenance costs (LEU, 2000); and notably after CVPIA act in 1992, for environmental regulation. To simulate the effects of surface water price changes in the Friant system, a few runs were made with prices listed in Table 12.

Table 12 - Changes in contract water price

Run	Class 1 price ($/af)	Class 2 price ($/af)
P1	24	14
P	44	34
P2	54	44
P3	64	54
P4	84	74
P5	104	94
P6	124	114
P7	144	134
P8	174	164
P9	204	194

Increase in surface water prices results in users switching to groundwater use and intensifying aquifer overdraft. This effect accumulates and is felt in later years where the volumes pumped actually drop when groundwater becomes too expensive. Higher surface water prices cause higher groundwater pumping in the first years. At the highest surface water prices the aquifer is so intensely exploited in the first years that groundwater pumping declines after 1961 and is pumped in much less quantity during the 1976-1977 drought compared to scenarios with lower surface water price (Figure 13). At this high surface water price there is a large economic impact and drought conjunctive use operations are compromised.

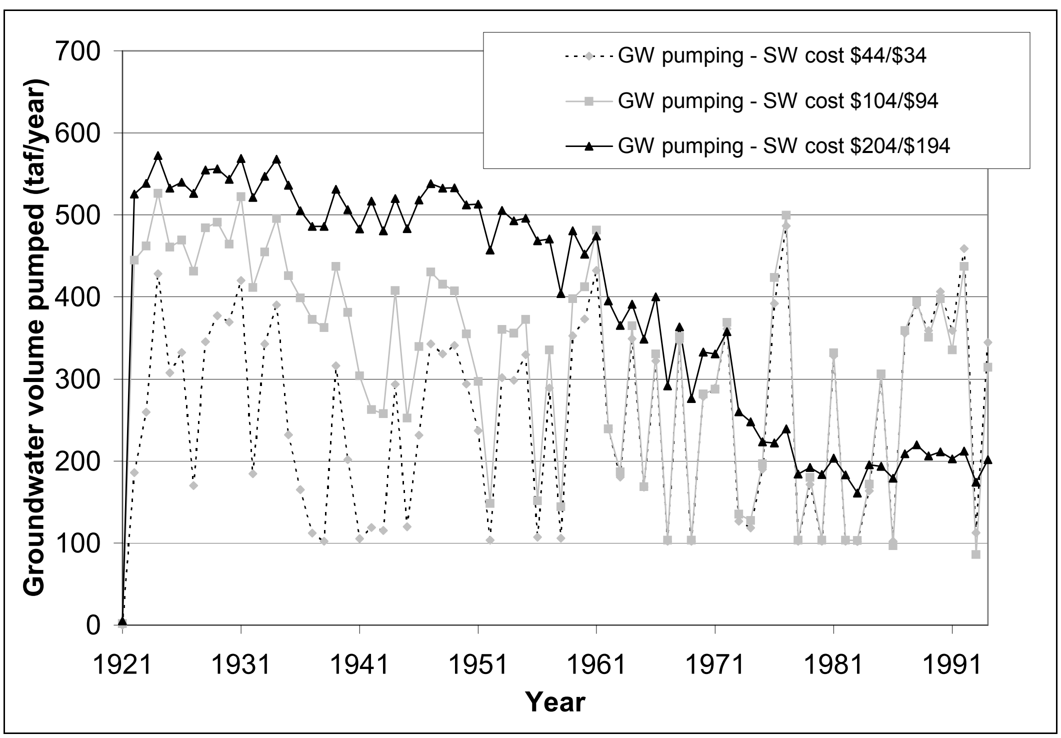

Figure 13- Groundwater pumping under different scenarios of surface water pricing

Economic impact appears in Figure 14 (scarcity costs related to surface water prices and End-of-Period overdraft). Reduction of supply options caused by significant increase in surface water prices leads to penalties over $35 million/year with severe overdraft conditions in parts of the system.

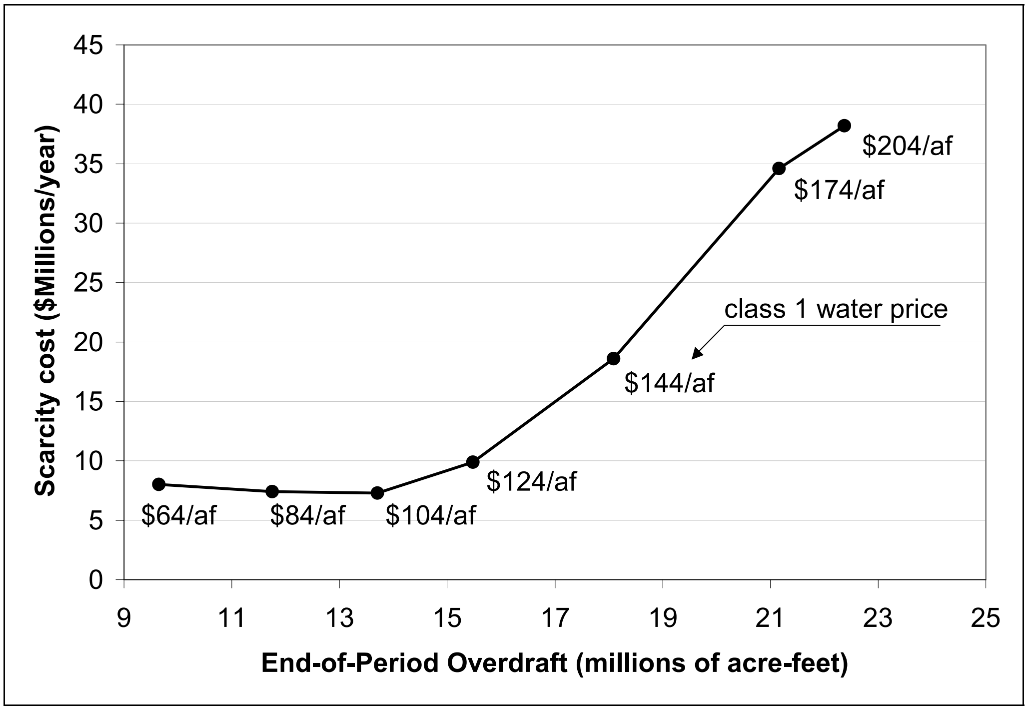

Figure 14 - End-of-Period overdraft and scarcity costs

Figures 15 and 16 present end-of-period (EOP) groundwater storage for the variable head modeled groundwater reservoirs and different contract Friant water. EOP starts being strongly affected when surface water costs surpasses the groundwater pumping cost and groundwater pumping starts replacing surface water. Groundwater basins exploited by irrigation districts with higher value crops and high demand are susceptible to higher overdraft impact. The largest groundwater reservoir considered, GW10, has its withdrawn water split between the Lower Tule River (LTID) and Pixley (PXID). Lower Tule has the highest groundwater demand, while Pixley has the highest percentage of total supply as groundwater. The result is the noticeable reduction in EOP storage in GW10 as soon as surface water price for Class 1 goes over $64/af.

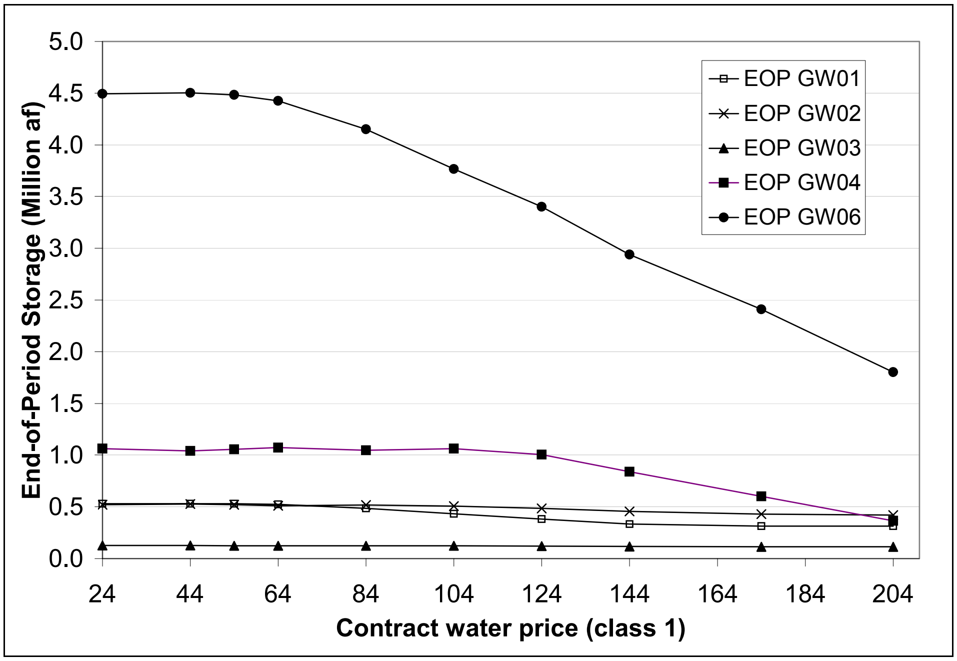

Figure 15 - EOP groundwater storage for varying surface water price

GW06 is shared by most districts and suffers a high overdraft impact as surface water price increases, with EOP storage dropping to half in the last run. GW04 suffers about the same reduction but it is not until the surface water price surpasses $124/af that a noticeable reduction in the EOP groundwater storage occurs. Most of the water in GW04 is used by Lindsay Strathmore (LSID) and Lindmore (LIID) irrigation districts with high value crops.

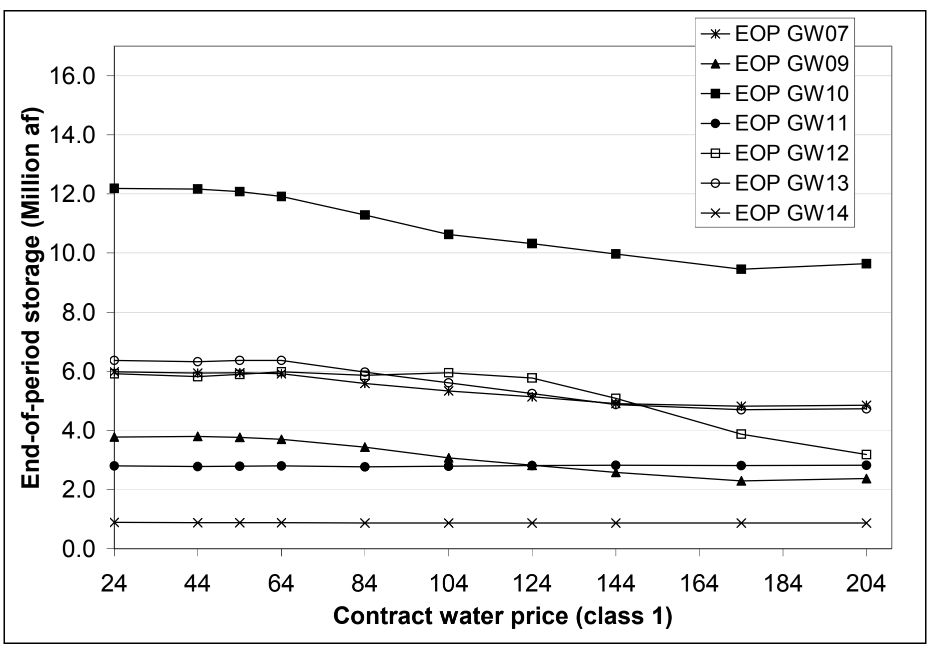

Figure 16 - EOP groundwater storage for varying surface water price

The impact of increases in surface water costs is high in scarcity and scarcity costs, but some distortions on the model behavior are also apparent. For increases in contract water up to $109/af class 1 and $94/af class 2 the scarcities actually are reduced for some districts (Tables 13 and 14). In a lower contract water price scenario, it will be prioritized over groundwater (if it costs less) and used whenever there is demand. During the drier, high demand months, the district will not have enough contract water available and resorts to groundwater, sometimes reaching the pumping capacity and facing scarcity. As the contract water price increases, groundwater will be prioritized (if it costs less) replacing contract water in early months (March-April). This contract water "saved" will be available during the dry months, when the pumping capacity is reached. the result is a lower scarcity.

Table 13 - Scarcity levels

		Scarcity level (taf/year)									
Friant contractor	C2/C1 Price ($/af)	14/ 24	34/ 44	44/ 54	54/ 64	74/ 84	94/ 104	114/ 124	134/ 144	164/ 174	194/ 204
Delano-Earlimart	DEID	5.7	6.3	6.3	5.2	3.8	2.1	13.9	35.6	47.0	47.7
Kern-Tulare WD	KTWD	1.3	1.3	1.3	1.3	1.3	1.3	1.3	1.3	1.3	1.3
Lindmore	LIID	1.2	1.3	1.3	1.3	1.3	1.3	0.9	1.5	12.3	14.3
Lindsay-Strathmore	LSID	7.3	7.3	7.3	7.3	7.3	7.3	7.2	6.6	5.8	10.0
Lower Tule River	LTID	14.8	14.9	13.4	12.0	9.9	9.3	14.2	46.4	106.9	112.5
Pixley	PXID	0.0	0.0	0.0	0.0	0.0	1.4	6.5	11.8	15.5	15.9
Porterville	POID	0.2	0.3	0.2	0.2	0.2	0.2	0.1	0.7	5.9	7.0
Rag Gulch	RGWD	1.0	1.0	0.9	0.9	0.9	0.9	0.5	0.2	0.1	0.1
Saucelito	SAID	0.9	1.0	1.0	1.0	0.9	1.3	2.7	5.3	14.1	20.6
Tea Pot Dome	TPWD	0.2	0.2	0.2	0.2	0.2	0.2	0.1	0.0	0.0	0.0
Terra Bella	TBID	0.1	0.1	0.1	0.1	0.1	0.1	0.1	2.6	6.6	6.6
Total (taf/yr)		**32.7**	**33.6**	**31.9**	**29.4**	**25.8**	**25.2**	**47.7**	**112.2**	**215.4**	**236.0**
Total all contractors (tafyr)		**142**	**119**	**97**	**105**	**152**	**192**	**254**	**340**	**454**	**476**

MODSIM is run as a simulation tool and does not optimize water use across time (i.e., the model has zero foresight even within an irrigation season). Farmer's actual decisions are based in some foresight, given forecasts and knowledge of water availability for coming months. Factors like groundwater pumping capacity and surface water availability are coordinated across months, so lower scarcity at the higher contract water price scenarios is highly improbable. Thus, increases in contract water price are expected to increase scarcity and scarcity costs, contrary to what the model presents for cost increases up to $94/$104.

For further increase in contract water prices, the model's behavior is coherent and scarcity and scarcity costs go up in total values. However, irrigation districts with high groundwater pumping costs and very high crop value continue to present distorted behavior for almost all scenarios, e.g., TPWD, LIID, LSID.

A possible improvement to correct this issue is to develop value functions for contract water use to capture the benefit of seasonal use, so the model can evaluate the trade-offs between paying more per af to start using groundwater earlier (if it is more expensive than surface water) and having more contract water available during high demand, very dry months.

Table 14 - Scarcity costs – year average

Friant contractor	C1/C2 Price Scenarios ($/af)	Scarcity cost ($1,000/year) 14/ 24	34/ 44	44/ 54	54/ 64	74/ 84	94/ 104	114/ 124	134/ 144	164/ 174	194/ 204
Delano-Earlimart	DEID	928	1062	1062	870	626	342	1782	4826	6880	7010
Kern-Tulare WD	KTWD	669	669	669	669	669	669	669	669	669	669
Lindmore	LIID	204	215	215	215	215	215	152	255	2082	2469
Lindsay-Strathmore	LSID	3747	3750	3750	3750	3750	3750	3696	3411	2022	2372
Lower Tule River	LTID	2044	2060	1846	1664	1369	1278	1958	6429	16375	17368
Pixley	PXID	0	0	0	0	0	179	877	1606	2141	2197
Porterville	POID	37	44	34	31	31	24	21	111	951	1153
Rag Gulch	RGWD	557	569	541	523	523	520	304	97	45	41
Saucelito	SAID	136	144	144	144	134	202	406	820	2333	3819
Tea Pot Dome	TPWD	70	71	71	71	71	71	46	15	6	2
Terra Bella	TBID	17	18	18	18	18	18	18	401	1108	1134
Total ($million/yr)		**8.4**	**8.6**	**8.4**	**8.0**	**7.4**	**7.3**	**9.9**	**18.6**	**34.6**	**38.2**
Total all contractors ($million/yr)		**26.2**	**24.0**	**21.8**	**22.1**	**25.6**	**29.4**	**36.7**	**48.2**	**65.7**	**69.6**

Energy prices change

Given the high groundwater use in the system, a significant part of supply operating costs depends on energy consumption and is susceptible to changes in energy prices. Energy prices have increased from around $0.06/kwh in the early eighties to about $0.1/kwh at the present (AECA, 2002). In the other hand, some irrigation districts can implement programs to stabilize power costs like development of power plants, long-term power contracts, and shifting irrigation schedules to off-peak hours (FWUA /MWDSC,2001).
This section investigates some potential impacts in the Friant division from increase and reduction in energy costs. The impact is evaluated in terms of groundwater operating costs. Three energy cost scenarios are evaluated, 0.08$/kwh, 0.1$/kwh and 0.12$/kwh. The 0.1$/kwh is the cost used in all previous runs and model analysis so far. The model is presently capable of running with energy cost varying per Friant contractor and per month, if data is available to do so.

A reduction of 20% in energy cost, from $0.1/kwh to $0.08/kwh has a relatively small effect on pumping amounts, about 2% increase overall with Delano Earlimart (DEID) and Rag Gulch (RGWD) presenting the highest increases (approximately 4% and 6% respectively) (Table 15). The impact on operating costs is noticeably higher as expected, 17% overall reduction. The increase in the amount pumped is expected to lower the heads and as more energy is required to extract the same amount of water, part of the gains of pumping with cheaper energy are reduced.

Table 15 - Groundwater pumping and operating cost for energy cost scenarios

	Avg. GW pumping (taf/yr)			Avg, GW operating cost (k$/yr)		
Energy cost scenario	0.08$/kwh	0.1$/kwh	0.12$/kwh	0.08$/kwh	0.1$/kwh	0.12$/kwh
Contractor						
DEID	20,491	19,673	19,607	1,294	1,529	1,818
KTWD	0	0	0	0	0	0
LIID	20,252	20,252	19,829	2,051	2,552	2,979
LSID	1,245	1,245	1,245	133	166	198
LTID	103,937	99,657	98,926	7,015	8,261	9,806
POID	6,401	6,707	5,065	654	851	761
PXID	93,458	92,334	91,479	6,255	7,527	8,894
RGWD	1,641	1,542	1,542	145	174	208
SAID	13,396	13,396	12,994	1,191	1,468	1,693
TBID	454	454	357	48	60	56
TPWD	1,998	1,998	1,998	209	261	312
Totals	**263,273**	**257,258**	**253,042**	**18,996**	**22,849**	**26,726**

An increase of 20% in energy costs causes a similar effect in the opposite direction. The reduction in the amount pumped and the lower heads alleviate part of the impact on the operating costs.

Further effects on scarcity costs are presented in Table 16. Reducing energy cost from $0.1/kwh to $0.08/kwh does not result in significant changes but an increase to $0.12/kwh heavily affects irrigation districts where the demand is smaller and groundwater is a significant portion of the total district water supply. like Pixley (PXID) and Porterville (POID). Other districts with higher value crops such as Lindsay (LIID) and Lindsay Strathmore (LSID) face smaller or zero impacts.

Table 16 - Scarcity costs for energy cost scenarios

	Avg. Scarcity cost (k$/year)		
Energy cost scenario / Contractor	0.08$/kwh	0.1$/kwh	0.12$/kwh
DEID	1050.7	1062.2	1062.2
KTWD	669.2	669.2	669.2
LIID	215.0	215.0	283.8
LSID	3749.9	3749.9	3749.9
LTID	1792.1	2059.9	2173.6
PXID	0	0	65.3
POID	34.2	44.3	184.9
RGWD	533.9	568.9	568.9
SAID	143.6	143.6	203.5
TPWD	70.5	70.5	70.5
TBID	17.7	17.7	33.8
Total ($Millions/year)	**8.3**	**8.6**	**9.1**

LIMITATIONS

Model limitations are presented here. These limitations provide orientation for results interpretation and future model improvement.

Artificial Recharge

Artificial recharge is conducted in the region but information regarding infrastructure and operations is still lacking. According to Naugle (2001), significant amounts of water are recharged through diversion ditches and natural streams, whenever irrigation districts have access to surplus water.

Applied Water Demands and Evapotranspiration of Applied Water (ETAW)

ETAW and applied water (AW) are required input in SWAP model. The AW/ETAW ratio is used to determine the optimal investment in irrigation technology and the demand functions are based on AW data. ETAW data provided by UZWB is based on monthly calculations where shorter time intervals mismatches between evapotranspiration, precipitation and soil moisture content may result in discrepancies in effective precipitation calculations and underestimates of ETAW. A model with higher detail in the temporal discretization is required to improve this calculation. Presently, the California Department of Water Resources (DWR) is developing a model to simulate weather variables including ETo, ETc, effective precipitation and ETAW in a daily basis (SIMETAW model) that could be used to improve the economic functions of FREDSIM.

Model Hydrology

The simulation was extended to a 73 years period. The Friant deliveries class 1 and class 2 were correlated to inflows at Millerton Lake during the same period (1985-1994) and extended to the rest of Millerton inflow time series. A longer times series of Friant deliveries is necessary for a sound statistical correlation.

Limited area modeled with groundwater model

The response factors (conductance) used to estimate subsurface flows require a detailed groundwater model to be estimated. So far only a small portion of the project area, including 11 irrigation districts, is included in this detailed study. Remaining irrigation district operations affect the groundwater supplies and these impacts are not yet fully represented.

Lack of model foresight and risk aversion

As currently set, the model optimizes water allocation in a monthly time step where no value is put on future water demands. Farmers do make decisions considering seasonal variability in both demand and supplies, as well as infrastructure capacity and risk aversion. To overcome this limitation, value functions that incorporate potential future use benefits of inputs should be added to the model on groundwater and surface water storage. These functions will enable it to evaluate trade-offs between supply sources with different prices and different seasonal availabilities, and trade-offs of some beneficial uses, like artificial recharge.

CONCLUSIONS

A scheme of variable groundwater heads and pumping costs was implemented at this stage of FREDSIM development, along with new developed economic functions at the irrigation district level. The groundwater system behaves coherently with heads and costs responding to increases in pumping and reduction in storage. The initial portion of the simulation is dominated by subsurface flows indicating that additional adjustments are necessary in the lag representation and initial conditions. The new calculated pumping costs are considerably higher that the original costs used but overdraft conditions still seem to be present in most of the modeled area, although at much lower rates with the new costs. With more detailed representation of artificial recharge a better insight could be drawn from on overdraft, and management options such as surface water price change could be evaluated in addressing overdraft problems.

Results show that users change supply sources and quantities, and transfer water reacting to variations in water price, economic value and water availability. Changes in surface and groundwater prices affected operations produced small variations in overall pumping and groundwater storage, except for contractors relying on groundwater for most of their supply.

Reduction of historical overdraft requires reduction of groundwater pumping. In terms of surface water this is equivalent to 33% of contract surface supplies. Without additional surface supplies, a 49% reduction in overdraft (9.8 maf) would cost an additional $5 million/yr average in scarcity costs, a 26% increase.

The direct effect of surface water availability and prices on supply balance between surface and groundwater has consequences for management programs including conjunctive use operations. Intensive groundwater pumping under high surface water prices resulted in aggravated overdraft conditions limiting considerably groundwater supply in dry seasons and dry years. With high surface water prices, the efficacy of conjunctive use programs relying on alternation between recharge in wet periods and pumping on dry periods is reduced.

ETAW values used in the development of the economic functions are systematically smaller than results from other models indicating that the economic demands used may be underestimated. A more detailed model to simulate ETAW for different weather conditions is required for further improvement.

High spatial and temporal variability in groundwater pumping was found by processing data from the groundwater model for use in FREDSIM. This variability is included as a constraint in the simulation model to enable a better characterization of present conditions when the model optimizes the water allocation for a given time step.

REFERENCES

AECA - Agricultural Energy Consumers Association (2002). Online document. http://www.aecaonline.com/aeca.html

ARVIN-EDISON Water Storage District (2000a). 2000 Water Year Summary Report

ARVIN-EDISON Water Storage District (2000b). The Arvin-Edison Water Storage District Water Resources Management Program).

Belaieh, G.; Peralta, R.C.; Hughes, T.C. (1999). Simulation/Optimization Modeling for Water Resources Management. *Journal Of Water Resources Planning and Management.* V.125, n.3

Charbeneau, R.J. (2000). *Groundwater hydraulics and pollutant transport.* Prentice Hall, New Jersey

Fredericks, J.W.; Labadie, J.W.(1998). Decisions Support System for Conjunctive Stream-Aquifer Management. *Journal of Water Resources Planning and Management.* V.124, n.2

FWUA / MWDSC (2001). FRIANT/MWD PARTNERSHIP DRAFT TECHNICAL MEMORANDA - TASK 801-809

Harter, T. (2001). *Estimating Energy Use of Irrigation Wells from Regional Water Level Data*. Department of Land, Air, and Water Resources, University of California, Davis, CA

Labadie, J.W.(1995). MODSIM: River Basin Network Flow Model for Conjunctive Stream-Aquifer Management. *Program User Manual and Documentation.*

Leu, M. (2001). Economics-Driven Simulation of the Friant Division of the Central Valley Project, California. Master's Thesis presented to the department of Civil and Environmental Engineering, University of California, Davis.

Naugle, A.W.(2001). A Hydrologic Budget Model for the Tule Basin Area, Southeastern San Joaquin Valley, California. Master's Thesis presented to the department of Land, Air and Water Resources, University of California, Davis.

Ruud, N.; Harter, T.; Naugle, A.(2002). A Conjunctive Use Model for the Tule Groundwater Sub-Basin Area in the Southern-Eastern San Joaquin Valley, California. *Report*

Zhang, M.. (1993). Arc/INFO® GIS landuse map for Tulare County based on the 1985 landuse survey by the California Department of Water Resources, Doctoral Research, University of California, Davis.

APPENDICES

Appendix A1 – Groundwater Pumping Pattern

Groundwater supply scheme for irrigation districts with variable head and pumping cost calculation is presented in Table 17. Values represent percentages of total groundwater supply that a given irrigation district withdraw from each groundwater site it has access to. In some examples, such as LTID, significant variations are present along the year, supply from GW09 goes from 13% in October to 30% in march. Inclusion of this data is important to constrain the solver to a supply mix pattern that is consequence of other factors, like present location of pumping infrastructure. Since the pumping cost is attached to the GW sites, the solver would tend to withdraw water from the cheapest source only if left unconstrained.

Table 17 - Percentages of supply withdrawn from groundwater sites

ID/Month	Oct	Nov	Dec	Jan	Feb	Mar	Apr	May	Jun	Jul	Aug	Sep
DEID												
GW01	0.00	0.00	0.00	0.00	0.00	0.00	0.06	0.03	0.05	0.06	0.05	0.05
GW06	0.00	0.00	0.00	0.00	0.00	0.00	0.12	0.13	0.11	0.11	0.12	0.12
GW07	0.21	0.25	0.21	0.21	0.32	0.25	0.28	0.25	0.23	0.29	0.27	0.28
GW12	0.00	0.00	0.00	0.00	0.15	0.18	0.20	0.13	0.14	0.10	0.10	0.08
GW13	0.79	0.75	0.79	0.79	0.53	0.57	0.34	0.45	0.47	0.45	0.46	0.48
KTWD												
GW03	0.00	0.00	0.00	0.00	0.62	0.62	0.27	0.22	0.15	0.17	0.19	0.26
GW12	0.64	0.00	0.00	0.00	0.00	0.00	0.67	0.62	0.68	0.64	0.62	0.54
GW13	0.36	1.00	1.00	1.00	0.38	0.38	0.06	0.17	0.18	0.19	0.19	0.21
LTID												
GW06	0.35	0.12	0.37	0.37	0.14	0.14	0.15	0.28	0.21	0.19	0.21	0.22
GW09	0.13	0.24	0.14	0.14	0.28	0.30	0.25	0.25	0.26	0.24	0.24	0.23
GW10	0.31	0.62	0.27	0.27	0.58	0.55	0.59	0.45	0.52	0.56	0.54	0.54
GW12	0.21	0.02	0.22	0.22	0.01	0.01	0.01	0.01	0.01	0.01	0.01	0.01
PXID												
GW01	0.00	0.00	0.00	0.00	0.00	0.00	0.00	0.00	0.00	0.00	0.00	0.00
GW06	0.00	0.07	0.00	0.00	0.09	0.10	0.09	0.13	0.14	0.11	0.10	0.10
GW07	0.03	0.37	0.00	0.00	0.36	0.33	0.31	0.31	0.26	0.24	0.26	0.27
GW10	0.97	0.54	1.00	1.00	0.53	0.52	0.54	0.53	0.57	0.63	0.62	0.62
GW14	0.00	0.02	0.00	0.00	0.02	0.05	0.06	0.03	0.03	0.02	0.02	0.01
LIID												
GW04	0.11	0.11	0.11	0.11	0.14	0.19	0.33	0.29	0.23	0.20	0.22	0.25
GW06	0.00	0.00	0.00	0.00	0.00	0.25	0.15	0.17	0.25	0.32	0.27	0.24
GW12	0.89	0.89	0.89	0.89	0.86	0.57	0.53	0.53	0.52	0.48	0.51	0.51
LSID												
GW04	0.35	0.36	0.33	0.33	0.57	0.63	0.43	0.42	0.38	0.40	0.41	0.44
GW12	0.65	0.64	0.67	0.67	0.43	0.37	0.57	0.58	0.62	0.60	0.59	0.56
POID												
GW06	0.05	0.03	0.05	0.05	0.04	0.05	0.07	0.11	0.10	0.12	0.11	0.11
GW12	0.95	0.97	0.95	0.95	0.96	0.95	0.93	0.90	0.90	0.88	0.89	0.89
RGWD												
GW03	0.00	0.00	0.00	0.00	0.00	0.00	0.00	0.10	0.03	0.08	0.14	0.19
GW12	0.00	0.00	0.00	0.00	0.00	0.00	0.96	0.83	0.85	0.81	0.72	0.56
GW13	1.00	1.00	1.00	1.00	1.00	1.00	0.04	0.07	0.12	0.11	0.14	0.25

SAID												
GW06	0.00	1.00	0.00	0.00	1.00	1.00	0.91	0.94	0.95	0.97	0.96	0.96
GW12	0.00	0.00	0.00	0.00	0.00	0.00	0.09	0.07	0.05	0.03	0.04	0.04
TPWD												
GW04	0.00	0.00	0.00	0.00	0.00	0.13	0.28	0.32	0.15	0.18	0.18	0.19
GW12	1.00	1.00	1.00	1.00	1.00	0.87	0.72	0.68	0.85	0.82	0.82	0.81
TBID												
GW02	0.00	0.00	0.00	0.00	0.14	0.09	0.09	0.05	0.03	0.04	0.04	0.04
GW04	0.00	0.00	0.00	0.00	0.00	0.31	0.13	0.14	0.13	0.14	0.15	0.19
GW12	1.00	1.00	1.00	1.00	0.86	0.60	0.78	0.81	0.84	0.82	0.81	0.77

Appendix A2 – Model Metadata

Metadata 1 - Seepage Data

Location folder	Data files
Friant project\Other data\Surface\Seepage_analysis	seepage split.xls other files in the location folder

Notes:

For seepage consideration it will be used the % diversion channel loss
from Naugle (2001) table 4.4.

This table lists percentage of water lost through seepage when water is conveyed through the diversion channel en route to each district. Information on the diversion channels that supply each district is in Naugle (2001) Table 4.5

In MODSIM, this loss is applied to each link connecting the district's total node to its supplies). The Return node the channel loss is applied to a "seepage node". Once the objective is to distribute the seepage through the GW sites under the channel network, and the link does not allow for multiple return nodes a intermediate seepage node is created. From the seepage node the water is split to the GW sites according to information available on location of the diversion network relative to the GW sites. This is described in more detail in the following:

LTID - Lower tule river
Main network delivering water to LTID icludes Poplar ditch, Woods-central ditch and Tule river. In the lack of more detailed information, It will be obtained the percentage of total length of all canals that is located over a given GW site as way to split the seepage.

APID - Alpaugh
Alpaugh receives water from FKC (CVC exchange) through Deer creek. It is accounted the Lower Deer Creek plus a extention to the district. The extention runs over GW site 7

ATID - Atwell Island
Same as Alpaugh

DEID - Delano Earlimart
Delano Earlimart receives FKC water through white River but it is ignored in alec model. Since only FKC turnouts are considered and no other information about the channel network is available, the seepage will be split to the GW sites based on area percentage that they have on DEID

PXID - Pixley
According to Naugle (2001), the certain diversion to Pixley is Deer Creek. Split of seepage is made based on percentage lengths of lower Deer creek over the GW sites

POID - Porterville
Since most of Porteville is over GW zone 12, 90% of all diversion seepage loss will be sent to GW12 and 10% to GW6.

Metadata 2 – Infiltration return from Irrigation districts

Location folder	Data files
Friant project\Other data\Economic Functions	Crop_acreage_per_ID.xls
Friant project\Other data\Groundwater	areas_district_vs_edit5.xls

Notes:

Irrigation efficiency data from Naugle (2001). Values were processed by taking average weighted by crop area

Metadata 3 – Time series of groundwater demand

Location folder	Data files
Friant project\Other data\Groundwater	pump_pattern.xls
Friant project\Other data\Nels_received\received_04_19_pump_pattern1977_corrected\gui-data	Grid-Pumpage-1977.DBF* Grid-Pumpage-1977.SHP* Grid-Pumpage-1977.SHX*
Friant project\Other data\Nels_received\Received_04_10_pump_pttn_cropac\gui-data	Grid-Pumpage-1980.DBF* Grid-Pumpage-1980.SHP* Grid-Pumpage-1980.SHX* Grid-Pumpage-1983.DBF* Grid-Pumpage-1983.SHP* Grid-Pumpage-1983.SHX*

* Files sent by Nels Ruud

Metadata 4 - Initial groundwater storages

Location folder	Data files
Friant project\Other data\Nels_received\Received_05_09_Initial_Storages\storage	Initial Storage F1985.DBF* Initial Storage F1985.SHP* Initial Storage F1985.SHX*

* Files sent by Nels Ruud

Metadata 5 – Hydraulic conductance values

Location folder	Data files
Friant project\Other data\Nels_received\updated_cond_12_16	districts.dbf* districts.shp* districts.shx* flux-del-districts.xls* flux-del-edit5.xls*
Friant project\Other data\Groundwater\conductance	flux-del_edit5_upd_04.xls

* Files sent by Nels Ruud

Metadata 6 – Economic functions

Location folder	Data files
Friant project\Other data\Hatchett_received	WATERDMDaw.txt*
Friant project\Model runs\VP\Data files	WATERDMDaw4_bcvp043.xls

* Files sent by Steve Hatchett

Metadata 7 – Inflows to surface reservoirs

Reservoir	Source
San Joaquin R at Millerton[a]	DWRSIM (IN18)
Chowchilla R at Eastman	DWRSIM (IN53)
Fresno R at Hensley	DWRSIM (IN52)
Kings R at Pine Flat	USACE
Kaweah R at Kaweah	USACE
Tule R at Success	USACE
Kern R at Isabella	USACE

Metadata 8 – Surface reservoir targets

Location folder	Data files
Friant project\Other data\Surface Reservoirs	res targets.xls*

*file developed by Marc Leu

Metadata 9 – Friant Kern Canal Capacities

Location folder	Data files (paper document)
-	Friant Water Users Authority (1998) *Friant Kern Canal Structures List.*

Appendix A3 – Reference Manual

The model reference manual uses the same basic instructions presented in Leu (2001) for preparation and running the model, since no structural modification was introduced. One program to convert the .txt MODSIM output into HEC DSS format was developed and it is presented here, along with three post-processing EXCEL spreadsheets where DSS data can loaded for faster results interpretation.

Preparation for a FREDSIM Model Run

1. Input inflow data into the model using the interface and ADA directory. Data files in the ADA directory do not need to be in the same directory as model files.

2. Check that reservoir targets and evaporation, and water demand time-series data correspond with hydrologic time-series data. Make adjustments.

3. In the MODSIM interface change the Time Scale to monthly and set the number of years in the model run plus one.

4. Name the FREDSIM file (*.xy) the same root name as the Perl script (*.pl). Naming model runs is critical because MODSIM will overwrite any output data files with the same name.

5. Place MODSIM and Perl software files into the same directory as the *.xy, *.pl, and the IRRPARAM data file.

Steps for Running FREDSIM

1. Open a DOS window and change the directory on the command line to the current model's directory. The executable MODSIM file is MODCMD.exe.

2. The command for running is MODCMD followed by the file name without file extensions. For example: C:\MODCMD bcvp043

Output files are placed in the same directory as the software and input files and have the same root name as the model input files. All model output must be post-processed in a spreadsheet for high quality plots and other data analysis. The MODSIM interface can be opened after the model run and used for simple plots of model run results. The output files along with a brief description are listed below.

MODSIM Output Files

File Ext.	Output Data	Notes
*.acc	Link output	Flow data in links.
*.flo	Link output	Flow data in links with notation of constrained flow.
*.dem	Demand results	Demands, supplies, and shortage data.
*.res	Reservoir operation results	Water balance data for storage nodes.
*.gw	Groundwater results	FREDSIM does not use the groundwater capabilities of MODSIM, thus the *.gw file is not used. Groundwater reservoir results are output to the *.res file.
test2.txt	groundwater pumping cost, per groundwater zone, per irrigation district, per month	
test3.txt	groundwater carryover storage, per groundwater zone, per month	

All the output files (except of test2.txt and test3.txt) can be converted to HEC DSS format running the program MODSS_v04. Once converted to DSS, the data can be loaded into EXCEL spreadsheets for easier processing. Three processing templates were developed:

Template processing file	Description
Charts_template_v4.xls	This file reads data of head, storage and pumping cost from test2.txt. and test3.txt output files and create two charts for each GW zone: a Head &. Cost vs. time and a Head & Storage vs. time
Scost_template.xls	This file reads economic data from IRRPARAM file and water supply data from DSS output and calculates scarcity values and scarcity costs
Scarcity&Supply.xls	Sorts DSS output data loaded for each irrigation district.